PNL-8000, Pt. 1
UC-408

PNL--8000-Pt.1

DE93 005013

Pacific Northwest Laboratory Annual Report for 1991 to the DOE Office of Energy Research

Part 1: Biomedical Sciences

J. F. Park and Staff

September 1992

Prepared for
the U.S. Department of Energy
under Contract DE-AC06-76RLO 1830

Pacific Northwest Laboratory
Richland, Washington 99352

Preface

This 1991 Annual Report from Pacific Northwest Laboratory (PNL) to the U.S. Department of Energy (DOE) describes research in environment and health conducted during fiscal year 1991. This year the report consists of four parts, each in a separate volume.

The four parts of the report are oriented to particular segments of the PNL program, describing research performed for the DOE Office of Health and Environmental Research in the Office of Energy Research. In some instances, the volumes report on research funded by other DOE components or by other governmental entities under interagency agreements. Each part consists of project reports authored by scientists from several PNL research departments, reflecting the multidisciplinary nature of the research effort.

The parts of the 1991 Annual Report are:

Part 1: Biomedical Sciences		
Program Manager:	J. F. Park	J. F. Park, Report Coordinator S. A. Kreml, Editor
Part 2: Environmental Sciences		
Program Manager:	R. E. Wildung	D. A. Perez, Editor
Part 3: Atmospheric Sciences		
Program Manager:	W. R. Barchet	L. K. Grove, Editor
Part 4: Physical Sciences		
Program Manager:	L. H. Toburen	L. H. Toburen, Report Coordinator R. C. Pedersen, Editor

Activities of the scientists whose work is described in this annual report are broader in scope than the articles indicate. PNL staff have responded to numerous requests from DOE during the year for planning, for service on various task groups, and for special assistance.

Credit for this annual report goes to the many scientists who performed the research and wrote the individual project reports, to the program managers who directed the research and coordinated the technical progress reports, to the editors who edited the individual project reports and assembled the four parts, and to Ray Baalman, editor in chief, who directed the total effort.

T. S. Tenforde
Health and Environmental Research Program

Previous reports in this series:

Annual Report for:

1951	HW-25021, HW-25709
1952	HW-27814, HW-28636
1953	HW-30437, HW-30464
1954	HW-30306, HW-33128, HW-35905, HW-35917
1955	HW-39558, HW-41315, HW-41500
1956	HW-47500
1957	HW-53500
1958	HW-59500
1959	HW-63824, HW-65500
1960	HW-69500, HW-70050
1961	HW-72500, HW-73337
1962	HW-76000, HW-77609
1963	HW-80500, HW-81746
1964	BNWL-122
1965	BNWL-280, BNWL 235, Vol. 1-4; BNWL-361
1966	BNWL-480, Vol. 1; BNWL-481, Vol. 2, Pt. 1-4
1967	BNWL-714, Vol. 1; BNWL-715, Vol. 2, Pt. 1-4
1968	BNWL-1050, Vol. 1;, Pt. 1-2; BNWL-1051, Vol. 2, Pt. 1-3
1969	BNWL-1306, Vol. 1;, Pt. 1-2; BNWL-1307, Vol. 2, Pt. 1-3
1970	BNWL-1550, Vol. 1;, Pt. 1-2; BNWL-1551, Vol. 2, Pt. 1-2
1971	BNWL-1650, Vol. 1;, Pt. 1-2; BNWL-1651, Vol. 2, Pt. 1-2
1972	BNWL-1750, Vol. 1;, Pt. 1-2; BNWL-1751, Vol. 2, Pt. 1-2
1973	BNWL-1850, Pt. 1-4
1974	BNWL-1950, Pt. 1-4
1975	BNWL-2000, Pt. 1-4
1976	BNWL-2100, Pt. 1-5
1977	PNL-2500, Pt. 1-5
1978	PNL-2850, Pt. 1-5
1979	PNL-3300, Pt. 1-5
1980	PNL-3700, Pt. 1-5
1981	PNL-4100, Pt. 1-5
1982	PNL-4600, Pt. 1-5
1983	PNL-5000, Pt. 1-5
1984	PNL-5500, Pt. 1-5
1985	PNL-5750, Pt. 1-5
1986	PNL-6100, Pt. 1-5
1987	PNL-6500, Pt. 1-5
1988	PNL-6800, Pt. 1-5
1989	PNL-7200, Pt. 1-5
1990	PNL-7600, Pt. 1-5

Foreword

This report summarizes progress in OHER biological research and general life sciences research programs conducted at PNL in FY 1991. The research develops the knowledge and scientific principles necessary to identify, understand, and anticipate the long-term health consequences of energy-related radiation and chemicals. Our continuing emphasis is to decrease the uncertainty of health risk estimates from existing and newly developed energy-related technologies through an increased understanding of the ways in which radiation and chemicals cause biological damage.

The sequence of this report of PNL research reflects the OHER programmatic structure. The first section, **Biological Research**, contains reports of biological research in laboratory animals and *in vitro* cell systems, including research with radionuclides and chemicals. The next section, **General Life Sciences Research**, reports research conducted for the OHER human genome research program.

Biological Research

Life-span studies in beagles with inhaled $^{239}Pu(NO_3)_4$ were in the 14th postexposure year. Thus far, 28 of 96 exposed dogs had bone tumors, 31 had lung tumors, and 9 had intrahepatic bile duct tumors. Because lung tumors were the primary plutonium exposure-related cause of death in the $^{239}PuO_2$-exposed dogs (51 of 116 dogs), four methods for calculating radiation dose to the lungs were compared to evaluate uncertainties in radiation dose estimates. Comparisons of mean accumulative average radiation dose to the lungs were not statistically different among the four different methods, and the fraction of dogs with lung tumors for the four highest dose-range groups was similar for each method of dose calculation. Other plutonium exposure-related effects included sclerosis of the tracheobronchial lymph nodes, lymphopenia, focal radiation pneumonitis, focal dystrophic osteolytic lesions in bone, adenomatous hyperplasia of the liver, and serum chemistry indicating liver damages.

In the project "National Radiobiology Archives," information from life-span radiation studies from DOE laboratories is stored in computerized databases with selected research documents and tissues for future research and analyses. The databases include information from records on about 7,000 beagle and 10,000 mice from seven laboratories, which is available on diskette.

Dose-effect-relationship studies on inhaled $^{239}PuO_2$ in rats are in progress to obtain lung tumor incidence data at lifetime lung doses of 0.07 to 20 Gy. Thus far, the lung cancer dose-response curve is well fitted by a quadratic function and a "practical" threshold of 1 to 2 Gy; maximum lung cancer incidence (75%) occurred at 8 Gy. The incidence of lung tumors in 1641 rats with lung doses <1 Gy was 0.2%; in 1004 rats with lung doses <0.1 Gy, it was 0.1%; and in 944 sham-exposed controls, the lung tumor incidence was 0.4%.

Rats exposed by inhalation to radon and decay products are under study to determine the influence of dose, dose rate, unattached fraction of radon progeny, and cigarette smoke on lung cancer incidence. Analyses of histopathological data for 100-WL (working-level) exposure rates showed that lung tumor incidence decreases in proportion to the decrease in cumulative exposure and remains elevated compared to that of controls at exposures comparable to those found in houses, that is, 40 WLM (working-level months). Exposures at 50 WLM/week produced a greater incidence of lung tumors than exposures at 500 WLM/week at cumulative doses larger than 640 WLM. Both lung and nasal carcinomas increased with increase in unattached progeny levels. Most (~80%) of the radon-induced tumors were considered to be peripheral in the lung. No particular association of lung tumor location was noted for unattached percentages, fp, ranging between 0.4% and 7%. Histopathological examination of rats exposed at 100 WL for 320 WLM and cigarette smoke on an initiation-promotion-initiation study showed that those with a

320-WLM continuous exposure had increased lung tumor incidence compared to those with split exposure with or without cigarette smoke. The majority of the smoke-exposure-related carcinomas were epidermoid carcinomas, in contrast to the generally greater incidence of adenocarcinomas in the non-smoke-related tumors.

The alkaline single-cell gel electrophoresis technique to estimate the fraction of cell nuclei "hit" by alpha particles during *in vitro* radon exposure was used to test PNL hit probability calculations. Preliminary data indicate that 47% of AL cells are hit by alpha particles when given 38 cGy of radon; the PNL model predicts that 61% would be transversed by an alpha particle.

After *in vitro* x irradiation or radon exposure, the largest category of CHO-HGPRT mutations was full deletions. The fraction of full deletions from radon (25 to 77 cGy) and 300-cGy x-ray exposure were similar (42% to 48%). Polymerase chain reaction exon analysis of *in vitro* x-ray- and radon-induced mutation at the CHO-HGPRT locus indicated that exon 5 was missing more often than would be expected in spontaneous mutations.

In our "Dosimetry of Radon Progeny" project, we used our lung dosimetry model and reported activity-size spectra of radon-progeny aerosols in mines and in homes to estimate dose received by the bronchial epithelium. The dose conversion factor for historical mine conditions was 20 mGy/WLM, compared to 16 mGy/WLM for homes. We used these results to reexamine lung cancer risk for radon exposure. In radon-exposed miners, we found that application of the risk factors currently recommended by the International Commission on Radiological Protection in the form of the calculated "effective dose" leads to an overestimation of lung cancer risk by a factor of approximately five; for the general public, the overprediction is greater. We have also developed physiologically based pharmacokinetics and dosimetry models for other body tissues, and have applied these models to evaluate marrow stem cell doses from exposure to radon, thoron, and their short-lived progeny.

An ultrafine radon progeny size-spectrometer, an integrating low-pressure impactor, and a past-exposure radon monitor have been developed using CR-39 alpha-track detectors to characterize radon-progeny exposures for experimental studies and for human exposure environments.

Studies to examine the role of oncogenes in radiation-induced cancer use tumor tissue from the animal studies previously described. We have identified mutations in K-*ras* and H-*ras* genes in radon-induced rat lung tumors, and H-*ras*, K-*ras*, and N-*ras* mutations in spleen cells from dogs with radiation-induced leukemia. A study of mutations of the tumor suppressor genes retinoblastoma susceptibility (RB) and p53, as targets in radiation carcinogenesis, was begun because large deletions are a major component of genetic damage by ionizing radiation, these genes are defective in human osteosarcoma and lung cancer, and plutonium has caused lung and bone tumors in experimental animals. We have prepared probes for mRNA analysis of dog RB and α-tubulin genes and found that the transcripts are the same as those of the rat and of humans.

In our chemical-related biological research, studies with well-defined DNA fragments adducted with the bulky chemical carcinogen benzo[a]pyrene demonstrated sequence-specific modification. Replication of the adducted DNA with polymerases consistently resulted in blockage of the polymerase at one base before the adducted deoxyguanine residues. A dose-dependent relationship was observed between the intensity of blocks and the level of modification. The level of adduction at any particular deoxyguanine residue varied by more than one order of magnitude, and the adduction of polydeoxyguanine sequences was invariably favored over adduction of single residues.

Interactions between cellular and genetic damage induced by radiation, chemicals, and oncogenes are being studied. Genotoxic responses to hexone and tributyl phosphate, present in large amounts at

nuclear waste sites, were investigated alone and in combination with gamma irradiation *in vitro*. The combined effects were not more than additive, and no interactive effects were observed between damage by radiation and that from the solvent. Mice given carbon tetrachloride plus mutated K-v-*ras* and ^{239}Pu had a higher frequency of liver nodules relative to those exposed to either agent alone.

In our fetal and juvenile radiation research we examined similarities and differences in coefficients for gastrointestinal, pulmonary, and placental transfer of several materials. To facilitate extrapolation to humans, a workshop was held on the effects of prenatal radiation on the central nervous septum to examine uncertainties about quantitative extrapolations to low dose levels from human and animal data and to explore new research approaches to decrease uncertainties. The workshop report (PNL-8009) summarized the current status of research. In our laboratory the involvement of fibronectin in cell migration during neurulation was evaluated in mice irradiated with 1 Gy at 13 days gestation (dg) and followed at 17 dg and 6 and 14 days postnatal life. These exposures produced reduction in brain weight and characteristic morphological changes, and the isoform patterns of fibronectin were altered.

General Life Sciences Research

PNL is developing a computer information system to graphically display and manipulate the vast amounts of information about the human genome. The user interface, named GnomeView, provides researchers with graphical representations of chromosomes, genetic and physical maps, and DNA sequences. The architecture of the GnomeView interface has been implemented. The test set of maps for superoxide dismutase as abstracted earlier manually from Human Genome Mapping Library, GenBank, and the literature have been, for the most part, supplemented with direct access capabilities to resident abstractions of GenBank and Genome Data Base.

PNL biomedical research is an interdisciplinary effort requiring scientific contributions from many research departments at PNL. Personnel in the Life Sciences Center are the principal contributors to this report.

Requests for reprints from the list of publications will be honored while supplies are available.

Contents

Biological
Research

Inhaled Plutonium Oxide in Dogs

Principal Investigator: *J. F. Park*

Other Investigators: *R. L. Buschbom, G. E. Dagle, E. S. Gilbert, G. J. Powers, C. R. Watson, and R. E. Weller*

Technical Assistance: *R. F. Flores, B. G. Moore, and M. J. Steele*

This project is concerned with long-term experiments to determine the life-span dose-effect relationships of inhaled $^{239}PuO_2$ or $^{238}PuO_2$ in beagles. The data will be used to estimate the health effects of inhaled transuranics. Beagle dogs given a single exposure to $^{239}PuO_2$ or $^{238}PuO_2$ aerosols to obtain dose-level groups with mean initial lung depositions approximately 1, 8, 40, 150, 700, and 2800 times the maximum permissible lung dose[(a)] for a plutonium worker have been observed for life-span dose-effect relationships; all the dogs have now died. Because lung tumors were the primary plutonium exposure-related cause of death in the $^{239}PuO_2$-exposed dogs, four methods for calculating radiation dose to the lungs were compared to evaluate uncertainties in radiation dose estimates. Accumulative average radiation dose to the lungs was caculated using: (1) initial plutonium lung deposition based on external thorax counting and a fitted plutonium lung retention function for all dogs; (2) initial lung deposition based on final body burden of plutonium and a fitted lung retention function for all dogs; (3) initial lung deposition based on external thorax counting and an individual lung retention function for each dog; and (4) initial lung deposition based on final body burden and an individual lung retention function for each dog. Comparisons of mean accumulative average radiation dose to the lungs for six dose-range groups (0-30, 30-100, 100-300, 300-1000, 1000-3000, and 3000-8500 rads) were not statistically different among the four different methods.

To determine the life-span dose-effect relationships of inhaled plutonium, 18-month-old beagle dogs were exposed to aerosols of $^{239}PuO_2$ [mean activity median aerodynamic diameter (AMAD), 2.3 μm; mean geometric standard deviation (GSD), 1.9], prepared by calcining the oxalate at 750°C for 2 hours; or to $^{238}PuO_2$ (mean AMAD, 1.8 μm; mean GSD, 1.9), prepared by calcining the oxalate at 700°C and subjecting the product to $H_2{}^{16}O$ steam in argon exchange at 800°C for 96 hours. This material, referred to as pure plutonium oxide, is used as fuel in space nuclear-power systems.

One hundred thirty dogs exposed to $^{239}PuO_2$ in 1970 and 1971 were selected for long-term studies; 14 were periodically sacrificed to obtain plutonium distribution and pathology data, and 116 were assigned to life-span dose-effect studies (Table 1). The 116 dogs exposed to $^{238}PuO_2$ in 1973 and 1974 were selected for life-span dose-effect studies (Table 2), and 21 additional dogs were exposed for periodic sacrifice. The Appendix (which follows Part 1 of this *Annual Report*) shows the status of the dogs in these experiments. The *Pacific Northwest Laboratory Annual Report for 1989 to the Office of Energy Research (Part 1)* summarized the results of the $^{239}PuO_2$ study, and the results of the $^{238}PuO_2$ study were summarized in the *Pacific Northwest Laboratory Annual Report for 1990 to the Office of Energy Research (Part 1)*. Because lung tumors were the primary plutonium exposure-related cause of deaths in the $^{239}PuO_2$-exposed dogs, this year we focused on dosimetry in the lungs.

(a) 15 rem/year, 16 nCi plutonium.

TABLE 1. Life-Span Dose-Effect Studies with Inhaled $^{239}PuO_2$ in Beagles[a]

Exposure-Level Group	Number of Dogs		Initial Lung Deposition[b]	
	Male	Female	nCi[c]	nCi/g Lung[c]
Control	10	10	0	0
1	12	12	3.5±1.3	0.029±0.011
2	10	11	22±4	0.18±0.04
3	10	10	79±14	0.66±0.13
4	11	11	300±62	2.4±0.4
5	11	10	1100±170	9.3±1.4
6	3	5	5800±3300	50±22
	67	69		

(a) Exposed in 1970 and 1971.
(b) Estimated from external thorax counts at 2 and 4 weeks after exposure and estimated lung weights (0.011 x body weight).
(c) Mean ± 95% confidence intervals around mean.

TABLE 2. Life-Span Dose-Effect Studies with Inhaled $^{238}PuO_2$ in Beagles[a]

Exposure-Level Group	Number of Dogs		Initial Lung Deposition[b]	
	Male	Female	nCi[c]	nCi/g Lung[c]
Control	10	10	0	0
1	10	10	2.3±0.8	0.016±0.007
2	11	10	18±3	0.15±0.03
3	12	10	77±11	0.56±0.07
4	10	10	350±81	2.6±0.5
5	10	10	1300±270	10±1.9
6	7	6	5200±1400	43±12
	70	66		

(a) Exposed in 1973 and 1974.
(b) Estimated from external thorax counts at 2 and 4 weeks after exposure and estimated lung weights (0.011 x body weight).
(c) Mean ± 95% confidence intervals around mean.

Fifty-one of the 116 life-span dogs exposed to $^{239}PuO_2$ had lung tumors at death. Table 3 shows the number of dogs with lung tumors for each exposure-level group based on initial plutonium lung deposition by external thorax counting. The dogs in the highest exposure-level group died early of respiratory insufficiency; 1 dog had lung tumors. Lung tumors were the primary cause of death in exposure-level groups 3, 4, and 5. Lung tumors were observed in 4 dogs in exposure-level group 2 and in 3 control dogs. Survival was decreased compared to controls in the three highest dose-level groups.

Reevaluation of the histopathology on these dogs was completed this year. Two dogs, 885F (control) and 865F (exposure-level group 1), previously reported with lung tumors, are now classified as metastatic sweat gland adenocarcinoma and pneumonia, respectively.

Lung dosimetry estimates in our previous reports have been based on initial lung deposition estimates derived from the mean of two external thorax counts of plutonium x-ray photons obtained at 2 and 4 weeks after exposure. We call this initial lung deposition (ILDCT). Error in ILDCT estimates based on external counting error for an individual dog with the mean ILDCT for each exposure-level group are shown in Table 4. Based only on external counting error calculations, the potential error in ILDCT estimates for the lowest dose-level group was large. These estimates do not include errors related to potential external contamination of the thorax at the time of counting. Because of the high attenuation of the 17-keV x rays by the thorax wall, small amounts of plutonium external to the thorax wall would cause high estimates of ILDCT.

At necropsy, representative samples were collected for histopathology, and the remainder of the tissues were analyzed radiochemically for plutonium. The results were adjusted by organ weight and summed to estimate the total plutonium present at death. We call this the final body burden (FBB). Similarly, the lung radioanalysis values were weight adjusted and summed to estimate total plutonium in the lung at death. We call this the final lung burden (FLB). Errors associated with this technique are considered to be lower than with external thorax counting, although they have not yet been evaluated.

The difficulty in making accurate *in vivo* plutonium lung deposition estimates was known at the time the dogs were exposed, and an alternate approach was planned. Excreta were collected daily for 1 week, weekly for 3 weeks, and then for 5 days in a year for plutonium analysis, as were tissues at death. Plutonium analysis of these samples allows estimation of initial body burden based

TABLE 3. Fraction of $^{239}PuO_2$-Exposed Dogs with Lung Tumors

Exposure-Level Group	Number of Dogs	Mean Initial Lung Deposition, nCi[(a)]	Number of Dogs with Lung Tumors	Percentage of Dogs with Lung Tumors	Survival Post Exposure, days[(b)]
Control	20	0	3	15	4447 (4140-4907)
1	24	3.5	0	0	4677 (4260-4950)
2	21	22	4	19	4811 (4669-5026
3	20	79	10	50	4723 (4107-5004)
4	22	300	16	73	3638 (3311-4034)
5	21	1100	20	85	2298 (1885-2856)
6	8	5800	1	13	460 (358-799)

(a) Estimated from mean of external thorax counts at 2 and 4 weeks after exposure.
(b) Median and 95% confidence limits.

TABLE 4. Estimated Error in ^{239}Pu Initial Lung Deposition Estimates Based on External Thorax Counting Error for an Individual Dog

Exposure-Level Group	Initial Lung Deposition, nCi[(a)]
1	3.5 ± 3
2	22 ± 3
3	79 ± 4
4	300 ± 5
5	1100 ± 9
6	5800 ± 19

(a) Mean ± standard error of the mean.

on adding estimated daily excretion to the FBB. Plutonium excreta analysis for such estimates are not yet complete. The costs for plutonium excreta analysis, especially for the low-level dogs, are large and exceed the current funding for this project. Further, the excreta analysis may not provide more accurate estimates of initial lung deposition than the ILDCT or the FBB. Therefore, before completing plutonium excreta analysis, we explored methods for estimating radiation dose to the lungs based on the ILDCT and the FBB.

Table 5 compares the mean and 95% confidence interval around the mean FBB with the mean ILDCT for the six exposure-level groups. In all groups the mean FBB was less than the mean ILDCT, and it was significantly different ($p < 0.05$) for exposure-level groups 2, 3, and 5. The mean fraction retained in the body ranged from 50% to 82% of the ILDCT, depending on exposure-level group. These were not significantly different ($p < 0.05$), except for the comparison of exposure-level group 2 with group 6. Survival time for exposure-level group 6 (see Table 4) was much shorter than the other groups, allowing less time for plutonium excretion.

Four methods for estimating radiation dose to the lungs were compared to evaluate uncertainties in radiation dose estimates. Mean lung doses for the four methods within each of six dose-range groups were compared using Tukey's studentized range test. The 0.05 level of significance was used for all statistical tests. The dose-range groups were 0-30, 30-100, 100-300, 300-1000, 1000-3000, and 3000-8500 rads.

Our approach was to obtain the fraction plutonium in lung at death (FLB) divided by plutonium initially deposited in the lung (ILD), fit it with an exponential retention function, and integrate under the curve. The general form of the dose calculation was:

$$D = \frac{(51.2)(E)(L)}{W}\left[\frac{1}{X}\left(1-e^{(x)t}\right)\right]$$

where:

D = Cumulative average radiation dose (rads) to the lungs
51.2 = Conversion factor for rads

TABLE 5. Comparison of ^{239}Pu Initial Lung Deposition and Final Body Burden

Exposure-Level Group	Number of Dogs	Initial Lung Deposition, nCi[(a)]	Final Body Burden, nCi[(b)]	Final Body Burden, %[(c)]
1	24	3.5 ± 1.3	2.3 ± 0.9	66 ± 28
2	21	22 ± 4	11 ± 5[(d)]	50 ± 14[(e)]
3	20	79 ± 14	57 ± 14[(d)]	72 ± 9
4	22	300 ± 62	231 ± 55	77 ± 10
5	21	1100 ± 170	806 ± 202[(d)]	73 ± 8
6	8	5800 ± 3300	4777 ± 2863	82 ± 18[(e)]

(a) Mean ± 95% confidence interval around the mean based on external thorax counting at 2 and 4 weeks after exposure.
(b) Mean ± 95% confidence interval around the mean based on radiochemical analysis of all tissues at death.
(c) Mean ± 95% confidence interval around the mean final body burden expressed as percent of initial lung deposition based on external thorax counting at 2 and 4 weeks after exposure.
(d) Significantly different ($p < 0.05$) from initial lung deposition estimates (t test).
(e) Underlined values are statistically different ($p < 0.05$) from each other (Tukey's studentized range test).

E = Alpha energy for ^{239}Pu = 5.15 MeV
L = Initial lung deposition in μCi
W = Lung weight in grams = 0.011 x body weight
X = Decay constant from retention curve
t = Days over which the dose was accumulated, survival after exposure.

The four methods we compared are based on alternate methods for estimating L and X.

Method 1: Initial Lung Deposition Based on External Thorax Counts (ILDCT)

The first method was to let L = ILDCT (from external thorax counting described earlier) and obtain X from a retention curve based on FLB/ ILDCT for all the dogs. The lung retention function $y = 100\ e^{-(0.000629)t}$, where y is the percent ILDCT remaining in the lungs at t days after exposure (Figure 1), was fitted by weighted nonlinear regression and shows the individual data points for each dog. The lung retention half-time for this retention function was 1102 days (1102 ± 80 days, 95% confidence interval). The spread of individual data points around the fitted curve in Figure 1 may be related to potential errors in estimating ILDCT or to individual dog variation in lung retention of plutonium, or both.

Method 2: Final Body Burden (FBB)

The second method used L = FBB and a lung retention function based on FLB/FBB for all the dogs. In this approach we assumed that initial lung deposition is equal to FBB. The retention function does not include the plutonium that was deposited in the lungs and then excreted; it includes only that plutonium which was deposited in the lung and retained in the body for the life of the dog. It eliminates the potential error associated with external thorax counting. The lung retention curve, $y = 100\ e^{-(0.000458)t}$, where y is the percent FBB remaining in the lungs at t days after exposure, was fitted by weighted nonlinear regression; the individual data points are shown in Figure 2. The lung retention half-time was 1513 days (1513 ± 92 days, 95% confidence interval). This retention function was significantly different ($p < 0.05$) from the function derived by method 1 (ILDCT) based on initial lung deposition (half-time, 1102 ± 80 days) determined by external thorax counting. The spread of individual data points around the fitted curve in Figure 2 suggests a large variation in lung retention for individual dogs.

Method 3: Individual Inital Lung Deposition Based on External Thorax Counts (IILDCT)

The third method was identical to method 1 (L = ILDCT, X based on FLB/ILDCT) except that we calculated radiation dose to the lungs using an individual exponential function for each dog. The lung retention half-times ranged from 376 to 3175 days with a mean of 1086 days (1086 ± 74 days, 95% confidence interval). The mean

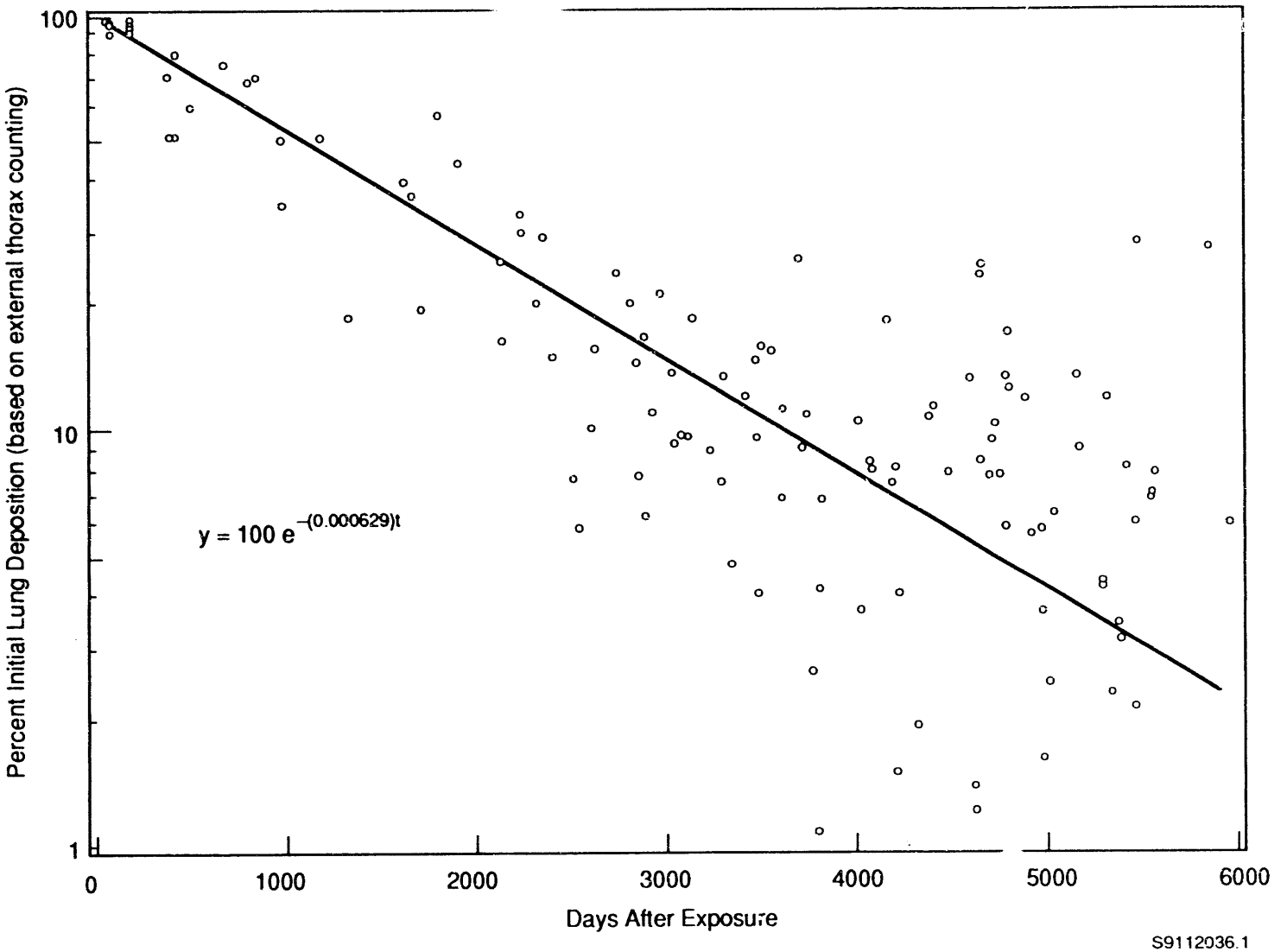

FIGURE 1. Lung Retention of Inhaled $^{239}PuO_2$ Determined by [(final lung burden of plutonium)/(initial lung deposition of plutonium based on external thorax counting)] x 100. Points represent data from individual dogs.

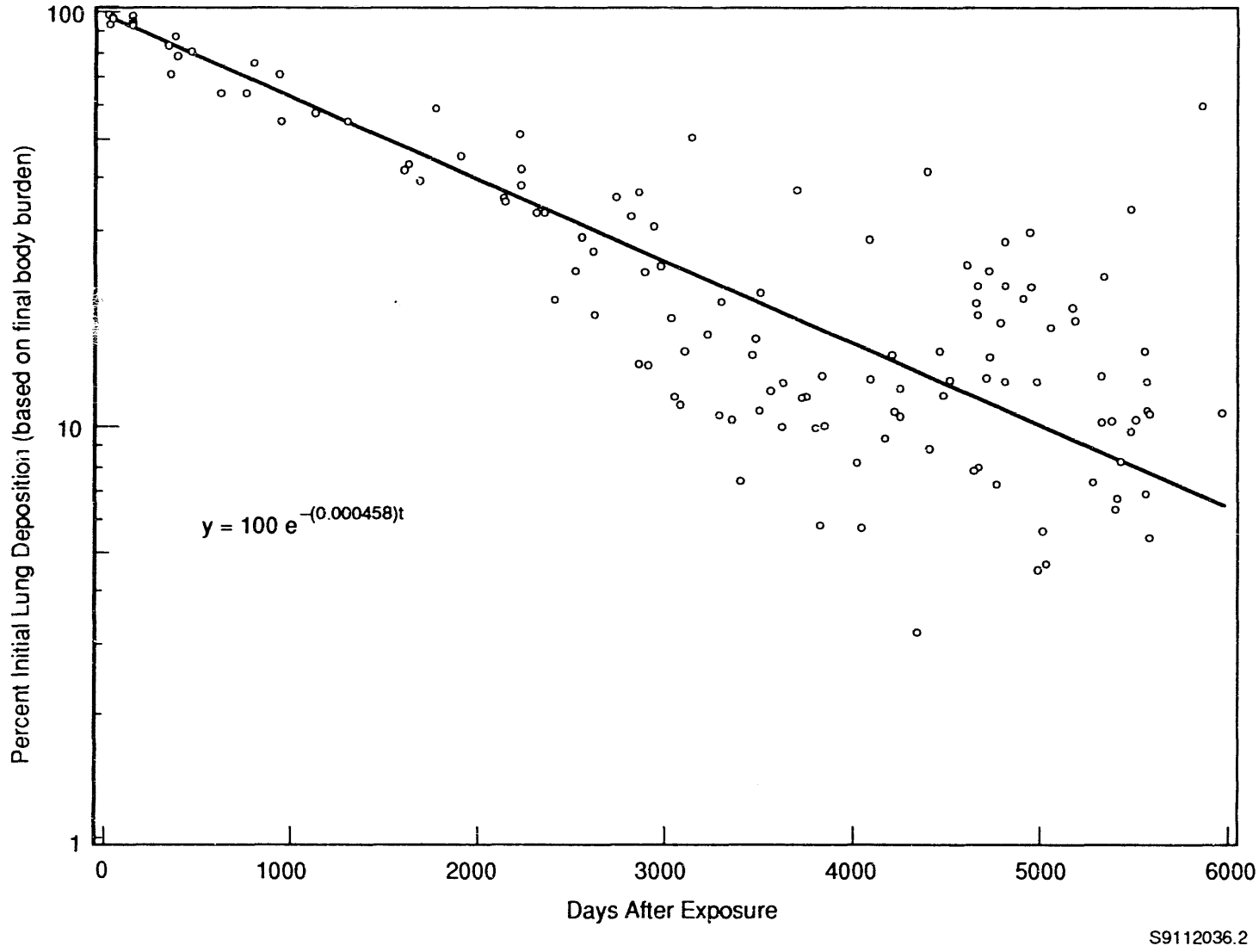

FIGURE 2. Lung Retention of Inhaled $^{239}PuO_2$ Determined by [(final lung burden of pl... m)/(initial lung deposition based on final body burden of plutonium)] x 100. Points represent data from individual dogs.

lung retention half-time for this method was not statistically different from the half-time obtained by method 1 (1102 ± 80 days, 95% confidence interval). Table 6 compares the mean and 95% confidence internal around the mean plutonium lung retention half-times for the six dose-range groups. Retention half-times were significantly different ($p < 0.05$) between dose-range groups at 100-300 rads and at 1000-3000 rads.

TABLE 6. Comparison of ^{239}Pu Lung Retention Half-Times Based on Initial Lung Deposition Estimated from External Thorax Counting for Individual Dogs

Dose Range, rads	Number of Dogs[a]	Lung Retention Half-Times, days[b]
Method 3:		
0 - 30	19	1133 ± 171
30 - 100	12	1247 ± 438
100 - 300	20	1533 ± 257[c]
399 - 1000	22	1250 ± 113
1000 - 3000	23	1012 ± 80[c]
3000 - 8500	13	1175 ± 321
0 - 8500	109	1086 ± 74
Method 1:		
0 - 8500	109	1102 ± 80

(a) Seven of the 0- to 100-rad dose-range dogs did not have initial lung deposition of plutonium based on external thorax counting.
(b) Mean ± 95% confidence interval around the mean.
(c) Underlined values are statistically different ($p < 0.05$) from each other (Tukey's studentized range test).

Method 4: Individual Final Body Burden (IFBB)

The fourth method was identical to method 2 (L = FBB, X based on FLB/FBB) except that we calculated radiation dose to the lungs using an individual exponential function for each dog. The lung retention half-times ranged from 730 to 7344 days with a mean of 1453 days (1453 ± 79 days, 95% confidence interval). The mean lung retention half-time for this method was not significantly different from the half-time obtained by method 2 (1513 ± 92 days, 95% confidence interval). Table 7 compares the mean plutonium lung retention half-times for the six dose-range groups. Retention half-times were significantly different ($p < 0.05$) between groups at 30 to 100 rads and at 1000 to 3000 rads.

TABLE 7. Comparison of ^{239}Pu Lung Retention Half-Times Based on Initial Lung Deposition Estimated from Final Body Burdens for Individual Dogs

Dose Range, rads	Number of Dogs	Lung Retention Half-Times, days[a]
Method 4:		
0 - 30	32	1571 ± 197
30 - 100	10	2073 ± 428[b]
100 - 300	18	2069 ± 685
300 - 1000	27	1440 ± 192
1000 - 3000	16	1381 ±158[b]
3000 - 8500	13	1480 ± 269
0 - 8500	116	1453 ± 79
Method 2:		
0 - 8500	116	1513 ± 92

(a) Mean ± 95% confidence interval around the mean.
(b) Underlined values are statistically different ($p < 0.05$) from each other (Tukey's studentized range test).

The mean and 95% confidence interval around the mean cumulative average radiation dose to the lungs at death for the six dose-range groups, calculated by the four methods, are shown in Table 8. The mean lung dose in Table 8 for each dose-range group was compared for each method of calculating doses using the Tukey's studentized range test. There were no significant differences ($p < 0.05$) among the methods. However, the number of dogs in each dose-range group and the individual dogs in each dose-range group varied depending on the method of calculating radiation dose to the lungs, and the dogs with lung tumors also varied among dose-range groups. Table 9 shows that the fraction of dogs with lung tumors for the four highest dose-range groups was similar for each method of dose calculation.

The large range of lung retention half-times observed for individual dogs, regardless of whether initial lung deposition was based on thorax counting at 2 and 4 weeks after exposure

TABLE 8. Comparison of ^{239}Pu Calculated Accumulative Average Radiation Dose to Lungs by Four Methods[a]

Dose Range, rads	Estimated Radiation Dose to the Lungs, rads[b]							
	IDCT[c]		FBB[d]		IILDCT[e]		IFBB[f]	
	Number of Dogs	Rads	Number of Dogs	Rads	Number of Dogs	Rads	Number of Dogs	Rads
0 - 30	27	13.6 ± 4.3	32	9.7 ± 2.4	26	12.7 ± 4.3	32	9.4 ± 2.2
30 - 100	14	68 ± 13	11	51 ± 12	12	59 ± 15	10	59 ± 13
100 - 300	18	180 ± 27	18	175 ± 27	20	195 ± 25	18	182 ± 24
300 - 1000	21	601 ± 90	19	578 ± 111	22	627 ± 80	27	629 ± 95
1000 - 3000	20	1856 ± 275	23	1580 ± 196	23	1880 ± 269	16	1663 ± 208
3000 - 8500	16	4773 ± 1044	13	4464 ± 769	13	4925 ± 893	13	4398 ± 735

(a) Comparison of mean doses among the four methods for each dose-range group were not significantly different ($p < 0.05$) from each other (Tukey's studentized range test).
(b) Mean ± 95% confidence interval around the mean.
(c) Calculated using the initial lung deposition based on the mean of individual external thorax counts at 2 and 4 weeks after exposure and a fitted plutonium lung retention function for all dogs.
(d) Calculated assuming initial lung deposition was equal to the final body burden of plutonium and using a fitted plutonium lung retention function for all dogs.
(e) Calculated using initial lung deposition based on the mean of individual external thorax counts at 2 and 4 weeks after exposure, the individual final lung burden of plutonium, and an individual lung retention function for each dog.
(f) Calculated using initial lung deposition equal to the final body burden of plutonium, the individual final lung burden of plutonium, and an individual lung retention function for each dog.

TABLE 9. Fraction of $^{239}PuO_2$-Exposed Dogs with Lung Tumors for Four Methods of Calculating Radiation Dose to the Lungs

Dose Range, rads	Number of Dogs with Lung Tumors / Number of Dogs (%)			
	ILDCT[a]	FEB[b]	IILDCT[c]	IFBB[d]
0 - 30	1/27 (4)	1/32 (3)	1/26 (4)	1/32 (3)
30 - 100	2/14 (14)	3/11 (27)	0/12 (0)	2/10 (20)
100 - 300	8/18 (44)	9/18 (50)	9/20 (45)	8/18 (44)
300 - 1000	13/21 (62)	12/19 (63)	14/22 (64)	19/27 (70)
1000 - 3000	18/20 (90)	20/23 (87)	21/23 (91)	15/16 (94)
3000 - 8500	9/16 (56)	6/13 (46)	6/13 (46)	6/13 (46)

(a) Radiation dose to the lungs calculated using the initial lung deposition based on the mean of individual external thorax counts at 2 and 4 weeks after exposure and a fitted plutonium lung retention function for all dogs
(b) Radiation dose to the lungs calculated assuming initial lung deposition was equal to the final body burden of plutonium and using a fitted plutonium lung retention function for all dogs.
(c) Radiation dose to the lungs calculated using initial lung deposition based on the mean of individual external thorax counts at 2 and 4 weeks after exposure, the individual final lung burden of plutonium, and an individual lung retention function for each dog.
(d) Radiation dose to the lungs calculated using initial lung deposition equal to the final body burden of plutonium, the individual final lung burden of plutonium, and an individual lung retention function for each dog.

or on final body burden, suggests that estimates of radiation dose to the lungs using individual plutonium lung retention functions for each dog would more accurately estimate the radiation dose to the lungs for individual dogs than using the same retention function for all dogs. Mean lung doses calculated using individual lung retention functions for each dog based on initial lung deposition determined from final body burden ("IFBB," Table 8) ranged from 88% to 100% of doses estimated using individual lung retention functions for each dog based on initial lung deposition determined from external thorax counting ("IILDCT," Table 8) for all dose-range groups except the 0- to 30-rad group, which was 75%. None of the dose-range groups was statistically different. Radiation dose estimates to the lungs using final body burden as initial lung deposition do not include dose from plutonium that was deposited in the lungs and then excreted. Therefore, these estimate the minimum dose to the lungs for individual dogs. Because of uncertainties related to external thorax counting for initial lung deposition in low-dose-level dogs, lung doses based on using final body burden for initial lung deposition may more accurately estimate radiation dose to the lungs for individual dogs in the 0- to 30-rad dose-range group.

Inhaled Plutonium Nitrate in Dogs

Principal Investigator: *G. E. Dagle*

Other Investigators: *R. R. Adee, R. L. Buschbom, K. M. Gideon, E. S. Gilbert, G. J. Powers, H. A. Ragan, C. O. Romsos, C. R. Watson, R. E. Weller, and E. L. Wierman*

Technical Assistance: *J. P. Bramson, B. M. Colley, K. H. Debban, R. F. Flores, B. B. Kimsey, B. G. Moore, C. R. Petty, D. L. Redetzke, R. P. Schumacher, and M. J. Steele*

The major objective of this project is to determine dose-effect relationships of inhaled plutonium nitrate in dogs to aid in predicting health effects of accidental exposure in man. For life-span dose-effect studies, beagle dogs were given a single inhalation exposure to $^{239}Pu(NO_3)_4$ in 1976 and 1977. The skeleton is generally considered the critical tissue with inhaled soluble plutonium that translocates to bone surfaces. Thus far, 14 years after exposure, 28 of 96 exposed dogs had bone tumors, 32 had lung tumors, and 9 had intrahepatic bile duct tumors.

The skeleton is generally considered the critical tissue after inhalation of "soluble" plutonium (e.g., plutonium nitrate), on the assumption that the plutonium will be rapidly translocated from the respiratory system to the skeleton. In several rodent studies, however, inhalation of "soluble" plutonium has resulted primarily in lung tumors. Skeletal tumors were seen less often, perhaps because they were not expressed within the short life span of the rodents. Therefore, beagle dogs were chosen for this study to compare relative risks with those from intravenously injected radionuclides in beagles at the University of Utah, inhalation studies with beta-, gamma-, and alpha-emitting radionuclides at the Inhalation Toxicology Research Institute (Lovelace), and external irradiation at the University of California (Davis) and at Argonne National Laboratory. More specifically, this study can be compared with inhaled $^{239}PuO_2$ and $^{238}PuO_2$ studies in beagle dogs at PNL (see *Inhaled Plutonium Oxide in Dogs*, this volume).

Six dose groups (105 dogs) were exposed, in 1976 and 1977, to aerosols of $^{239}Pu(NO_3)_4$ for life-span observations (Table 1). In addition, 20 dogs were exposed to nitric acid aerosols as vehicle controls; 25 dogs were exposed to aerosols of $^{239}Pu(NO_3)_4$ for periodic sacrifice to obtain plutonium distribution and pathogenesis data in developing lesions; 7 dogs were selected as controls for periodic sacrifice; and 20 dogs were selected as untreated controls for life-span observations. The Appendix (at the end of this volume of the *Annual Report*) shows the current status of each dog on these experiments.

TABLE 1. Life-Span Dose-Effect Studies with Inhaled $^{239}Pu(NO_3)_4$ in Beagles[a]

Dose-Level Group	Number of Dogs		Initial Lung Deposition[b]	
	Male	Female	nCi[c]	nCi/g Lung[c]
Control	10	10	0	0
Vehicle	10	10	0	0
1	10	10	2±2	0.02±0.02
2	10	10	8±4	0.06±0.04
3	10	10	56±17	0.5±0.2
4	10	10	295±67	2±0.8
5	10	10	1709±639	14±6
6	3	2	5445±1841	47±17

(a) Exposed in 1976 and 1977.
(b) Estimated from external thoracic counts at 2 weeks post exposure and estimated lung weights (0.011 x body weight).
(c) Mean ± standard deviation.

The average amount of plutonium in the lungs decreased to approximately 1% of the final body burden in dogs surviving 5 years or more (Table 2). More than 90% of the burden translocated to the liver and skeleton; only about 1% translocated to thoracic and abdominal lymph nodes. This was in contrast to dogs that inhaled $^{239}PuO_2$; in these dogs, ~50% of the final body burden was present in thoracic lymph nodes, but only about 2% in the skeleton at 10 to 11 years after exposure.

The earliest observed biological effect was on the hematopoietic system: lymphopenia occurred at the two highest dose levels at 4 weeks after exposure to $^{239}Pu(NO_3)_4$. Total leukocyte concentrations were reduced significantly in the two highest dose groups, that is, Group 5 (mean initial lung deposition, ~1700 nCi) and Group 6 (~5500 nCi).

The reduction in white cells in Groups 5 and 6 resulted from an effect on most leukocyte types (neutrophils, lymphocytes, monocytes, and eosinophils). This is in contrast to the effects of both $^{239}PuO_2$ and $^{238}PuO_2$, which significantly depressed lymphocyte concentrations in groups with initial lung burdens of approximately 80 nCi or more. The lymphopenia at lower dose levels of plutonium oxides may be related to the more extensive translocation of plutonium oxide to the tracheobronchial lymph nodes and subsequent higher dosage levels to lymphocytes circulating through those lymph nodes. The results of these continuing evaluations are shown in Figure 1.

Serum enzyme assays have been performed throughout the postexposure period in an attempt to identify specific damage to liver or bone by plutonium translocated from the lung. Evaluation of these data has revealed a biphasic elevation of serum alkaline phosphatase (ALP) and serum glutamic pyruvic transaminase (GPT) in individual dogs. There was an early increase followed by a return to control values and then a late effect characterized by persistent, increased elevations of both ALP and GPT. Calculation of the cumulative average radiation dose to mean time after exposure, when serum chemistry values were first observed to be different from controls for dose-level Group 5 dogs, revealed a mean dose to liver of 280 rads for the late effect, which occurred 4.1 years post exposure. At this time, the dose rate was 60 to 70 rads per year. GPT and ALP values in dose-level Groups 3 and 4 were significantly higher ($p \leq 0.05$) than those for the control group (Figures 2 and 3).

Table 3 summarizes, by dose-level group, the mortality and lesions associated with deaths through 14 years after exposure to $^{239}Pu(NO_3)_4$. All five dogs at the highest dose level (Group 6) died from radiation pneumonitis 14 to 41 months after exposure. Histopathological examination of the lungs of these dogs revealed interstitial fibrosis, alveolar epithelial hyperplasia, increased numbers of alveolar macrophages, occasional small emphysematous cavities and, at times, very small nodules of squamous metaplasia at the termini of respiratory bronchioles. One dog at the highest dose level had a small bronchioloalveolar carcinoma as well as radiation pneumonitis.

All the dogs in dose-level Group 5 died or were euthanized 34 to 92 months after plutonium exposures. The principal cause of death at this exposure level was osteosarcoma, which occurred in 17 of 20 dogs. Other deaths in dose-level Group 5 were caused by radiation pneumonitis (2 dogs) and multiple lung tumors (1 dog). The multiple lung tumors, in different lobes, were papillary adenocarcinomas, combined epidermoid and adenocarcinoma, and bronchioloalveolar carcinoma; metastases were present in the tracheobronchial lymph nodes.

Malignant but nonfatal lung tumors were also present in nine dogs from dose-level Group 5 that died from osteosarcomas and in one dog that died from radiation pneumonitis. Typically, these arose subpleurally, proximal to areas of interstitial fibrosis or small cavities communicating with bronchioles. They consisted of bronchioloalveolar carcinomas in four dogs; papillary adenocarcinomas in two dogs; both bronchioloalveolar carcinoma and papillary adenocarcinoma in one dog; both papillary and tubular adenocarcinomas in one dog; a combined epidermoid and adenocarcinoma in one dog; and a bronchioloalveolar carcinoma, a papillary adenocarcinoma, and a mixed lung tumor in one dog. No metastases of these lung tumors were observed.

TABLE 2. Tissue Distribution of Plutonium in Beagles After Inhalation of $^{239}Pu(NO_3)_4$

Dog Number	Time After Exposure, months[a]	Final Body Burden, μCi	Percent of Final Body Burden					Cause of Death
			Lungs	Thoracic Lymph Nodes[b]	Abdominal Lymph Nodes[c]	Liver	Skeleton	
1359M	0.1	0.080	90.50	0.15	0.06	2.46	3.20	Sacrifice
1375F	0.1	0.073	89.61	0.14	0.01	0.97	4.68	Sacrifice
1407F	0.1	0.092	51.87	0.41	0.13	10.99	18.70	Sacrifice
1389M	0.5	0.053	24.07	0.38	0.08	41.28	26.21	Sacrifice
1390M	0.5	0.051	24.62	0.32	0.11	20.05	44.45	Sacrifice
1445F	0.5	0.057	26.42	0.32	0.11	21.28	44.73	Sacrifice
1329F	1	0.485	70.05	0.16	0.04	8.28	18.79	Sacrifice
1346M	1	0.902	76.81	0.32	0.03	10.45	10.30	Sacrifice
1347F	1	0.699	71.71	0.36	0.08	9.33	14.09	Sacrifice
1336M	1	0.032	71.38	0.22	0.05	5.72	19.73	Sacrifice
1341F	1	0.022	64.43	0.29	0.10	12.92	18.63	Sacrifice
1344F	1	0.052	58.68	0.25	0.04	21.87	16.09	Sacrifice
1335M	1	0.003	19.52	0.07	0.06	6.68	25.04	Sacrifice
1339F	1	0.001	19.08	0.13	0.08	20.92	45.47	Sacrifice
1351M	1	0.002	40.68	1.22	0.09	17.09	28.89	Sacrifice
1522F	3	0.059	54.68	0.57	0.10	11.52	28.24	Sacrifice
1529F	3	0.049	51.68	0.40	0.07	18.48	23.74	Sacrifice
1539M	3	0.072	52.45	0.31	0.05	18.58	25.03	Sacrifice
1564F	12	0.037	18.00	1.27	0.11	33.53	42.63	Sacrifice
1571F	12	0.053	22.37	1.47	0.11	28.76	42.91	Sacrifice
1588M	12	0.053	13.14	0.40	0.12	35.85	46.18	Sacrifice
1424M	14	4.625	33.10	1.43	0.16	26.49	36.88	Radiation pneumonitis
1517F	16	4.025	18.99	0.94	0.18	29.51	47.88	Radiation pneumonitis
1510F	17	4.048	22.00	1.15	0.05	20.71	52.00	Radiation pneumonitis
1420M	25	1.616	16.51	0.86	0.20	7.77	70.06	Radiation pneumonitis
1471M	34	1.375	9.25	0.73	0.12	26.92	58.34	Radiation pneumonitis
1518M	42	1.880	6.87	0.24	0.07	21.31	67.51	Radiation pneumonitis, lung tumor
1512M	42	2.136	4.31	0.60	0.08	49.93	42.66	Bone tumor
1508M	43	1.730	3.24	0.62	0.08	41.53	52.70	Bone tumor
1459F	51	1.567	4.40	0.15	0.12	30.86	61.41	Radiation pneumonitis, lung tumor
1492F	52	1.202	2.81	0.20	0.17	27.02	66.38	Bone tumor
1485F	54	1.052	0.82	0.35	0.07	31.13	63.94	Bone tumor
1502F	55	3.113	0.80	0.39	0.09	33.33	62.51	Bone tumor, lung tumor
1387F	55	0.167	1.41	0.22	0.12	45.48	49.10	Bone tumor
1429M	59	1.159	4.14	0.35	0.10	37.06	54.70	Bone tumor, lung tumor
1598F	60	0.058	0.90	0.14	0.17	24.44	31.62	Sacrifice
1576M	60	0.065	1.54	0.36	0.13	46.23	39.15	Sacrifice
1605F	60	0.025	1.87	0.11	0.12	52.32	39.37	Sacrifice
1646F	60	0.806	0.72	0.20	0.40	46.92	48.42	Bone tumor
1619F	62	1.361	0.55	0.59	0.13	37.87	58.63	Bone tumor
1589F	63	0.029	0.68	0.04	0.13	46.43	50.32	Sacrifice
1636M	66	0.634	1.21	0.27	0.52	53.97	39.09	Bone tumor
1652F	68	0.658	1.46	0.23	0.29	50.47	44.32	Bone tumor, lung tumor
1498F	69	0.845	0.59	0.32	0.13	26.63	53.37	Bone tumor, lung tumor
1659F	69	0.736	1.14	0.34	0.40	38.90	55.89	Bone tumor
1640M	76	0.177	4.01	0.64	0.63	54.41	36.59	Lung tumor
1419M	76	0.873	0.69	0.28	0.39	44.06	50.70	Bone tumor, lung tumor
1660M	82	0.854	0.76	0.53	0.53	37.51	56.17	Bone tumor, lung tumor
1621M	84	0.840	0.94	0.56	0.29	40.87	54.55	Bone tumor, lung tumor
1655M	88	0.505	1.05	0.22	0.93	41.83	52.14	Lung tumor, Bone tumor
1501M	92	0.002	1.62	0.50	0.79	38.05	48.41	Thyroid tumor
1648M	92	0.639	1.12	0.25	0.73	42.83	50.61	Bone tumor, lung tumor
1641M	92	0.869	0.78	0.24	0.48	45.72	48.89	Lung tumor

TABLE 2. Continued

Dog Number	Time After Exposure, months[a]	Final Body Burden, μCi	Percent of Final Body Burden					Cause of Death
			Lungs	Thoracic Lymph Nodes[b]	Abdominal Lymph Nodes[c]	Liver	Skeleton	
1408F	93	0.181	0.60	0.19	0.37	49.47	45.52	Bone tumor
1404M	93	0.217	0.82	0.28	0.72	46.24	48.62	Pleuritis
1470F	95	0.001	1.11	0.48	0.34	43.21	50.23	Meningioma
1489F	98	0.002	1.23	0.73	0.70	41.36	48.52	Esophageal tumor
1565F	101	0.001	0.77	1.55	0.87	43.62	44.09	Hemangiosarcoma
1385M	101	0.362	0.62	0.51	0.42	46.38	49.36	Bone tumor, lung tumor
1364M	102	0.370	1.13	0.32	0.40	49.46	46.17	Lung tumor
1503F	103	0.007	0.37	0.64	0.25	60.15	35.37	Thyroid tumor
1645F	105	0.182	0.73	0.41	0.46	55.96	40.70	Lung tumor
1587M	106	0.027	0.65	0.74	0.51	20.11	74.97	Hemangiosarcoma, lung tumor
1534M	106	0.201	0.96	0.43	0.49	50.78	43.95	Congestive heart failure
1521F	106	0.146	0.88	0.34	0.36	51.77	44.41	Bone tumor, lung tumor
1599F	106	0.007	0.69	0.54	0.48	34.04	60.60	Adrenal tumor
1413F	109	0.026	1.16	0.39	0.51	58.06	37.78	Malignant lymphoma
1391M	111	0.004	1.21	0.34	0.47	50.40	45.49	Thyroid tumor, lung tumor
1581M	111	0.002	0.52	0.95	0.31	38.21	56.46	Hemangiosarcoma
1602M	111	0.006	1.95	1.29	0.97	42.80	46.45	Epilepsy
1428F	114	0.230	0.72	0.62	0.56	35.16	60.14	Bone tumor, lung tumor
1386M	116	0.028	1.59	0.26	0.82	56.40	38.62	Hemangiosarcoma
1568M	116	0.034	0.93	0.50	0.54	42.27	52.10	Pneumonia
1590F	119	0.003	0.48	0.35	1.00	59.61	31.23	Mammary tumor
1530F	122	0.017	0.89	0.77	0.84	42.50	50.30	Bone tumor, lung tumor
1570F	122	0.001	0.34	0.91	0.42	30.80	63.13	Stomach tumor
1535F	122	0.145	0.62	0.67	0.74	19.27	73.73	Bone tumor, lung tumor
1446F	123	0.165	0.40	0.56	0.63	27.06	67.94	Pyometra, liver tumor
1540M	124	0.037	0.61	0.45	0.38	39.21	55.37	Lung tumor
1414F	126	0.121	1.29	0.42	0.54	44.44	49.50	Bone, lung, and liver tumors
1569F	126	0.031	0.53	0.42	0.31	50.23	45.17	Lung tumor
1575M	128	0.004	0.43	0.54	0.51	55.53	37.17	Prostate tumor
1456F	132	0.041	0.33	0.60	0.49	41.34	52.74	Pneumonia
1637M	132	0.105	1.22	0.64	0.31	45.50	49.64	Lung tumor
1607M	135	0.001	0.53	1.80	0.44	37.49	55.95	Liver tumor
1363M	135	0.046	0.51	0.69	0.44	55.62	40.23	Pneumonia, adrenal/liver tumor
1582F	136	0.034	0.64	0.69	4.82	31.22	57.87	Mammary tumor, liver tumor
1380M	136	0.041	0.57	0.70	0.82	34.11	58.90	Pneumonia
1618F	140	0.134	0.38	0.23	1.05	38.34	56.67	Bone tumor
1439F	143	0.033	0.41	0.69	0.75	25.65	68.09	Malignant lymphoma
1379M	144	0.202	0.56	0.72	0.85	25.30	67.38	Liver, lung, and bone tumors
1507M	144	0.002	1.69	0.38	0.58	51.27	38.98	Malignant melanoma
1639F	145	0.094	0.84	0.70	0.73	35.42	57.73	Radiation pneumonitis, lung tumor
1647M	146	0.155	0.78	0.46	0.17	45.84	51.38	Lung tumor, liver tumor
1591M	147	0.007	0.68	0.56	0.70	31.49	59.61	Malignant lymphoma
1585F	148	0.005	1.03	0.80	0.85	28.77	60.90	Thyroid tumor
1490F	149	0.013	0.45	0.42	0.34	46.01	49.06	Mammary tumor
1583F	149	0.001	1.20	3.65	1.33	29.96	57.51	Thyroid tumor
1592F	150	0.001	0.63	0.47	0.48	44.39	50.24	Pneumonia
1595M	154	0.030	0.61	0.68	0.53	43.98	50.01	Nephropathy
1362M	155	0.167	0.45	0.44	0.61	36.97	58.06	Bone, liver, and lung tumor
1465F	156	0.001	1.71	0.37	1.31	45.84	44.12	Nephropathy
1604M	156	0.032	0.91	0.72	0.58	21.71	70.83	Encephalopathy

(a) Radioanalysis not completed in dogs that died more than 156 months after exposure.
(b) Includes tracheobronchial, mediastinal, and sternal lymph nodes.
(c) Includes hepatic, splenic, and mesenteric lymph nodes.

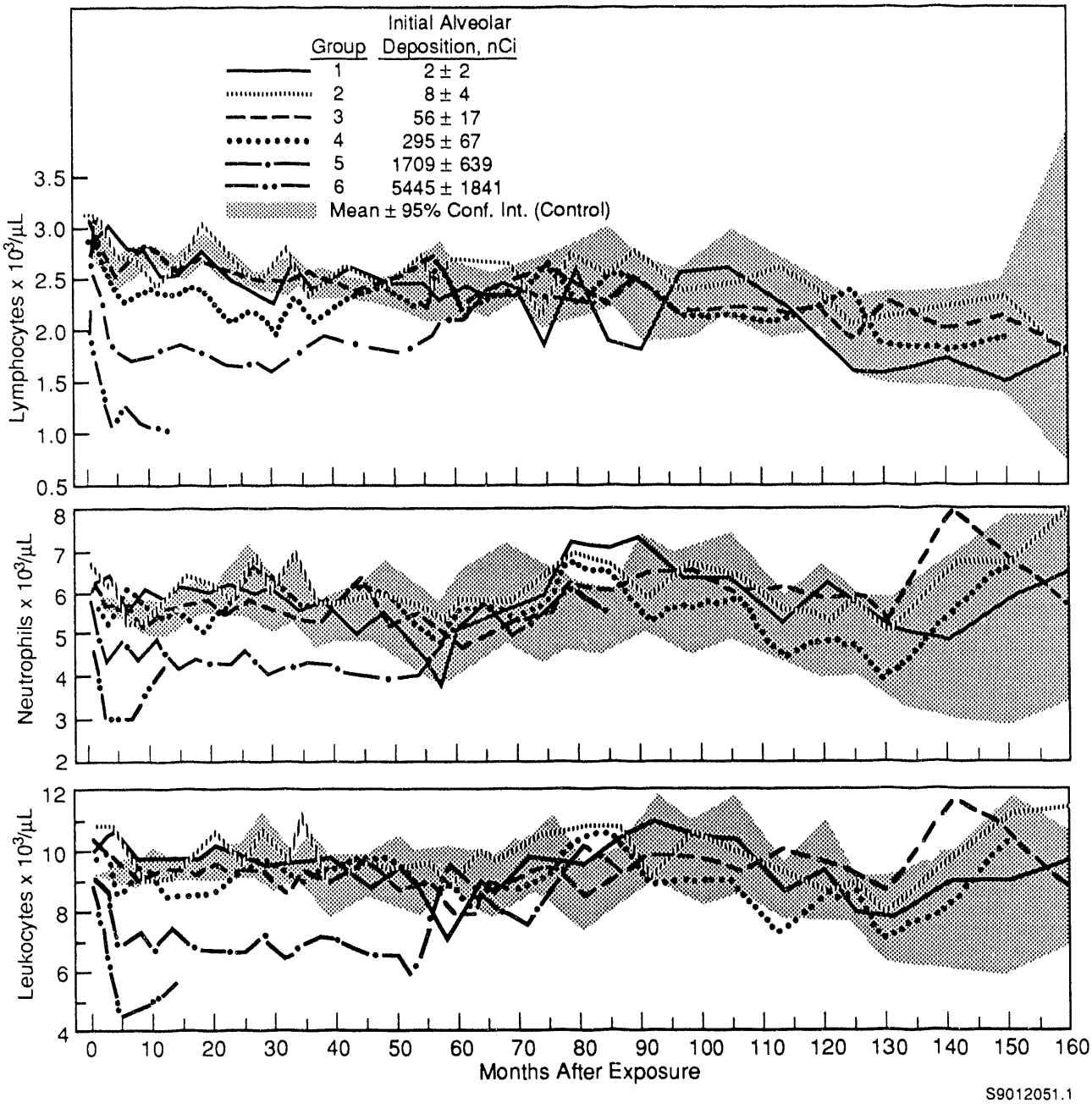

FIGURE 1. Mean Leukocyte, Neutrophil, and Lymphocyte Values in Dogs After Inhalation of $^{239}Pu(NO_3)_4$.

In dose-level Group 4, all the dogs died or were euthanized 54 to 157 months after plutonium exposure. The causes of death, probably related to plutonium exposure, included bone tumors (9 dogs), lung tumors (5 dogs), a delayed-onset radiation pneumonitis (1 dog), and a bile duct carcinoma (1 dog). Intrahepatic bile duct tumors were present in the livers of 4 additional dogs that died of other causes. Nonfatal lung tumors were present in 9 dogs that died of other causes.

In dose-level Group 3, 18 dogs have now died up to 14 years after exposure. Three dogs have died of lung tumors, and lung tumors were present in

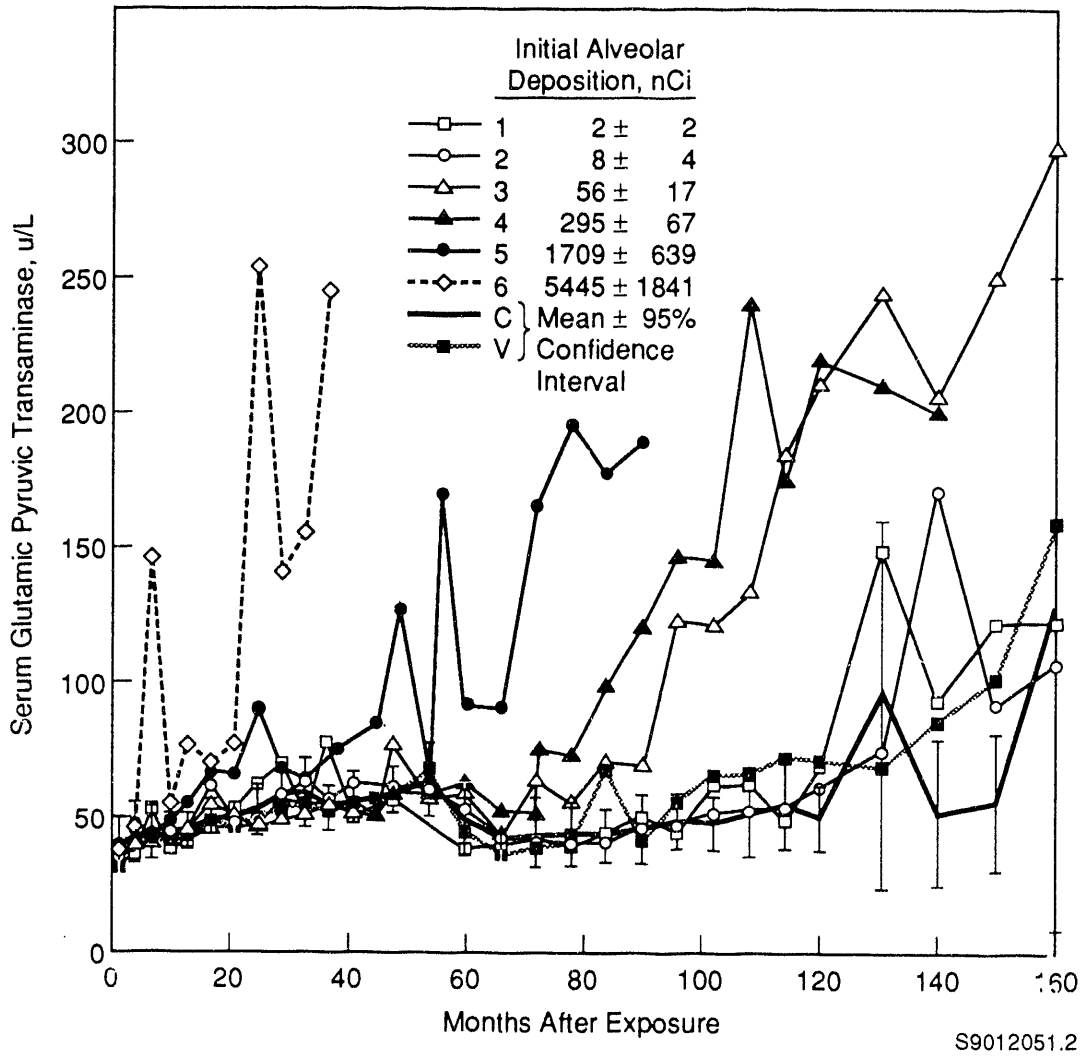

FIGURE 2. Serum Glutamic Pyruvic Transaminase (GPT) in Dogs After Inhalation of $^{239}Pu(NO_3)_4$.

each of 3 additional dogs that died of a bone tumor, a thyroid tumor, and a hemangiosarcoma. Two dogs had bile duct tumors.

In the lower dose levels (Groups 1 and 2), the incidence of lesions to 14 years after exposure was not significantly different from that of the control groups. Of uncertain relationship to plutonium exposure, however, were bile duct carcinomas in 2 dogs from dose-level Group 2 and fatal hepatocellular carcinomas in 1 dog each from dose-level Group 2 and dose-level Group 1. Bile duct tumors have not yet been observed in any control dogs, but we have observed a nonfatal hepatocellular carcinoma in a control dog.

Although the skeleton is generally considered the critical tissue after inhalation of soluble plutonium, and 28 of 96 exposed dogs had died with bone tumors by 14 years after exposure, it should be noted that 32 of these 96 exposed dogs also had lung tumors. We have calculated that lung cancer risks for these dogs, based on estimated cumulative dose to the lung, are approximately 12 times higher for $^{239}Pu(NO_3)_4$ than for inhaled $^{239}PuO_2$ and 50 times higher than for inhaled $^{238}PuO_2$.

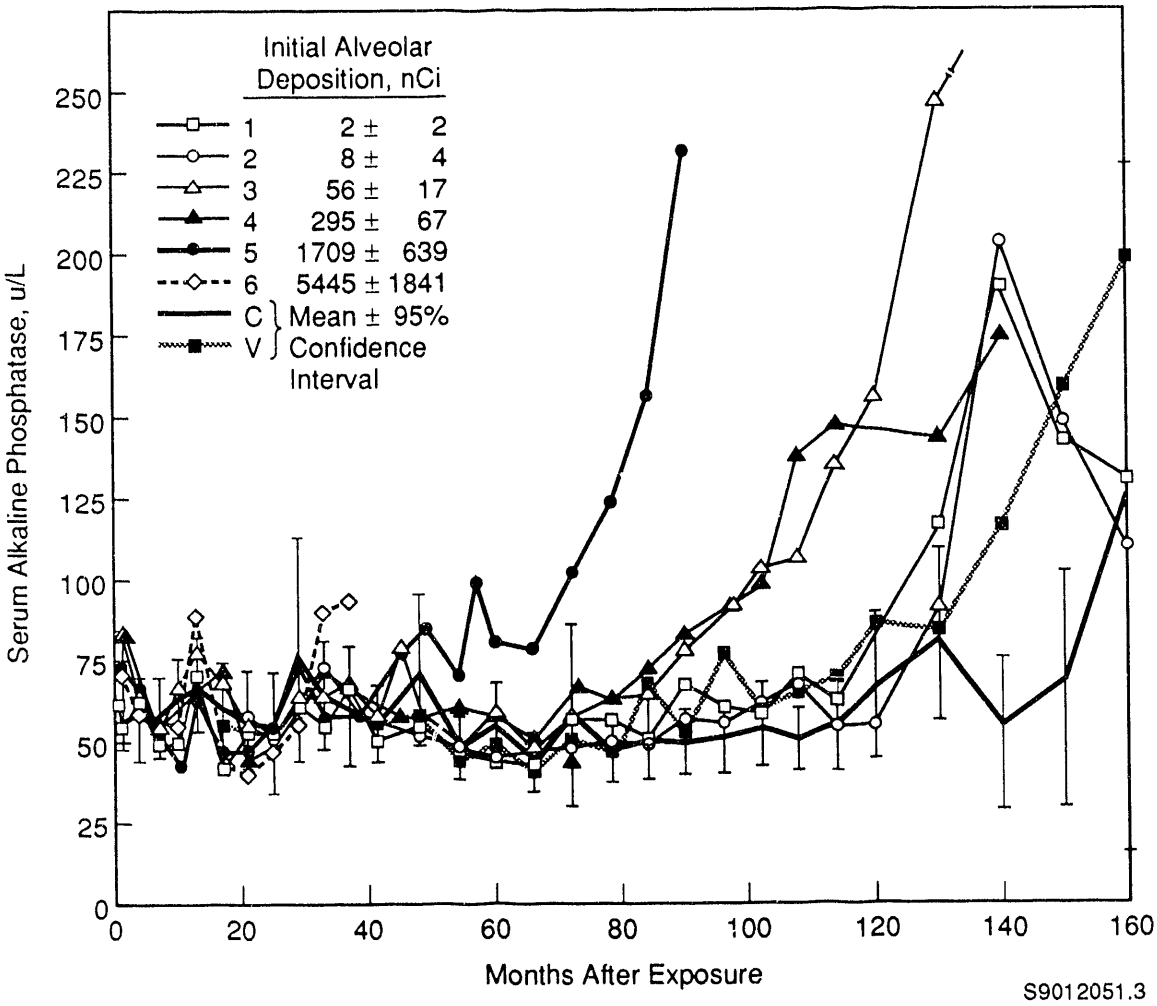

FIGURE 3. Serum Alkaline Phosphatase (ALP) in dogs After Inhalation of $^{239}Pu(NO_3)_4$.

The bone tumor incidence, relative to total skeletal dose in the dose levels having bone tumors, is given in Table 4. The sites of the bone tumors were lumbar vertebrae (6 dogs), humerus (6 dogs), cervical vertebrae (4 dogs), pelvis (4 dogs), thoracic vertebrae (3 dogs), sacrum (3 dogs), ribs (3 dogs), facial bones (2 dogs), femur (2 dogs), radius (1 dog), scapula (1 dog), and nasal turbinates (1 dog); several dogs had tumors at more than one site, and metastases were frequent. Further, intrahepatic bile duct tumors have now occurred in 9 of the 96 exposed dogs.

TABLE 3. Lesions in Beagle Dogs 14 Years After Inhalation of $^{239}Pu(NO_3)_4$

	Dose Group							
	6	5	4	3	2	1	Vehicle	Control
Number of Dogs/Group	5	20	20	20	20	20	20	20
Number of Dead Dogs/Group	5	20	20	18	17	16	17	16
Condition[(a)]								
Radiation pneumonitis	4	1						
Radiation pneumonitis and lung tumor	1	1	1					
Bone tumor		8	3					
Bone and lung tumor		9	4	1				
Bone, lung, and liver tumor			2					
Lung tumor		1	4	3				
Liver, lung, and bone tumor			1					
Lung and liver tumor			1					
Hemangiosarcoma and lung tumor				1				
Thyroid and lung tumor				1				
Pneumonia and lung tumor			1					
Pyometra and liver tumor			1					
Pneumonia and liver tumor				1				1
Mammary and liver tumor				1				
Nephropathy liver tumor					1			
Liver tumor					2	1		
Pneumonia or pleuritis			1	3		1		3
Lymphoma				2	2		4	
Thyroid tumor					2	2		2
Meningeal tumor						1		
Status epilepticus/encephalopathy				1	1			1
Congestive heart failure			1			1	1	
Hemangiosarcoma				1	1	2		
Adrenal tumor					1	1		1
Esophageal/stomach tumor						2		
Intervertebral disc protrusion							2	2
Mammary tumor					2		3	
Cerebral hemorrhage								1
Prostate tumor					1			1
Urinary bladder tumor				1	1			
Pyometra								1
Mastocytoma							1	
Splenic tumor								1
Endocarditis								1
Nephropathy				1	1	3	3	
Malignant melanoma (oral)				1		1	1	
Nephritis					1			
Panophthalmitis					1			
Gastric dilatation						1		
Skin tumor (lung metastasis)							1	
Hypothyroidism							1	
Pituitary tumor								1

(a) Number of dogs with lesions associated with death.

TABLE 4. Bone Tumor Incidence in Beagle Dogs 14 Years After Inhalation of $^{239}Pu(NO_3)_4$

Dose-Level Group	Number of Dogs	Mean Survival, years	Skeletal Dose, cGy[(a)]	Bone Tumor Incidence
Control	20	11.8	--	0
Vehicle	20	12.6	--	0
1	20	11.9	--	0
2	20	12.4	--	0
3	20	11.5	17 ± 6	7%
4	20	9.8	99 ± 68	53%
5	20	5.4	192 ± 64	85%
6	5	1.9	72 ± 70	0

(a) Skeletal dose 1 year before death. Inadequate numbers of dogs were analyzed for dose levels 1 and 2, and not all the dogs have been analyzed in dose levels 3 and 4.

National Radiobiology Archives

Principal Investigator: *C. R. Watson*

Other Investigators: *M. T. Karagianes, E. K. Ligotke, J. C. Prather, L. G. Smith, and S. K. Smith*

The National Radiobiology Archives is a comprehensive effort to gather, organize, and catalog data, tissues, and documents related to radiobiology studies. This will provide future researchers with materials for analysis by advanced molecular biology techniques and with information for statistical analysis to compare results of these and other studies. The project concentrated initially on three tasks associated with studies of beagle dogs exposed to ionizing radiation at five DOE laboratories: (1) implementing an interlaboratory computerized **information system** containing a summarized dose-and-effects database with results for each of more than 5,000 life-span-observation dogs, a collection inventory database, and a bibliographic database; (2) establishing a **document archives** of research materials such as logbooks, clinical notes, radiographic films, and pathologists' observations; and (3) establishing a **specimen archives** for research materials such as biopsy and necropsy tissue samples or histopathology blocks and slides. The databases were designed, and the scope of the information system has been expanded to include about 7,000 beagle and 10,000 mouse records from seven laboratories. An introduction to the system is available on diskette. Tissue specimens and histopathology blocks from more than 1,000 University of California at Davis dogs are organized and available; gerontologists from the University of California visited the tissue archives to harvest brain specimens from selected aged dogs.

Since the initiation of the Manhattan project, many investigations have been conducted into the biological effects of ionizing radiation. The focus of these studies has been on understanding the degree of risk and the nature of human health effects. When the acute effects of relatively large doses had been characterized, attention shifted to the relationship between low doses and cancer. This led to initiation of life-span studies of experimental animals in several DOE-supported laboratories. As these studies are completed, the National Radiobiology Archives (NRA) provides integration and preservation of this unique body of information and materials, and encourages and facilitates its continued use.

Radiobiology Studies

Nearly 40 years ago, the U.S. Atomic Energy Commission made a far-reaching commitment to conduct life-span radiation effect studies in a relatively long-lived animal, the beagle dog, at five laboratories. As a consequence, a group of closely related experiments are now coming to fruition. These studies, conducted at the University of Utah (U of Utah), the University of California at Davis (UC Davis), Argonne National Laboratory (ANL), Pacific Northwest Laboratory (PNL), and the Inhalation Toxicology Research Institute (ITRI) were summarized in 1989 by Roy Thompson in *Life-Span Effects of Ionizing Radiation in the Beagle Dog* and became the initial focus of Archives activities. A similar study in beagle dogs was supported by the Food and Drug Administration at Colorado State University (CSU). Information from CSU about the effect of gamma rays is being included in the Archives.

There have been many life-span studies of rodents, notably those conducted at Oak Ridge National Laboratory (ORNL), ANL, Brookhaven National Laboratory (BNL), and PNL. This year, the Archives accessioned information about 9765 mice of various strains exposed to gamma

rays at ORNL. These experiments are listed in Table 1, showing the NRA study code, the time period over which the exposures were conducted, the nature of the exposures, and the number of animals held for life-span observation.

Three tasks are associated with integrating and preserving information from these studies. The computerized **information system** provides electronic access to summary data on each animal, the document and specimen collection catalogs, and bibliographic citations; the **document archives** houses and preserves nonbiological materials; and the **specimen archives** houses and preserves biological materials. This year, we made significant progress toward implementing the databases and report an interesting use of the specimen archives. Procedures were developed for cataloging the written materials in the document archives. Documents will be shipped to the NRA as studies are completed; this year, the documents were still in active use in the laboratories.

Advisory Committee

The NRA is guided by an advisory committee (NRAAC) consisting of five external advisors:

Stephen A. Benjamin, Colorado State University: Dog Studies
J. A. Louis Dubeau, University of Southern California: Molecular Biology
Nancy Knight, American College of Radiologists: Archivist
Kenneth L. Jackson, University of Washington: Radiobiology
Philip R. Watson, Oregon State University: Databases

and eight participating advisors:

Bruce B. Boecker, Inhalation Toxicology Research Institute
Marvin E. Frazier, U.S. Department of Energy
Thomas E. Fritz, Argonne National Laboratory
Ronald L. Kathren, Washington State University, Tri-Cities
Scott C. Miller, University of Utah
James F. Park, Pacific Northwest Laboratory
Otto G. Raabe, University of California at Davis
Roy C. Thompson, Pacific Northwest Laboratory.

The NRAAC met in March 1991 to review progress and help set priorities. Major recommendations were to expand the archives to include rodent studies and to develop a demonstration diskette for potential users. Future activities of the NRAAC include sponsorship of a workshop on current and future research uses of archived tissue specimens.

Information System

Computer database technology is essential to integrating this broad and diverse collection of information. The NRA is developing several interrelated databases, each of which follows the relational model. There are three major databases: the dose-effects summary, the collection inventory, and the bibliography. These systems were initially developed on two hardware platforms, the DEC VAX configuration at ANL and the IBM PC systems at PNL. We evaluated two database management software products, Oracle on the VAX and PC and Paradox on the PC, and have decided to concentrate on Paradox on the PC.

The computerized summary database contains the dose to and the effect on each significant tissue in each animal. It has six major tables:

LAB	- describing each laboratory
STUDY	- describing each study (as shown in Table 1)
GROUP	- describing groups of animals within each study
ANIMAL	- summarizing each animal
TEFFECT	- effect (and diagnosis dates) observed in each significant tissue category
TDOSE	- dose to each significant tissue category at diagnosis dates in TEFFECT.

The summary database also includes laboratory-specific supporting tables for information such as serial hematological determinations or clinical observations. Progress toward populating the summary database is shown in Table 2.

TABLE 1. Major Life-Span Studies Being Incorporated into the National Radiobiology Archives

NRA Study ID[a]	Date of Exposures	Description of Study	Number of Life-Span Animals
Beagle Dogs:			
A-01	1956	^{90}Sr, Transplacental	53
A-02	1957	^{90}Sr, SC injection (multiple, various ages)	98
A-03	1960-1964	^{144}Ce, IV injection	49
A-04	1961-1963	^{137}Cs, IV injection	65
A-05	1968-1978	Gamma ray, whole body (continuous to death)	311
A-06	1968-1977	Gamma ray, whole body (continuous to predetermined dose)	343
C-03	1967-1973	Gamma ray, whole body, F_3 and F_4 generations	1680
D-01	1952-1958	X ray, whole body (fractionated)	360
D-02	1961-1969	^{90}Sr, ingested (*in utero* to 540 days)	483
D-03	1964-1969	^{90}Sr, IV injection	45
D-04	1964-1969	^{226}Ra, IV injection (multiple)	335
I-01	1965-1967	$^{90}SrCl_2$, Inhalation	63
I-02	1966-1967	$^{144}CeCl_3$, Inhalation	70
I-03	1966-1967	$^{91}YCl_3$, Inhalation	54
I-04	1967-1971	^{144}Ce (FAP)[b], Inhalation	126
I-05	1968-1969	$^{137}CsCl$, IV injection	66
I-06	1969-1971	^{90}Y (FAP), Inhalation	101
I-07	1970-1971	^{91}Y (FAP), Inhalation	108
I-08	1970-1974	^{90}Sr (FAP), Inhalation	124
I-09	1972-1976	^{144}Ce (FAP), Inhalation (juvenile)	54
I-10	1972-1975	^{144}Ce (FAP), Inhalation (aged)	54
I-11	1972-1975	^{144}Ce (FAP), Inhalation (multiple)	36
I-12	1973-1976	$^{238}PuO_2$, Inhalation (3.0 μm)	84
I-13	1974-1976	$^{238}PuO_2$, Inhalation (1.5 μm)	84
I-14	1977-1979	$^{239}PuO_2$, Inhalation (0.75 μm)	60
I-15	1977-1979	$^{239}PuO_2$, Inhalation (1.5 μm)	108
I-16	1977-1979	$^{239}PuO_2$, Inhalation (3.0 μm)	83
I-17	1977-1978	$^{239}PuO_2$, Inhalation (multiple, 0.75 μm)	72
I-18	1979-1983	$^{239}PuO_2$, Inhalation (juvenile, 1.5 μm)	108
I-19	1979-1982	$^{239}PuO_2$, Inhalation (aged, 1.5 μm)	60
P-01	1959-1962	$^{239}PuO_2$, Inhalation	35
P-02	1967	$^{238}PuO_2$, Inhalation	22
P-03	1970-1972	$^{239}PuO_2$, Inhalation	136
P-04	1972-1975	$^{238}PuO_2$, Inhalation	136
P-05	1975-1977	$^{239}Pu(NO_3)_4$, Inhalation	148
U-01	1952-1974	^{239}Pu, IV injection	285
U-02	1953-1970	^{226}Ra, IV injection	164
U-03	1954-1963	^{228}Ra, IV injection	89
U-04	1954-1963	^{228}Th, IV injection	94
U-05	1955-1966	^{90}Sr, IV injection	99
U-06	1966-1975	^{241}Am, IV injection	117
U-07	1971-1974	^{249}Cf, IV injection	36
U-08	1971-1973	^{252}Cf, IV injection	35
U-09	1972-1978	^{239}Pu, IV injection (juvenile)	75
U-10	1973	^{253}Es, IV injection	5
U-11	1975-1978	^{239}Pu, IV injection (aged)	34
U-12	1975-1978	^{226}Ra, IV injection (juvenile)	53
U-13	1975-1980	^{226}Ra, IV injection (aged)	33
U-14	1977-1979	^{224}Ra, IV injection (multiple)	128
Total:	1952-1983		7061
Mice:			
R-01	1977	Gamma ray, single exposure at 10 wk, BALB/c & RFM females	4728
R-02	1987	Gamma ray, single exposure at 10 wk, C3Hf & C57BL/6, both sexes	5037
Total	1977-1987		9765

(a) Laboratory codes: A, ANL; C, Colorado State University; D, University of California at Davis; I, ITRI; P, PNL; R, ORNL; U, University of Utah. Study numbers: arbitrarily assigned by NRA.

(b) FAP: radionuclide was adsorbed to an insolubie fused aluminosilicate vector aerosol.

The collection inventory database contains information about each of the bar code labels affixed to materials (or containers of materials) in the NRA collections. The database defines the materials and also tracks the location of items to allow rapid retrieval. More than 2000 items, related to 9000 animals, are currently managed by this system.

The bibliographic database uses the same bar code label system as the collection inventory database to identify reference materials. Location information about the materials is stored in the collection inventory database, and a complete bibliographic citation is stored in the bibliography system. The bibliography system includes more than 400 items of a supporting nature; animal-specific documents will arrive in 1992.

An introduction to the NRA information system is available as a stand-alone application that can be self-loaded from diskette onto a DOS-based microcomputer. The accompanying documentation, "National Radiobiology Archives Distributed Access User's Manual," explains usage and extensively describes the fields (Watson et al. 1991). This document and software are an important summary of the meta data (information describing data) collected by the Archives.

Document Archives

The research document archives collects the detailed research findings associated with each study. These include handwritten "raw" data such as exposure logbooks, clinical notes, laboratory analysis forms, hematological profiles, and animal care observations. A significant class of research document from these studies is photographic film-autoradiographs, radiographs, and photographs. "Summarized" data, usually reduced to computer files or publication reprints, are also included. Each document (or document container such as a folder) is given a bar-coded accession number label and is stored in a controlled environment. This material is cataloged in the bibliographic database for rapid selection and retrieval.

TABLE 2. Progress Toward Populating the Summary Database

NRA Lab and Study ID[a]	Status of NRA Database Tables[b]						
	LAB	STUDY	GROUP	ANIMAL	TEFFECT	TDOSE	LAB SPECIFIC
A-01, A-02, A-03	F	C	C	P			
A-04	F	C	C	C	C		C
A-05, A-06	F	C	C	P			
C-03	P	P	P	I			
D-01	F	C	C	P			
D-02, D-03, D-04	F	C	C	C	C	C	
I-01 to I-19	F	C	C	C			
P-01, P-02	F	C	C	P		P	
P-03, P-04, P-05	F	C	C	C		P	
R-01, R-02	C	C	C	C	C	C	C
U-01 to U-14	F	C	C	C	C	C	C
Number of Records:	7	62	444	19,661	47,700	1,886	>200,000

(a) Laboratory Codes: A, ANL; C, Colorado State University; D, University of California at Davis; I, ITRI; P, PNL; R, ORNL; U, University of Utah. Study numbers are defined in Table 1.

(b) Status Codes:
C, Complete; database records are complete, all significant fields have complete information.
F, Final; database records are complete and reviewed by investigator.
I, Incomplete; database tables are partially filled with representative rows.
P, Partial; database records are partially complete, some fields have no information.

The first contribution to the document archives is the extensive collection of supportive documentation that provided the basis for *Radioactivity and Health: A History*, by J. Newell Stannard; more than 30 boxes of material have been accessioned. The UC Davis clinical and radiographic records will be shipped to the Archives at the conclusion of their contract with DOE in 1992. Documents such as clinical records, radiographs, photographs, and autoradiography preparations, as well as specimens such as organs, histology blocks, and slides, at the U of Utah were accessioned in 1990; these materials will reside in Utah pending completion of the studies.

Specimen Archives

The biological specimen archives contains collected research materials such as tissues preserved in formalin or alcohol, tissue samples embedded in paraffin or plastic for histopathological analysis, microscope slides, and radiographic films. Many of these materials are radioactive and are associated with hazardous materials such as formalin, alcohol, or paraffin. An existing 1200-ft^2 cinder block building, 331-G, has been renovated as the repository of these specimens. It contains a specimen manipulation laboratory and storage bays with an automatic fire suppression system. Materials are nominated for donation to the Archives by an institution that recognizes that specific completed studies are worthy of consideration for inclusion in the Archives.

Collaborations with Participating Laboratories

The cooperation of participating institutions and investigators is essential to achieve the goals of the NRA project. Collaboration has been excellent with the seven institutions that have donated information and materials. The NRA staff has participated in, or has been invited to participate in, several site visits; collaborative projects were initiated, and these laboratory directors serve on the NRAAC.

This year, two NRA collaborations were active. The NRA encourages analysis of studies that examine previous information from a new perspective by applying different analytical approaches or by combining results of studies performed at different institutions. This year we continued our collaboration with ANL and ITRI to combine information from two studies (I-05 and A-04) of injected $^{137}CsCl$. We also collaborated with investigators at UC Davis to harvest brain specimens of dogs whose clinical records indicated Alzheimer-like symptoms. The NRA retrieved the tissues and provided laboratory facilities, and the UC Davis team prepared histopathology slides for staining and interpretation.

Future Activities

The Archives will continue the orderly accessioning of life-span beagle study information and shipment of selected specimens and documents to PNL. While these studies are being completed, the NRA will play an increasing role in facilitating cross-cutting and interspecies analysis. For example, the NRA will compile and publish a combined data set of control animals based on consensus-building meetings of the donating investigators. Because most rodent-based radiobiology studies involved thousands of animals, access to unsummarized, unpublished data from them is limited. As the NRA project matures, additional rodent studies, initially those conducted at ANL, ORNL, and PNL, will be included in the NRA information system.

References Cited

Stannard, N. J. 1988. *Radioactivity and Health: A History*, R. W. Baalman, ed. DOE/RL/10830-T59 (DE88013791), Office of Scientific and Technical Information, Springfield, Virginia.

Thompson, R. C. 1989. *Life-Span Effects of Ionizing Radiation in the Beagle Dog: A Summary Account of Four Decades of Research by the U.S. Department of Energy and Its Predecessor Agencies.* PNL-6822, Pacific Northwest Laboratory, Richland, Washington.

Watson, C. R., J. C. Prather, and S. K. Smith. 1991. *National Radiobiology Archives Distributed Access User's Manual.* PNL-7877, Pacific Northwest Laboratory, Richland, Washington.

Low-Level $^{239}PuO_2$ Life-Span Studies

Principal Investigator: *C. L. Sanders*

Other Investigator: *K. E. Lauhala*

Wistar, Long-Evans, and Fischer-344 rats are being examined during their life span for spatial-temporal dose-distribution patterns and pathological sequelae, including lung tumors. Histopathological analyses have been completed on 2821 of 3192 female Wistar rats. The dose-response curve for lung tumors was well fitted by a quadratic function and a "practical" threshold of 1 to 2 Gy; maximum lung tumor incidence (75%) was seen at about 8 Gy. The incidence of all lung tumors in 1641 rats with lung doses <1 Gy was only 0.2% and in 1004 rats with lung doses <0.1 Gy only 0.1%; in 944 sham-exposed controls, the lung tumor incidence was 0.4%. Dose-response relationships for carcinoma formation in the lung of the rat from either highly genotoxic ^{239}Pu or from a variety of nongenotoxic dusts may be best explained by a threshold model.

Introduction

This project is one of only a few that provide lung cancer risk data from an animal model at radiation doses as low as those received by nuclear workers, using a sufficient number of animals in control and low-dose groups to estimate tumor risk. The accurate determination of lung dose for each animal and the large numbers of animals in control and low-dose groups provide new information for decreasing the uncertainty of carcinogenic risk estimate in the lung. Quantitative light and scanning electron microscopic autoradiography, cell kinetics, morphometry, and pathological studies are used to evaluate and quantitate radiation dose received by type II alveolar epithelium as it progresses to carcinoma.

Lung Tumors in Female Wistar Rats

A total of 3192 young-adult, female, specific-pathogen-free (SPF) rats were used in the initial life-span study. Of these, 2134 were exposed to $^{239}PuO_2$ at initial lung burdens (ILB) ranging from about 0.007 kBq to 6.7 kBq, and 1058 control rats were sham-exposed. Histopathological analyses have been completed on 2821 of 3192 rats, including 944 sham-exposed controls and 1877 exposed animals. At a lung dose >1 Gy, the incidence of lung tumors rapidly increases, with a maximum tumor incidence of about 75% being seen at a lung dose of approximately 8 Gy. Only four lung tumors (one adenocarcinoma, one squamous carcinoma, one mesothelioma, and one fibrosarcoma) have been found in exposed rats with lung doses <1 Gy, for a malignant lung tumor incidence of 0.2%. Only one lung tumor (an adenocarcinoma) was found in 1004 exposed rats with lung doses <0.1 Gy, for a malignant lung tumor incidence of 0.1%. Four lung tumors were seen in 944 sham-exposed control rats, for a malignant lung tumor incidence of 0.4% (Table 1).

These data also continue to indicate the presence of a possible "threshold" dose of about 1 Gy for lung tumor formation; below this threshold, lung tumors are unlikely to be seen (Figures 1 and 2). They may actually be less likely to occur in exposed animals than in controls. We are continuing to suggest that ^{239}Pu acts as a promoter of pulmonary carcinogenesis, at lung doses >1 Gy, which provides ILB levels sufficient to cause focal aggregation of $^{239}PuO_2$ particles; this leads to a sequence of focal inflammation, fibrosis, type II alveolar epithelial hyperplasia, differentiated and undifferentiated cuboidal metaplasia, and squamous metaplasia in alveolar regions preceding carcinoma formation.

TABLE 1. Lung Tumor Incidences in Female Wistar Rats Following Inhalation of $^{239}PuO_2$

Dose to Lung, Gy[a]	Number of Rats[b]	Incidence of Malignant Lung Tumors, %				
		Squamous Carcinoma	Adeno-carcinoma	Sarcoma[c]	Mesothelioma	Total
21.4 ± 1.3	9 (9)	33.3	11.1	22.2	0	66.7
18.5 ± 0.97	11 (11)	54.5	18.2	0	0	72.7
15.6 ± 0.82	14 (14)	35.7	14.3	7.1	0	57.2l
13.0 ± 0.55	16 (16)	62.5	18.8	18.8	0	100
11.5 ± 0.25	15 (15)	40.0	20.0	13.3	0	73.3
10.0 ± 0.51	16 (16)	43.8	12.5	6.3	0	62.5
7.94 ± 0.47	20 (20)	60.0	10.0	0	5.0	75.0
5.93 ± 0.63	17 (17)	23.5	11.8	17.6	5.9	58.8
4.48 ± 0.23	17 (17)	0	29.4	5.9	0	35.3
3.40 ± 0.28	29 (29)	10.3	10.3	0	0	20.7
2.56 ± 0.24	35 (35)	5.1	5.1	0	0	10.2
1.40 ± 0.32	37 (37)	5.4	0	0	0	5.4
0.89 ± 0.05	39 (39)	0	0	0	0	0
0.68 ± 0.06	63 (63)	0	0	0	0	0
0.49 ± 0.06	60 (60)	0	0	1.7	1.7	3.3
0.28 ± 0.05	140 (138)	0.7	0	0	0	0.7
0.13 ± 0.03	373 (337)	0	0	0	0	0
0.07 ± 0.02	1211 (1004)	0	0.1	0	0	0.1
0.005[d]	1058 (944)	0	0.2	0.1	0.1	0.4

(a) Mean ± standard deviation.
(b) Number of rats with completed histopathology is given in parentheses.
(c) Hemangiosarcoma, fibrosarcoma, carcinosarcoma.
(d) Estimated background lung dose.

Pathological Sequelae Leading to Pulmonary Carcinoma

The radiation dose to various cell types in focal regions of Pu particle aggregation is being determined using dose estimates from studies of quantitative light microscopic autoradiography (Sanders et al. 1988), and data from current morphometric studies; early results are presented in Table 2. Type II alveolar epithelium, the most probable target cell for carcinomas in the lung of the rat, accounts for only 3%-4% of the alveolar surface in normal rat lung. A marked increase is seen in alveolar histiocytes at about 6 months after exposure, along with a two- to threefold increase

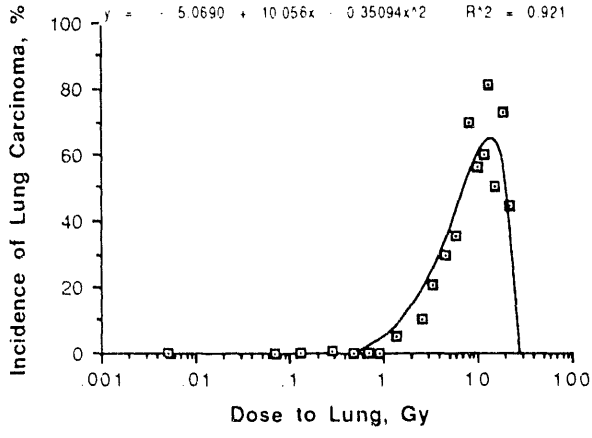

FIGURE 1. Incidence of Malignant Lung Tumors as a Function of Dose to the Lung Following Inhalation of $^{239}PuO_2$. Data fitted by polynomial function.

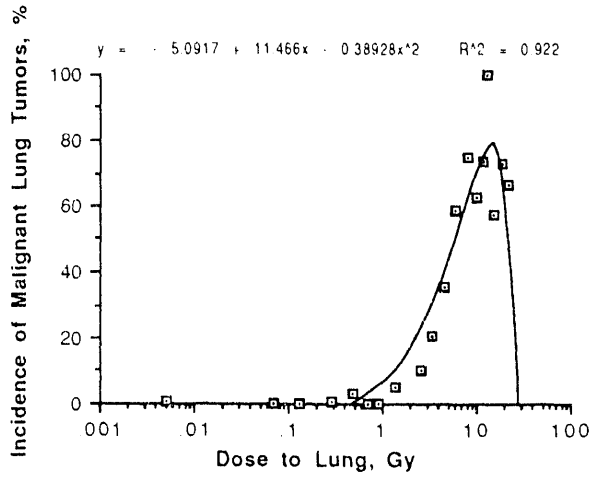

FIGURE 2. Incidence of Lung Carcinomas as a Function of Dose to the Lung Following Inhalation of $^{239}PuO_2$. Data fitted by polynomial function.

TABLE 2. Morphometric Determination of Numerical and Volumetric Abundance of Alveolar Cell Types in Regions of Focal $^{239}PuO_2$ Aggregation[a]

Time After Exposure, Days	Alveolar Histiocyte/ Macrophage		Type II Alveolar Epithelium		Mast Cell,	Metaplastic Epithelium	
	%#	% vol	%#	% vol	% #	%#	% vol
Control[b]	2.4 ± 3.2	1.4 ± 1.2	9.4 ± 5.9	3.2 ± 2.0	0	0	0
180 (3)[c]	16.2 ± 4.8	11.7 ± 1.7	12.8 ± 4.1	3.6 ± 1.6	4.9 ± 2.0	9.6 ± 8.2	2.3 ± 2.2
210 (4)[c]	21.2 ± 8.6	18.3 ± 5.2	14.0 ± 2.8	4.7 ± 1.6	4.2 ± 1.5	17.6 ± 7.4	3.5 ± 1.7
240 (7)[c]	12.5 ± 3.6	11.4 ± 3.7	22.1 ± 5.0	5.4 ± 1.3	5.7 ± 0.8	12.2 ± 7.9	2.1 ± 1.4
400 (1)[c]	15.3	11.3	27.6	4.9	7.1	--	--

(a) Lung dose in exposed rats = 12 ± 0.5 Gy; values are mean ± standard deviation.
(b) From Rhoads et al. (1981).
(c) ^{239}Pu-exposed (number of focal sites in parentheses).

in type II cell numbers by 8 months after exposure. Increased cell proliferation of type II cells in regions of focal $^{239}PuO_2$ aggregation is not surprising, in view of the vulnerability of type I alveolar epithelium to damage and because type II cell proliferation is required to renew type I cells.

Mast cells are associated with fibroblast proliferation and collagen formation. Increasing numbers of mast cells are also associated with radiation-induced fibrosis in focal, high-dose regions. These morphometric studies will be expanded and continued from 1 to 700 days post exposure. Focal areas of type II cell hyperplasia (Figure 3) may be replaced by alveolar bronchiolization (Figure 4). Alveolar bronchiolization does not appear to differentiate further into cuboidal or squamous epithelial cells, but it does appear to represent a terminal and reversible change. On the other hand, undifferentiated cuboidal metaplasia along the alveolar walls (Figure 5) appears to present a premalignant change leading to adenocarcinoma

FIGURE 3. Type II Alveolar Epithelial Hyperplasia (arrow) Following Inhalation of $^{239}PuO_2$ (x1000).

FIGURE 4. Alveolar Bronchiolization (arrow) Comprises Ciliated and Nonciliated "Bronchiolar-Like" Epithelium Along Surface of Alveolar Wall Following Inhalation of $^{239}PuO_2$ (x1000).

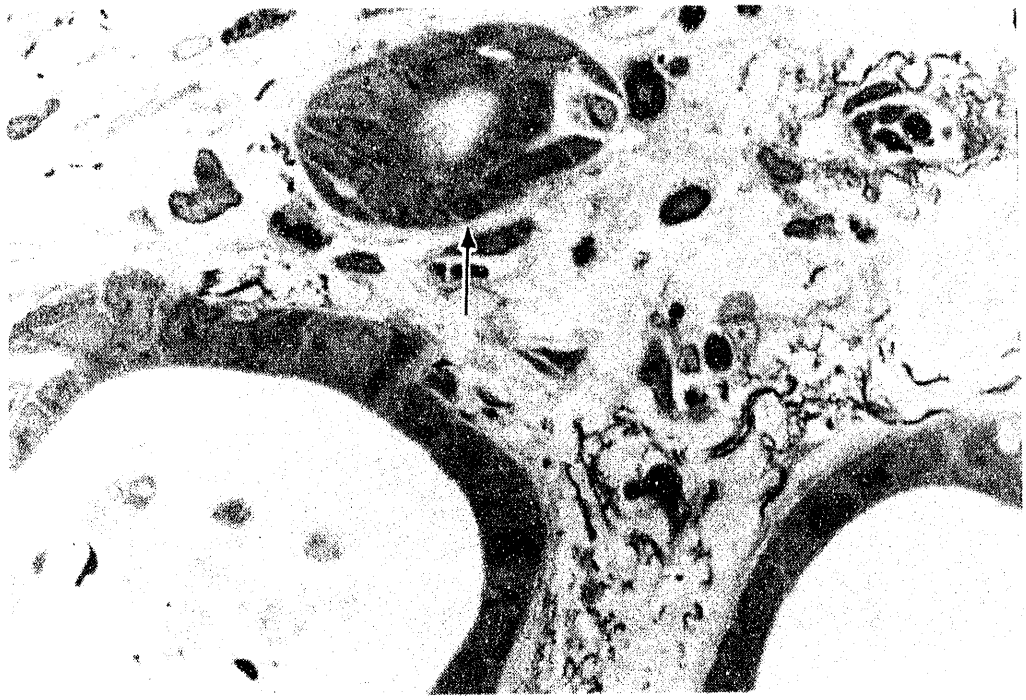

FIGURE 5. Undifferentiated Cuboidal Metaplasia (arrow) Along Alveolar Walls in Area of Intense Alveolar Fibrosis Following Inhalation of $^{239}PuO_2$ (x1000).

formation. Small focal regions of squamous cell differentiation (Figure 6) are seen adjacent to undifferentiated cuboidal metaplastic cells lining the alveoli in regions of more intense interstitial fibrosis. Thus, squamous metaplasia, a precursor to squamous carcinoma, seems to require both cuboidal metaplasia and alveolar fibrosis.

Predictions of Lung Tumor Risk

Many examples in rodents suggest a nonlinearity in tumor response to ionizing radiation. Initiation events involving damage to DNA appear to increase in a linear fashion with radiation dose for high-LET radiation. The availability of a promoter that stimulates cell proliferation may determine the fate of initiated cells. Thus, proliferation of "target" stem cells plays a critical role in the expression of tumors, with tumors most often seen at doses associated with increased cell proliferation.

Otto Raabe (University of California, Davis) has fitted a Gomperzian survival function using age to death in sham-exposed rats in this study. He then used this function to predict the distribution of deaths with ^{239}Pu-induced lung cancer. The results of his analyses (Figure 7) indicate a practical threshold in rats at a cumulative lung dose of 1.3 Gy (0.4 kBq ILB), below which radiation-induced lung cancer would be extremely unlikely. The dose-response curve for lung tumors in beagle dogs following inhalation of $^{239}PuO_2$ is similar to that seen in our rat studies. The Syrian hamster is resistant to lung tumor induction by inhaled $^{239}PuO_2$. Limited data in primates indicate a dose- response curve similar to that seen in the hamster (Figure 8).

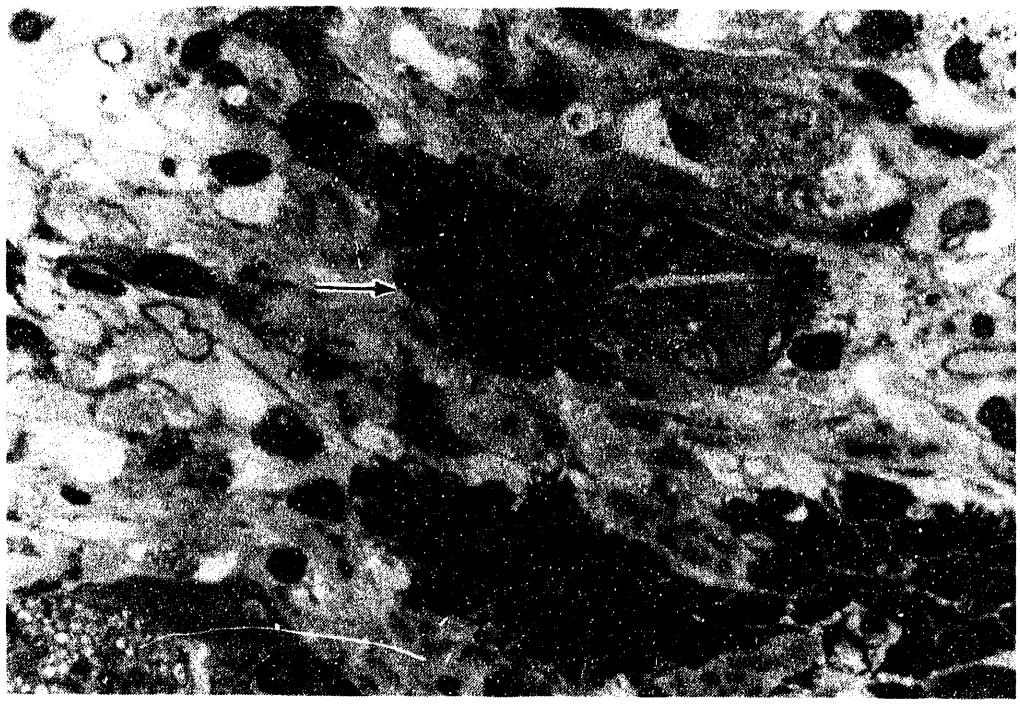

Figure 6. Squamous Metaplasia (arrow) in Region of Intense Alveolar Fibrosis Following Inhalation of $^{239}PuO_2$ (x1000).

Common Carcinogenic Mechanism for Plutonium and Nongenotoxic Particulates

No unique genetic alteration has yet been associated with radiation-induced hyperplastic, metaplastic, or neoplastic lesions in the lung of animals. Many weakly genotoxic or nongenotoxic particulates (titanium dioxide, Kevlar fibrils, coal dust, quartz, shale dust, petroleum coke, chromium dioxide, volcanic ash) have been shown to induce lung carcinomas at high doses such that the particle load in the lung is sufficient to overcome normal clearance processes. This leads to particle aggregate formation and subsequent pathological sequelae similar to that seen with inhaled $^{239}PuO_2$. These studies indicate the presence of a threshold lung tumor response that is also similar to that seen with $^{239}PuO_2$. Insoluble particulates could not mechanically interfere with chromosome distribution within progeny cells during mitosis of type II cells because type II cells are not phagocytic. Thus, even though ^{239}Pu is markedly genotoxic, its biological behavior in the rat lung is similar to that seen with a variety of nongenotoxic particulates. Pulmonary studies with quartz and alpha emitters in rats indicate that alpha irradiation may actually promote the formation of lung tumors following quartz deposition (Spiethoff et al., in press). Thus, in spite of its ability to break DNA and chromosomes, alpha irradiation from inhaled $^{239}PuO_2$ does not have to exhibit its greatest carcinogenic effect through initiation events but can also do so by the nature of carcinogenic promotion.

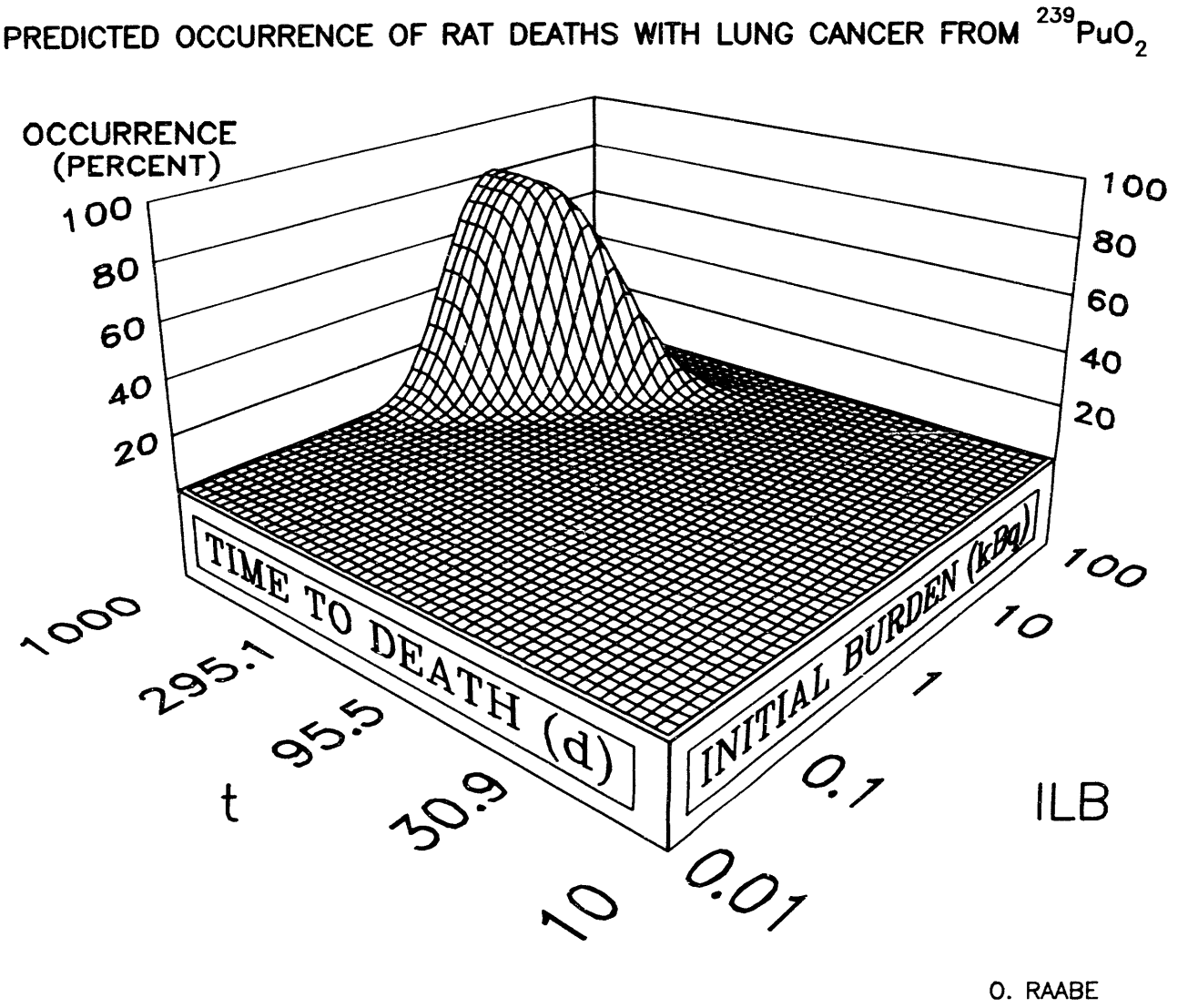

FIGURE 7. Predicted Occurrence of Rat Deaths with Lung Tumors Following Inhalation of $^{239}PuO_2$ Based on an Analysis of Survival in Sham-Exposed rats. (Photograph supplied by Otto G. Raabe, with permission.)

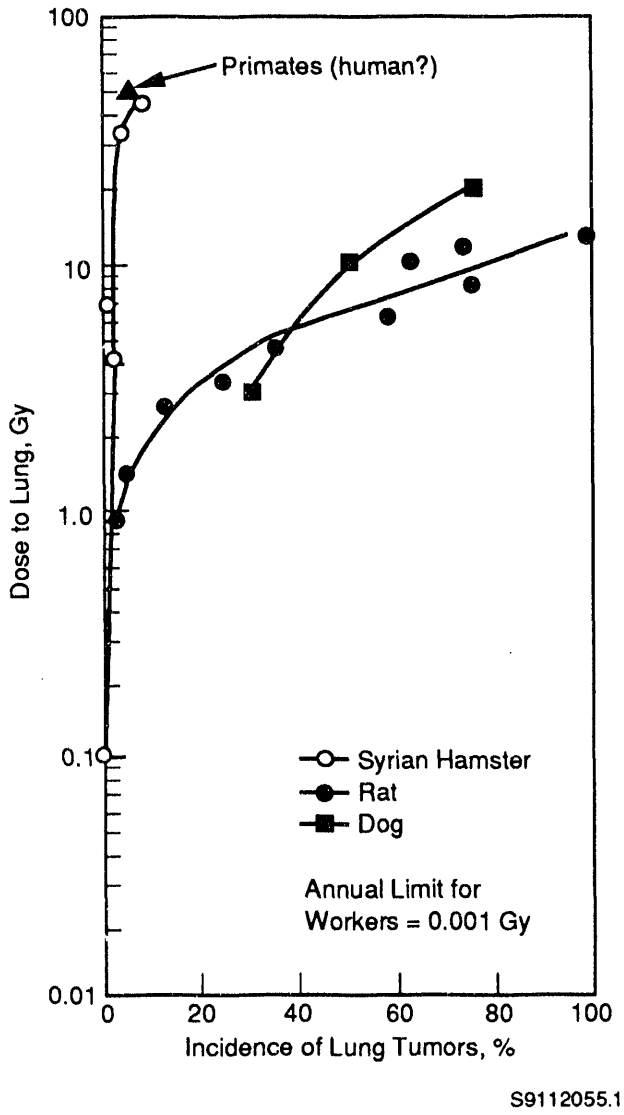

FIGURE 8. Incidence of Lung Tumors in Several Mammalian Species as a Function of Dose to the Lung Following Inhalation of $^{239}PuO_2$. Curves fitted by eye.

REFERENCES CITED

Rhoads, K., J. A. Mahaffey, and C. L. Sanders. 1981. A morphometric study of rat and hamster lung following inhalation of $^{239}PuO_2$. *Radiat. Res.* 88:266-279.

Sanders, C. L., K. E. McDonald, and K. E. Buhala. 1988. Promotion of pulmonary carcinogenesis by plutonium particle aggregation following inhalation of $^{239}PuO_2$. *Radiat. Res.* 116:393-405.

Spiethoff, A., H. Wesch, K. Wegener, and H.-J. Klimish. The effects of Thorotrast and quartz on the induction of lung tumors in rats. *Health Phys.* (in press).

Inhalation Hazards to Uranium Miners

Principal Investigator: *F. T. Cross*

Other Investigators: *R. L. Buschbom, G. E. Dagle, K. M. Gideon, and R. A. Gies*

Technical Assistance: *C. R. Petty*

Using experimental animals, we are investigating levels of air contaminants that produce respiratory system and other organ disease in radon-exposed populations. Lung cancer incidence and deaths from degenerative lung disease are significantly elevated among uranium miners, but the cause-effect relationships for these diseases are based on inadequate epidemiologic data. More recent human data suggest that radon is also implicated in other organ disease, although confirmatory data are lacking in animal systems. This project identifies agents or combinations of agents (both chemical and radiological), and their exposure levels, that produce respiratory tract and other system lesions, with emphasis on the development of lung carcinoma and collaborative mechanistic data.

Histopathological data on radon-, radon-progeny-, and uranium ore-dust-exposed life-span rats showed the overall trend in lung tumor incidence decreases in proportion to the decrease in cumulative radon-progeny exposure and remains elevated at exposures comparable to those found in houses. Exposures at 50 working-level months (WLM)/wk produced a greater overall incidence of lung tumors than exposures at 500 WLM/wk. The lower exposure rate also produced more epidermoid carcinoma, multiple primary lung tumors (more often of different types than of the same type), and fatal lung tumors. The origin of most radon-induced tumors was considered to be peripheral in the lung. Finally, the assumption that tumors appear where the doses and radiation sensitivity are high was examined by reanalysis of our limited database on inhalation exposure to various levels of unattached fractions of radon progeny. Both lung and nasal carcinomas increased with increase in unattached progeny levels. No particular association of lung tumor location was noted for unattached percentages, f_p, ranging between 0.4% and 7%.

Wistar Rat Exposure Protocols

The 6000 Series (1000-working level; WL) and 7000 Series (100-WL) experiments (Table 1) are designed to develop the relationships between response and exposure to radon progeny (at two rates of exposure) and carnotite uranium ore dust. The 8000 Series (100-WL) experiments (Table 2) are designed to extend the exposure-response relationships to cumulative exposure levels comparable to current conditions in the mines and to lifetime environmental exposures. The 9000 Series experiments (Table 3) continue the "low-dose" studies at exposure rates comparable to former occupational working levels (10 WL). They will help to further evaluate the hypothesis that the tumor probability per working-level month (WLM) exposure increases with decreasing exposure rate. In addition, concurrent exposure to varying levels of uranium ore dust tests the hypothesis that irritants (both specific and nonspecific) act synergistically with radiation exposures. The exposures of 6000, 7000, and 8000 Series animals are complete. Exposures of 9000 Series animals have been temporarily discontinued, ceasing with the 80-WLM and 15 mg/m^3 ore-dust exposures, pending analyses of existing data. Exposures of rats to uranium ore dust alone (10,000 Series experiments; Table 4) have been completed.

The ore-dust studies address the potential link of silica exposures to lung cancer. Exposures of rats to radon progeny, uranium ore dust, and cigarette-smoke mixtures [initiation-promotion-initiation (IPI; 11,000 Series) experiments; see *Mechanisms of*

TABLE 1. Exposure-Response Relationship Study for Radon-Progeny Carcinogenesis in Rats (6000 and 7000 Series Experiments)

Number of Animals[a]		Exposure Regimen[b,c]	Total Exposure, WLM[d]
6000 Series	7000 Series		
64	0	1000-WL radon progeny 15 mg/m^3 uranium ore dust	10,240
56	32	1000-WL radon progeny 15 mg/m^3 uranium ore dust	5,120
56	32	1000-WL radon progeny 15 mg/m^3 uranium ore dust	2,560
56	32	1000-WL radon progeny 15 mg/m^3 uranium ore dust	1,280
88	64	1000-WL radon progeny 15 mg/m^3 uranium ore dust	640
152	128	1000-WL radon progeny 15 mg/m^3 uranium ore dust	320
64	96	Controls	

(a) Number of animals is sufficient to detect the predicted incidence of lung tumors at the 0.05 to 0.1 level of significance, assuming linearity of response between 0 and 9200 WLM (see footnote d) and 0.13% spontaneous incidence.
(b) Exposure rate, 90 hr/wk; planned periodic sacrifice.
(c) Study is repeated at 100-WL rate (without periodic sacrifice) to augment previous limited exposure-rate data (7000 Series experiments).
(d) Working level (WL) is defined as any combination of the short-lived radon progeny in 1 liter of air that will result in the ultimate emission of 1.3 x 10^5 MeV of potential α energy. Working-level month (WLM) is an exposure equivalent to 170 hours at a 1-WL concentration. Previous exposure at 900 WL for 84 hr/wk to 9200 WLM produced an 80% incidence of carcinoma.

Radon Injury project, this volume] have been completed. These experiments clarify the induction-promotion relationships of radon and cigarette-smoke exposures. Exposures of female rats (12,000 Series experiments; Table 5) are complete. These experiments provide comparative risk data to exposures of male animals. Tables 1 through 5 are shown here with the actual numbers of animals (including serial-sacrifice animals) used at each exposure level.

Rat Respiratory Tract Pathology

A current summary of primary tumors of the respiratory tract for 8000 Series animals, shown in Table 6, is updated from the 1990 *Annual Report*. While the incidence of primary lung tumors at 320-WLM exposure is lower than that which is historically (7000 Series) observed, these sampled data show that the incidence of lung tumors decreases in proportion to the decrease in

cumulative radon-progeny exposure and, in comparison to an assumed 0.13% spontaneous incidence, remains elevated at exposures comparable to those found in houses (20 to 40 WLM). Histopathological examinations are in progress on the remainder of tissues from 8000, 9000, 10,000, 11,000, and 12,000 Series animals.

TABLE 2. Low Exposure-Response Relationship Study for Radon-Progeny Carcinogenesis in Rats (8000 Series Experiments)

Number of Animals[a]	Exposure Regimen[b]	Total Exposure, WLM[c]
96	100-WL radon progeny 15 mg/m^3 uranium ore dust	640[d]
96	100-WL radon progeny 15 mg/m^3 uranium ore dust	320[d]
192	100-WL radon progeny 15 mg/m^3 uranium ore dust	160
384	100-WL radon progeny 15 mg/m^3 uranium ore dust	80
480	100-WL radon progeny 15 mg/m^3 uranium ore dust	40
544	100-WL radon progeny 15 mg/m^3 uranium ore dust	20
192	Controls	

(a) Number of animals is sufficient to detect lung tumors at the 0.05 to 0.1 level of significance, assuming linearity of response between 0 and 640 WLM (see footnote c) and 0.13% spontaneous incidence.
(b) Exposure rate, 90 hr/wk; planned periodic sacrifice.
(c) Previous exposures indicated a tumor incidence of 16% at 640 WLM. Working level (WL) is defined as any combination of the short-lived radon progeny in 1 liter of air that will result in the ultimate emission of 1.3 x 10^5 MeV of potential α energy. Working-level month (WLM) is an exposure equivalent to 170 hours at a 1-WL concentration.
(d) Repeat exposure is for normalization with Table 1 data.

TABLE 3. Ultralow Exposure-Rate Study for Radon-Progeny Carcinogenesis in Rats (9000 Series Experiments)

Number of Animals[a]	Exposure Regimen[b]	Total Exposure, WLM[c]
64	10-WL radon progeny 15 mg/m^3 uranium ore dust	320
64	10-WL radon progeny 3 mg/m^3 uranium ore dust	320
384	10-WL radon progeny 15 mg/m^3 uranium ore dust	80
384	10-WL radon progeny 3 mg/m^3 uranium ore dust	80
512	10-WL radon progeny 15 mg/m^3 uranium ore dust	20
512	10-WL radon progeny 3 mg/m^3 uranium ore dust	20
192	Controls	

(a) Number of animals is sufficient to detect lung tumors at the 0.05 to 0.1 level of significance, assuming linearity of response between 0 and 640 WLM (tumor incidence is approximately 16% at 640 WLM) and 0.13% spontaneous incidence.
(b) Exposure rate, 90 hr/wk; planned periodic sacrifice.
(c) Working level (WL) is defined as any combination of the short-lived radon progeny in 1 liter of air that will result in the ultimate emission of 1.3 x 10^5 MeV of potential α energy. Working-level month (WLM) is an exposure equivalent to 170 hours at a 1-WL concentration.

TABLE 4. Control Study for Uranium Ore-Dust Carcinogenesis in Rats (10,000 Series Experiments)

Number of Animals	Exposure Regimen[a]
96	15 mg/m^3 uranium ore dust
64	Sham-exposed controls

(a) Exposures, 12 to 18 months at 72 hr/wk; planned periodic sacrifice.

TABLE 5. Exposure of Female Rats to Radon Progeny and Uranium Ore Dust (12,000 Series Experiments)

Number of Animals	Exposure Regimen[a]
96	100-WL radon progeny; 640 WLM 5 mg/m^3 uranium ore dust
96	Sham-exposed controls

(a) Exposure rate, 72 hr/wk; planned periodic sacrifice. Working level (WL) is defined as any combination of the short-lived radon progeny in 1 liter of air that will result in the ultimate emission of 1.3×10^5 MeV of potential α energy. Working-level month (WLM) is an exposure equivalent to 170 hours at a 1-WL concentration.

Influence of Exposure Rate and Level on the Incidence and Type of Primary Lung Tumors in Rats Exposed to Radon

Previous databases were reexamined to determine the incidence, type, fatality, and origin of tumors primary to the lung as a function of radon-progeny exposure rate and level. The reexamination was done, in part, to determine consistency over time in histopathological analysis, but mainly for the purposes of clarifying risk and dosimetric modeling to aid in the extrapolation of animal data to man. Risk model development, in particular, depends on proper classification of tumors regarding their lethality to the animal. Table 7 examples part of the database on the percent incidence of primary and fatal lung tumors in rats versus radon-progeny exposure rate and level. The data in brackets are significantly ($p<0.05$) higher at 50 WLM/wk (100-WL concentrations) than at 500 WLM/wk (1000-WL concentrations) exposure rates.

The principal tumor type that increased at the lower exposure rate was epidermoid carcinoma, which also generally accounted for the increase in fatal lung tumors. Protraction of exposures in rats also produced a significantly higher incidence of multiple primary lung tumors (more often of a different type than of the same type; see Table 8). Most (>70%) epidermoid carcinomas but only about 20% of adenocarcinomas were classified as fatal. Finally, most (~80%) radon-induced lung tumors in rats exposed to a wide range of exposure rates and levels are considered to originate peripherally and to occur at the bronchiolar-alveolar junction. The remaining 20% are considered to be centrally located (bronchi-associated); the actual percent depends somewhat on exposure rate and possibly on exposure level.

TABLE 6. Current Summary of Primary Tumors of the Respiratory Tract in Life-Span Animals (8000 Series Experiments)

		Extrathoracic Tumors			Lung Tumors							
Nominal Exposure, WLM	Nominal Ore Dust Conc., mg/m^3	Nasal	Laryngeal	Tracheal	No. Animals Examined	No. Animals to be Examined	Adenoma	Adenocarcinoma	Epidermoid Carcinoma	Adenosquamous Carcinoma	Sarcoma[a]	Animals with Lung Tumors, %
20	15	0/122[b]	0/82	0/119	127	399	0	0	1	0	0	0.8
40[c]	15	0/135	0/91	0/132	142	320	0	1	0	0	1	1.4
160	15	0/161	0/97	0/158	171	0	4	5	1	0	1	6.4
320	15	0/74	0/56	0/69	77	0	0	1	0	0	1	2.6
640	15	0/72	0/44	0/71	76	0	5	3	2	1	0	13
Controls		0/92	0/68	0/84	96	77	0	0	0	0	0	0

(a) One malignant hemangiopericytoma, one malignant fibrous histiocytoma, and one malignant mesothelioma considered radon-progeny-exposure related.
(b) Number tumors/number examined.
(c) One malignant oropharyngeal hemangiosarcoma, considered radon-progeny-exposure related; found in tissue not routinely sectioned for histopathology.

TABLE 7. Percent Incidence of Primary and Fatal Lung Tumors in Rats Versus Radon-Progeny Exposure Rate and Level[a]

WLM at 500 WLM/wk	No. Animals Examined	Percent Incidence						
		Adenoma	Adeno-carcinoma	Epidermoid Carcinoma	Adeno-squamous Carcinoma	Sarcoma	Fatal Lung Tumors	Animals with Lung Tumors, %
320	131	5	8	1	0	0	2	15
640	70	3	7	0	0	0	1	10
1280	38	0	26	0	3	0	5	29
2560	38	3	24	3	0	3	11	32
5120	41	2	44	2	0	2	15	49
WLM at 50 WLM/wk								
320	127	5	5	1	1	1	2	0
640	64	3	[20][b]	3	3	2	6	[28]
1280	32	[22]	41	[13]	9	3	[22]	[66]
2560	32	9	41	[47]	[9]	0	[50]	[69]
5120	32	[22]	53	[44]	3	0	[44]	[75]

(a) 15 mg/m^3 ore-dust exposures accompanied radon and radon-progeny exposures.
(b) Data in brackets at 50 WLM/wk are significantly ($p<0.05$) higher than corresponding data at 500 WLM/wk; see previous tables for WL and WLM definitions.

TABLE 8. Percent Incidence of Multiple Primary Lung Tumors in Rats Versus Radon-Progeny Exposure Rate and Level[a]

WLM at 500 WLM/wk	No. Animals Examined	Multiple Tumors of Same Type	Multiple Tumors of Different Type
320	131	1	0
640	70	0	0
1280	38	5	3
2560	38	0	3
5120	41	17	5
WLM at 50 WLM/wk			
320	127	0	2
640	64	5	3
1280	32	6	[22][b]
2560	32	[22]	[28]
5120	32	22	[44]

(a) 15 mg/m^3 ore-dust exposures accompanied radon and radon-progeny exposures.
(b) Data in brackets at 50 WLM/wk are significantly ($p<0.05$) higher than corresponding data at 500 WLM/wk; see previous tables for WL and WLM definitions.

Effect of Unattached Fraction on Location of Tumors

One of the assumptions in the currently proposed lung model of the ICRP Lung Model Task Group is that tumor development coincides with respiratory tract regions of high dose and high sensitivity. To test this assumption, we reanalyzed histological slides on groups of rats that were exposed to various levels of unattached radon progeny. Biophysical dose modeling predicts higher proximal than distal respiratory tract doses with higher percentages of unattached progeny such as occur in homes. Limited tumor data from rats confirm that both lung and nasal carcinomas increase with increase in unattached progeny levels. Lung tissues were examined "blind" to determine by histological criteria whether there was a correlation of bronchial involvement with the degree of radon-progeny unattachment. All tumors not "peripheral" were considered central or bronchi-associated.

Our limited database on unattached fraction indicates no particular association of lung tumor location for total short-lived progeny unattached percentages, f_p, ranging between 0.4% and 7%. Our criteria for ascertaining tumor location may not be rigorous enough in the absence of special stains and other techniques. On the other hand, tissue sensitivity may be sufficiently high in rat peripheral areas to cause more tumors to appear there, despite the tendency for modeled doses to increase to the more proximal lung regions. Because modeled doses from unattached progeny occur mainly to bronchi and essentially disappear at the terminal bronchioles and alveoli, the more rigorous test of this assumption would be inhalation exposures to only unattached progeny.

Mechanisms of Radon Injury

Principal Investigator: *F. T. Cross*

Other Investigators: *G. E. Dagle, E. W. Fleck,[a] M. E. Foreman, R. A. Gies, J. E. Hulla, R. F. Jostes, L. S. McCoy, T. L. Morgan, and G. L. Stiegler*

Technical Assistance: *T. L. Curry and C. R. Petty*

In this project we conduct dosimetric, molecular, cellular, and whole-animal research relevant to understanding the mechanisms of radon and radon-progeny injury to the respiratory tract. The work specifically addresses the exposure-rate effect in radon-progeny carcinogenesis; the induction-promotion relationships associated with exposure to radon and cigarette-smoke mixtures; the role of oncogenes and suppressor genes in radon-induced cancers; and the effects of radon exposure on chromosomal aberrations, mutations, and strand break production and repair.

PNL collaborative efforts to correlate oncogene data with pathological data derived from animal radon studies continued; codon 13 K-*ras*- and codon 62 H-*ras*-activating lesions were identified in radon-induced lung tumors. Studies to determine the involvement of tumor suppressor genes in radon-induced rat lung cancers were initiated. Collaborative mechanistically based cellular studies with researchers at PNL and at other institutions also continued. Collaborations with researchers at other institutions included: (1) Dr. Earl Fleck, Whitman College, on molecular analysis of radon-induced HGPRT mutations using Southern blot and PCR exon analyses; (2) Dr. Helen Evans, Case-Western Reserve University (CWRU), on mutational response of radiosensitive and radioresistant L5178Y cells as well as the dosimetric evaluation of the CWRU *in vitro* radon exposure system; (3) Drs. Sheldon Wolff and John Wiencke, University of California San Francisco (UCSF), on adaptation studies using x irradiation followed by radon exposure and vice versa; and (4) Drs. James Cleaver and Louise Lutze, UCSF, on radon exposure of shuttle vectors for molecular analysis of induced mutations. The alkaline single-cell gel (SCG) electrophoresis technique to estimate the percentage of cell nuclei "hit" by alpha particles during *in vitro* radon exposure was used to test PNL hit probability calculations. Preliminary data indicate that 47% of A_L cells are hit by alpha particles when given 38 cGy of radon; the PNL dosimetry model predicts that 61% would be traversed by an alpha particle. Polymerase chain reaction (PCR) exon analysis was added to Southern blot analyses of x-ray- and radon-induced mutations at the CHO-HGPRT locus. Processing of tissues and analyses of data from initiation-promotion-initiation experiments in male SPF Wistar rats exposed to radon and cigarette-smoke mixtures also continued. The majority of smoke-exposure-related carcinomas were epidermoid carcinomas in contrast to the generally greater incidence of adenocarcinomas in non-smoking-related tumors.

Oncogene/Suppressor Gene Studies

In an effort to correlate molecular data with pathological data derived from the animal radon studies, Drs. Marla Foreman, Linda McCoy, and Jan Hulla (PNL) were supplied fresh, frozen, and fixed, archived, radon-induced rat tumor tissue to determine the involvement of oncogenes and suppressor genes in radon carcinogenesis. The involvement of oncogenes in archived radon- and plutonium-induced lung tumors in rats was compared. A 12th-codon activating lesion was identified in one plutonium-induced lung tumor. Two 13th-codon K-*ras*-activating mutations have been identified in radon-induced lung tumors, and an activating lesion that may be unique occurred

(a) Whitman College, Walla Walla, Washington.

at codon 62 in the H-*ras* 2nd exon in four radon-induced lung tumors in which GAA is mutated to GAT, bringing about a glutamate-to-aspartate substitution. The potential of this mutation to induce *ras* transformational effects is not known. (This collaborative work appears in *Oncogenes in Radiation-Induced Carcinogenesis*, this volume.)

In Vitro Radon Cell-Exposure System and Molecular/Cellular Studies

The PNL *in vitro* radon cell-exposure system was extensively employed in PNL experiments as well as in several collaborative experiments with other laboratories. Collaborations included, first, Dr. Earl Fleck, Whitman College, on molecular analysis of radon-induced HGPRT mutations using Southern blot and PCR exon analyses; we have completed the Southern blot studies and our preliminary work is in press (*Indoor Radon and Lung Cancer: Reality or Myth?*, Proceedings of the 29th Hanford Symposium on Health and the Environment). Three exons require evaluation to complete the PCR exon analysis; this work is ongoing at PNL (Jostes/Stiegler). The second collaboration is with Dr. Helen Evans, Case-Western Reserve University (CWRU), on mutational response of radiosensitive and radioresistant L5178Y cells as well as the dosimetric evaluation of the CWRU *in vitro* radon exposure system; we have recently completed experimentation on this project and have started to calculate the dosimetry for three exposure systems. The survival and mutation response of the two cell lines at CWRU, PNL, and the University of Chicago are expected to be ready for publication in FY 1992.

The third collaboration is with Drs. Sheldon Wolff and John Wiencke, University of California San Francisco (UCSF), on adaptation studies using x irradiation followed by radon exposure and vice versa. We have noted that pretreating human lymphocytes with a small x-ray dose reduces the chromosomal damage induced by a subsequent acute radon exposure. This work has been published in *Mutation Research* (Wolff et al. 1991). We are currently investigating the effect of a small radon pretreatment followed by an acute x-ray dose. The fourth joint effort, with Drs. James Cleaver and Louise Lutze, UCSF, is radon exposure of shuttle vectors for molecular analysis. This work indicates that a high proportion of radon-induced mutations are large deletions that are not randomly distributed but appear to begin and end in defined regions of the episome. Deletion ends were rejoined by nonhomologous recombination involving up to 6 base pairs of homology. (This work has been submitted to *Cancer Research* for publication.) Dose-response studies are currently being evaluated; we are initiating studies to evaluate the response of shuttle vectors in repair-proficient and repair-deficient human cell lines.

Dosimetry of *In Vitro* Radon Exposures

Theoretical models of hit probability require experimental validation. We have used the single-cell gel (SCG) electrophoretic technique to evaluate hit probability calculations based on a dosimetry model developed at PNL (Jostes et al. 1991). The SCG technique measures DNA strand breaks as increased migration of the DNA out of lysed cells embedded in the middle layer of a three-layer gel formed on a microscope slide. We have used the alkaline SCG technique to estimate the percentage of cell nuclei "hit" by alpha particles after irradiation with an *in vitro* radon exposure system. One of the advantages of this system is that individual cells of an exposed population can be evaluated and histograms (Figure 1) constructed to estimate the population response. A_L cells, held at 0°C to prevent repair of single-strand breaks, were given 38 cGy of radon, a dose at which our dosimetry model predicts that 61% of the cell nuclei will be traversed by an alpha particle. A 150-cGy x-ray response was also evaluated as a low-LET control. As expected, the x-ray profile of DNA damage was shifted from the unirradiated profile, in the direction of greater DNA migration, and approximated a normal distribution. The profile of the radon-exposed cells was biphasic with one distribution corresponding to the control (nonirradiated) response and the other profile showing increased DNA migration. We interpret the second profile as representing the cells that had received an alpha "hit." The percentage of cells in the "hit" category (approximately 47%) was in reasonable agreement with the hit probability calculations derived from our dosimetry model. A similar result has been obtained using the CHO-C18 cell line. We are currently writing an image analysis program to enhance our ability to resolve hit from nonhit cells using the SCG technique.

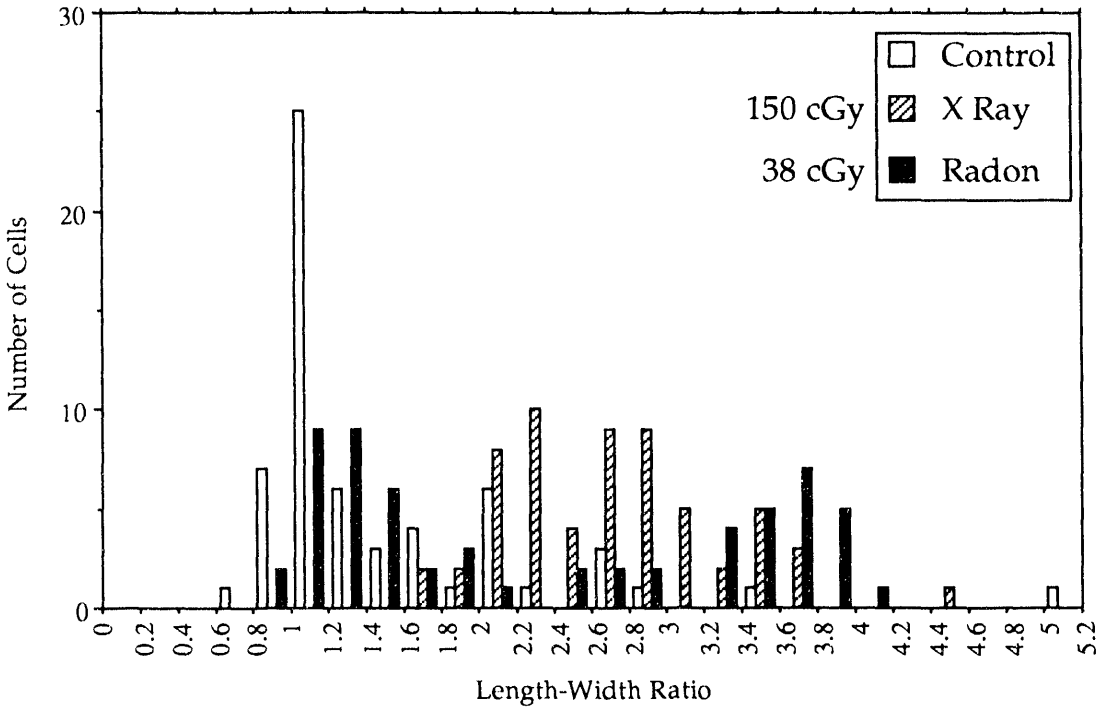

FIGURE 1. Length-Width Ratios of Control, X-Irradiated, and Radon-Irradiated A_L Cell DNA (single-strand break, 0°C)

HGPRT Mutation Analysis

Data on the type, location, and frequency of mutations in control, x-irradiated, and radon-exposed mammalian cells will help us to understand mechanisms in radiation mutagenesis and clarify risk assessment of radon exposures. We have added polymerase chain reaction (PCR) exon analysis to our evaluation of CHO-HGPRT mutations induced by radon exposure. Mutations obtained after low- and high-level radon exposures (25 and 30 cGy versus 75 and 77 cGy) are compared with mutations from 300-cGy x-ray exposures, as well as with mutations of spontaneous origin. The results of these analyses are presented in Table 1. The largest category of mutation types obtained after x-irradiation or radon exposure is the full deletion. Further, the percentages of full deletions obtained from both levels of radon exposure, as well as from the 300-cGy x-ray exposure, are essentially the same. The largest category of mutations in the spontaneous population have no changes from the parental cell line that are detectable by Southern blot or PCR exon analysis. Mutations were carefully isolated to prevent the analysis of sibling isolates.

Initiation-Promotion-Initiation Studies

Processing of tissues and analyses of data from initiation-promotion-initiation (IPI) experiments in male SPF Wistar rats with radon and cigarette-smoke mixtures continued. The exposure protocols are shown in Table 2.

Initial radon-progeny exposures were at 100-working-level (100-WL) concentrations with cumulative levels of 320 working-level months (WLM); uranium ore-dust concentrations ranged from about 5 to 6 mg/m^3. Cigarette smoke from Kentucky 1R4F cigarettes, in exposures of 1 hr/day, 5 days/week, for 17 weeks, contained total particulate mass concentrations of about 0.5 mg/L and carbon monoxide concentrations between 650 and 700 ppm. Mean plasma concentrations of nicotine and cotinine were about 260 and 125 ng/mL, respectively, in cigarette-smoke-exposed animals; carboxyhemoglobin levels were about 29%. Blood samples were obtained within 15 minutes after exposures ended.

Histopathological examination was completed on all IPI series life-span rats exposed to radon, radon

TABLE 1. Current Summary of CHO-HGPRT Mutation Types[a]

Treatment	Full Deletion[b]	Alteration[c]	No Change[d]	Total
None (spontaneous)	4 (13%)	12 (39%)	15 (48%)	31
Low-dose radon (25 and 30 cGy)	13 (48%)	8 (30%)	6 (22%)	27
High-dose radon (75 and 77 cGy)	11 (42%)	11 (42%)	4 (16%)	26
300-cGy x rays	16 (47%)	13 (38%)	5 (15%)	34

(a) DNA from each mutant cell line was digested with one or more restriction enzymes.
(b) Full deletion, no residual HGPRT-specific coding sequences detectable.
(c) Alteration, loss of bands and/or appearance of new bands.
(d) No change, banding pattern not different from that of untreated parental controls.

TABLE 2. Initiation-Promotion-Initiation (IPI) Protocol for Radon (R), Dust (D), and Cigarette-Smoke (S) Inhalation Exposure of Rats[a]

	Duration of Exposure, weeks					
Group	0	4	8	17	21	25
1	R+D---------->					
2	R+D----->					R+D->
3	R+D---->S---------->					R+D->
4	R+D---------->	S---------->				
5	S---------->			R+D---------->		
6	D---------->	S---------->				

(a) Moderately low concentrations of uranium ore dust (D) accompany radon exposures as the carrier aerosol for radon progeny; sham-exposed control animals (not shown) are included in each exposure group. Animals from each group are killed at 25, 52, and 78 weeks to evaluate developing lesions. Protocol may be repeated for different radon-progeny and cigarette-smoke exposure rates and levels.

progeny, uranium ore dust, and cigarette smoke, as well as on one sham-exposed group of animals (Table 3). These data are based on our historical protocol examination of one central section per lung lobe, plus any observed lesion at necropsy, rather than the multiple-slicing technique employed in the serially sacrificed rats reported in the 1990 *Annual Report*, Part 1. Multiple slicing of the remainder of the IPI life-span rat lungs for histopathological examination is in progress. As in the serially sacrificed rats, exposure-related lesions were limited to the lungs and tracheobronchial lymph nodes. Curiously, the majority of smoke-exposure-related carcinomas were epidermoid carcinomas in contrast to the generally greater incidence of adenocarcinomas in non-smoking-related tumors. Smoking-related tumors were also generally larger than non-smoking-related tumors; assuming spherical volumes, the average volume of smoking-related carcinomas was about twice as large as that of non-smoking-related carcinomas.

Table 4 shows the average severity grade of pulmonary adenomatosis observed in groups of IPI rats sacrificed at 25, 52, and 78 weeks from start of exposure in comparison with the average grade observed in life-span animals. Resolution of adenomatosis with time suggests that this preneoplastic lesion has both a repairable and nonrepairable component.

References Cited

Jostes, R. F., T. E. Hui, A. C. James, F. T. Cross, J. L. Schwartz, J. Rotmench, R. Atcher, H. H. Evans, J. Mencl, G. Bakale, and P. S. Rao. 1991. *In vitro* exposure of mammalian cells to radon: Dosimetric considerations. *Radiat. Res.* 127:211-219.

Wolff, S., R. Jostes, F. T. Cross, T. E. Hui, V. Afzal, and J. K. Wiencke. 1991. Adaptive response of human lymphocytes for the repair of radon-induced chromosomal damage. *Mutat. Res.* 250:299-306.

TABLE 3. Current Summary of Primary Lesions of the Lung in Life-Span Initiation-Promotion-Initiation (IPI) Rats (11,000 Series Experiments)[a]

Group Number	Exposure Regimen[c]	Number of Rats (and Group Average Severity Grade)[b]				
		Interstitial Reaction	Dust Macrophages	Adenomatosis	Tumors	
					Malignant	Benign
1	320	16(0.7)	34(1.5)	5(0.3)	5	0
2	Sham-exposed controls	9(0.4)	0	0	1	0
3	160/Shelf/160	19(0.8)	33(1.1)	1(~0)	1	2
4	Sham-exposed controls	-	-	-	-	-
5	160/Smoke/160	10(0.4)	33(1.4)	6(0.3)	3	0
6	Sham-exposed controls	-	-	-	-	-
7	320/Smoke	24(1.1)	34(1.5)	6(0.3)	3	1
8	Sham-exposed controls	-	-	-	-	-
9	Smoke/320	15(0.6)	32(1.2)	2(0.1)	-[d]	1
10	Sham-exposed controls	-	-	-	-	-
11	Ore dust/smoke	14(0.6)	34(1.6)	0	0	0
12	Sham-exposed controls	-	-	-	-	-

(a) Moderately low concentrations (5-6 mg/m^3) of uranium ore dust (2% U content) accompanied radon exposures as a carrier aerosol for the progeny; 34 animals were in each group. Data are based on examination of one central section per lung lobe plus any observed lesion at necropsy.

(b) Group average lesion severity grade is given in parentheses: +1 (very slight); +2 (slight); +3 (moderate); +4 (marked); +5 (extreme).

(c) Radon-progeny exposures shown are nominal;
320 = 320-WLM (100-WL) radon progeny + uranium ore dust delivered in 8-wk exposure period
160/Shelf/160 = 160 WLM (4 wk)/Shelf (17 wk)/160 WLM (4 wk).
All exposures except group 1 were completed in 25 weeks; cigarette-smoke exposures were 1 hr/d, 5 d/wk for 17 weeks at 0.5 mg/L total particulate mass concentration. Working level (WL) is defined as any combination of the short-lived radon progeny in 1 liter of air that will result in the ultimate emission of 1.3×10^5 MeV of potential α energy. Working-level month (WLM) is an exposure equivalent to 170 hours at a 1-WL concentration.

(d) Multiple primary hemangiosarcomas were found in the lungs of one Group 9 rat.

TABLE 4. Progression of Group Average Severity Grade of Adenomatosis in Initiation-Promotion-Initiation (IPI) Rats[a]

Exposure Regimen	Adenomatosis			
	25 wk	52 wk	78 wk	Death
320	0	1.0	2.2	0.3
160/Shelf/160	0.1	1.4	1.5	0
160/Smoke/160	0.5	1.2	2.1	0.2
320/Smoke	0.1	1.1	1.3	0.3
Smoke/320	0	0.1	0.9	0.1
Ore dust/smoke	0	0	0	0
Sham-exposed controls	0	0.1	0.1	0

(a) All exposures except Group 1 were completed at 25 weeks; see Table 3 footnote for additional information on these exposures.

Dosimetry of Radon Progeny

Principal Investigator: *A. C. James*

Other Investigators: *T. E. Hui, K. D. Thrall,[a] D. R. Fisher, and F. T. Cross*

This project provides the dosimetric and biokinetic models needed to integrate findings of the DOE Radon Research Program into a coherent and comprehensive assessment of human cancer risks from exposures to radon and thoron progeny. In particular, we contribute modeling and assessments needed to develop more defensible standards of radiological protection from radon progeny and other internal alpha emitters. We report here the dosimetric implications of new and more comprehensive data on the complete activity-size spectra of radon-progeny aerosols in underground mines and in homes. The new data enable evaluation of the variability in the coefficient that relates exposure to ^{222}Rn progeny potential α-energy to the critical dose received by bronchial epithelium in both underground miners and the general public exposed in their homes. We have used these results to reexamine each step in extrapolating to the general population the age- and time-dependency of radon-related lung cancer observed in underground miners by means of comparative dosimetry. For radon-exposed miners, we find that application of the risk factors currently recommended by the International Commission on Radiological Protection in the form of the calculated "effective dose" leads to an overestimate of lung cancer risk by a factor of approximately five. For the general public, the overprediction is greater. This highlights the need for further review of the validity of extrapolating risk factors that apply to high-dose-rate gamma radiation to the alpha radiation associated with radon exposure. We have also developed physiologically based pharmacokinetic and dosimetry models for other body tissues (using the available experimental data from laboratory animals and human subjects), and have applied these models to evaluate tissue doses to the U.S. population from exposure to radon, thoron, and their short-lived progeny.

Last year we reported contributions made by this project to the dosimetric modeling carried out by the National Research Council/National Academies of Science's panel on "Comparative Dosimetry of Radon in Mines and Homes" (NRC 1991). In this report we update the dosimetric analyses carried out for the NRC panel by applying the new data on the complete activity-size spectra of radon progeny in mines and homes that have been produced by the DOE Radon Research Program. These data represent a significant advance on the information available to the NRC panel, particularly for evaluating the large variability in radon-progeny aerosol characteristics both between and within mines and homes, and the resulting variability in the dose per unit exposure to potential alpha (α) energy (James, in press, a). Further, a recent study (Li and Hopke 1991) has measured, in homes, the effects of air cleaning on both the radon-progeny concentrations (degree of equilibrium with radon gas) and the activity-size spectrum of the airborne progeny (fraction of potential α-energy present as "unattached" atoms and that present as "ultrafine" aerosol particles). We have assessed elsewhere the dosimetric implications of this study (James, in press, a).

New Data for Projecting Lung Cancer Risk from Mines to Homes

We applied our lung dosimetry model developed in FY 1990 for the National Research Council's study to evaluate the new data on the complete activity-size spectrum in the underground mine environment obtained by Knutson and George (in press), and for a variety of home environments by Li (1990), Tu et al. (1991), and Wasiolek et al. (in press). Figure 1 shows the variation in bronchial dose per unit exposure to radon-progeny potential

(a) NORCUS Postdoctoral Fellow.

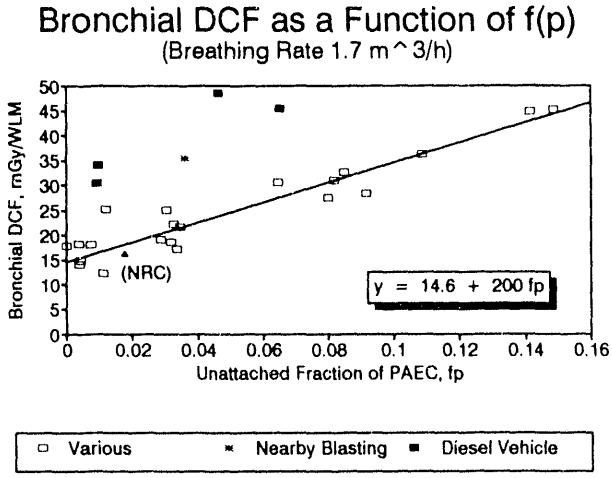

FIGURE 1. Dose Conversion Factor in Uranium Mines Versus Unattached Fraction.

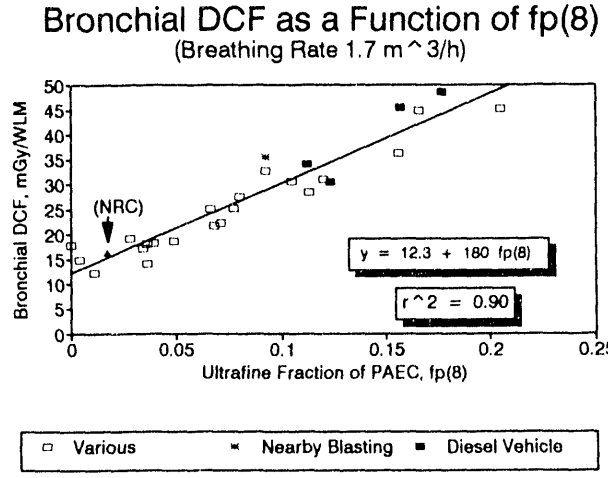

FIGURE 2. Correlation of the Dose Conversion Factor in Mines with Ultrafine Fraction.

α-energy modeled for 26 locations in underground uranium mines. The dose conversion factor (DCF) is here plotted as a function of the measured unattached fraction, f_p. Knutson and George used modern analytical techniques to derive complete activity-size spectra from original measurements made by George et al. (1975). According to their results, the dose per unit exposure varied over a fivefold range, with all except three values exceeding the reference exposure-DCF derived in the NRC (1991) study. Examination of these data showed that higher values of the DCF were associated with proximity to operating diesel-powered vehicles (see Figure 1). The modeled DCF is in general closely related to the unattached fraction of potential α-energy (which was found to vary over a surprisingly large range), but four measurements close by operating diesel trucks, and one made shortly after blasting, gave anomalously high values of the DCF. Overall, we found that the calculated DCF is more closely related to an "ultrafine" fraction of potential α-energy rather than the classical "unattached" fraction (Figure 2). The data are most highly correlated (r^2 = 0.9) when the modeled DCF is compared with the measured fraction of potential α-energy associated with airborne particles smaller than 8 nm in diameter, which we denote in Figure 2 by $f_p(8)$.

There are no other data (other than those of Knutson and George) of equivalent quality that can be used to calculate accurately the variability of the bronchial DCF in mine environments, neither for modern-day mining conditions nor, most emphatically, for the more primitive conditions relevant to the epidemiologic studies. However, assuming that values of f_p higher than about 4% would have been unlikely in the dusty mines of the 1950s and 1960s, and excluding high values associated with diesel exhaust, we derived from the data of Knutson and George an estimate of 20 mGy/WLM as a likely dose conversion factor under these historical mine conditions. This is 25% higher than the value of 16 mGy/WLM derived from the NRC (1991) assumed aerosol-size distribution.

Figure 3 shows the average values of bronchial DCF modeled from three recent studies of the complete radon-progeny activity-size spectra in 10 North American homes (Li 1990; Tu et al. 1991; Wasiolek et al., in press). In each of these homes multiple measurements were made; in the case of the studies of Li and Wasiolek, they were made repeatedly over week-long periods. It is seen that the DCF varies over an approximately fourfold range among these homes. Overall, we again found that the DCF derived from the assumed (NRC 1991) "typical" aerosol-size distribution in homes is low in comparison with the measured range. Figure 4 shows that the modeled DCF is again more closely correlated with an "ultrafine"

fraction of potential α-energy ($r^2 = 0.95$) than it is with the classical "unattached" fraction; in this case the relevant limit on particle size is found to be 15 nm in diameter. This ultrafine fraction is denoted in Figure 4 by $f_p(15)$.

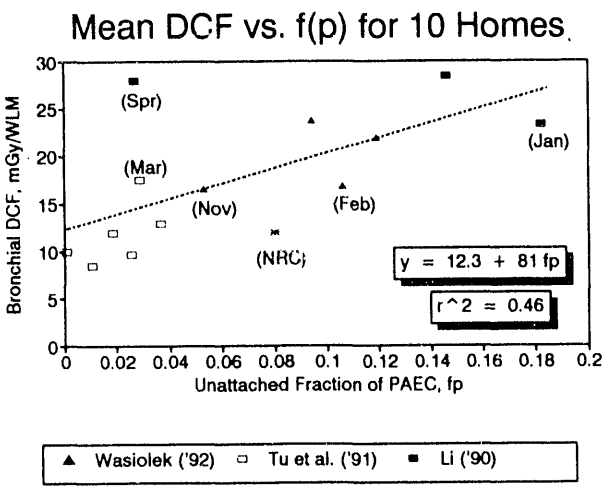

FIGURE 3. Dose Conversion Factor in 10 North American Homes Versus Unattached Fraction.

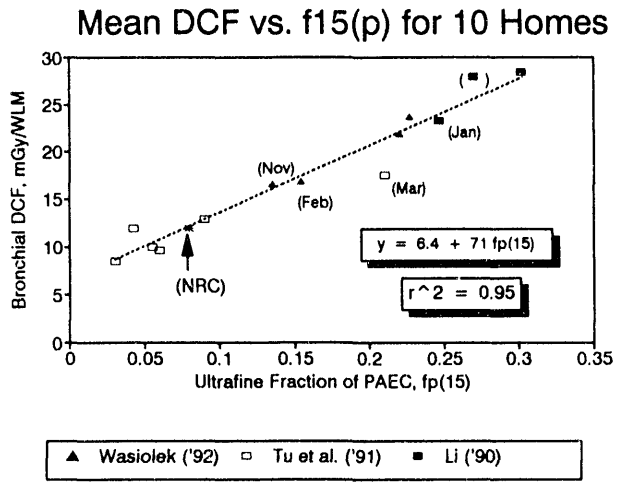

FIGURE 4. Correlation of the Dose Conversion Factor in Homes with Ultrafine Fraction.

By excluding one clearly unusual home environment, and giving equal weight to the data from each of the nine remaining homes, we derived a midrange value for the bronchial dose conversion factor of 16 mGy/WLM, which is 80% of the value estimated for a uranium miner. The modeled DCF in a home does not vary substantially with age or gender. It is about 40% higher for very young children than for a male or female adult.

Analysis of large numbers of measurements of the radon-progeny activity-size spectrum in normally occupied homes showed that, in a given home, the spot value of the DCF with respect to either radon-progeny or radon gas concentration varies over approximately a threefold range. Thus, to obtain representative values it is necessary to average the results of many spot measurements. Alternatively, it is clearly advantageous to extend a measurement over several days or a week to average out both hourly and daily variations in the indoor environment. In the related "Aerosol Technology Development" project we apply our specially designed ultrafine radon progeny particle-size spectrometer (URPSS) to make protracted (and unattended) measurements of the DCF in a range of different homes.

For the present, we have used our current estimate of the comparative dose per unit exposure between historical uranium mines and North American homes with the BEIR IV Committee's model (NRC 1988), to extrapolate to the home environment the lung cancer risk coefficient determined for uranium miners. According to the BEIR IV Committee's model, in which exposure early in life causes a relatively small increase in the expression of lung cancer (which occurs predominantly in old age), the higher dose per unit exposure modeled for children has a negligible impact on lung cancer risk. The projected risk for an average male from lifetime exposure to 150 Bq/m^3 radon gas concentration in the home (the current USEPA "Action Level") is estimated to be 2%, and that for an average female approximately 0.8%. For nonsmokers the projected risks are four- to fivefold lower, and for smokers approximately twofold higher, than the population average values.

We found that the effective dose calculated according to the ICRP Lung Modeling Task Group's proposed apportionment of radiation detriment of 0.85:0.15:0.05 between bronchial, bronchiolar, and alveolar tissue (Bair 1991; James et al. 1991) is 44 mSv/WLM for the uranium miner

and 35 mSv/WLM for indoor exposure. Table 1 compares the lifetime excess risks per unit exposure to radon progeny that are implied by these values of effective dose (ICRP 1991) with the values projected from the uranium miner epidemiologic data using the BEIR IV Committee model. Values range from 0.004%/WLM for a nonsmoking female member of the public to 0.088%/WLM for a smoking uranium miner. In comparison, the risk coefficients recommended by ICRP are constant at 0.0056%/mSv for a worker and 0.0073%/mSv for a member of the public. When defined in terms of equivalent risks, the conversion coefficient from exposure to effective dose is found to range from 0.5 mSv/WLM for a nonsmoking female member of the public to 16 mSv/WLM for a smoking uranium miner. The population average values are 9 mSv/WLM for a uranium miner and 4 mSv/WLM for a member of the public. To obtain these values using the ICRP dosimetry methods, it would be necessary to change the weighting factor for α-particle irradiation from the recommended value of 20 to a minimum value 0.3 for a nonsmoking female and a maximum value of 7 for a smoking uranium miner. The population-average values are $w_R = 4$ for the uranium miner and $w_R = 2.2$ for the public as a whole.

In the case of radon exposure and human lung cancer, the ICRP current formulation of effective dose leads to gross overpredictions of risk (James, in press, b). The fundamental question arises as to whether significantly lower risk weighting factors should also be applied for other α-emitters, and for other tissues, or whether these apply only to radon-progeny irradiation of the lung. We will continue to address this issue in this project.

Modeling Radon-Progeny Doses to Other Tissues

We have developed and tested, by comparing with human and laboratory animal data, physiologically based pharmacokinetic models for inhalation and ingestion of radon, thoron, and their short-lived progeny. We based our inhalation model for radon and thoron on the inert gas model developed by Peterman and Perkins (1988). We extended this model to develop the general pharmacokinetic model shown in Figure 5, which also represents the kinetic behavior of the short-lived polonium, lead, and bismuth progeny. We have factored parameters into the model to allow for body weight (degree of obesity) and ventilation and perfusion rates of individual subjects appropriate to their level of physical exertion (i.e., minute volume and blood flow through tissues). As an example of our results, Figure 6 (A and B) shows the measured and predicted exhalation of radon gas during a 2-day period following an 8-hour exposure (Harley et al. 1958). Figure 7 shows the measured and modeled whole-body retention of radon following ingestion in water. This was found to depend strongly on the subject's breathing rate as well as the quantity of water consumed. We are extending this modeling to include the effects of food intake on transit and uptake through the stomach and small intestine (in collaboration with C. T. Hess, University of Maine).

As an example of our preliminary dosimetric findings, Table 2 shows the doses calculated for stem cells in active bone marrow of adults and children. We consider here adults and children exposed in the home to radon and thoron concentrations of 55 and 50 Bq/m, respectively, the estimated average value for U.S. homes. Our current modeling results for radon confirm in general the doses calculated by Richardson et al. (1991), but not their estimates of dose contributed by inhaled progeny. However, the calculated dose from radon depends critically on assumptions made about the fat content of active marrow, the size distribution of the fat cells, and the degree of retention in the fat of ^{214}Pb, which is produced by the decay of ^{222}Rn and ^{218}Po (^{214}Bi is fat soluble). In the absence of more specific data we have temporarily adopted the assumptions of Richardson et al. regarding fat content and fat cell dimensions as a function of age. We are investigating these factors experimentally.

In the case of exposure to thoron and its progeny, only the progeny (principally ^{212}Pb) contribute significantly to tissue doses. The dose calculated for stem cells in bone marrow then depends critically on the assumptions made about ^{212}Pb uptake and retention in the marrow itself and on the contribution from ^{212}Pb uptake on bone surfaces (see Table 2). Again, carefully designed studies using the laboratory rat will enable us to refine our

TABLE 1. Comparison of Coefficients of Lifetime Excess Risk (L-ER) Per Unit Exposure to ^{222}Rn Progeny Derived from Uranium Miner Epidemiologic Data Using BEIR IV Model with Risk Coefficients Derived from Atomic Bomb Survivor Data and Calculated Effective Dose

Subjects	Smoking Status	BEIR IV L-ER Coefficient, %/WLM	ICRP 60 L-ER Coefficient, %/mSv	Derived DCF, mSv/WLM	Calculated DCF, mSv/WLM	Normalization Factor,[a] N_{Rn}	Implicit Radiation Weighing Factor,[b] w_{Rn}
Uranium miners	Smokers	0.088	0.0056	16	44	0.36	7
	Nonsmokers	0.009	0.0056	1.6	44	0.04	1
	Population Average	0.052	0.0056	**9**	44	**0.2**	**4**
Male public	Smokers	0.071	0.0073	10	35	0.29	6
	Nonsmokers	0.007	0.0073	1.0	35	0.03	0.6
	Population Average	0.042	0.0073	5.8	35	0.17	3
Female public	Smokers	0.038	0.0073	5.2	35	0.15	3
	Nonsmokers	0.004	0.0073	0.5	35	0.014	0.3
	Population Average	0.017	0.0073	2.3	35	0.10	1.4
Total public	Smokers	0.055	0.0073	7.5	35	0.21	4
	Nonsmokers	0.006	0.0073	0.8	35	0.02	0.4
	Population Average	0.030	0.0073	**4**	35	**0.11**	**2.2**

(a) Factor by which calculated effective dose has to be multiplied to obtain the value derived from BEIR IV model (based on epidemiologic data from underground miners).

(b) Factor needed to replace $w_R = 20$ in calculated effective dose to give the same estimated of lifetime excess risk as BEIR IV model (i.e., $w_{Rn} = N_{Rn} \times w_R$).

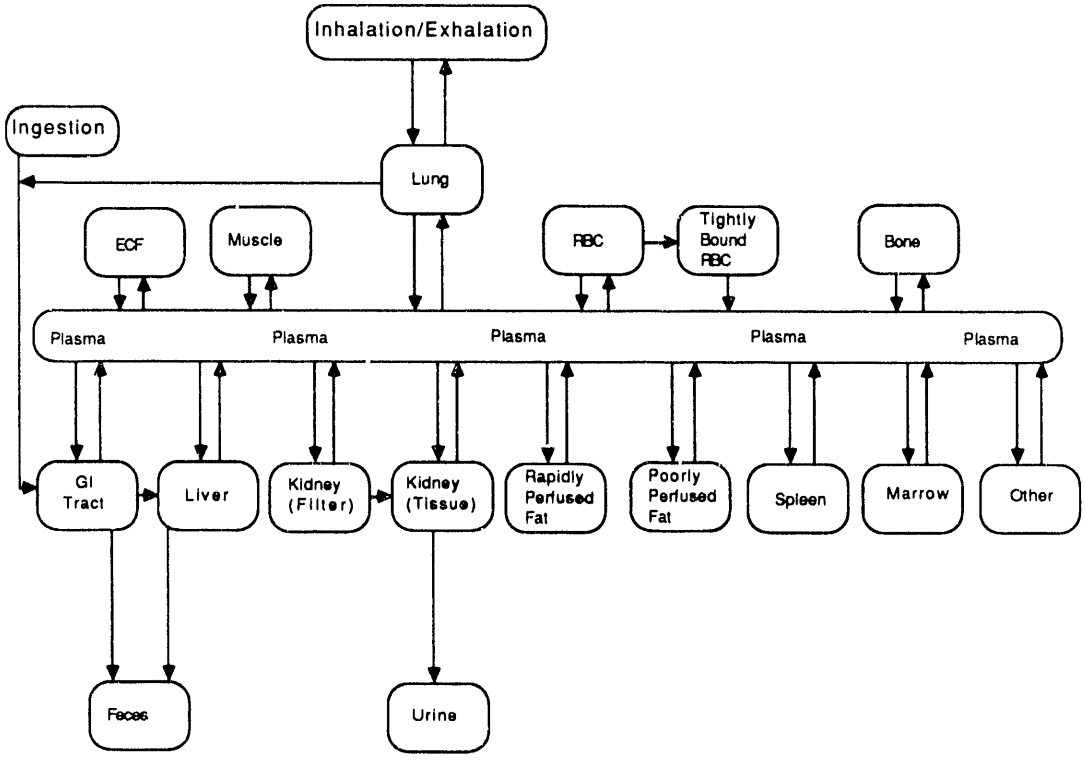

FIGURE 5. General Biokinetic Model for Radon, Thoron, and Their Short-Lived Progeny.

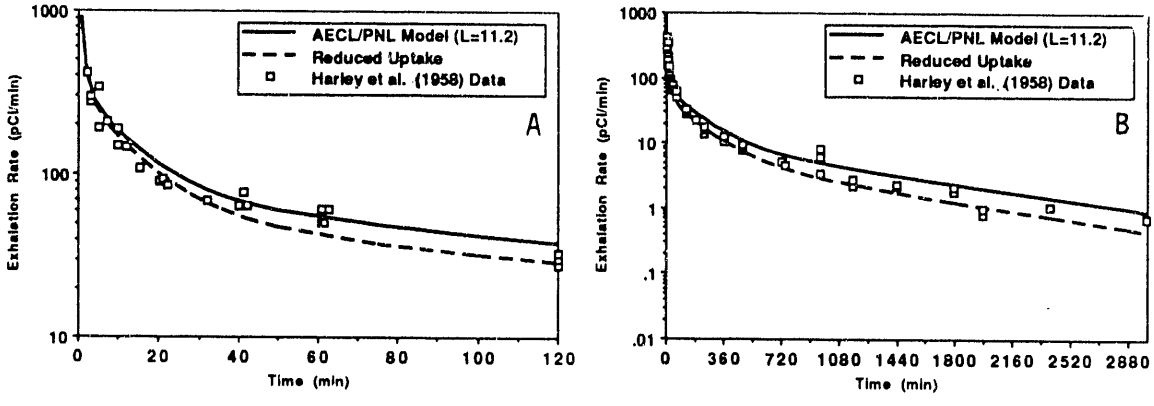

FIGURE 6. Short- and Long-Term Exhalation of Radon Following an 8-Hour Exposure.

TABLE 2. Estimates of Annual Average Equivalent Dose (in μSv/yr) to Active Bone Marrow from Exposure of U.S. Population to Radon (^{222}Rn), Thoron (^{220}Rn), and Their Short-Lived Progeny

Model	Source	Subject/Timeframe					
		Man	Woman	10 yr	5 yr	1 yr	3 mo
Richardson et al. (1991)	^{222}Rn	154	136	128	92	-	31
	Progeny	11	20	33	55	-	26
	Total	165	156	160	147	-	57
	^{220}Rn progeny	75	115	193	301	-	125
This project	^{222}Rn	145	121	126	111	89	64
	Progeny	0.5	0.5	0.8	1.0	1.5	1.1
	Total	145	121	127	112	90	65
	(excluding activity in fat)	(26)	(32)	(35)	(44)	(62)	(58)
	^{220}Rn	3	3	4	5	6	6
	Progeny	11	13	21	30	53	40
	Total	14	16	24	34	59	46
	(excluding activity in fat)	(5)	(6)	(8)	(11)	(18)	(15)

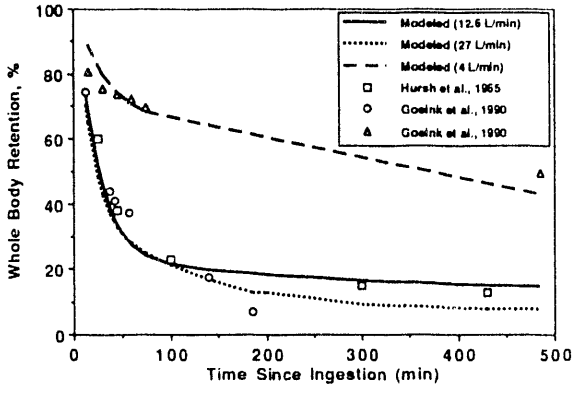

FIGURE 7. Whole-Body Retention of Radon Following Ingestion.

physiologically based model of bone marrow dosimetry, and also our models of the dosimetry of kidney, liver, and circulating blood cells, both in animals and the human (in collaboration with Dr. C. Badger, Fred Hutchinson Cancer Research Center, Seattle).

References Cited

Bair, W. J. 1991. Overview of ICRP respiratory tract model. *Radiat. Prot. Dosim.* 38(3/4):179-188.

George, A. C., L. Hinchliffe, and R. Sladowski. 1975. Size distribution of radon daughter-particles in uranium mine atmospheres. *Am. Ind. Hyg. Assoc. J.* 36:484-490.

Gosink, T. A., M. Baskaran, and D. E. Holleman. 1990. Radon in the human body from drinking water. *Health Phys.* 59:919-924.

Harley, J. H., E. Jetter, and N. Nelson. 1958. *Elimination of Radon from the Body.* Report No. HASL-32. U.S. Atomic Energy Commission Health and Safety Laboratory, New York.

Hursh, J. B., D. A. Morken, T. P. Davis, and A. Lovaas. 1965. The fate of radon ingested by man. *Health Phys.* 11:465-476.

International Commission on Radiological Protection (ICRP). 1991. *1990 Recommendations of the International Commission on Radiological Protection.* ICRP Publication 60. *Ann. ICRP* 21(1-3).

James, A. C. *The Dosimetry of Human Exposures to Radon, Thoron, and Their Progeny: I. Quantification of Lung Cancer Risk from Indoor Exposure.* DOE/OHER Radon Technical Report Series (in press, a).

James, A. C. Dosimetry of radon and thoron exposures: Implications for risks from indoor exposure. In: *Indoor Radon and Lung Cancer: Reality or Myth?*, F. T. Cross, ed., Proceedings of the 29th Hanford Symposium on Health and the Environment, Richland, Washington. Battelle Press, Columbus, Ohio (in press, b).

James, A. C., P. Gehr. R. Masse, R. G. Cuddihy, F. T. Cross, A. Birchall, J. S. Durham, and J. K. Briant. 1991. Dosimetry model for bronchial and extrathoracic tissues of the respiratory tract. *Radiat. Prot. Dosim.* 37:221-230.

Knutson, E. O., and A. C. George. Reanalysis of data on the particle-size distribution of radon progeny in uranium mines. In: *Indoor Radon and Lung Cancer: Reality or Myth?*, F. T. Cross, ed. Battelle Press, Columbus, Ohio (in press).

Li, C.-S. 1990. *Field Evaluation and Health Assessment of Air Cleaners in Removing Radon Progeny Decay Products in Domestic Environments.* Ph.D. Thesis. Report No. DOE ER61029-2. University of Illinois at Urbana-Champaign, Ilinois.

Li, C.-S., and P. K. Hopke. 1991. Efficiency of air cleaning systems in controlling indoor radon decay products. *Health Phys.* 61:785-797.

National Research Council (NRC). 1988. *Health Risks of Radon and Other Internally Deposited Alpha-Emitters.* BEIR IV, Committee on the Biological Effects of Ionizing Radiation. National Academy Press, Washington, D.C.

National Research Council (NRC). 1991. *Comparative Dosimetry of Radon in Mines and Homes.* Report by a scientific panel. National Academy Press, Washington, D.C.

Peterman, B. F., and C. J. Perkins. 1988. Dynamics of radioactive chemically inert gases in the human body. *Radiat. Prot. Dosim.* 22:5-12.

Richardson, R. B., J. P. Eatough, and D. L. Henshaw. 1991. Dose to red bone marrow from natural radon and thoron exposure. *Br J. Radiol.* 64:608-624.

Tu, K. W., E. O. Knutson, and A. C. George. 1991. Indoor radon progeny aerosol size measurements in urban, suburban, and rural regions. *Aerosol Sci. Technol.* 15:170-178.

Wasiolek, P. T., P. K. Hopke, and A. C. James. Assessment of exposure to radon decay products in realistic living conditions. *J. Exposure Anal. Environ. Epidemiol.* (in press).

Aerosol Technology Development

Principal Investigator: *A. C. James*

Other Investigators: *J. K. Briant, M. A. Parkhurst, and J. A. Mahaffey*

The purpose of this project is to develop and transfer aerosol technology to basic and applied research in biology and chemistry, especially in the areas of health and environmental effects of energy-related materials. We report here further development of PNL's Ultrafine Radon Progeny Size-Spectrometer (URPSS) and manufacture of a series of instruments for deployment in experimental animal studies and characterization of human exposure environments; the development of CR-39 α-track detectors for the Integrating Low-Pressure Impactor (ILPI) and the application of the ILPI to measure the activity-size distribution of airborne radon progeny and uranium aerosols; the development of the Past-Exposure Radon Monitor (PERM) and basic techniques for automated α-track recognition and analysis; progress in modeling the relationship between ^{210}Po activity accumulated on an exposed surface in a room and bronchial dose; and progress in developing a computational model based on fluid mechanical principles that predicts the volumetric dispersion and particle recovery as a function of breath-hold time and heartbeat rate for an aerosol bolus inhaled to a shallow depth by a human subject.

The ongoing objectives of this project are (1) to improve systems for the control, monitoring, and characterization of exposures of laboratory animals to toxic aerosols, gases, and vapors; (2) to develop simpler and more widely applicable techniques to characterize ultrafine and attached radon progeny in domestic and occupational settings, especially to transfer PNL's CR-39 (poly-[ethylene glycol *bis*-(allyl)]carbonate) track-etch and analysis technology to improve the monitoring and characterization of occupational and environmental exposures to radon progeny and other alpha (α) emitters; (3) to deploy these techniques in the field to obtain representative data for human dosimetry and risk assessment; and (4) to apply fluid mechanical concepts to resolve paradoxical experimental findings that appear to imply protracted retention of particles on the surface of human bronchi after deposition from an aerosol bolus inhaled to a shallow depth.

Development of the Ultrafine Radon Progeny Size-Spectrometer (URPSS)

Last year we reported the design and testing of a prototype URPSS instrument. We have improved on the original design by adding a proportional flow sampling system and detector collimator to the final filter stage (Figure 1). The proportional flow-sampler reduces the amount of airflow passing through the central part of the filter (which is viewed by the small CR-39 α-detector chip) to only 3% of the total flow. The flow-reducer was needed to match the dynamic response of the "attached" radon-progeny detector to that of the 15-cm-long CR-39 plate, which measures the activity-size spectrum of "ultrafine" progeny. Reducing the fraction of airflow sampled by the small CR-39 detector chip prevented overloading with α-tracks of too high density.

We also developed a technique to coat the surfaces of the CR-39 detectors with a thin, electrically conductive layer of aluminum. This has been shown to prevent nonuniformity in the recorded pattern of α-tracks caused by the buildup of electric charge. Distortion of the theoretically predicted pattern of radon-progeny deposition along the CR-39 detector strip caused by charging effects was found to be a major problem in the prototype URPSS; the original coating of carbon was not sufficiently conductive and also interfered with the chemical etching process. The same thin coating with aluminum was found to solve charging problems in CR-39 detectors developed for the Integrating Low-Pressure Impactor (ILPI).

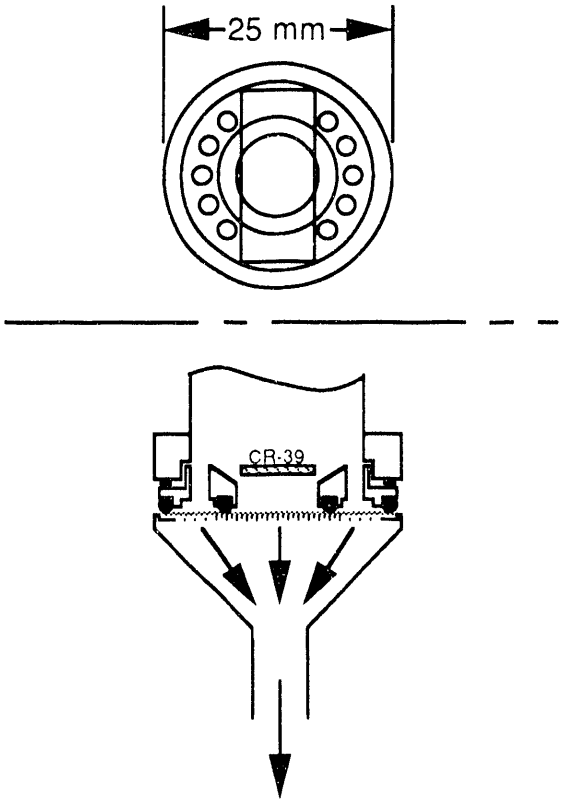

FIGURE 1. Proportional Flow Sampling Stage of the URPSS Device for Measuring Attached Radon Progeny.

Development and Application of the Integrating Low-Pressure Impactor (ILPI)

We designed a set of CR-39 detector plates to fit each of the 10 particle-collection stages of the Andersen SE-218 radial-slot low-pressure impactor (Andersen Samplers Inc., Atlanta, Georgia). With the thin aluminum coating developed for the URPSS applied to these detector plates, test samples from PNL's experimental animal radon exposure system showed a well-defined Gaussian pattern of α-tracks at each size-selective stage. When exposed to airborne radon progeny, the ILPI device gives an α-track density under each radial slot that is proportional to the total amount of potential α-energy collected by that size-selective stage.

We also used CR-39 α-track autoradiography to increase the sensitivity of the Andersen SE-218 low-pressure impactor in measuring the activity-size distribution of airborne uranium at an uranium fuels fabrication facility. The low background of CR-39 enabled the uranium α-activity collected at each stage to be measured with high statistical precision by exposing the CR-39 detectors to the collection media for several days. We applied the same technique to obtain statistically valid α-counts from all collection stages of an Andersen 2000 Ambient Cascade Impactor. However, we found from side-by-side samples at the fuels facility that the activity-size distributions unfolded from the two impactors consistently differed. Of these two instruments, the multiple circular-jet Andersen 2000 impactor has been more widely studied, and its particle-sizing characteristics are better established. Because the smaller SE-218 impactor with its radial-slot jets provides an ideal pattern of α-tracks for automatic counting, we plan to carry out a thorough laboratory calibration of its particle-sizing characteristics.

Development of Past-Exposure Radon Monitor (PERM) and CR-39 α-Track Technology

The logistical aspects of measuring *in situ* (in a subject's home) the ^{210}Po activity that had accumulated on the surface of a personal possession over a common period of past exposure to radon were addressed in a joint PNL study funded by the National Cancer Institute. In this project (with additional PNL discretionary research funding), we developed the basic technology to apply small CR-39 detectors to this task. Figure 2 compares the ^{210}Po activity measured on 13 different glass artifacts belonging to subjects included in a case-control study of radon and lung cancer in nonsmoking women with independent estimates of their total exposure to radon in each of their previous homes (Mahaffey et al., in press). These measurements, made *in situ* with CR-39 α-track detectors, were compared with results reported by Samuelsson et al. (in press) in Sweden, who used a pulse ionization chamber in his laboratory to measure ^{210}Po activity on samples of glass

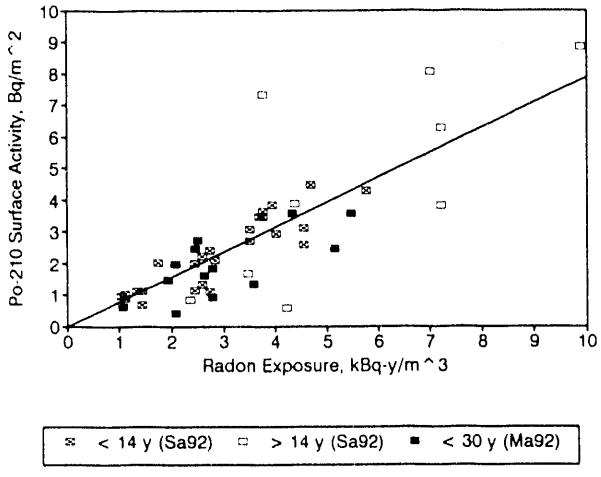

FIGURE 2. Relationship Between ^{210}Po Surface Activity and Past Radon Exposure Measured in Homes in the United States (Ma92) and Sweden (Sa92).

removed from homes. We found the same relationship between ^{210}Po activity and past radon exposure in the U.S. homes (in Missouri) as did the Swedish study. Our measurements were of gross α-activity, corrected for the average background α-activity of glass samples. Regression analysis of the measured gross α-activity as a function of past radon exposure showed the average bulk-activity (background) of glass samples to be approximately 1.3 Bq/m^3. This value was confirmed in the laboratory by measuring 10 pieces of glass from various sources but was found to be highly variable between samples. These results demonstrated that the *in situ* measurement of surface α-activity yields meaningful estimates of past radon exposure, but for unbiased estimates it is necessary to resolve the ^{210}Po activity from the variable glass background. We are developing integrated software for the automatic recognition and dimensional analysis of α-tracks in CR-39, which discriminates tracks with dimensions consistent with the 5.3-MeV incident energy of the ^{210}Po α particle.

Relating ^{210}Po Accumulated on an Exposed Surface to Bronchial Dose

In the project "Dosimetry of Radon Progeny," we used the available data on the variation of radon-progeny unattached fraction and equilibrium factor between 10 different North American homes to estimate a set of "typical" values, including an average conversion coefficient between the radon gas concentration and bronchial dose rate. In this project we have modeled the associated rates of progeny plate-out on exposed surfaces and the resulting buildup and decay of trapped ^{210}Pb and ^{210}Po activity. Figure 3 summarizes our resulting estimates of a direct conversion coefficient between duration of exposure to radon gas (at an assumed concentration of 1 kBq/m^3) and risk-normalized effective dose (in mSv) per Bq/m^2 measured surface concentration of ^{210}Po. Based on the available direct measurements of ^{210}Po surface activity and past radon exposure in homes (ours and the Swedish results), and our model relating room plate-out behavior to lung dose, we obtained an estimated conversion coefficient of about 40 mSv per Bq/m^2 measured ^{210}Po. Alternatively, using the surface plate-out rate modeled directly from what we assume to be a "typical" radon progeny activity-size distribution in U.S. homes yielded an estimate of about 20 mSv per Bq/m^2 calculated ^{210}Po activity. To achieve a closer match between modeled results (which provide the direct link with bronchial dose) and measured ^{210}Po surface activity, further experimental studies are needed to relate surface plate-out rates more specifically to the airborne activity-size spectra in a wider selection of normally occupied homes and in the laboratory.

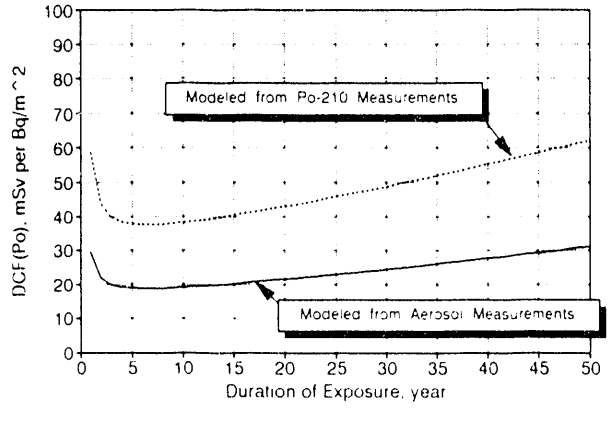

FIGURE 3. Conversion Coefficient from ^{210}Po Surface Activity to Effective Dose Modeled as a Function of Exposure Duration.

Fluid Mechanical Model of Aerosol Bolus Dispersion in Human Lungs

Aerosol bolus dispersion has been used to characterize airway morphometry and to deduce the location of aerosol particle deposition in studies of particle clearance from the human bronchi. A bolus as small as 10 cm^3 is placed at some volumetric point in an inhaled breath, and then inhaled to a controlled depth in the lungs. The concentration of aerosol particles in the exhaled air is then measured as a function of the volume exhaled after some period of breath-hold. The bolus is spread to a much broader form upon exhalation, as shown in Figure 4 from measurements made by Scheuch and Stahlhofen (1990). In this example, a 10-cm^3-wide bolus (full width, half maximum) is spread to a width of 175 cm^3 on exhalation with essentially no breath-hold (0.5 s).

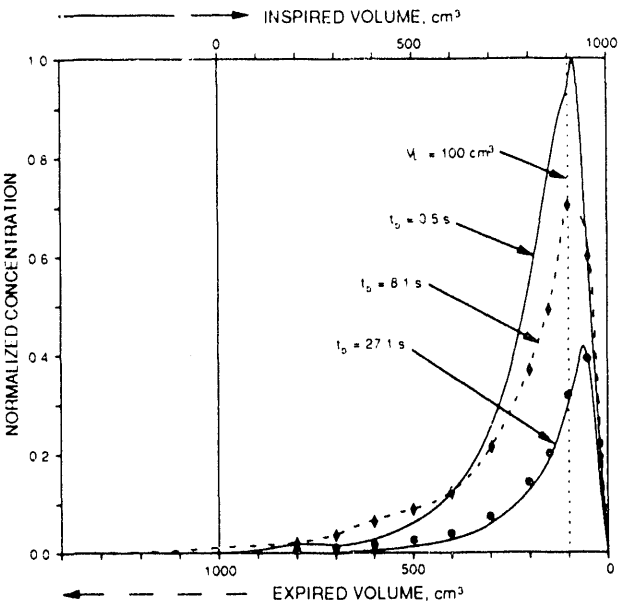

FIGURE 4. Comparison of the Exhaled Aerosol Particle Bolus Measured in a Human Subject as a Function of Breath-Hold with That Predicted by the PNL Computational Model.

The measurement of dispersion shows the volumetric standard deviation of the expired bolus to initially increase with time of breath-hold, then gradually decrease as the total number of exhaled particles decreases. Scheuch and Stahlhofen (1990) interpreted the decreasing dispersion as "a result of particle losses due to gravitational settling in small airways." Because the bolus is shallow, this implies that the particles have settled onto airway surfaces which should be cleared rapidly by the mucociliary mechanism. However, Scheuch and Stahlhofen (1991) observed that a large fraction (up to 70%) of these particles are cleared slowly. They concluded that bronchial clearance is not completed rapidly, as previously assumed. This inference has a major impact on the absorbed dose from long-lived α-emitters that would be received by bronchial epithelium, and on the implied risks of bronchogenic cancer from these materials (Bair 1991; James et al. 1991).

We are developing a computational model, based on the fluid mechanics of bolus penetration and cardiogenic transport, which is leading to a very different conclusion about the site of particle deposition from a shallow aerosol bolus. To interpret these experiments, it is necessary to establish a fundamental premise for the mechanism of particle loss. Scheuch and Stahlhofen assumed that particles are lost from the spread bolus solely by gravitational deposition in the ciliated airways. Our model differs in that particles are shown to disappear from the spread bolus by a convective mechanism which carries some of them to peripheral (nonciliated) airways of the lungs, in conjunction with gravitational deposition. The convective mechanism is caused by motion of the beating heart (cardiogenic air-motion). The fluid mechanical basis of cardiogenic transport is the same mechanism responsible for the transport of particles by shallow, high-frequency ventilation (Briant et al. 1988, 1992, in press). Cardiogenic air-motion during a breath-hold resembles a weak and somewhat localized form of high-frequency ventilation. A quasi-steady, bidirectional stream of convective air-motion is conducted by the motion of the heart. Aerosol particles suspended in the inhaled bolus are carried in the core of airways by the cardiogenic air-motion to regions of the lung far beyond the inhaled volume, where many deposit on nonciliated surfaces.

In the computational model, particles are transported by cardiogenic air-motion from a given volumetric compartment to one immediately below

it (distal from the trachea) with an empirically determined efficiency. Particles are transported from the initial compartment to the one which is two levels below with a lesser efficiency, and to the one which is three levels below with even lesser efficiency. At shallow depths, in the most central airways, the transport efficiency is relatively low. Deeper airways have much higher efficiency of transport to lower airways by each cycle of cardiogenic air-motion. Using the data shown in Figure 4, for example, the actual efficiencies are derived empirically by aligning the position of the curve predicted for 8-sec breath-hold with respect to the initial spread of the bolus (0.5-sec breath-hold). This alignment serves to calibrate the computational model for the particular subject under study.

Because the transport efficiencies remain constant, changes in the shape of the bolus with time of breath-hold are caused directly by the transport process. Having calibrated the model, we found that the spread of the exhaled bolus with further breath-hold is predicted with remarkable precision (see Figure 4). In this example, the change in computed shape of the bolus from the initial spread at 0.5 sec to the spread at 8 sec (dispersion) involves 6 cycles of computation corresponding to complete cardiac cycles, and the predicted change from 8 sec to 27 sec, an additional 13 cycles. Any unrealistic relationship in the empirical model would be dramatically amplified by 13 cycles of computation beyond the calibration point.

Particles experiencing transport by cardiogenic motion are kept airborne much longer than would occur during settling to airway surfaces in undisturbed air. Figure 5 shows the agreement of the modeled aerosol recovery with experimental values. According to our model, aerosol particles suspended in the air of the spread bolus are carried by the cardiogenic air-motion in the core of airways to regions of the lung far beyond the exhaled volume, where they eventually do deposit. The deposition in peripheral airways by deep bolus penetration, and farther transport by cardiogenic air-motion, result in the observed slow clearance of a large fraction of the total lung deposition by the established slow mechanisms of clearance from the respiratory airways and alveoli.

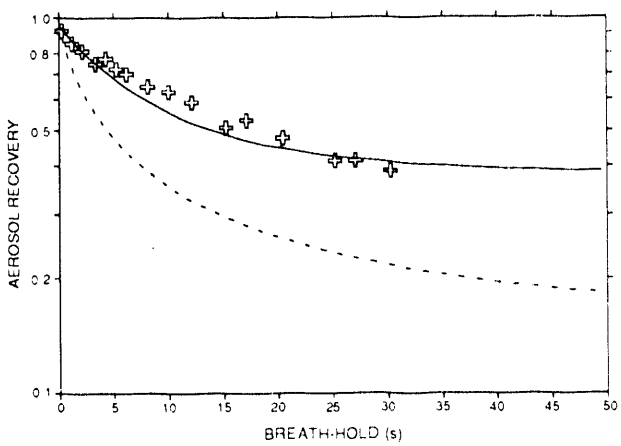

FIGURE 5. Measured Aerosol Recovery as a Function of Breath-Hold for a Shallow Bolus of 2.6-μm Particles Compared with PNL Prediction.

As a further illustration of the predictive power of our particle transport model, Figure 6 compares the predicted standard deviation of the exhaled bolus as a function of breath-hold time with the values measured by Scheuch and Stahlhofen (1990) in an experimental subject at two different heartbeat rates. The actual heartbeat rate of 40 per minute is used in the model for the rest condition. The dotted curve in Figure 6 is computed for twice this resting heartbeat rate. It is seen that the transport efficiencies predicted by the model are consistent with both the shape of the bolus dispersion and the magnitude of dispersion as a function of breath-hold time and heartbeat rate.

Bronchial dosimetry for radioactive materials emitting short-range radiations and also for chemically toxic particles is profoundly influenced by the interpretation put on the studies of particle clearance following deposition of an aerosol bolus that has been assumed to have been inhaled to a shallow depth. We are collaborating with Dr. Stahlhofen and his colleagues at the GSF Aerosol Biophysics Laboratory, Frankfurt, Germany, to develop our model to the point where we believe we can resolve the paradoxical issue of "slow bronchial clearance."

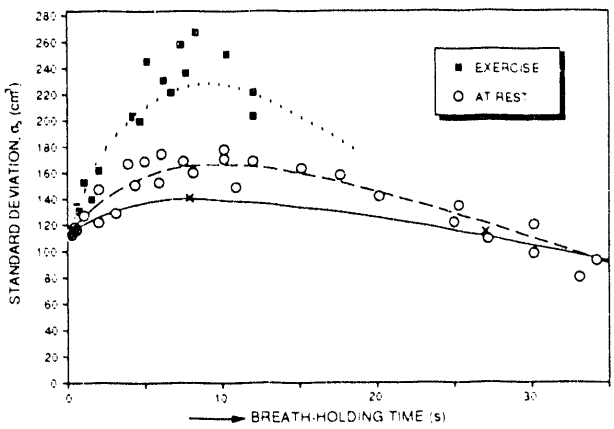

FIGURE 6. Measured and Predicted Standard Deviation of an Exhaled Aerosol Bolus as Functions of Breath-Hold Time and Hearbeat Rate.

References Cited

Bair, W. J. 1991. Overview of ICRP respiratory tract model. *Radiat. Prot. Dosim.* 38(3/4):179-188.

Briant, J. K. 1988. *Distinction of Reversible and Irreversible Convection by High-Frequency Ventilation of a Respiratory Airway Cast.* Ph.D. Thesis, New York University, New York.

Briant, J. K., and M. Lippmann. 1992. Particle transport through a hollow canine airway cast by high-frequency oscillatory ventilation. *Exp. Lung Res.* 18:385-407.

Briant, J. K., D. D. Frank, A. C. James, and L. L. Eyler. Numerical simulation of aerosol particle transport by oscillating flow in respiratory airways. *Ann. Biomed. Eng.* (in press).

James, A. C., P. Gehr, R. Masse, R. G. Cuddihy, F. T. Cross, A. Birchall, J. S. Durham, and J. K. Briant. 1991. Dosimetry model for bronchial and extrathoracic tissues of the respiratory tract. *Radiat. Prot. Dosim.* 37:221-230.

Mahaffey, J. A., M. A. Parkhurst, A. C. James, F. T. Cross, M. C. R. Alavanja, S. Ezrine, P. Henderson, and R. M. Brownson. Feasibility study to evaluate affixing CR-39 to glass artifacts for estimating past exposure to radon. *Health Phys.* (in press).

Samuelsson, C., L. Johansson, and M. Wolff. Po-210 as a tracer for radon in dwellings. In: *Proceedings of the Fifth International Symposium on the Natural Radiation Environment, NRE V,* September 22-28, 1991, Salzburg, Austria. *Radiat. Prot. Dosim.* (in press).

Scheuch, G., and W. Stahlhofen. 1990. Dispersion of aerosol boluses in the human tracheobronchial-tract during periods of breath-holding. *J. Aerosol Sci.* 21:S431-S434.

Scheuch, G., and W. Stahlhofen. 1991. Effect of heart rate on aerosol recovery and dispersion in human conducting airways after periods of breath-holding. *Exp. Lung Res.* 17:763-787.

Oncogenes In Radiation-Induced Carcinogenesis

Principal Investigator: *G. L. Stiegler*

Other Investigators: *M. E. Foreman, M. F. Minnick,[a] T. M. Seed,[b] E. C. Sisk, and L. C. Stillwell*

We are analyzing how oncogenes are molecularly activated in radiation-induced carcinogenesis. Radon-induced rat lung tumors and leukemia cells from dogs exposed to gamma radiation are being analyzed for mutations in the *ras* gene family by polymerase chain reaction (PCR) amplification, molecular cloning, and DNA sequence analysis. We have identified mutations in K-*ras* and H-*ras* genes in radon-induced rat lung tumors and H-*ras*, K-*ras*, and N-*ras* mutations in spleen cells from dogs with radiation-induced leukemia. To facilitate analysis of a large number of available tumor samples, we have adapted more rapid mutation assays: the single-strand conformational polymorphism (SSCP) assay and the chemical mismatch cleavage (CMMC) assay.

Carcinogenesis is a multistage process caused by genetic changes that alter the normal function of proto-oncogenes or tumor suppressor genes. Proto-oncogenes are normal cellular genes that become oncogenes when mutationally activated. Proto-oncogenes and tumor suppressor genes are critical genes in the highly regulated pathways of growth and differentiation, and their oncogenic activation increases the probability of neoplastic transformation. Tumor initiation can be produced in normal cells by inherited genetic defects or by exposure to chemical or physical agents that cause somatic mutation. The genetic changes can be point mutations, small deletions, or the loss of an entire allele. These changes can cause a decreased responsiveness to cellular signals such as growth factors and inducers of cell differentiation, and this change can result in a cellular growth advantage. Populations of cells that are expanding more rapidly have an intrinsic genomic instability and a greater probability that additional mutations will occur, resulting in an evolving increase in growth aggressiveness.

(a) University of Montana, Missoula, Montana.
(b) Argonne National Laboratory, Argonne, Illinois.

Molecular Analysis of Gene Mutations

Colorectal tumor developmental progression from the benign adenoma to the fully malignant phenotype has been studied using molecular analysis. A model developed by Fearon and Vogelstein (1990) proposed that mutational activation of oncogenes and tumor suppressor genes contributes to the development of the colorectal tumors and that the malignant tumor phenotype requires a mutational event in at least four or five genes, whereas fewer genetic changes are found associated with benign colorectal tumors. Their studies indicate that the accumulation of gene mutations, rather than the order of mutational activating events, contributes to carcinogenesis.

Activated *ras*, found in 40% to 50% of colon carcinomas, is often an early event in tumorigenesis correlated with aggressive growth and cell survival. The occurrence of a mutated *ras* gene is closely associated with tumor size; adenomas and carcinomas greater than 1 cm in diameter show a much higher frequency of activated *ras* than do smaller tumors. In addition to *ras* gene activation, frequent rearrangements on chromosomes 5, 17,

and 18 have been identified in colorectal tumors, correlating with the alteration of the FAP, p53, and DCC gene loci, respectively.

Role of Oncogenes in Carcinogenesis

The association of malignant tumor progression with the activation of several critical proto-oncogenes supports the hypothesis that molecular genetic markers can be used to characterize tumor initiation and development. Radiation-induced versus chemically induced oncogenesis may preferentially activate certain genes. It is also possible that radiation and chemical mutagens might produce a predictable type of damage; radiation may preferentially induce damage by deletion whereas chemicals more often cause damage by point mutation. Research directed toward identifying and characterizing radiation-damaged oncogenes will provide molecular markers that might distinguish radiation-induced and nonradiation-induced carcinogenesis. The focus of our research effort is to identify and characterize oncogenes that are associated with radiation-induced damage.

Both dominant and recessive oncogenes are associated with carcinogenesis. Dominant oncogenes, such as *ras*, are activated by mutational events so that the products of the genes have a direct effect on tumor progression. Tumor suppressor genes act in a recessive or negative manner by decreasing the activity of other genes that regulate growth or differentiation. Mutations that occur at these loci usually cause inactivation of the suppressor gene rather than a dominant activation. PNL studies that focus on the involvement of tumor suppressor genes in radiation-induced carcinogenesis are described in *Mutation of DNA Targets* (this volume).

This project has been investigating the dominant-acting *ras* oncogene family. We have focused on characterization of lesions that activate *ras* oncogenes because the *ras* oncogene family is the best characterized group of oncogenes, with a large database available on gene activation induced by chemicals; however, little is known about radiation-induced *ras* activation. It is known that *ras* oncogenes are activated by point mutations in codons 12, 13, 59, and 61. Codon position 12 must always code for the amino acid glycine, and gene activation results from substitution of any other amino acid residue. Only two amino acids, glutamic acid and proline, are acceptable at position 61; any other amino acid yields a transformationally active *ras* gene. Amino acid substitutions at codons 13 and 59 also lead to *ras* gene activation. The exact function of the *ras* genes is not known, but they are believed to be involved in signal transduction through transmembrane signaling systems.

Lesions in *ras* Genes Induced by Radiation

During this past year we have concentrated our research efforts on frozen spleen samples from myelomonocytic leukemic dogs, in which leukemia was induced by exposing the dogs to whole-body gamma radiation at Argonne National Laboratory (ANL), and on rat lung tumor samples from studies of animals exposed to radon progeny or to radon-progeny and cigarette-smoke inhalation at PNL (see *Mechanisms of Radon Injury*, this volume). The 1st exon of the N-*ras*, H-*ras*, and K-*ras* genes has been examined by polymerase chain reaction (PCR) amplification, molecular cloning of the products, and characterization by DNA sequence analysis. We are examining a number of cloned PCR samples from each tumor. The analysis has not been completed; however, a list of the tumors thus far analyzed and the accumulated sequence data are shown in Tables 1 and 2.

In summary, we have found 12th-codon activating lesions in H-*ras* and K-*ras* in one leukemic dog spleen sample and identified an N-*ras* 13th-codon lesion in another spleen sample. The 12th-codon activating lesions of H-*ras* and K-*ras* that occur in the same tumor sample are unusual, and we hope that these lesions may provide molecular markers in tumor progression. The leukemic tumors provide an excellent source of experimental material for this type of study because blood lymphocyte samples have been collected and frozen throughout the course of the disease.

The frozen samples provide experimental material useful for PCR mRNA amplification as well as DNA. For example, the N-*ras* mutation in the 13th codon was determined by PCR analysis of isolated

TABLE 1. Analysis of *ras* Gene Activation in Leukemic Spleen Samples from Dogs Exposed to Whole-Body Gamma Radiation

Dog Number	Number of Clones Analyzed	*ras* Genes Examined	Number of Mutations Found
4256	5	1 N-*ras*	0
		4 K-*ras*	0
4141	14	10 N-*ras*	5 N-*ras* (codon 13)
		4 K-*ras*	0
4335	5	1 N-*ras*	0
		4 K-*ras*	0
1606	12	12 K-*ras*	0
4164	3	3 N-*ras*	0
4077	5	5 K-*ras*	0
4345	6	2 K-*ras*	2 K-*ras* (codon 12)
		3 N-*ras*	1 H-*ras* (codon 12)
		1 H-*ras*	0
4334	1	1 K-*ras*	0
1688	1	1 N-*ras*	0

total tumor RNA. The analysis is based on the exon-connection strategy of Fearon et al. (1990). Briefly, complementary DNA (cDNA) is prepared from total tumor tissue RNA by direct PCR analysis of mRNA. Two primers are chosen from different exons so that amplification results in a PCR product of the N-*ras* exons 1 and 2 in which the intron has been removed and the exons have been properly spliced. Trace amounts of DNA will not amplify into the same size fragment, and the DNA-directed PCR products contain unspliced exons separated by a large intron sequence. The strategy when applied to total mRNA from leukemic samples produced a 310-bp fragment found to be the correctly spliced N-*ras* product. The spliced 1st- and 2nd-exon products were molecularly cloned and sequenced. When several recombinants were analyzed, approximately 50% showed a mutation in the 13th codon that resulted in the substitution of an asparagine for a glycine.

Studies of rats exposed to radon-progeny and mixed radon-progeny and cigarette-smoke inhalation have yielded similar information (Table 2). An activating lesion that may be unique occurs at codon 62 where GAA is mutated to GAT, bringing about a glutamate-to-aspartate substitution.

TABLE 2. *ras* Gene Activation in Lung Tumors from Rats Exposed to Radon Progeny or Radon Progeny and Cigarette Smoke

Type of Exposure	Rat Number	Number of Clones Analyzed	Number of Mutations Found
Radon progeny[a,b]	283-437-2	13	2, Codon 13; 7, codon 12
	282-687-2	13	0
	282-1198-2	3	0
	282-1197-2	4	1, Codon 13
Radon progeny and cigarette smoke[a,b]	38T	9	0
	26T	5	0
	53T	5	0
Radon progeny[c,d]	281-1541-1	-	Codon 62
	282-1547-2	-	Codon 62
	282-1247-1	-	Codon 62
	281-198	-	0
	283-69-1	-	0

(a) K-*ras* gene (exon 1) was examined
(b) Sequence of cloned polymerase chain reaction (PCR) products
(c) H-*ras* gene (exon 2) was examined
(d) PCR samples were sequenced directly

Future Studies with Single-Strand Conformational Polymorphism Assay

Molecular cloning and DNA sequence analysis of PCR-generated sequences are time consuming and labor intensive. We are introducing new methods of research analysis that will expedite our effort. The single-strand conformational polymorphism (SSCP) assay provides an initial rapid PCR product point mutation screening by comparing electrophoretic migrational differences in nearly identical denatured PCR templates. The method is sensitive and can detect strand migrational differences induced by a single base-pair change (see SSCP gel example in Figure 1A).

The SSCP method is limited, however, in that it cannot identify the position or chemical nature of the point mutation. Thus, we have introduced a second assay, the chemical mismatched-cleavage (CMMC) assay, that can identify the position of a point mutation in a PCR product. This assay can also provide limited information about the chemical nature of a base change. The CMMC assay is based on the single-base-pair-mismatch chemical reactivity of cytosine and thymine with hydroxylamine and osmium tetroxide, respectively. The assay is carried out by denaturing and annealing a mixture of normal and mutated PCR-generated sequences. The annealed heterologous products contain a mismatched base differing between the mutant and normal sequence. The complementary strands are chemically cleaved selectively at the point of mismatch, and the resulting products are separated and molecularly sized on a denaturing polyacrylamide gel. Illustration and description of the method are shown in Figure 1B.

Our future work will continue the analysis of *ras* gene activation in radiation-induced tumors. We hope to coordinate these data with ongoing tumor suppressor gene research (see *Mutation of DNA Targets*, this volume). We are introducing new methods of mutation analysis, such as the SSCP and CMMC, to expedite our research. As we have had difficulties with analyzing mixed populations of normal and tumor cells and because tumor cell enrichment is an important step in tumor analysis, we intend to integrate cell sorting as a first step in molecular tumor analysis.

We are using a flow cytometer to sort nuclei on the basis of DNA content differences, which allows isolation of aneuploid and diploid cell populations. Aneuploid cell populations have progressed the furthest in tumorigenesis and have accumulated the greatest number of contributing mutations; thus, molecular analysis of these populations will be the most informative. Mutations found in the diploid populations precede ploidy alterations and can be classified as early events in tumorigenesis. Mutation profiles based on cell-sorting analysis may provide molecular markers that will differentiate forms of physical genetic insult. Implementing these types of techniques for tumor analysis will contribute to our overall goal of identifying molecular markers that characterize radiation-induced or chemical-induced carcinogenesis.

References Cited

Fearon, E. R., and B. Vogelstein. 1990. A genetic model for colorectal tumorigenesis. *Cell* 61:759-767.

Fearon, E. R., K. R. Cho, J. M. Nigro, S. E. Kern, J. W. Simons, J. M. Ruppert, S. R. Hamilton, A. C. Preisinger, G. Thomas, K. W. Kinzler, and B. Vogelstein. 1990. Identification of a chromosome 18q gene that is altered in colorectal cancers. *Science* 247:49-55.

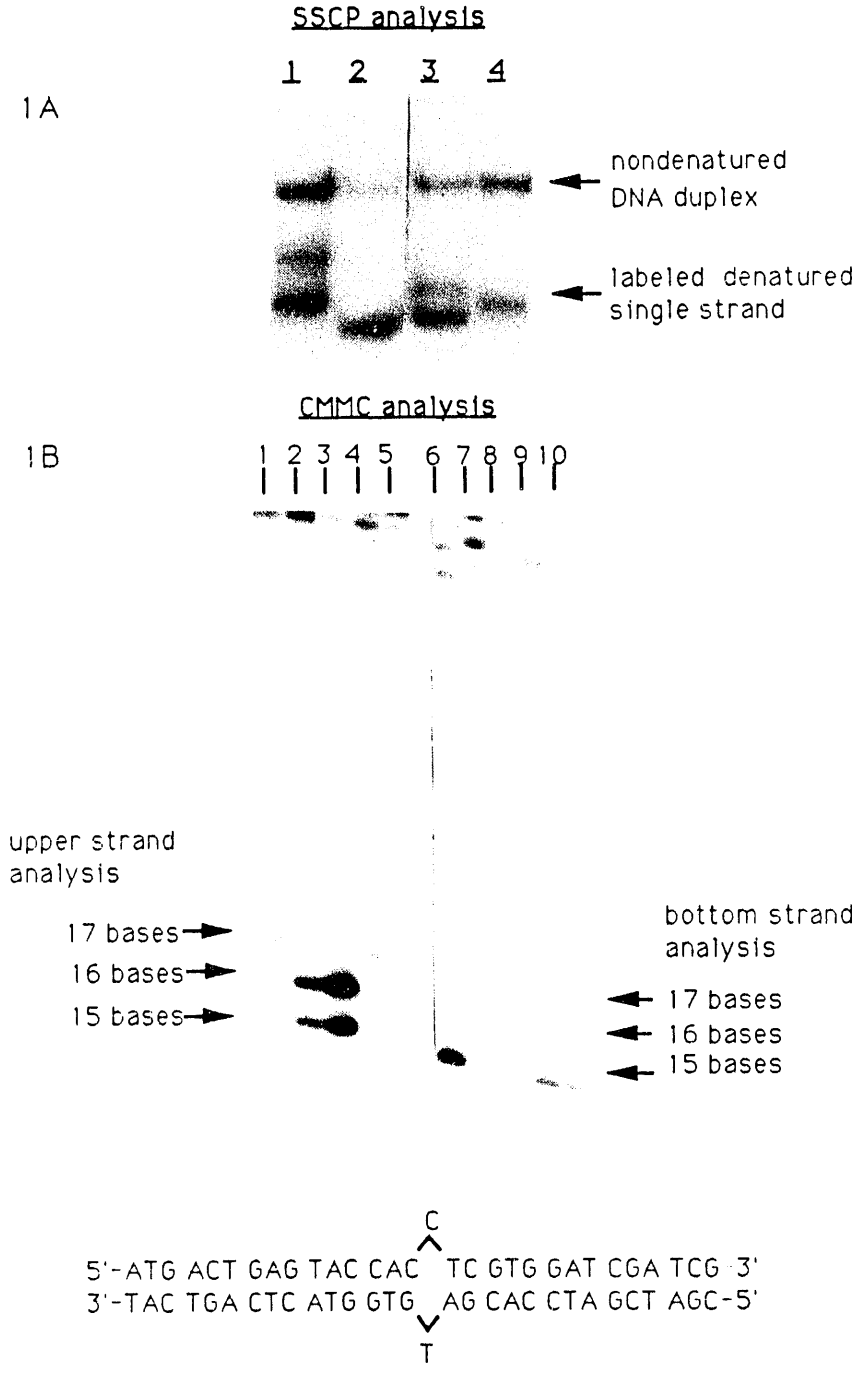

FIGURE 1. A. Single-Strand Conformational Polymorphism (SSCP) Analysis. Lanes 1 and 2 show single-strand migrational differences of same labeled strand from tumors 1606 (normal sequence) and 4141 (mutant sequence), respectively; lanes 3 and 4 show migrational differences in labeled complementary strand for tumors 1606 and 4141, respectively. Indicated nondenatured duplexes migrate at same rate. A 1-bp difference in codon 13 is seen in tumors 1606 and 4141. **B.** Chemical mismatch cleavage (CMMC) analysis of two complementary synthetic deoxyoligonucleotides with a 1-bp (C,T) mismatch is shown at bottom of Figure 1B. Reactive bases in mismatched region are numbered from the 5' end of the top strand: 15C, 16C, and 17T. The only reactive base in the bottom strand is T at base position 15.

Mutation of DNA Targets

Principal Investigator: *R. P. Schneider*

Other Investigators: *J. E. Hulla and G. L. Stiegler*

The project is testing the hypothesis that tumor suppressor genes are important targets in radiation carcinogenesis. We have concentrated our work on characterizing the dog retinoblastoma susceptibility (RB) and the rat p53 genes. We have been able to amplify two new fragments of RB cDNA (795 and 705 bp). We have also prepared probes for mRNA analysis of dog RB and α-tubulin genes and found that the transcripts are the same as those of the rat and human. Evidence of a second p53 pseudogene was discovered, and we have been studying p53 gene structure by amplification, sequencing, and, in some cases, cloning of regions containing exon-intron junctions.

Tumor suppressor genes have been recently discovered by analyses of the genetics of inherited forms of cancer, chromosomal aberrations, and polymorphic DNA markers of homozygosity. This class of genes is defined by functional criteria; that is, loss of normal function leads to neoplastic growth deregulation. About six of these genes have recently been described, and one or another has been found to be altered in virtually every type of human cancer. We suspect that inactivation of tumor suppressor genes is a common mechanism of radiation carcinogenesis because deletions are a major component of genetic damage from ionizing radiation. We are testing this hypothesis by studying the two tumor suppressor genes that have been described best, the retinoblastoma susceptibility (RB) and p53 genes in tumors from animals exposed to ionizing radiation.

Defects in the RB gene are found in retinoblastoma, osteosarcoma, small-cell cancer of the lung (SCCL), and some non-small-cell lung, breast, and bladder cancers in humans. The p53 gene has been found to be altered in almost all types of human cancers and is the gene most commonly mutated in human cancer. The p53 gene differs from the recessive nature of RB because mutations can confer a dominant phenotypic expression pattern. Some mutated forms of p53 protein can complex the wild-type gene product from the other nonmutated allele. The gene products of both these genes act in the nucleus, probably by interacting with transcription regulatory factors, and both gene products are inactivated by viral oncoproteins. In infected cells, the viral proteins complex the RB and p53 gene products and thereby effectively inactivate the genes.

Our approach is to examine p53 and RB genes in tumor tissue preserved from life-span animal experiments at PNL and other DOE laboratories. We have a small number of frozen rat and dog lung tumors and dog bone tumors (osteosarcomas) induced by inhaled plutonium, and a large number of radon-induced rat lung tumors and plutonium-induced rat and dog lung tumors that have been fixed in formalin and embedded in paraffin. Frozen myelogenous leukemia cells from dogs that were chronically exposed to x rays and gamma radiation at Argonne National Laboratory are also available. When tissue of sufficient quality is available, we plan to analyze RB and p53 gene expression of mRNA with the polymerase chain reaction (PCR) of RNA and northern blot methods. The fixed and embedded tissues do not have the mRNA or high molecular weight DNA required for northern or Southern analyses. Thus, PCR is used to amplify specific regions of these genes for analysis by gel electrophoresis and methods that detect base-pairing mismatches caused by mutations and deletions. The first step required for this approach has been to prepare primers for PCR and for RB and p53 gene-specific DNA probes for northern blot analysis.

Preliminary characterization of these genes was required so that we could analyze the dog and rat tumors, because neither the gene structure nor

the cDNA sequence of dog p53 or RB gene is known. The rat p53 cDNA sequence has been published, but its gene structure has not been previously described. We have therefore focused our efforts on obtaining the information we needed, including the location and sequence of splice junctions in rat p53 and generation of DNA probes for most of the RB cDNA. These data are also of more general interest concerning the relatedness of the genes between species and will aid cancer research with animal models. For example, information describing the p53 structure and the sequences near its splice junctions can be used by other investigators to study the role of this important gene in rats.

Because the RB gene is commonly defective in human osteosarcomas and some lung tumors, and because dogs exposed to $^{239}Pu(NO_3)_4$ and $^{238}PuO_2$ developed these forms of cancer, we have prepared reagents for analysis of the dog RB gene. The human gene is encoded in 200 kb containing 27 exons with a 4.7-kb mRNA and a coding sequence of 2.7 kb; the human and mouse cDNA sequences are known but that of the dog is not. Our original strategy was to amplify specific exons of the gene in archived tissues by PCR, assuming a high degree of sequence homology with the human gene, and then to analyze these regions for mutations. This plan has not been feasible due to difficulty in amplifying the exons, probably because the sequences from dogs and humans differ. Also, because of the complexity of the gene, we must study mRNA and cDNA rather than the gene itself. In last year's report we described a 600-bp fragment that we amplified from a phage cDNA library and sequenced. It had a high degree of sequence homology with the human RB gene from exons 17 to 20. This year we amplified two other fragments of the cDNA from RNA extracted from dog kidney that include regions corresponding to exons 8 to 17 (795 bp) and 3 to 8 (703 bp) of the human gene. The results of a Southern blot using a synthetic probe specific for regions common to both fragments confirm their identity (Figure 1). We now have generated fragments that include 70% of the coding region of the gene, and we will continue to attempt to amplify more of the cDNA. These gene fragments will serve as probes for northern blots and will provide a means to search for mutations and deletions in experiments planned for FY92.

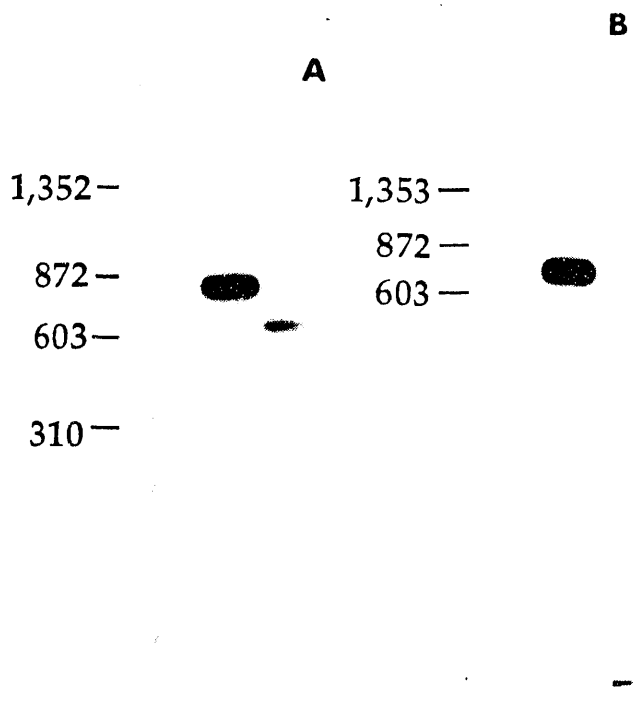

FIGURE 1. Autoradiograms of Southern Blots of Fragments of Dog RB cDNA Amplified from Dog Kidney RNA. Positions of DNA molecular size standards and corresponding size in base pairs (bp) are shown to left of both parts of this autoradiogram. **A.** Left lane, fragment corresponding to exons 8 to 17 in the human gene; right lane, exons 17 to 20. Probe was a synthetic 21-bp oligonucleotide from exon 17. **B.** Fragment corresponding to exons 1 to 8 of human gene; probe was a 21-bp oligonucleotide from exon 4.

We have hybridized RB cDNA probes to northern blots of poly-A RNA and total RNA from frozen dog kidney (Figure 2) and shown that the dog RB mRNA is about the same size as that of humans (4.7 kb). Using primers derived from the sequence of the rat α-tubulin gene, we also amplified a 300-bp fragment of this gene from dog RNA for a probe for α-tubulin mRNA on northern blots. The size of dog α-tubulin message (Figure 3) is the same as that of human and rat (1.7 kb). The tubulin is expressed at much higher levels than RB, and its mRNA will provide a control for the quality and amounts of mRNA in northern blots.

Several years ago, cell lines from dog plutonium-induced osteosarcomas and lung tumors were developed at PNL. These lines have been stored in liquid nitrogen for as long as 15 years, and we have begun a systematic study of their viabilities.

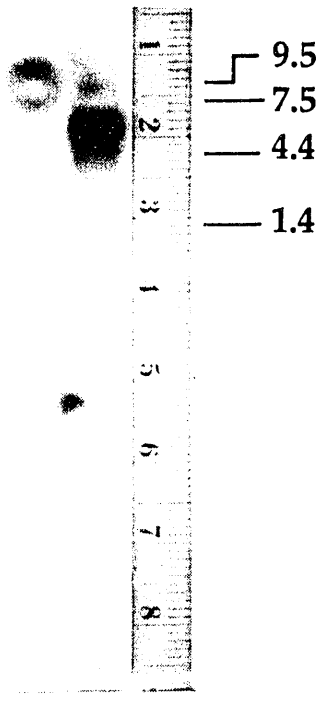

FIGURE 2. Autoradiogram of Northern Blot of Poly-A RNA Isolated from Dog Kidney RNA. Positions of RNA molecular size in base pairs (bp) are shown to right of this autoradiogram. Probes are the same fragments as shown in Figure 1A, labeled by random primer extension.

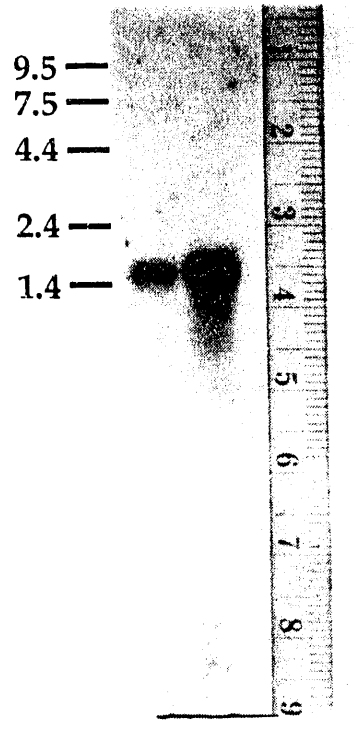

FIGURE 3. Autoradiogram of Northern Blots of Total Dog Kidney RNA Hybridized with a 300-bp Fragment Amplified from Dog α-Tubulin mRNA. Positions and corresponding sizes (bp) of RNA molecular size standards are shown on left of autoradiogram. Probe was labeled by random primer extension.

These cell lines may be a valuable resource for evaluating genetic changes in the cancer cells because of the opportunity to study gene expression and mutations. These lines can also be used for experiments that can more closely define the role of tumor suppressor genes by gene transfection experiments.

We previously deduced a tentative structure of the rat p53 gene based on sizes and locations of introns within the mouse and human p53 genes. Polymerase chain reaction (PCR) assays made apparent the occurrence of a p53 pseudogene within the rat genome. We found that the pseudogene is a "processed" sequence; it lacks introns and retains close homology to the cDNA. This year, we sequenced a major portion of the rat pseudogene by using PCR to amplify the sequencing templates. When these sequence fragments were compiled, we found that at least two pseudogene sequences are present in the rat genome. We have sequenced a pseudogene fragment corresponding to bases 250-296 of the cDNA. This fragment contains 9 base substitutions and a 15-base deletion. A second pseudogene fragment from the same region contains 10 substitutions and a 2-base deletion (Figure 4).

Because of sequence homologies, the gene and pseudogenes are co-amplicons. We are investigating the potential for using a pseudogene amplicon as a PCR internal control. A 1200-base fragment of pseudogene 1 was recently amplified. We expect to clone and sequence this fragment if the sequence is determined to be a suitable internal control.

The p53 gene structures are established for the p53 genes from human, mouse, and *Xenopus* (Figure 5). We are currently defining the rat p53 gene structure. Preliminary results suggest the rat gene contains only 10 of the 11 exons present in other species. We found intron 6 missing from the PCR

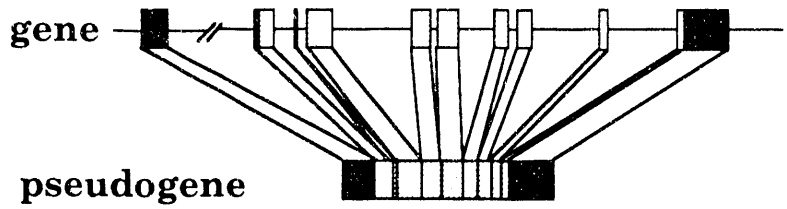


```
I      250      AT  • • • • • • • • • • • • • • • •  A T     C   T T A       C
cDNA   GCCCCTGCACCCGTGGCCCCTGCTTCAGCTACACCGTGGCCTCTGT
II           T            ACT                CT   TC   T   A         • •
```

FIGURE 4. The Rat Genome May Contain More than One Processed Pseudogene. Two sequences (I, II) tentatively identified as pseudogenes contain rat p53 gene homology and lack the intervening sequence. Each sequence contains mutations that define its uniqueness.

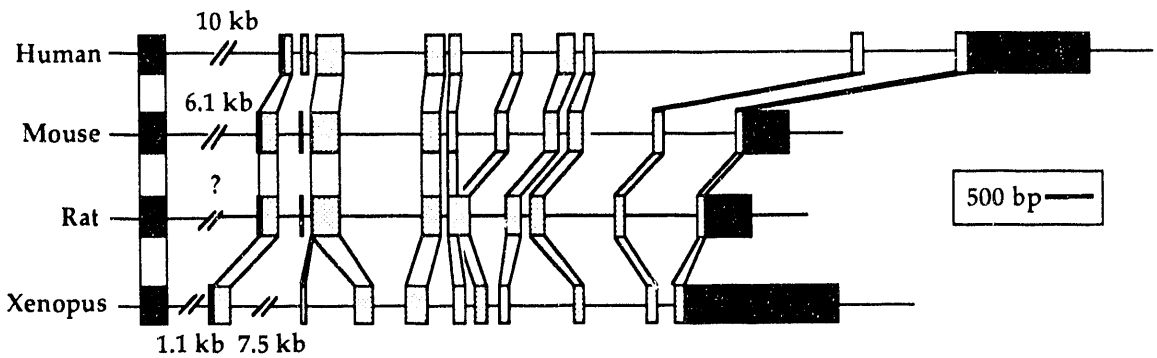

FIGURE 5. Comparison of Rat p53 Gene Structure with Human, Mouse, and *Xenopus* p53 Gene Structures. Preliminary results suggest that the rat gene may lack the intervening sequence between exons 6 and 7. Size of the first intron is not yet determined; sizes of all other introns are estimated from differences in length of p53 gene fragments and corresponding fragments of the processed pseudogene. These estimates are consistent with lengths of introns within mouse p53 gene. Symbols: solid bars, not transcribed; shaded bars, transcribed; scale bar, 500 bp.

fragment that contains a portion of intron 5, all of exon 6, and a portion of exon 7. We are now preparing the clones to verify this sequence. To date, gene regions containing exons 2-6, 7-9, 8-10, and 9-11 have been cloned. Data from these clones and from PCR fragments were compiled to provide the tentative rat gene structure shown in Figure 5. No information is yet available from the 5′ end of the rat gene. Once established, intron sequences will be used as gene-specific priming sites. We have analyzed the base sequence of 16 of 18 sites present in the p53 gene by direct sequencing of PCR products and sequencing of plasmid clones (Figure 6).

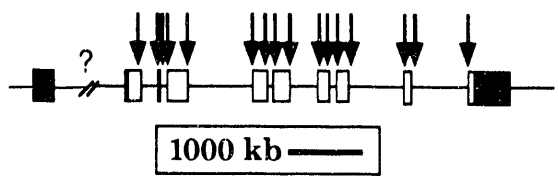

FIGURE 6. Several Fragments of the Rat p53 Gene Have Been Cloned and Sequenced. Of 18 splice junctions presumed to occur, 16 have been defined; their locations are indicated by arrows in this diagram. Scale bar, 1000 bp.

Molecular Events During Tumor Initiation

Principal Investigator: *D. L. Springer*

Other Investigators: *D. B. Mann, G. L. Stiegler, and B. D. Thrall*[a]

Benzo[a]pyrene diol epoxide (BPDE) is a highly reactive metabolite of benzo[a]pyrene and forms a number of covalent adducts with DNA. Of these adducts, 85% to 95% are on the exocyclic nitrogen of deoxyguanine, resulting in a bulky lesion that interferes with the progression of DNA and RNA polymerases. We are using this phenomenon to map the distribution of damage in plasmid DNA modified with BPDE to better understand the sequence-specific factors involved in DNA adduction. Replication of BPDE-modified DNA with T7 DNA polymerase (Sequenase) consistently results in blockage of the polymerase at 1 base prior to adducted dG residues. Densitometric analysis demonstrates that this blockage is quantitative, with a dose-dependent relationship between the intensity of blocks and the level of modification. The level of adduction at any particular dG residue varies by 11 fold and is distinctly nonrandom. Adduction of poly dG sequences is invariably favored over single dG residues, and within a poly dG region there is a bias for adduction of the 5′ bases. Similarly, transcription of the DNA using SP6 RNA polymerase results in decreasing amounts of full-length RNA with increasing levels of DNA template modification. However, the position of blockage of the RNA polymerase appears different from the DNA polymerase, showing a less consistent relationship to adducted dG residues. The results suggest that there are clear differences in the manner by which DNA and RNA polymerases process DNA templates that are modified with BPDE.

Benzo[a]pyrene diol epoxide (BPDE) forms a number of covalent adducts with DNA that impede the progression of DNA and RNA polymerases. We are using this phenomenon to map the distribution of damage in DNA modified with BPDE to better understand the sequence-specific factors involved in DNA adduction. Replication of BPDE-modified DNA with T7 DNA polymerase consistently results in blocks occurring 1 base prior to dG residues. This blockage is quantitative, with a linear relationship between the intensity of blocks and the level of modification. Adduction of poly-dG sequences is invariably favored over single dG residues, and within a poly-dG region there is bias for adduction of the 5′ bases. Transcription of the DNA using SP6 RNA polymerase results in decreasing amounts of full-length RNA with increasing template modification.

It is well established that DNA binding is a necessary, but not sufficient, requirement for the tumorigenicity of polyaromatic hydrocarbons (PAH). Benzo[a]pyrene (BaP), a prototypical PAH, has been well studied in this regard, and it is clear that metabolism of BaP to the (+)-*anti*-7,8-diol-9,10-epoxide [(+)-*anti*-BPDE] is associated with the tumor-initiating potential of this compound. Although a number of DNA adducts are associated with BPDE, it is estimated that up to 95% of the adducts formed are on the exocyclic nitrogen of guanine and reside within the minor groove of the DNA helix. Adduction of DNA by BPDE occurs in a nonrandom fashion, because not all guanines in DNA have equal susceptibility to adduction. Bulky DNA adducts such as those from BPDE are effective inhibitors of both DNA replication and transcription, acting as complete or nearly complete blocks to the progression of DNA and RNA polymerases. We are using this phenomenon to study the sequence-specific factors involved in DNA modification by BPDE as well

---

(a) The name of J. E. Hulla was inadvertently omitted from the list of Other Investigators on Dr. Springer's article in last year's *Annual Report* (1990)

as to characterize the effect of these adducts on the enzymatic processing of DNA and RNA.

Modification of DNA by [^{3}H]BPDE

The plasmid pGEM-5S, developed in our laboratory, contains the 5S rRNA gene from *Xenopus borealis* and serves as a unique system for the study of site-specific adduct formation by BPDE. pGEM-5S DNA is incubated in the presence of 0 to 50 μM radiolabeled (±)-*anti*-r-7,t-8-dihydroxy-t-9,10-epoxy-7,8,9,10-tetrahydrobenzo[a]pyrene [(±)-*anti*-BPDE] in 10 mM Tris-Cl buffer, followed by removal of unbound BPDE metabolites and its degradation products by consecutive extractions with diethylether and precipitation with ethanol. As is demonstrated in Figure 1, adduction in this system occurs in a near-linear fashion and is dependent on both BPDE and DNA concentrations.

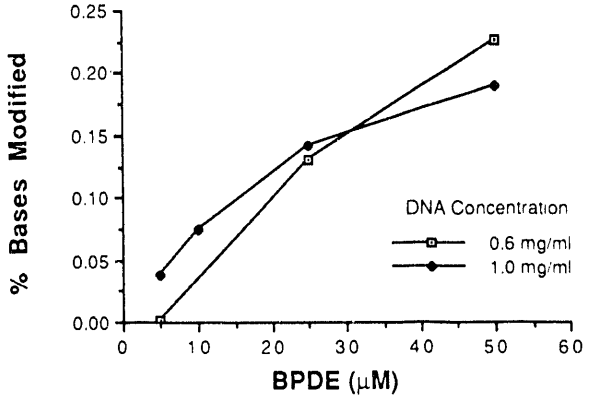

FIGURE 1. Adduction of pGEM-5S Plasmid DNA with ^{3}H-(+)-*anti*-BPDE. Plasmid DNA (0.6 or 1 mg/ml) was incubated with 0 to 50 μM [^{3}H]BPDE for 2 h in 10 mM Tris-Cl (pH 7.1) at 37 C. Nonreacted BPDE and its degradation products were removed by 10 consecutive extractions with water-saturated diethylether, followed by 2 ethanol precipitations. Average adduction level was determined by liquid scintillation counting.

Analysis of BPDE Binding Sites

The distribution of BPDE binding sites can be determined by a number of methods. We are determining the sequence specificity of BPDE binding by analyzing the points at which DNA and RNA polymerases are blocked by these bulky adducts. Native and modified pGEM-5S DNA are denatured by alkali, and primers are annealed to the DNA. Using a cloned version of T7 DNA polymerase (Sequenase, U.S. Biochemical), the DNA is then replicated, incorporating [α-^{32}P]dCTP. The stoichiometry of the labeling reaction is such that approximately the first 25 bases are labeled, resulting in a short-patch "end label" of high specific activity in the nascent DNA. The replicated DNA is separated by electrophoresis, and the position of replication blocks is determined by comparison to standard dideoxy sequencing reactions (Figure 2). Replication of nonadducted DNA is unimpeded, resulting in a clean lane on the autoradiograph. Replication of adducted DNA, however, results in a series of shortened DNA fragments that reflect the distribution of guanines within the DNA. Similar results were found with other DNA polymerases, including DNA polymerase I (Klenow fragment) and Taq DNA polymerase.

Analysis of the total adduction of bases 58 to 65, as determined by laser densitometry, correlates very closely to the total adduction level calculated by liquid scintillation analysis of the total amount of [^{3}H]BPDE bound (Figure 3). Thus, these blocks in T7 DNA polymerase are clearly related to BPDE adducts. Densitometric analysis also reveals that binding of BPDE occurs in a nonrandom fashion and that the susceptibility of a guanine to adduction varies as much as 11 fold (Figure 4). In addition, the potential of a guanine for modification is significantly influenced by neighboring bases, as has been suggested by other investigators using different methods of analysis (Boles and Hogan 1984, 1986). Within long tracts of guanines, there is a bias toward modification of the 5′-end guanines. This trend is not observed in regions with two consecutive guanines.

Transcription of BPDE-Modified DNA

It has long been known that BPDE adducts, in addition to inhibiting DNA replication, also block transcriptional processes (Leffler et al. 1977). However, few studies have carefully characterized this effect. Using the pGEM-5S plasmid system and a simple monomeric RNA polymerase (SP6 polymerase), we are also investigating the effect of DNA adducts on RNA polymerization. Transcription conducted with SP6 RNA polymerase on

nonadducted, *Eco*RI-linearized plasmid results in primarily full-length RNA (242 bases) (Figure 5).

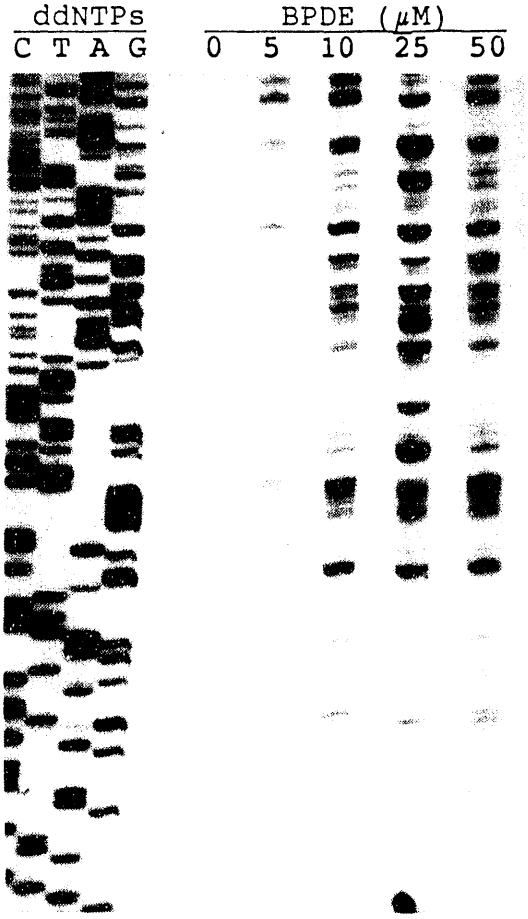

FIGURE 2. Replication of Adducted pGEM-5S by T7 DNA Polymerase. Plasmid DNA (4 μg) was denatured by alkali and annealed with 75 ng of primer DNA (17-mer). Initial labeling reactions were in the presence of 3 units T7 DNA polymerase (Sequenase, U.S. Biochemical), 1.5 μM each of dGTP, dATP, and dTTP, and 3.3 pmol [α-^{32}P]dCTP (3000 Ci/mmol) for 2 min. Labeling was immediately chased with 200 μM each of dGTP, dATP, dCTP, and dTTP for 5 min, and the reaction was stopped by the addition of gel-loading buffer containing 90% formamide. Samples were heated to 80°C for 90 sec and immediately electrophoresed on an 8% denaturing polyacrylamide gel. Locations of adduct-induced blocks in replication were determined by comparison to standard dideoxynucleotide triphosphate sequencing lanes.

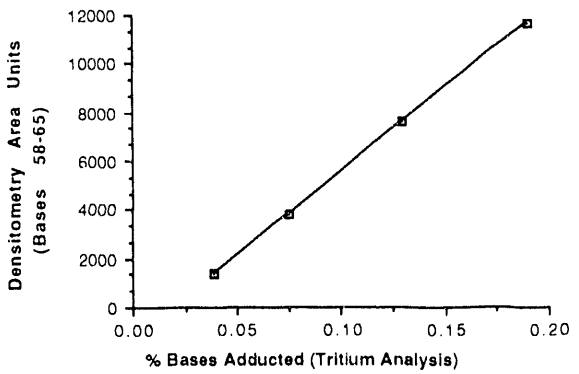

FIGURE 3. Comparison of BPDE Binding Using Densitometric Analysis and Liquid Scintillation Values. Autoradiographs of samples produced by Sequenase (see Figure 2) were scanned by laser densitometry using a Zeneih Model SL/2D laser densitometer. Scans were run between bases 58 to 65 (poly dG_8) and the total area of each lane was determined. Average intensity (area) determined by densitometry correlated significantly with average total adduction levels determined by liquid scintillation counting (r^2 = 0.999).

However, with adducted DNA templates, the amount of full-length RNA decreases with increasing template modification. In addition, RNA produced from adducted templates shows a series of shorter, aborted transcripts that align with adducted sites on the DNA (see Figure 5). Densitometric analysis of the amount of full-length RNA produced as a function of total adduction level shows that the inhibition of full-length RNA production occurs in an approximately linear fashion. Based on this trend, inhibition of 50% is predicted in templates that have an average of 0.5 adducts per molecule (Figure 6).

These studies provide mechanistic information on the reactivity of particular bases in DNA toward BPDE. For example, the enhanced reactivity of guanines with sequence specificity may in part explain the activation of specific codons within proto-oncogenes. In addition, because the regulatory regions of many genes, including proto-oncogenes, contain poly-G sequences, these findings may be important to understanding the effects of BPDE adducts on gene expression. For example, studies by Kootstra et al. (1989) showed

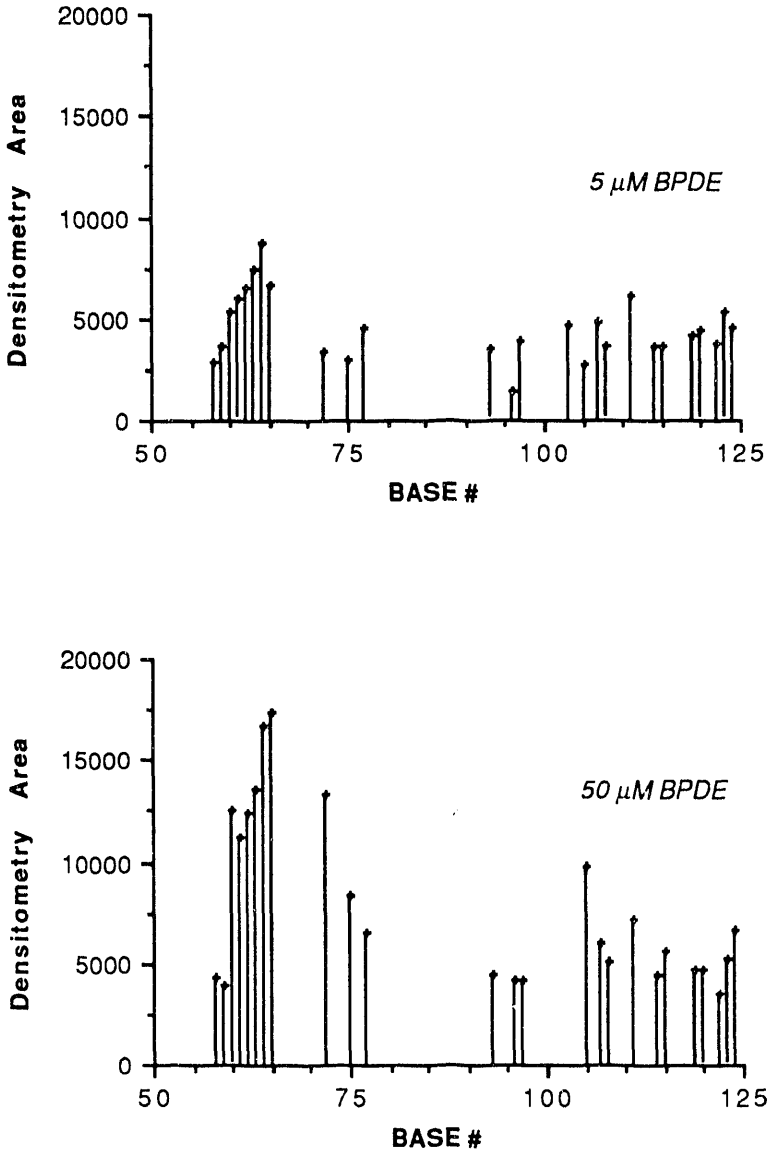

Sequence Analyzed:

^{55}
3' - CCCGGGGGGGGTCTTCCGTCGTGTTCCCCTCCTTTT

^{91}
CAGTCGGAACACGAGCGGATGCCGGTATGGTGGGAC - 5'

FIGURE 4. Site-Specific Adduction Levels within BPDE-Modified pGEM-5S DNA. pGEM-5S DNA modified with either 5 μM or 50 μM BPDE was replicated with Sequenase as described in Figure 2; the intensities of replication blocks were determined at individual bases by laser densitometry. Replicated strand (3' → 5') is shown from bases #55 to #125 (where base #1 is the first base transcribed by SP6 RNA polymerase).

FIGURE 5. Transcription of BPDE-Modified pGEM-5S by SP6 RNA Polymerase. pGEM-5S DNA was linearized with *Eco*RI, which cuts 242 bases downstream (3′) from start of SP6 transcription. Transcription reactions were conducted in presence of 600 ng DNA, in 40 mM Tris-Cl (pH 7.5), 6 mM $MgCl_2$, 2 mM spermidine, 5 mM dithiothreitol, 1 mM NTP, 12.5 pmol [α-^{32}P]UTP, 1 unit RNase inhibitor (Promega), and 750 units/ml SP6 RNA polymerase 37°C for 45 min. After reaction was terminated, RNA was precipitated with cold ethanol, electrophoresed in 8% denaturing polyacrylamide gels, and exposed to autoradiographic film for 16 h.

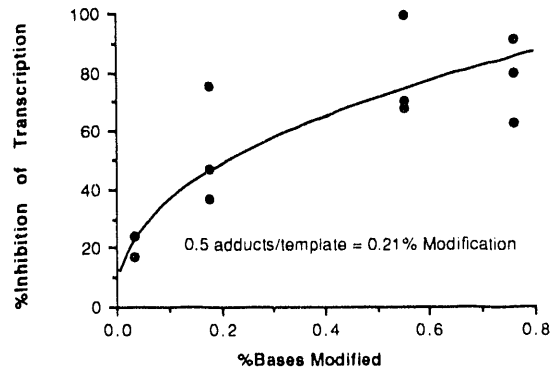

FIGURE 6. Inhibition of Transcription in BPDE-Modified pGEM-5S. Transcription reactions were carried out in modified and unmodified pGEM-5S as described in legend of Figure 5. After exposure to autoradiographic film for 2.5 h, relative amounts of full-length RNA (242 bases) were determined by laser densitometry. Inhibition of RNA synthesis is shown as a percentage of full-length RNA produced with unmodified templates.

that transcription of plasmid DNA is terminated in regions containing GC boxes (GGGCGG), which are important eukaryotic promoter elements found in the 5′ region of some oncogenes. Because the chromatin structure of many active genes is in open (nonnucleosomal) conformation (Benezra et al. 1986), these regions may be highly susceptible to modification by BPDE. Studies designed to test this hypothesis are currently under way. Another possible consequence of the preferential modification of poly-G regions by BPDE is that damage to these sites may promote chromosomal rearrangements, which could conceivably result in an oncogenic recombinant gene. Chromosomal translocations are known to be involved in the activation of several proto-oncogenes, including *myc* genes; however, the mechanism of such rearrangements is not understood. The ability of agents that preferentially modify GC-rich regions of DNA to promote chromosomal rearrangements has not been extensively studied and deserves further experimentation.

Reconstitution of the 5S Gene

Although chemically induced or radiation-induced DNA damage is being extensively studied in naked DNA, tumor initiation involves alteration of cellular DNA that is associated extensively with histones and other proteins. In an effort to obtain information that more closely resembles the cellular environment, we are studying damage to DNA in a simple reconstituted nucleosome model. For this, a 218-bp restriction fragment that includes the 5S rRNA gene is obtained by digestion of pGEM-5S followed by purification by agarose electrophoresis. The restriction fragment is end labeled, incubated with chick erythrocyte mononucleosomes at high salt concentration, and

dialyzed to remove excess salt. Under these conditions the core histones are known to become associated with the DNA fragment, forming a fixed position nucleosome with the dyad located at the beginning of the 5S gene. When this preparation is separated by 4% nondenaturing polyacrylamide gel electrophoresis (PAGE), reconstituted nucleosome migration is retarded relative to the naked DNA (Figure 7). In addition, cleavage of the DNA is inhibited when the nucleosome is incubated with the restriction enzyme *Bsp* 1286 I. This result is taken as confirmatory evidence of nucleosome formation because the *Bsp* 1286 I restriction sites are located within the nucleosome. Subsequent studies will use this model along with the mapping procedure to determine whether (1) the association of DNA with core histones protect certain regions from BPDE adduction relative to naked DNA and (2) whether nucleosome formation and positioning is altered by bulky chemical adducts.

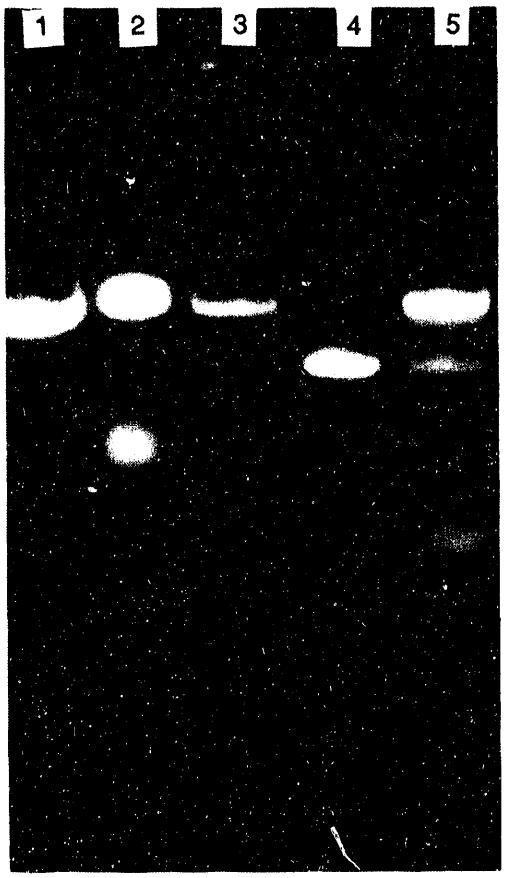

FIGURE 7. Autoradiograph Following Polyacrylamide Gel Electrophoresis (PAGE) Separation of Reconstituted 5S Gene. A 218-bp restriction fragment containing the 5S rRNA gene was incubated with a chick erythrocyte chromatin preparation under conditions that favor exchange of core histones to form nucleosomes with the 5S gene. Lane 1, reconstituted 218-bp fragment after digestion with proteinase K; lane 2, native 218-bp DNA; lane 3, reconstituted 218-bp DNA. Data from these three lanes suggest that a portion of 218-bp DNA was reconstituted, because the reconstituted DNA migrated slower than the native DNA and because treatment with a proteolytic enzyme eliminated the slower migrating DNA. Lane 4, native 218-bp DNA digested with *BSP* 1286 I to yield radiolabeled 79-bp fragment. Lane 5, digestion of 218-bp reconstituted DNA with *BSP* 1286 I resulted in both 79- and 218-bp fragments, suggesting that nucleosomal DNA is unavailable to the restriction enzyme.

References

Benezra, R., C. R. Cantor, and R. Axel. 1986. Nucleosomes are phased along the mouse ß-major globin gene in erythroid and nonerythroid cells. *Cell* 44:697-704.

Boles, T. C., and M. E. Hogan. 1984. Site-specific carcinogen binding to DNA. *Proc. Natl. Acad. Sci. USA* 81:5623-5627.

Boles, T. C., and M. E. Hogan. 1986. High-resolution mapping of carcinogen binding sites on DNA. *Biochemistry* 25:3039-3043.

Kootstra, A., L. K. Lew, R. S. Nairn, and M. C. MacLeod. 1989. Preferential modification of GC boxes by benzo[a]pyrene-7,8-diol-9,10-epoxide. *Mol. Carcinog.* 1:239-244.

Leffler, S., P. Pulkrabek, D. Grunberger, and I. B. Weinstein. 1977. Template activity of calf thymus DNA modified by a dihydrodiol epoxide derivative of benzo[a]pyrene. *Biochemistry* 16:3133-3136.

Genotoxicity of Inhaled Energy Effluents

Principal Investigator: *A. L. Brooks*

Other Investigators: *R. M. Kitchin, K. E. McDonald, C. Mitchell, and W. K. Yang*

The interaction between cellular and genetic damage induced by low- and high-LET radiation and damage produced by chemicals and oncogenes is being studied. We are concentrating our research on materials associated with the nuclear industry and those that are present at nuclear waste sites. Genotoxic responses to the organic solvents methyl isobutyl ketone (hexone) and tributyl phosphate (TBP), present in large amounts in nuclear waste sites, have been investigated *in vitro*. Both hexone and TBP produced a concentration-related increase in cell killing. An extensive genotoxicity analysis was conducted for hexone given alone and in combination with ^{60}Co gamma rays. The combined effects were not more than additive for the induction of cell cycle delay, chromosome aberrations, or sister chromatid exchanges. For the TBP cell cycle, changes and the induction of micronuclei were evaluated, and no interactive effects were observed between the damage from radiation and that from the solvent.

The potential interaction of mutated *ras* oncogenes with ^{239}Pu and the organic solvent carbon tetrachloride (CCl_4) has been studied. To date, a higher frequency of liver nodules has been observed in mice that are given combined exposure to *ras* and ^{239}Pu relative to those exposed to either agent alone. This research develops a mechanistic foundation of the interaction of radiation and chemicals in the production of cancer. Understanding of these mechanisms identifies potential interactions and allows for adequate worker protection both in the nuclear industry and during nuclear waste-site cleanup.

Introduction

This research uses *in vitro* cellular toxicology to understand potential interactions between damage produced by agents in the work environment. Several difficulties are associated with health protection problems associated with mixed wastes and the nuclear industry. First, the site of action and responses produced may be different for each insult. Second, the dose-exposure terms for radiation and chemicals are hard to express in common units. Third, converting exposure to a biologically significant dose for chemicals and relating this dose to a measured response is also difficult. Finally, the interactive effects of damage from two or more carcinogens may be additive, synergistic, or antagonistic depending on the concentrations, time of exposure, biological site of attack, and endpoint evaluated. All these factors complicate the relationships and extrapolations needed to relate how risk from radiation compares with risk from exposure to carcinogenic chemicals and how these risks are expressed for combined exposure.

Studies are being conducted *in vitro* to define the relationships between combined exposures and cellular responses, measured as cell killing, induction of micronuclei, sister chromatid exchanges, chromosome aberrations, and changes in cell cycle to provide preliminary information on potential interactions. The presence of mutated oncogenes can also cause a predisposition for the induction of cancer. How this predisposition is altered by radiation and/or chemical exposure is also being studied. The data derived from this approach provide a mechanistic foundation for evaluating health risks in the nuclear industry and during nuclear waste-site cleanup.

Results and Discussion

Exposure to Radiation and Organic Solvents

The organic chemicals selected for study were methyl isobutyl ketone (hexone) and tributyl phosphate (TBP). Hexone was used to separate uranium and plutonium from fission products, and TBP was used to recover americium and to separate uranium, plutonium, and neptunium from fission products. These materials were then discarded in large volumes in the nuclear waste sites. To study these solvents, we evaluated both lung epithelial cells (LEC) and Chinese hamster ovary cells (CHO) for genotoxic changes.

The survival of CHO cells as a function of organic solvent exposure is shown in Figure 1. There was a concentration-related increase in cell killing for both solvents, TBP (Figure 1A) being more toxic than hexone (Figure 1B).

Hexone

The combined effects of hexone and radiation were studied at a concentration that resulted in some cell killing: 1.25 mM hexone and radiation at a dose of 2.0 Gy. The results of the combined exposures are shown in Table 1. With a few exceptions, the table indicates that combined exposure to radiation and hexone resulted in no greater change in cell cycle, induction of micronuclei, chromosome aberrations, or sister chromatid exchanges than that produced by the radiation alone.

Two measurements suggested that the hexone may have some potential effect. First, the frequency of chromosome aberrations was higher in CHO cells exposed to hexone than was observed in the controls. With the sample size scored, this was not significant at the $p > 0.05$ level. Second, more micronuclei were produced in confluent LEC cells with combined treatment than were measured in those that were exposed to radiation alone. This observation was not consistent with the other measures of genotoxic potency such as chromosome aberrations and micronuclei in dividing cells and as such requires additional validation to be considered biologically significant.

Tributyl Phosphate

The influence of tributyl phosphate (TBP) on the induction of micronuclei and the progression of CHO cells through the cell cycle was determined. The cell cycle effects were measured by determining the fraction of the cells that had divided and formed binucleated cells at 24 hours after a 2-hour TBP treatment. The results of these studies (Figure 2) demonstrate that, over the range of concentrations evaluated, there were no changes as a function of TBP concentration in either cell cycle measured as the number of binucleated cells or the frequency of micronuclei.

To study the combined effects of TBP and radiation, CHO cells were exposed to TBP at concentrations of 0.0, 0.1, and 0.2 mM alone and in combination with 0.0 or 1.5 Gy of Co gamma rays.

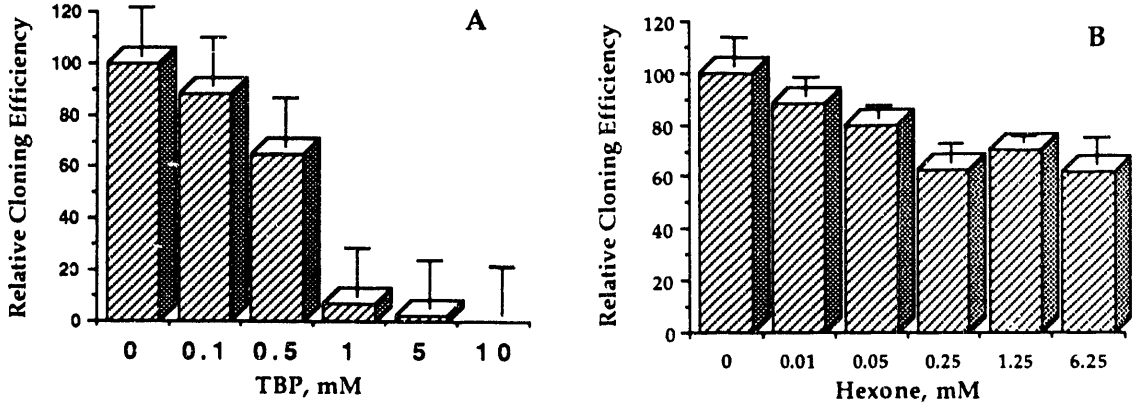

FIGURE 1. Cell Killing in CHO Cells by TBP (A) and Hexone (B) Measured by Colony-Forming Assay

TABLE 1. Combined Genotoxic Effects of Hexone and ^{60}Co Gamma Rays on Cells in Culture[a]

Treatment	LEC Cells			CHO Cells	
	Second Division, %	Micronuclei, %		Chromosome Aberrations/Cell	SCE/Cell[b]
		Dividing	Confluent		
Control	74.0 ± 5.7	11.5 ± 3.9	6.5 ± 1.0	0.05 ± 0.01	8.2 ± 1.3
Hexone	69.0 ± 4.2	12.3 ± 4.6	6.2 ± 1.1	0.10 ± 0.03	7.2 ± 0.5
Radiation	51.0 ± 4.2	29.0 ± 2.4	14.7 ± 2.4	0.38 ± 0.05	11.8 ± 0.2
Radiation + hexone	53.0 ± 7.1	28.6 ± 2.2	23.8 ± 1.7[c]	0.35 ± 0.04	11.7 ± 1.2

(a) Radiation exposure, 2.0 Gy; hexone exposure, 1.25 mM.
(b) SCE, sister chromatid exchanges.
(c) Significantly increased above the level observed for radiation only.

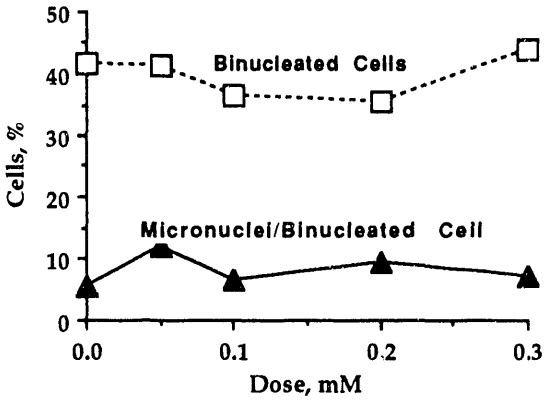

FIGURE 2. Frequency of Binucleated Cells and Micronuclei in CHO Cells Exposed to TBP at Graded Concentrations.

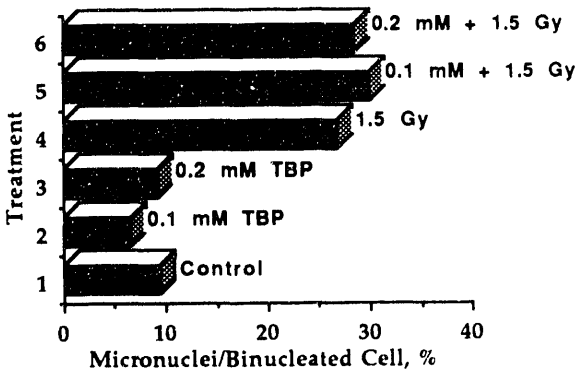

FIGURE 3. Interaction of Damage from Ionizing Radiation with TBP in Induction of Micronuclei in CHO Cells. There was no interaction between the two insults and no indication that TBP produced genotoxic damage.

The percentage of cells with micronuclei per binucleated cells (Figure 3) illustrates that radiation increases the frequency of micronuclei but that addition of the solvent has no influence on micronuclei frequency when given either alone or in combination with radiation.

Data derived from these short-term tests suggest that these solvents are not genotoxic. They also illustrate that genetic damage from these solvents is minimal and has little interaction with damage induced by ionizing radiation.

Combined Effects of Oncogenes and Plutonium

B_6C_3 F_1 mice were injected with 7.4 Bq/g body weight of ^{239}Fu citrate 30 days before or after intraperitoneal injection of retroviral oncogenes. The oncogenes used were mutated K-v-*ras* or the *neo* gene as a control. To obtain incorporation of the genes in the liver, the mice were gavaged with 0.15 ml of 20% carbon tetrachloride (CCl_4) in saline 24 hours before the oncogenes were given. The CCl_4 caused liver cell necrosis and cell proliferation, which aided in incorporation of the

retroviral vectors and oncogenes into the liver cells. Appropriate control groups with ^{239}Pu only, with CCl_4, with *neo*, and with no treatment were also included.

At 300 days after exposure to the oncogenes, 30 animals with 5 animals per group were sacrificed, and the frequency of liver nodules and the incorporation of the *ras* and *neo* genes were evaluated. The frequency of liver nodules (Figure 4) demonstrates that the injection of the *ras* gene was the most important variable in the production of liver nodules. The nodules were analyzed for the presence of the mutated K-v-*ras* oncogene; in all animals treated with the *ras* gene, the gene was expressed in the cells of the liver nodules, suggesting that the nodules were clonal in nature. Preliminary histopathology of the nodules suggests that most nodules were not neoplastic at this time. As the animals age, additional sacrifices will be conducted to further characterize the potential interaction between the chemicals, radiation, and mutated oncogenes.

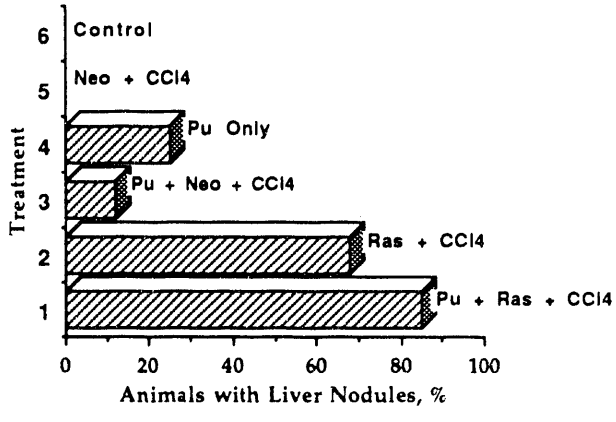

FIGURE 4. Induction of Liver Nodules in Mice Exposed to Mutated K-v-*ras* and ^{239}Pu Alone and In Combination. *Neo* genes served as controls for experimental treatment.

Summary

The effects of hexone and TBP combined with radiation were never more than additive for the induction of cell cycle delay, chromosome aberrations, or sister chromatid exchanges. TBP produced no interaction with damage from radiation in the production of micronuclei. Incorporation of the *ras* oncogene into the liver caused a marked increase in the frequency of liver nodules, which was not greatly altered by the presence of ^{239}Pu.

Information from this research can help us understand some basic mechanisms involved in the induction of chromosome damage and cancer. This understanding is useful in evaluation of occupational radiation exposure, radiation accidents, and nuclear waste-site cleanup.

Fetal and Juvenile Radiotoxicity

Principal Investigator: *M. R. Sikov*

Other Investigators: *R. L. Buschbom, G. E. Dagle, and H. K. Meznarich*

This project obtains and integrates information concerning the deposition, dosimetry, and toxicity of radionuclides relative to prenatal or postnatal age. Recent emphasis has been directed toward performing comparative and predictive analyses, modeling patterns and phenomenologic interactions to facilitate extrapolations to man, and investigating teratogenic mechanisms. This information is being used in setting radiological protection practices for pregnant women and for rapidly growing infants and children.

We continued to explore factors controlling placental radionuclide transfer and its general relationship to radionuclide absorption from gut or lung; accepted metabolites showed greater similarities and toxic materials showed greater differences, implicating binding and transport processes, metabolic specificities, and concentration gradients.

The paucity of information about the mechanisms of radiation teratogenesis led us to begin evaluating changes in the extracellular matrix and cell surfaces during development *in vitro*. These studies have detected molecular-level alterations of the extracellular matrix, especially fibronectin, that correlate with radiation-induced histological and histochemical changes in growth and differentiation.

We continued to evaluate our specimens and data and the literature to integrate and extend our information and concepts about placental transfer, fetoplacental radiation doses, and perinatal or long-term toxicity. These efforts address continuing questions about the identity of target cells and tissues associated with teratogenesis or oncogenesis during prenatal life and the magnitude of the radiation doses to these targets from radionuclides. Examination of tissue preparations and related experimental materials, plus additional data evaluation, provided correlations with previous information to complete our projects and extrapolate the results.

Analyses of prenatal radionuclide disposition included both further estimation of radiation doses to the human embryo/fetus from radionuclides and prediction of effects. We also extrapolated data from studies of laboratory species, with scaling for species-specific developmental stage and for gestational time relationships and maturities at birth. Earlier, we had begun estimating general values for expressing fractional transfer across the placenta (θ) and examining their relationships to tabulated values for fractional absorption (f_1) from the gastrointestinal (GI) tract (see *Annual Report*, Part 1, 1989, 1990). These approaches have been expanded to include estimates and comparisons for several additional elements as well as comparisons with fractional absorption from the respiratory tract. We have emphasized materials expected to exhibit differences exploitable for examining reasons for agreement or disagreement among values (Table 1).

The well-studied differences between the fractional transfer of inorganic and organic mercury, which pertain for GI tract, lung, and placenta, serve as a benchmark for comparisons. Other discrepancies, such as the marked differences between clearance values for cadmium transfer calculated from human and guinea pig placental perfusion measurements, have not been satisfactorily explained. Uranium transfer is similar at all three sites, but the site-dependent differences exhibited by cerium and many transuranic elements illustrate the impact of differences in the chemical form of materials at the site of deposition (gut or lung) compared to their form after they have entered into the blood circulation.

TABLE 1. Examples of Materials for Which Tabulated Values of Fractional Absorption into Transfer Compartment (f_1) from Gastrointestinal (GI) Tract or Lung Differ Among Themselves or from Estimates (θ) of Fractional Placental Transfer

Material	f_1, GI Tract	f_1, Lung	θ, Placenta
Americium	0.001	0.0005	0.006
Cadmium	0.05	0.05	0.6 (guinea pig)
Cadmium	0.05	0.05	0.06 (human)
Cerium	0.0003	0.0003	0.06
Cobalt	0.3	0.05	0.2
Einsteinium	0.001	0.0004	0.02
Mercury (inorganic)	0.02	0.02	0.02
Mercury (methyl)	1.0	1.0	0.8
Neptunium	0.001	0.01	0.06
Plutonium	0.001	0.0001	0.063
Polonium	0.3	0.1	0.01
Thorium	0.001	0.0004	≤0.001
Uranium	0.05	0.05	0.03
Vanadium	0.01	0.01	0.1

Other identified factors include differences among the physicochemical behavior, toxicity, and altered blood flow in experimental systems that have been observed with various materials. Placental transfer tends to be more bidirectional than absorption from gastrointestinal tract or lung, and between-site differences may include the extent of the involvement of transport processes and proteins. The relationships between placental transfer kinetics and the development of specific target tissues are clearly implicated in certain cases, and these factors are also of concern relative to radiation effects.

Absorption of relatively insoluble or poorly absorbed materials differs for the placenta and GI tract or lung, including the extent of involvement and the roles of transport proteins. To illustrate, consider a material that is a mixture of (physico) chemical forms such that 20% of the total in the gut or lung is in absorbable form and enters the blood within hours after intake; this affects the composition of the mixture that is available for placental transfer (Figure 1). A greater fraction of the material would be expected to be in this absorbable form in the bloodstream than it was in the gut or lung. In this case, calculations of placental transfer are based on the absorbed fraction, which may be involved with a transport protein or chelate. Accordingly, binding and transport processes, metabolic specificities, and concentration gradients must be examined to understand both similarities and differences in absorption values.

This line of investigation has raised additional questions relative to radiation doses to fetoplacental structures. The answers are relatively straightforward when considering target tissues for prenatal or early postnatal effects, but targets are more difficult to identify when delayed lesions are involved, as, for example, in carcinogenesis, when the structure in which a tumor is detected may not yet exist at the time of exposure. This consideration has mechanistic implications, but also illustrates a need to develop additional concepts. In addition, biological effects that result from the insult can alter the temporal relationships between placental transfer kinetics and concentrations, and transfer patterns often further implicate the role of target tissue development.

Evaluations of the radiation dose levels needed to produce specific developmental effects and to quantify the dose-response relationship provided a basis against which to weigh some of this mechanistic information and resulting inferences. Processes initially involved include cytotoxicity, which leads to embryolethality or reduced cell numbers in progenitor tissue and to interference with induction and differentiation. Altered integrity of chromosomes or the mitotic apparatus, as well as defective behavior of cells and cell populations that is related directly to the genome or indirectly to altered cell-to-cell communication, have been shown to yield an array of lesions ranging from abnormal cytoarchitecture, malformations, and histopathology on one hand to pathophysiology or

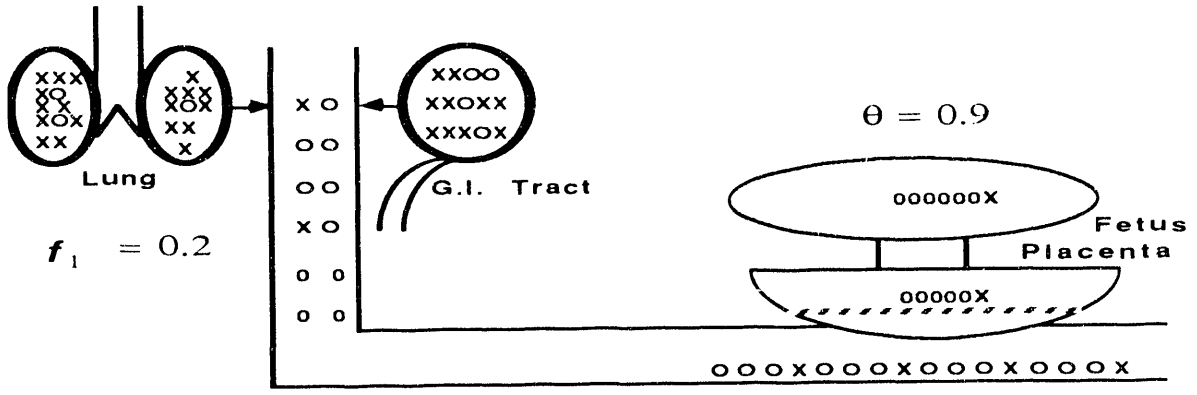

FIGURE 1. Diagrammatic Representation of Explanation for Differences Between Coefficients for Fractional Gastrointestinal or Pulmonary Absorption and Placental Transfer. As described in the text, this is based on greater fractions of readily absorbable (o) than poorly absorbed material (x) in blood than originally present in gut or lung.

reduced longevity and other delayed lesions on the other. Communication defects may be mediated through cell surfaces or the extracellular matrix (ECM), and susceptibility to subsequent insult by radiation or normal aging changes also can be affected by abnormal control through induced endocrine or immune system deficits of structure or function.

Comparisons showed commonalities of many deficits in these basic processes with those that pertain in derangements associated with neoplasia, whether "spontaneous" or produced by etiologic agents, including radiation. The similarities are especially striking with prenatal or perinatal irradiation. Extension of these analyses, which derive from earlier efforts by other investigators who did not consider mechanisms, led to the relationships summarized in Table 2. It further became clear that similar derangements play a role in abnormalities of tissue repair and that these may interfere with processes which are responsible for compensatory changes that reduce the impact of prenatal irradiation.

With the support of OHER/DOE, a workshop was held on the effects of prenatal radiation effects on the central nervous system to examine uncertainties about quantitative relationships and the underlying interpretations and conclusions. The subject was developed through a sequence of synoptic presentations and discussions from experimental and clinical perspectives. Participation by scientists from basic neuroscience and molecular biology provided other concepts and approaches, while pragmatic viewpoints were provided by representatives of agencies that might be involved in using current and future knowledge in their regulatory mission. A workshop report summarized salient features (Sikov 1992).

Deficits in morphological development of the brain at the cytoarchitectural, histological, and gross levels have been among the most striking effects of prenatal irradiation. These changes are much more striking after acute exposure to external photon beams than with exposure to protracted radiation or to radionuclides. The specific morphological changes and behavioral effects, although inconclusively correlated with each other, are clearly stage dependent, but there are difficulties in equating these motor and behavioral deficits in animals with observed intelligence changes induced in humans after prenatal irradiation. The latter, however, had been thought by others to be the most sensitive endpoint, and risk coefficients that have been calculated by UNSCEAR on the assumption of a nonthreshold, linear relationship indicate that sensitivity for such defects is even greater than for carcinogenesis.

We have been studying the role of the altered ECM and cell surfaces as mechanisms in radiation teratogenesis in limb development *in vitro* (*Annual Report*, Part 1, 1989, 1990). These experiments

TABLE 2. Parallels Between Three Pathophysiological Expressions of Radiogenic Alterations of Developmental Processes

Process	Teratogenesis	Oncogenesis	Tissue (Mis)repair
Proliferation	Delayed or decreased	Uncontrolled	Incomplete or overgrowth; Hypoplastic scar; keloid
Differentiation	Defective interactions Malformations	Incomplete or undifferentiated	Abnormal composition/structure; Scarring
Adhesion/Migration	Abnormal positioning Spatial arrangement defects	Invasion or metastasis	Incomplete or defective healing; Hypoplastia; hypertrophy
Definitive structural and functional maturation	Teratisms, structure or function Later display of latent defects Premature degenerations Decreased longevity Increased neoplasia	Neoplasms	Deficiencies of parenchyma; Connective tissue replacement

demonstrated changes in the ECM, especially fibronectin, that were correlated with histological and histochemical changes in cartilage differentiation. These results are consistent with the involvement of ECM in cell migration during neurulation and with the action of ECM components as promoters of gene expression through expression on the cell surface. These relationships suggested a need for pilot experiments to obtain parallel information about the consequences of prenatal irradiation on intercellular communication during brain corticogenesis. Mice were irradiated with 1 Gy at 13 days of gestation (dg) and were followed by evaluation of morphology and composition at 17 dg and at 6 and 14 days of postnatal life as well as morphological examination at 35 days.

These exposures produced the expected reduction of head size and brain weight and the characteristic morphological changes. Western analysis (gel electrophoresis and immunoblotting) detected fibronectin bands in the insoluble matrix fraction from brains of mice at all three ages. Isoforms were found in irradiated brains at 17 dg and in control brains at 6 days of age. A protein band of about 120 kD was detectable in normal brains at 17 dg and at 6 days of age, but this band was not present in the irradiated brains at these ages nor in control brains or brains from irradiated mice at 14 days. These findings suggest that the distribution of isoforms was altered by prenatal irradiation.

Northern analyses (gel electrophoresis followed by hybridization to fibronectin or tubulin probes) found expression of brain tubulin mRNA at both 17 dg and 6 days of age, but no exposure-related difference was found. Fibronectin mRNA was found in both control and irradiated brains at 17 dg, but expression was not detected at 6 days of age. The relative intensities of the mRNA bands, however, were affected by the prenatal irradiation. The intensity of band 1 in preparations from irradiated fetuses was increased while the intensity of band 2 was decreased (Figure 2). Additional experiments are required to confirm that the shift in the molecular weight of fibronectin represents altered mRNA expression. Fibronectin cDNA probes encoding alternative gene-splicing regions are being investigated to detect differences in mRNA expression.

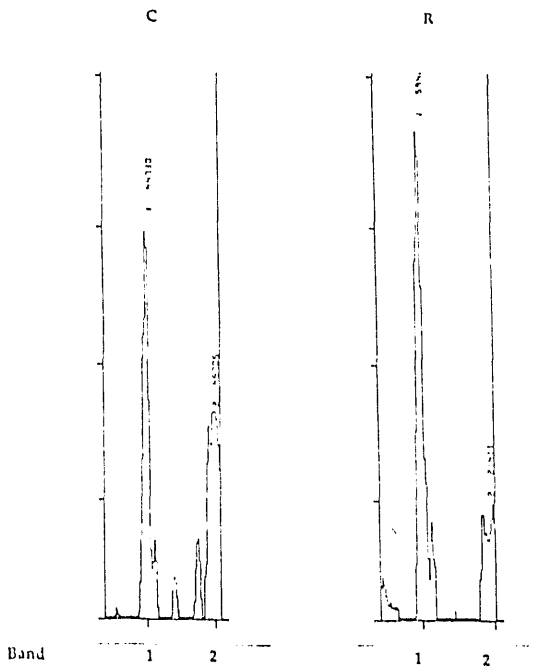

FIGURE 2. Effect of Irradiation on Intensity of Bands 1 and 2 in Northern Blots of Fibronectin from Brains of Mice at 17 dg.

Reference Cited

Sikov, M. R. 1992. *Effects of Low-Dose Prenatal Irradiation on the Central Nervous System.* PNL-8009, Pacific Northwest Laboratory, Richland, Washington.

General
Life Sciences
Research

GnomeView III: Database Information Integration and Graphics Representation

Principal Investigator: *R. J. Douthart*

Other Investigators: *J. Pelkey and G. Thomas*

The architecture of the GnomeView interface has been planned and implemented. The test set of maps for superoxide dismutase as abstracted earlier manually from the Human Genome Mapping Library, GenBank, and the literature have been, for the most part, supplanted by direct access capabilities to resident abstractions of GenBank and Genome Data Base (GDB). GnomeView is now an efficient integrated graphics user interface to GenBank and GDB that should be useful to the Genome community. Testing at a few chosen sites will begin in the latter part of FY 1992.

GnomeView is a graphical interface to the huge amounts of information generated by the Human Genome Initiative. As previously described (see GnomeView II: A Graphical Interface to the Human Genome, *OHER Annual Report for 1990, Part 1*), the central data organization theme of GnomeView is the genomic map. GnomeView utilizes the db_VISTA data management system to store, organize, and assemble information objects (map_objects) that constitute genomic maps. GnomeView is not a repository database per se, but utilizes information obtained from databases such as GenBank and the Genome Data Base (GDB) to obtain information about map_objects.

A dominant theme during the development of the architecture of the interface has been the preservation of the pictorial quality of the genomic map. The human genome effort will produce hundreds of thousands of map_objects, making pictorial map representation increasingly more difficult. It is likely that pictorial representations will tend to be abandoned as the number of map_objects increase. If this happens, insights regarding genomic topology and the relationships between different maps and map_objects that such representations convey may be lost.

Object Crowding

Maps and Labels

The problem of object crowding manifests itself in both the drawing of maps and the labeling of objects located to the maps. GnomeView handles these problems in a number of different ways.

Filtering by Query

Query tools are being developed that allow the user to map objects with common characteristics. At the first pass, objects are retrieved and can be represented as color-coded density maps. For the sake of comparison, it is possible to send out a number of independent queries that return separate density maps which are displayed adjacent to each other.

The query returns a list of objects used to construct the density maps. From this list, more detailed information about individual selected objects can be obtained.

Label Display

On individual maps, distinct objects are displayed but their labels are shown only if space permits. Labels for all displayed objects are available by selection even if their labels are not displayed on the active map. By selecting the object either from the display or from the object list associated with the display, its label is highlighted in the foreground.

Dynamic Zooming

Maps are initially presented at the magnification level corresponding to the map set constructed by the db_VISTA DBMS (Data Base Management System) in response to a query. This lowest existing magnification for a specific map is fitted to occupy a single x-window. The zoom widget can be used to present magnified views of any selected portion of the map. The zooming is dynamic in the sense that the display can change with magnification. For sequence maps, a solid line representation changes to color-coded tick marks, and eventually to color-coded symbols for the bases as magnification increases. Objects can be color filled at lower magnification, changing to outlines to reveal other objects contained within as magnification increases. Object labels become progressively displayed as magnification increases. Theoretically almost all label overwrite to the limit of the display is resolvable by zooming with progressive disclosure. In practice, a combination of zooming and selection from a list is most often used to select appropriate labels for display.

System Design and Demonstration

GnomeView was designed to accept minimal information describing map_objects that allows appropriate queries to present efficiently graphic representation of genomic maps. The definition of map_object is quite general and represents anything that can be located to the metric of a given genomic map. In this broad sense, even objects such as an investigator's name or a particular vector can conceivably be mapped to a genomic representation, that is, the investigator's name to a particular region, gene, loci, sequence, etc. that he/she may be working on and the vector to all genes, loci, probes, etc. cloned into it. Although all map_objects are intrinsically equivalent within GnomeView, it is appropriate for the sake of clarity to define a particular class of objects as landmarks. Landmarks are map_objects that are or relate to specific physical regions or structures that make up genomic maps. In GnomeView, chromosome bands are map_objects that are definitely landmarks. Landmarks can often be linked together on a metric to form a map and must be represented as map_objects in the GnomeView schema. On the other hand, objects that are definitely not landmarks, such as descriptive attributes or literature references, need not always be represented as individual map objects but could be assigned as tables or entities to give more flexibility in query response and possibly increased speed in query searching.

To test and demonstrate the GnomeView interface, data on the chromosome, restriction map, and sequence-level mapping of the superoxide dismutase genetic loci were obtained from various sources including the literature and appropriate genomic databases (see GnomeView II: A Graphical Interface to the Human Genome, *OHER Annual Report for 1990, Part 1*). This test case allowed a first-draft structuring of the interface. Practical links between various mapping levels were demonstrated to be feasible. The representation, zooming, and display modules were developed using this single example.

Databases

Sequence-Level Maps from GenBank

To be a useful interface, GnomeView must access available genomic databases such as GenBank and GDB. Direct access to GenBank for sequence information has been implemented; access is obtained by accession number, symbol, or description (keyword). Reference from GDB or to GDB from GenBank can occur. Cross-referencing among various databases and between various map representations in GnomeView may not be completely internally consistent, reflecting the idiosyncrasies of the queried databases. The rule that has been incorporated into GnomeView is that the cross-references given at the map level or database to which the initial query is given are searched first. If the object

is not found, then the cross-referenced map type or database is searched. For example, a search for sequence maps after finding loci SODI (superoxide dismutase) on 21q22.1, using GDB-generated map_ objects, first searches the appropriate GDB entity that cross-references GenBank. If a cross-reference is not found, the GenBank cross-reference file is then searched. If the query is initiated at the sequence level after finding sequence HUMSODG1 in GenBank, its cross-reference file is searched first. If the locus SODI is not found, the GDB cross-reference is then searched.

Unless all the cross-references are internally consistent, there is no guarantee that searches initiated at different levels will return identical sets of maps. Because database entries correspond to map objects, one-to-many and many-to-many relationships are expected to be usual. Queries from one level of mapping to other levels will often be one to many. Other complications arise from independence of formation of the cross-reference tables and hidden bias on definition of map_ objects in compiling a database. One extremely important feature of the GnomeView interface is the capability of simultaneous viewing of different and possibly conflicting maps and mapping pathways for critical review by the user. When one-to-many mappings are encountered, a list is presented from which maps to be viewed graphically can be chosen.

GnomeView directly accesses the GenBank features table. Information on name and location is rendered directly into a color-coded representation of objects (features) on a linear representation of the sequence. Objects (features) are labeled according to short acronyms defined by GenBank. Short definitions with regional flavor can be viewed by selecting these labels. For any given GenBank entry, the entire sequence header or portions of it can be viewed by the user on request.

Chromosome Maps: The Genome Data Base

As previously reported, the loci listed by the Human Genome Mapping Library (HGML) were manually entered into GnomeView's database. A set of descriptive attributes were devised to aid querying at the chromosome level. A utility has been written that greatly facilitates attribute assignment; it is being used to assign attributes to loci now obtained automatically from GDB.

Color Density Maps

Queries can be sent at the chromosome level to symbol, description/name, number, or attribute. It is assumed that numbers assigned by databases will be unique so that the relationship between query and output objects will be one to one when numbers are used as query input. Symbols and description/names for the most part yield one-to-one with occasional one-to-few mappings. Contrastingly, queries using descriptive attributes such as "oncogene" more often than not are one-to-many mappings. Other non-one-to-one mappings are probes and GenBank sequence entries mapped to chromosome loci. The distribution of objects found as the result of such queries is presented graphically as color-coded density maps where frequency of occurrence in defined regions of the map representation is color coded.

Consecutive queries of any sort can be made to the same map representation. Responses of single (label displayed) or multiple (color density map displayed) objects are presented adjacent to one another on the appropriate landmark map representation. The density maps of the consecutive queries of all loci and sequenced loci for chromosome 16 and chromosome 19 are shown in Figure 1.

The GDB Interface

GnomeView is presently being configured to accommodate map_objects as defined by GDB. When completed, this will include objects defined as loci and probes by this database. Excluded for the time being are pure linkage map_objects because the map_widget has not yet been scripted for linkage maps. Also excluded is side figure bibliographic information and information on verification, people, and sources which are not directly related to mapping. This information can be easily obtained using the network available interface to the GDB relational DBMS.

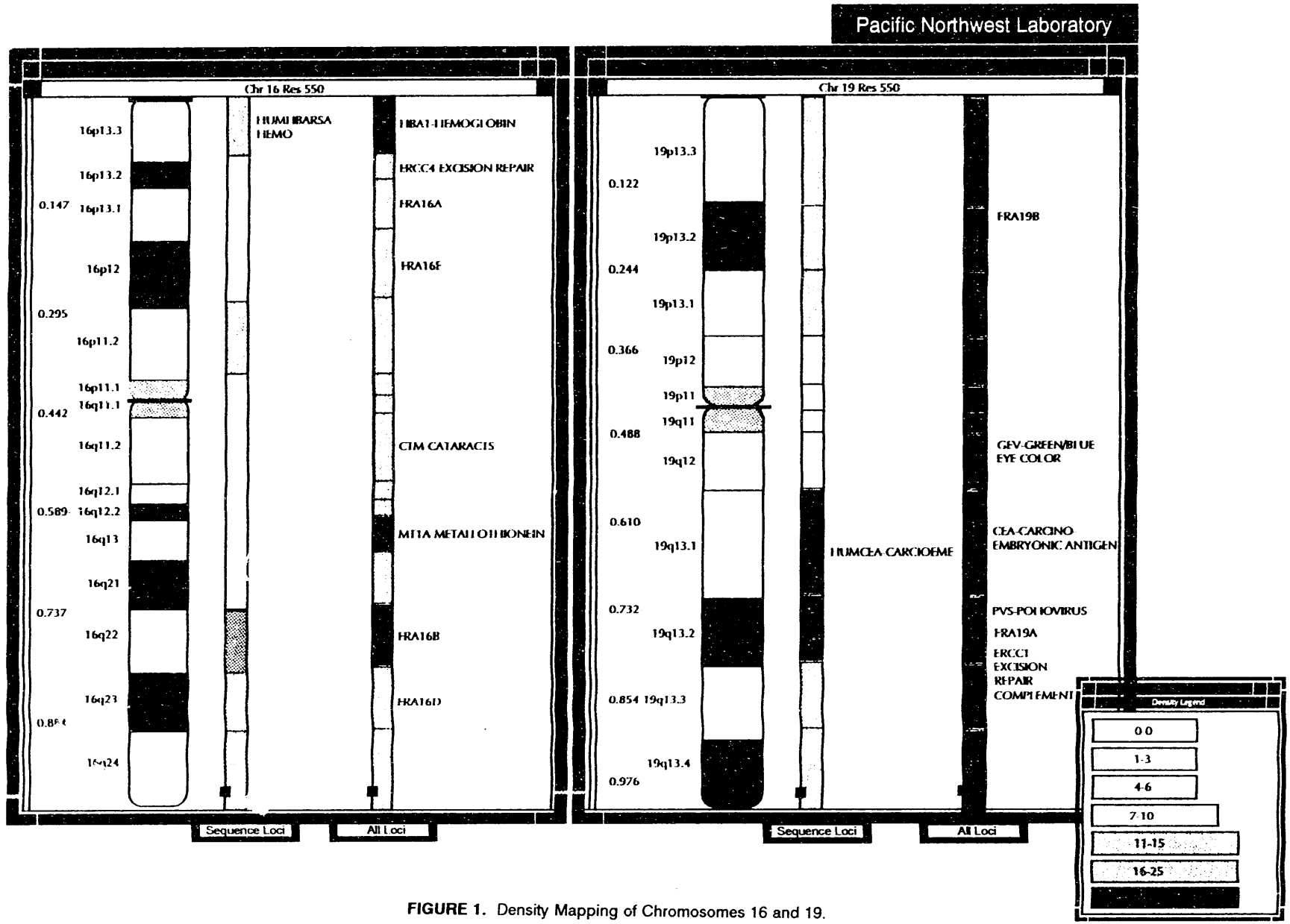

FIGURE 1. Density Mapping of Chromosomes 16 and 19.

Acknowledgment

A special note of thanks to Dr. Peter Pearson for providing us direct access to the relational tables that constitute the Genome Data Base (GDB).

Appendix

Appendix

Dose-Effect Studies with Inhaled Plutonium in Beagles

On the following pages (pp. 99 to 123), data are presented for all dogs assigned to current life-span dose-effect studies with inhaled $^{239}PuO_2$, $^{238}PuO_2$, and ^{239}Pu nitrate. Information is presented on the estimated initial lung deposition, based on external thorax counts and on estimated lung weights (0.011 x body weight) at time of exposure. Information is also provided (see column headed "Comments on Dead Dogs") on the current interpretation of the most prominent clinicopathological features associated with the death of animals. These data represent information presently available, and are presented as reference material for scientists who desire to follow in detail the progress of these experiments.

DOSE-EFFECT STUDIES WITH INHALED PU-239 OXIDE IN BEAGLES

			INITIAL ALVEOLAR DEPOSITION			INHALATION EXPOSURE			DEATH INFORMATION			
DOSE GROUP	DOG IDENT	BIRTH DATE	NCI	NCI/G LUNG	NCI/ KG	WEIGHT (KG)	AGE (MO)	EXPO DATE	DEATH DATE	MONTHS POST INH	AGE (MO)	COMMENTS ON DEAD DOGS
CONTROL	738 F	4/25/69	0	0.00	0.00	10.5	25.4	6/08/71	8/11/83	146.1	171.5	Hemangiosarcoma, Heart
CONTROL	740 F	4/25/69	0	0.00	0.00	11.0	25.4	6/08/71	6/18/83	144.3	169.8	Malignant Lymphoma
CONTROL	749 F	6/03/69	0	0.00	0.00	11.0	19.5	1/19/71	9/14/84	163.8	183.4	Adrenalitis
CONTROL	755 M	6/05/69	0	0.00	0.00	12.0	19.5	1/19/71	12/10/82	142.7	162.2	Renal Papillary Necrosis; Epileptic Seizures
CONTROL	766 M	6/16/69	0	0.00	0.00	11.5	19.1	1/19/71	6/26/84	161.2	180.3	Lung Tumor
CONTROL	775 F	6/28/69	0	0.00	0.00	12.0	18.7	1/19/71	10/05/81	128.5	147.3	Pulmonary Thromboembolism
CONTROL	785 M	7/19/69	0	0.00	0.00	12.0	19.5	3/04/71	9/02/87	198.0	217.5	Herniated Vertebral Disc
CONTROL	789 M	7/29/69	0	0.00	0.00	11.5	19.2	3/04/71	7/25/83	148.7	167.9	Malignant Lymphoma
CONTROL	792 M	9/11/69	0	0.00	0.00	12.5	20.9	6/08/71	4/28/76	58.7	79.5	Malignant Melanoma, Oral Cavity
CONTROL	800 F	10/21/69	0	0.00	0.00	10.0	16.4	3/04/71	11/17/86	188.5	204.9	Malignant Pheochromocytoma, Adrenal
CONTROL	801 M	10/21/69	0	0.00	0.00	12.5	19.5	6/08/71	2/23/82	128.6	148.1	Lung Tumor
CONTROL	811 F	11/23/69	0	0.00	0.00	11.5	15.3	3/04/71	2/24/85	167.8	183.1	Malignant Melanoma, Oral Cavity
CONTROL	846 M	12/19/69	0	0.00	0.00	13.5	18.5	7/06/71	4/08/83	141.1	159.6	Chronic Nephropathy
CONTROL	861 M	12/29/69	0	0.00	0.00	13.0	18.2	7/06/71	11/18/86	184.4	202.6	Cushing's Disease; Carcinoma, Intestine
CONTROL	868 F	2/08/70	0	0.00	0.00	9.5	16.9	7/06/71	3/24/87	188.6	205.4	Chronic Nephropathy
CONTROL	872 F	2/11/70	0	0.00	0.00	8.0	16.8	7/06/71	11/05/82	136.0	152.8	Lung Tumor
CONTROL	878 M	4/10/70	0	0.00	0.00	12.0	19.0	11/10/71	1/22/85	158.4	177.4	Chronic Nephropathy
CONTROL	882 M	4/15/70	0	0.00	0.00	12.5	18.9	11/10/71	11/06/81	119.9	138.7	Hemangiosarcoma, Liver
CONTROL	885 F	5/04/70	0	0.00	0.00	11.5	18.2	11/10/71	2/18/83	135.3	153.5	Sweat Gland Adenocarcinoma, Skin (Lung Metastases)
CONTROL	903 F	7/14/70	0	0.00	0.00	7.0	15.9	11/10/71	1/30/85	158.7	174.6	Malignant Lymphoma

DOSE-EFFECT STUDIES WITH INHALED PU-239 OXIDE IN BEAGLES

			INITIAL ALVEOLAR DEPOSITION			INHALATION EXPOSURE			DEATH INFORMATION			
DOSE GROUP	DOG IDENT	BIRTH DATE	NCI	NCI/G LUNG	NCI/ KG	WEIGHT (KG)	AGE (MO)	EXPO DATE	DEATH DATE	MONTHS POST INH	AGE (MO)	COMMENTS ON DEAD DOGS
CONTROL-SAC	701 F	3/17/69	0	0.00	0.00	9.0	19.8	11/10/70	4/18/79	101.2	121.0	Sacrificed
CONTROL-SAC	703 M	3/17/69	0	0.00	0.00	14.5	19.8	11/10/70	3/24/77	76.4	96.2	Sacrificed
CONTROL-SAC	724 M	4/01/69	0	0.00	0.00	14.0	18.8	10/26/70	3/30/78	89.1	107.9	Sacrificed
LOWEST	756 M	6/05/69	0	0.00	0.00	13.0	19.5	1/19/71	4/21/83	147.0	166.5	Epileptic Seizures
LOWEST	847 M	12/19/69	0	0.00	0.00	13.0	18.5	7/06/71	1/23/85	162.6	181.2	Chronic Nephropathy
LOWEST	858 M	12/29/69	0	0.00	0.00	13.5	18.2	7/06/71	10/01/86	182.9	201.1	Lymphocytic Leukemia
LOWEST	865 F	1/23/70	0	0.00	0.00	9.0	17.4	7/06/71	9/16/86	182.4	199.8	Pneumonia
LOWEST	879 M	4/10/70	0	0.00	0.00	14.5	17.9	10/07/71	7/27/84	153.7	171.6	Hemangiosarcoma, Liver, Spleen
LOWEST	886 F	5/04/70	0	0.00	0.00	10.5	18.2	11/10/71	4/04/84	148.8	167.0	Meningioma, Malignant
LOWEST	907 F	7/14/70	0	0.00	0.00	11.5	15.9	11/10/71	5/10/86	174.0	189.9	Pneumonia
LOWEST	825 F	12/03/69	1	0.01	0.12	11.5	18.1	6/08/71	11/17/82	137.3	155.5	Hemangiosarcoma, Spleen
LOWEST	904 F	7/14/70	1	0.01	0.07	9.5	15.9	11/10/71	12/19/83	145.3	161.2	Chondrosarcoma, Nasal
LOWEST	832 F	12/10/69	2	0.02	0.22	9.0	16.5	4/26/71	3/03/86	178.2	194.7	Malignant Lymphoma
LOWEST	900 M	7/12/70	3	0.02	0.22	13.0	16.0	11/10/71	5/21/82	126.3	142.3	Extramedullary Myeloma
LOWEST	870 F	2/08/70	4	0.03	0.32	12.0	16.9	7/06/71	5/04/84	154.0	170.8	Pneumonia
LOWEST	899 F	7/12/70	4	0.03	0.31	11.5	16.0	11/10/71	3/29/81	112.6	128.6	Hemangiosarcoma, Heart
LOWEST	867 M	1/23/70	5	0.04	0.41	11.5	17.4	7/06/71	2/07/86	175.1	192.5	Malignant Lymphoma
LOWEST	891 M	7/11/70	6	0.04	0.41	14.0	16.0	11/10/71	6/26/81	115.5	131.5	Septicemia
LOWEST	853 M	12/28/69	8	0.05	0.51	15.0	21.3	10/07/71	12/12/84	158.2	179.5	Pneumonia
LOWEST	875 M	2/11/70	8	0.05	0.54	14.0	16.8	7/06/71	5/21/78	82.5	99.3	Malignant Lymphoma
LOWEST	770 F	6/16/69	6	0.06	0.63	9.5	19.1	1/19/71	11/29/84	166.3	185.5	Chronic Nephropathy

DOSE-EFFECT STUDIES WITH INHALED PU-239 OXIDE IN BEAGLES

			INITIAL ALVEOLAR DEPOSITION			INHALATION EXPOSURE			DEATH INFORMATION			
DOSE GROUP	DOG IDENT	BIRTH DATE	NCI	NCI/G LUNG	NCI/ KG	WEIGHT (KG)	AGE (MO)	EXPO DATE	DEATH DATE	MONTHS POST INH	AGE (MO)	COMMENTS ON DEAD DOGS
LOWEST	788 M	7/19/69	8	0.06	0.62	13.0	18.8	2/10/71	4/13/84	158.1	176.8	Chronic Nephropathy
LOWEST	850 F	12/28/69	5	0.06	0.63	8.0	21.3	10/07/71	6/06/83	140.0	161.2	Bone Tumor; Chronic Nephropathy
LOWEST	893 M	7/11/70	9	0.06	0.61	14.0	14.9	10/07/71	7/01/86	176.8	191.7	Pneumonia
LOWEST	807 F	11/23/69	8	0.07	0.73	11.0	14.6	2/10/71	7/24/81	125.4	140.0	Pituitary Tumor; Cushing's Disease
LOWEST	841 F	12/16/69	6	0.07	0.75	8.0	17.7	6/08/71	4/01/86	177.8	195.5	Malignant Lymphoma
LOWEST	908 M	7/14/70	9	0.07	0.77	11.0	15.9	11/10/71	4/01/80	100.7	116.6	Unknown Cause; Pulmonary Hyalinosis
LOWEST-SAC	762 M	6/11/69	0	0.00	0.00	11.5	19.3	1/19/71	1/24/77	72.2	91.5	Sacrificed
LOWEST-SAC	849 F	12/28/69	1	0.01	0.10	10.0	21.3	10/07/71	10/26/72	12.6	33.9	Sacrificed
LOW	776 M	6/28/69	10	0.07	0.74	13.5	20.2	3/04/71	9/19/84	162.6	182.7	Pneumonia
LOW	842 M	12/16/69	10	0.07	0.77	13.5	18.6	7/06/71	5/01/85	165.8	184.5	Lung Tumor; Chronic Nephropathy
LOW	767 M	6/16/69	10	0.08	0.83	12.0	18.2	12/21/70	12/09/85	179.6	197.8	Heart Failure
LOW	862 M	12/29/69	13	0.09	1.00	13.0	17.3	6/08/71	6/25/83	144.6	161.8	Peritonitis
LOW	871 M	2/08/70	13	0.09	0.96	13.5	16.9	7/06/71	7/24/86	180.6	197.5	Malignant Melanoma, Oral Cavity
LOW	874 M	2/11/70	16	0.11	1.24	13.0	16.8	7/06/71	4/09/85	165.1	181.9	Chronic Nephropathy
LOW	754 M	6/05/69	22	0.15	1.69	13.0	19.5	1/19/71	1/10/78	83.7	103.2	Epileptic Seizures
LOW	845 F	12/19/69	19	0.15	1.63	11.5	17.6	6/08/71	8/09/84	158.1	175.7	Transitional Carcinoma, Urinary Bladder
LOW	748 F	6/03/69	14	0.16	1.75	8.0	19.5	1/19/71	8/19/81	127.0	146.5	Unknown Cause
LOW	826 F	12/03/69	19	0.17	1.90	10.0	19.1	7/06/71	4/17/84	153.4	172.5	Hemangioma, Spleen
LOW	831 F	12/10/69	21	0.18	2.00	10.5	17.9	6/08/71	5/14/84	155.2	173.1	Pneumonia
LOW	881 F	4/15/70	19	0.19	2.09	9.0	17.7	10/07/71	12/20/86	182.4	200.2	Pneumonia
LOW	780 F	7/13/69	24	0.22	2.40	10.0	18.2	1/19/71	4/08/82	134.6	152.8	Malignant Pheochromocytoma, Adrenal

DOSE-EFFECT STUDIES WITH INHALED PU-239 OXIDE IN BEAGLES

			INITIAL ALVEOLAR DEPOSITION			INHALATION EXPOSURE			DEATH INFORMATION			
DOSE GROUP	DOG IDENT	BIRTH DATE	NCI	NCI/G LUNG	NCI/ KG	WEIGHT (KG)	AGE (MO)	EXPO DATE	DEATH DATE	MONTHS POST INH	AGE (MO)	COMMENTS ON DEAD DOGS
LOW	859 M	12/29/69	35	0.22	2.41	14.5	18.2	7/06/71	4/22/84	153.6	171.8	Transitional Carcinoma, Urinary Bladder
LOW	757 M	6/05/69	36	0.23	2.57	14.0	18.5	12/21/70	11/26/86	191.2	209.7	Leiomyosarcoma,Kidney; Lung Tumor
LOW	876 F	4/10/70	19	0.24	2.69	7.0	17.9	10/07/71	5/05/86	174.9	192.8	Nephropathy; Lung Tumor
LOW	806 F	11/23/69	26	0.25	2.74	9.5	15.3	3/04/71	10/29/82	139.9	155.2	Malignant Melanoma, Oral Cavity
LOW	813 F	11/30/69	32	0.29	3.20	10.0	15.1	3/04/71	12/15/83	153.4	168.5	Multilobular Sarcoma, Skull
LOW	877 F	4/10/70	34	0.29	3.24	10.5	17.9	10/07/71	5/06/86	174.9	192.9	Lung Tumor
LOW	769 F	6/16/69	28	0.32	3.50	8.0	18.2	12/21/70	6/23/78	90.1	108.2	Granulosa Cell Tumor, Ovary
LOW	802 M	10/21/69	40	0.33	3.64	11.0	18.1	4/26/71	12/28/84	164.1	182.2	Pneumonia
LOW-SAC	920 M	2/08/71	11	0.08	0.92	12.0	16.0	6/08/72	7/07/72	1.0	16.9	Sacrificed
LOW-SAC	798 F	10/21/69	16	0.16	1.78	9.0	15.7	2/10/71	8/29/74	42.6	58.3	Sacrificed
MED-LOW	781 F	7/13/69	48	0.38	4.17	11.5	17.3	12/21/70	2/20/81	122.0	139.3	Hemangiosarcoma, Kidney; Lung Tumor
MED-LOW	771 F	6/16/69	44	0.40	4.40	10.0	19.2	1/20/71	11/02/83	153.4	172.6	Lung Tumor
MED-LOW	782 M	7/13/69	62	0.42	4.59	13.5	19.0	2/10/71	5/27/83	147.5	166.4	Neurofibrosarcoma, Brachial Plexus
MED-LOW	786 M	7/19/69	62	0.42	4.59	13.5	19.5	3/04/71	5/29/86	182.8	202.3	Adrenocortical Carcinoma; Lung Tumor
MED-LOW	752 M	6/03/69	62	0.43	4.77	13.0	18.6	12/21/70	2/22/79	98.1	116.7	Lung Tumor
MED-LOW	823 M	11/30/69	65	0.44	4.81	13.5	16.8	4/26/71	5/24/84	156.9	173.8	Transitional Carcinoma, Urethra
MED-LOW	883 M	4/15/70	63	0.44	4.85	13.0	17.7	10/07/71	1/25/88	195.6	213.4	Chronic Nephropathy
MED-LOW	778 M	6/28/69	74	0.46	5.10	14.5	20.2	3/04/71	8/26/79	101.7	121.9	Pulmonary Thromboembolism
MED-LOW	838 M	12/12/69	56	0.46	5.09	11.0	17.8	6/08/71	7/20/84	157.4	175.2	Malignant Lymphoma; Lung Tumor
MED-LOW	795 F	10/21/69	54	0.49	5.40	10.0	15.0	1/20/71	9/06/83	151.5	166.5	Lung Tumor
MED-LOW	851 F	12/28/69	53	0.54	5.89	9.0	21.3	10/07/71	12/07/86	182.0	203.3	Carcinoma, Thyroid; Hypothyroidism

DOSE-EFFECT STUDIES WITH INHALED PU-239 OXIDE IN BEAGLES

			INITIAL ALVEOLAR DEPOSITION			INHALATION EXPOSURE			DEATH INFORMATION			
DOSE GROUP	DOG IDENT	BIRTH DATE	NCI	NCI/G LUNG	NCI/ KG	WEIGHT (KG)	AGE (MO)	EXPO DATE	DEATH DATE	MONTHS POST INH	AGE (MO)	COMMENTS ON DEAD DOGS
MED-LOW	834 F	12/12/69	67	0.68	7.44	9.0	17.8	6/08/71	7/05/79	96.9	114.7	Pyometra
MED-LOW	797 F	10/21/69	85	0.70	7.73	11.0	16.4	3/04/71	5/16/86	182.4	198.8	Lung Tumor
MED-LOW	848 F	12/28/69	75	0.72	7.94	9.5	21.3	10/07/71	10/02/86	179.8	201.1	Pneumonia
MED-LOW	827 F	12/03/69	89	0.74	8.09	11.0	16.7	4/26/71	1/06/85	164.4	181.1	Pneumonitis
MED-LOW	697 M	3/16/69	140	0.85	9.33	15.0	19.5	10/30/70	5/08/80	114.3	133.7	Heart Failure
MED-LOW	750 M	6/03/69	118	0.93	10.26	11.5	19.6	1/20/71	6/28/84	161.2	180.8	Lung Tumor; Malignant Lymphoma
MED-LOW	884 M	4/15/70	123	1.12	12.30	10.0	17.8	10/08/71	9/12/84	155.2	172.9	Lung Tumor
MED-LOW	844 F	12/19/69	135	1.17	12.86	10.5	17.6	6/08/71	8/08/85	170.0	187.6	Nephropathy; Lung Tumor
MED-LOW	905 F	7/14/70	127	1.36	14.94	8.5	15.9	11/10/71	2/07/83	134.9	150.8	Malignant Lymphoma
MED-LOW-SAC	815 M	11/30/69	68	0.52	5.67	12.0	16.8	4/26/71	5/22/73	24.9	41.7	Sacrificed
MED-LOW-SAC	918 M	2/08/71	74	0.58	6.43	11.5	16.0	6/08/72	7/06/72	0.9	16.9	Sacrificed
MEDIUM	866 M	1/23/70	200	1.35	14.81	13.5	17.4	7/06/71	6/27/84	155.7	173.1	Lung Tumor
MEDIUM	809 F	11/23/69	157	1.36	14.95	10.5	15.3	3/04/71	5/28/81	122.8	138.1	Liver Cirrhosis; Carcinoma, Thyroid
MEDIUM	764 F	6/16/69	158	1.37	15.05	10.5	18.2	12/21/70	7/07/82	138.5	156.7	Lung Tumor
MEDIUM	835 F	12/12/69	163	1.48	16.30	10.0	16.4	4/26/71	6/25/78	86.0	102.4	Reticulum Cell Sarcoma
MEDIUM	839 F	12/16/69	189	1.49	16.43	11.5	16.3	4/26/71	2/03/86	177.3	193.6	Lung Tumor; Carcinoma, Bile Duct
MEDIUM	814 F	11/30/69	140	1.50	16.47	8.5	15.1	3/04/71	10/17/79	103.5	118.5	Lung Tumor
MEDIUM	836 M	12/12/69	256	1.66	18.29	14.0	17.8	6/08/71	3/16/81	117.3	135.1	Lung Tumor
MEDIUM	819 F	11/30/69	163	1.74	19.18	8.5	18.2	6/08/71	8/20/85	170.4	188.6	Nephropathy; Lung Tumor
MEDIUM	888 M	5/04/70	274	1.78	19.57	14.0	17.1	10/08/71	7/02/79	92.8	109.9	Lung Tumor
MEDIUM	824 F	12/03/69	227	1.79	19.74	11.5	18.1	6/08/71	1/26/81	115.6	133.8	Pneumonia

DOSE-EFFECT STUDIES WITH INHALED PU-239 OXIDE IN BEAGLES

			INITIAL ALVEOLAR DEPOSITION			INHALATION EXPOSURE			DEATH INFORMATION			
DOSE GROUP	DOG IDENT	BIRTH DATE	NCI	NCI/G LUNG	NCI/ KG	WEIGHT (KG)	AGE (MO)	EXPO DATE	DEATH DATE	MONTHS POST INH	AGE (MO)	COMMENTS ON DEAD DOGS
MEDIUM	860 M	12/29/69	254	1.85	20.32	12.5	17.3	6/08/71	6/24/82	132.5	149.8	Lung Tumor
MEDIUM	833 F	12/10/69	248	2.37	26.11	9.5	16.5	4/26/71	4/04/83	143.3	159.8	Metritis
MEDIUM	810 F	11/23/69	302	2.39	26.26	11.5	15.3	3/04/71	9/09/81	126.2	141.5	Lung Tumor
MEDIUM	794 M	9/11/69	444	2.60	28.65	15.5	17.7	3/04/71	2/17/81	119.5	137.2	Adenoma, Pituitary; Cushing's Disease
MEDIUM	854 M	12/28/69	465	2.64	29.06	16.0	21.3	10/08/71	1/25/82	123.6	144.9	Lung Tumor
MEDIUM	808 F	11/23/69	270	2.89	31.76	8.5	14.6	2/10/71	9/09/82	138.9	153.5	Lung Tumor
MEDIUM	805 F	11/23/69	257	3.12	34.27	7.5	18.5	6/08/71	7/22/82	133.5	151.9	Leiomyoma, Esophagus; Lung Tumor
MEDIUM	812 M	11/23/69	438	3.19	35.04	12.5	17.1	4/26/71	11/12/79	102.6	119.6	Lung Tumor
MEDIUM	857 M	12/29/69	486	3.40	37.38	13.0	17.3	6/08/71	7/01/80	108.8	126.1	Lung Tumor
MEDIUM	892 M	7/11/70	494	3.59	39.52	12.5	16.0	11/10/71	10/26/81	119.5	135.5	Lung Tumor
MEDIUM	777 M	6/28/69	546	3.97	43.68	12.5	20.2	3/04/71	3/26/80	108.7	128.9	Lung Tumor
MEDIUM	803 M	10/21/69	547	4.32	47.57	11.5	18.1	4/26/71	11/10/77	78.5	96.7	Interstitial Pneumonitis
MEDIUM-SAC	478 M	6/08/65	298	2.71	29.80	10.0	64.0	10/09/70	10/16/70	0.2	64.3	Sacrificed
MEDIUM-SAC	816 M	11/30/69	398	3.62	39.80	10.0	16.8	4/25/71	5/11/71	0.5	17.3	Sacrificed
MED-HIGH	787 M	7/19/69	651	4.73	52.08	12.5	19.5	3/04/71	2/08/79	95.2	114.7	Lung Tumor; Leiomyosarcoma, Intestine
MED-HIGH	840 F	12/16/69	703	4.92	54.08	13.0	17.7	6/08/71	4/29/80	106.7	124.4	Lung Tumor
MED-HIGH	727 M	4/03/69	733	5.33	58.64	12.5	18.8	10/26/70	11/10/76	72.5	91.3	Lung Tumor
MED-HIGH	898 F	7/12/70	711	5.39	59.25	12.0	16.0	11/10/71	2/03/81	110.8	126.8	Transitional Carcinoma, Urinary Bladder; Lung Tumor
MED-HIGH	856 F	12/29/69	818	5.72	62.92	13.0	18.2	7/07/71	5/02/79	93.8	112.1	Lung Tumor
MED-HIGH	759 M	6/11/69	809	6.13	67.42	12.0	18.3	12/21/70	6/02/75	53.4	71.7	Lung Tumor
MED-HIGH	864 F	1/23/70	801	6.62	72.82	11.0	17.4	7/07/71	11/02/79	99.9	117.3	Lung Tumor

DOSE-EFFECT STUDIES WITH INHALED PU-239 OXIDE IN BEAGLES

			INITIAL ALVEOLAR DEPOSITION			INHALATION EXPOSURE			DEATH INFORMATION			
DOSE GROUP	DOG IDENT	BIRTH DATE	NCI	NCI/G LUNG	NCI/ KG	WEIGHT (KG)	AGE (MO)	EXPO DATE	DEATH DATE	MONTHS POST INH	AGE (MO)	COMMENTS ON DEAD DOGS
MED-HIGH	909 M	7/14/70	737	6.70	73.70	10.0	15.9	11/10/71	6/04/81	114.8	130.7	Lung Tumor
MED-HIGH	837 M	12/12/69	1283	8.04	88.48	14.5	18.8	7/07/71	7/21/77	72.5	91.3	Lung Tumor
MED-HIGH	863 F	1/23/70	980	8.48	93.33	10.5	17.4	7/07/71	10/21/77	75.5	92.9	Lung Tumor
MED-HIGH	820 F	11/30/69	847	8.56	94.11	9.0	18.2	6/08/71	6/01/79	95.8	114.0	Lung Tumor
MED-HIGH	852 F	12/28/69	1187	9.38	103.22	11.5	21.3	10/08/71	2/22/78	76.5	97.8	Lung Tumor
MED-HIGH	880 F	4/15/70	840	9.55	105.00	8.0	17.8	10/08/71	12/04/78	85.9	103.7	Lung Tumor
MED-HIGH	889 F	7/11/70	1089	9.90	108.90	10.0	16.0	11/10/71	9/20/79	94.3	110.3	Lung Tumor; Osteoarthropathy
MED-HIGH	783 M	7/13/69	1394	10.14	111.52	12.5	19.0	2/10/71	12/03/75	57.7	76.7	Lung Tumor
MED-HIGH	804 M	10/21/69	1344	10.18	112.00	12.0	20.5	7/07/71	8/18/74	37.4	57.9	Lung Tumor; Radiation Pneumonitis
MED-HIGH	873 M	2/11/70	1767	10.71	117.80	15.0	16.8	7/07/71	9/03/76	61.9	78.7	Lung Tumor
MED-HIGH	760 M	6/11/69	1378	10.89	119.83	11.5	19.3	1/20/71	8/15/73	30.8	50.1	Radiation Pneumonitis
MED-HIGH	796 F	10/21/69	1318	11.41	125.52	10.5	15.7	2/10/71	9/17/75	55.2	70.9	Lung Tumor; Osteoarthropathy
MED-HIGH	761 M	6/11/69	1460	12.07	132.73	11.0	19.3	1/20/71	11/02/76	69.4	88.7	Lung Tumor
MED-HIGH	772 M	6/16/69	1896	14.99	164.87	11.5	19.8	2/10/71	6/26/75	52.5	72.3	Lung Tumor; Osteoarthropathy
MED-HIGH-SAC	734 M	4/04/69	914	6.92	76.17	12.0	19.2	11/10/70	4/01/71	4.7	23.9	Sacrificed
MED-HIGH-SAC	709 M	3/24/69	1726	12.55	138.08	12.5	19.6	11/10/70	3/31/71	4.6	24.2	Sacrificed
MED-HIGH-SAC	702 F	3/17/69	1682	15.29	168.20	10.0	19.8	11/10/70	3/31/71	4.6	24.4	Sacrificed
MED-HIGH-SAC	739 F	4/25/69	1511	17.17	188.88	8.0	18.5	11/10/70	4/01/71	4.7	23.2	Sacrificed
HIGH	753 F	6/05/69	2448	23.43	257.68	9.5	18.5	12/21/70	10/02/76	69.4	87.9	Lung Tumor
HIGH	817 M	11/30/69	3164	23.97	263.67	12.0	19.2	7/07/71	3/26/73	20.6	39.8	Radiation Pneumonitis
HIGH	829 M	12/03/69	3515	24.58	270.38	13.0	19.1	7/07/71	9/13/73	26.3	45.3	Radiation Pneumonitis

DOSE-EFFECT STUDIES WITH INHALED PU-239 OXIDE IN BEAGLES

			INITIAL ALVEOLAR DEPOSITION			INHALATION EXPOSURE			DEATH INFORMATION			
DOSE GROUP	DOG IDENT	BIRTH DATE	NCI	NCI/G LUNG	NCI/ KG	WEIGHT (KG)	AGE (MO)	EXPO DATE	DEATH DATE	MONTHS POST INH	AGE (MO)	COMMENTS ON DEAD DOGS
HIGH	890 F	7/11/70	3101	31.32	344.56	9.0	16.0	11/10/71	6/13/74	31.1	47.1	Radiation Pneumonitis
HIGH	906 F	7/14/70	6632	63.46	698.11	9.5	15.9	11/09/71	11/22/72	12.5	28.3	Radiation Pneumonitis
HIGH	896 F	7/12/70	5515	66.85	735.33	7.5	16.0	11/10/71	2/12/73	15.1	31.1	Radiation Pneumonitis
HIGH	747 F	6/03/69	7476	97.09	1068.00	7.0	19.6	1/20/71	1/13/72	11.8	31.3	Radiation Pneumonitis
HIGH	910 M	7/14/70	14267	103.76	1141.36	12.5	15.9	11/10/71	10/12/72	11.1	27.0	Radiation Pneumonitis
HIGH-SAC	435 F	7/21/64	3840	33.25	365.71	10.5	75.5	11/05/70	11/12/70	0.2	75.7	Sacrificed
HIGH-SAC	913 M	2/04/71	4900	35.64	392.00	12.5	17.4	7/19/72	8/18/72	1.0	18.4	Sacrificed

DOSE-EFFECT STUDIES WITH INHALED PU-238 OXIDE IN BEAGLES

			INITIAL ALVEOLAR DEPOSITION			INHALATION EXPOSURE			DEATH INFORMATION			
DOSE GROUP	DOG IDENT	BIRTH DATE	NCI	NCI/G LUNG	NCI/ KG	WEIGHT (KG)	AGE (MO)	EXPO DATE	DEATH DATE	MONTHS POST INH	AGE (MO)	COMMENTS ON DEAD DOGS
CONTROL	939 M	5/05/71	0	0.00	0.00	13.5	19.5	12/19/72	10/01/82	117.4	136.9	Transitional Carcinoma, Urinary Bladder
CONTROL	949 F	5/11/71	0	0.00	0.00	12.0	19.3	12/19/72	10/30/84	142.4	161.7	Malignant Lymphoma
CONTROL	978 M	5/15/71	0	0.00	0.00	15.5	19.2	12/19/72	4/07/88	183.6	202.8	Herniated Vertebral Disc
CONTROL	990 F	5/26/71	0	0.00	0.00	8.0	18.8	12/19/72	7/08/79	78.6	97.4	Pyometra
CONTROL	996 F	5/31/71	0	0.00	0.00	11.5	19.6	1/18/73	7/06/84	137.6	157.2	Malignant Lymphoma
CONTROL	1005 M	5/31/71	0	0.00	0.00	10.0	19.6	1/18/73	2/24/87	169.2	188.8	Lung Tumor
CONTROL	1007 F	6/02/71	0	0.00	0.00	11.0	19.6	1/18/73	3/29/88	182.3	201.9	Chronic Nephropathy
CONTROL	1024 M	6/15/71	0	0.00	0.00	14.5	19.2	1/18/73	7/13/87	173.8	192.9	Transitional Carcinoma, Urethra
CONTROL	1038 M	8/19/71	0	0.00	0.00	14.0	18.2	2/22/73	12/16/86	165.7	183.9	Hemangiosarcoma, Spleen
CONTROL	1045 M	8/20/71	0	0.00	0.00	11.5	18.1	2/22/73	6/08/86	159.5	177.6	Renal Amyloidosis; Hemangiosarcoma, Spleen
CONTROL	1054 F	8/27/71	0	0.00	0.00	9.0	17.9	2/22/73	12/05/88	189.4	207.3	Chronic Nephropathy
CONTROL	1061 F	8/30/71	0	0.00	0.00	13.0	17.8	2/22/73	7/07/81	100.4	118.2	Malignant Lymphoma
CONTROL	1093 M	12/22/71	0	0.00	0.00	14.0	17.3	5/31/73	11/04/83	125.1	142.4	Adenoma, Pituitary; Cushing's Disease
CONTROL	1097 F	1/11/72	0	0.00	0.00	7.5	16.6	5/31/73	9/15/88	183.5	200.1	Nasal Transitional Carcinoma
CONTROL	1112 M	1/19/72	0	0.00	0.00	13.5	16.4	5/31/73	12/02/86	162.1	178.4	Malignant Lymphoma
CONTROL	1116 F	1/27/72	0	0.00	0.00	12.0	16.1	5/31/73	4/07/89	190.2	206.3	Hemangiosarcoma, Omentum
CONTROL	1186 F	8/16/72	0	0.00	0.00	9.5	18.3	2/25/74	7/26/85	137.0	155.3	Transitional Carcinoma, Urinary Bladder
CONTROL	1197 M	8/31/72	0	0.00	0.00	12.0	17.8	2/25/74	4/25/89	181.9	199.8	Pneumonia
CONTROL	1209 M	9/09/72	0	0.00	0.00	12.5	17.5	2/25/74	12/27/88	178.0	195.6	Pulmonary Interstial Fibrosis
CONTROL	1225 F	10/04/72	0	0.00	0.00	8.0	16.8	2/26/74	10/10/87	163.4	180.2	Adenoma, Pituitary
CONTROL-SAC	966 M	5/14/71	0	0.00	0.00	13.0	19.2	12/19/72	4/30/77	52.3	71.6	Sacrificed

DOSE-EFFECT STUDIES WITH INHALED PU-238 OXIDE IN BEAGLES

			INITIAL ALVEOLAR DEPOSITION			INHALATION EXPOSURE			DEATH INFORMATION			
DOSE GROUP	DOG IDENT	BIRTH DATE	NCI	NCI/G LUNG	NCI/ KG	WEIGHT (KG)	AGE (MO)	EXPO DATE	DEATH DATE	MONTHS POST INH	AGE (MO)	COMMENTS ON DEAD DOGS
CONTROL-SAC	1011 F	6/04/71	0	0.00	0.00	11.0	19.5	1/18/73	6/01/78	64.4	83.9	Sacrificed
CONTROL-SAC	1013 F	6/04/71	0	0.00	0.00	11.5	19.5	1/18/73	5/29/79	76.3	95.8	Sacrificed
CONTROL-SAC	1087 M	12/15/71	0	0.00	0.00	13.5	17.5	5/31/73	12/14/76	42.5	60.0	Sacrificed
CONTROL-SAC	1118 M	1/27/72	0	0.00	0.00	8.5	16.1	5/31/73	1/13/76	31.4	47.5	Sacrificed
CONTROL-SAC	1223 M	9/16/72	0	0.00	0.00	12.0	19.0	4/18/74	5/15/75	12.9	31.9	Sacrificed
CONTROL-SAC	1227 M	10/04/72	0	0.00	0.00	9.5	18.4	4/18/74	12/01/76	31.5	49.9	Sacrificed
CONTROL-SAC	1228 M	10/04/72	0	0.00	0.00	14.5	18.4	4/18/74	10/31/78	54.4	72.9	Sacrificed
LOWEST	958 M	5/31/71	0	0.00	0.00	10.5	19.6	1/18/73	4/11/86	158.7	178.4	Lung Tumor
LOWEST	1003 M	5/31/71	0	0.00	0.00	14.0	19.6	1/18/73	4/01/87	170.4	190.0	Transitional Carcinoma, Urinary Bladder
LOWEST	1023 F	6/15/71	0	0.00	0.00	12.5	19.2	1/18/73	3/27/88	182.2	201.4	Pneumonia
LOWEST	1039 M	8/19/71	0	0.00	0.00	11.0	17.0	1/18/73	7/04/86	161.5	178.5	Heart Failure
LOWEST	1044 F	8/20/71	0	0.00	0.00	11.5	17.0	1/18/73	8/31/88	187.4	204.4	Epileptic Seizures
LOWEST	1055 M	8/27/71	0	0.00	0.00	13.0	16.8	1/18/73	6/04/87	172.5	189.2	Malignant Melanoma, Oral Cavity
LOWEST	1063 M	8/30/71	0	0.00	0.00	14.5	16.7	1/18/73	11/11/80	93.8	110.4	Brain Tumor
LOWEST	1105 F	1/19/72	0	0.00	0.00	10.0	16.4	5/31/73	2/08/85	140.3	156.7	Malignant Lymphoma
LOWEST	1194 F	8/24/72	0	0.00	0.00	10.5	19.8	4/18/74	12/03/85	139.5	159.3	Malignant Lymphoma
LOWEST	1230 M	10/04/72	0	0.00	0.00	12.5	18.4	4/18/74	9/30/86	149.4	167.9	Hemangiosarcoma, Liver
LOWEST	951 M	5/11/71	2	0.01	0.14	14.0	19.3	12/19/72	2/14/83	121.9	141.2	Anesthetic Death
LOWEST	1008 M	6/02/71	2	0.01	0.15	13.5	19.6	1/18/73	10/24/85	153.2	172.7	Fibrosarcoma, Spleen
LOWEST	1193 F	8/24/72	2	0.01	0.16	12.5	19.8	4/18/74	1/22/86	141.2	161.0	Immune Hemolytic Anemia
LOWEST	959 M	5/14/71	3	0.02	0.22	13.5	19.2	12/19/72	6/22/84	138.1	157.3	Liver Abscess

DOSE-EFFECT STUDIES W INHALED PU-238 OXIDE IN BEAGLES

DOSE GROUP	DOG IDENT	BIRTH DATE	INITIAL ALVEOLAR DEPOSITION NCI	NCI/G LUNG	NCI/ KG	INHALATION EXPOSURE WEIGHT (KG)	AGE (MO)	EXPO DATE	DEATH INFORMATION DEATH DATE	MONTHS POST INH	AGE (MO)	COMMENTS ON DEAD DOGS
LOWEST	1069 F	11/26/71	2	0.02	0.24	8.5	18.1	5/31/73	6/24/83	120.8	138.9	Malignant Lymphoma
LOWEST	1095 F	1/11/72	2	0.02	0.19	10.5	16.6	5/31/73	8/12/87	170.4	187.0	Chronic Nephropathy
LOWEST	989 F	5/26/71	3	0.03	0.32	9.5	18.8	12/19/72	3/05/81	98.5	117.3	Bone Tumor
LOWEST	1204 M	9/05/72	6	0.04	0.43	14.0	17.7	2/26/74	2/23/89	179.9	197.6	Transitional Carcinoma, Urethra
LOWEST	993 F	5/26/71	6	0.05	0.50	12.0	18.8	12/19/72	7/01/86	162.4	181.2	Malignant Lymphoma
LOWEST	1106 F	1/19/72	5	0.05	0.50	10.0	16.4	5/31/73	3/14/83	117.4	133.8	Carcinoma, Adrenal; Osteoarthropathy
LOWEST-SAC	1215 M	9/09/72	0	0.00	0.00	15.5	19.3	4/18/74	4/26/77	36.3	55.5	Sacrificed
LOWEST-SAC	921 F	4/15/71	3	0.03	0.31	10.0	19.5	11/30/72	12/27/72	0.9	20.4	Sacrificed
LOWEST-SAC	923 F	4/15/71	3	0.03	0.35	8.5	19.5	11/30/72	1/26/73	1.9	21.4	Sacrificed
LOWEST-SAC	925 M	4/15/71	5	0.04	0.40	12.5	19.5	11/30/72	2/27/73	2.9	22.5	Sacrificed
LOWEST-SAC	970 F	5/15/71	6	0.05	0.55	11.0	19.2	12/19/72	1/04/77	48.5	67.7	Sacrificed
LOW	1065 F	11/20/71	6	0.05	0.60	10.0	18.3	5/31/73	4/10/86	154.3	172.6	Malignant Lymphoma; Lung Tumor
LOW	1082 M	11/29/71	11	0.06	0.69	16.0	18.0	5/31/73	12/04/79	78.1	96.2	Paralysis, Spinal Cord Degeneration
LOW	1188 M	8/16/72	11	0.06	0.71	15.5	18.4	2/26/74	1/15/84	118.6	137.0	Metastatic Lung Tumor, Primary Site Unknown
LOW	1084 M	12/15/71	13	0.07	0.76	17.0	17.5	5/31/73	8/19/89	194.6	212.1	Malignant Lymphoma, Heart
LOW	1090 F	12/22/71	10	0.08	0.83	12.0	17.3	5/31/73	5/10/87	167.3	184.6	Heart Failure
LOW	1222 M	9/16/72	15	0.10	1.07	14.0	19.0	4/18/74	3/19/86	143.0	162.0	Malignant Mesothelioma
LOW	971 F	5/15/71	13	0.11	1.24	10.5	19.2	12/19/72	5/04/83	124.5	143.6	Hemangiosarcoma, Spleen
LOW	999 F	5/31/71	11	0.11	1.16	9.5	18.7	12/19/72	1/31/86	157.4	176.1	Nasal Sarcoma; Lung Tumor
LOW	1229 M	10/04/72	16	0.11	1.19	13.5	16.8	2/26/74	5/25/84	122.9	139.7	Pneumonia; Carcinoma, Thyroid
LOW	1070 M	11/26/71	22	0.12	1.33	16.5	18.1	5/31/73	12/13/83	126.4	144.6	Malignant Lymphoma

DOSE-EFFECT STUDIES WITH INHALED PU-238 OXIDE IN BEAGLES

			INITIAL ALVEOLAR DEPOSITION			INHALATION EXPOSURE			DEATH INFORMATION			
DOSE GROUP	DOG IDENT	BIRTH DATE	NCI	NCI/G LUNG	NCI/ KG	WEIGHT (KG)	AGE (MO)	EXPO DATE	DEATH DATE	MONTHS POST INH	AGE (MO)	COMMENTS ON DEAD DOGS
LOW	955 M	5/14/71	17	0.14	1.55	11.0	19.2	12/19/72	1/27/87	169.3	188.5	Lung Tumor; Adenoma, Bile Duct
LOW	1033 M	7/23/71	17	0.14	1.55	11.0	19.1	2/22/73	12/17/85	153.8	172.8	Lung Tumor
LOW	1036 F	8/19/71	16	0.14	1.52	10.5	18.2	2/22/73	5/06/87	170.4	188.6	Malignant Melanoma, Oral Cavity
LOW	1216 M	9/09/72	23	0.16	1.77	13.0	19.3	4/18/74	4/22/87	156.1	175.4	Malignant Lymphoma
LOW	1000 F	8/30/71	22	0.18	2.00	11.0	17.8	2/22/73	12/21/84	141.9	159.7	Pneumonia
LOW	981 M	5/20/71	30	0.21	2.31	13.0	19.0	12/19/72	1/12/89	192.8	211.8	Chronic Nephropathy
LOW	1046 M	8/20/71	27	0.22	2.45	11.0	18.1	2/22/73	12/15/87	177.7	195.8	Lung Tumor
LOW	1050 F	8/22/71	22	0.22	2.44	9.0	18.1	2/22/73	5/14/86	158.7	176.7	Lung Tumor
LOW	1078 F	11/29/71	29	0.22	2.42	12.0	18.0	5/31/73	11/09/83	125.3	143.3	Malignant Meningioma
LOW	1207 F	9/09/72	22	0.24	2.59	8.5	17.6	2/26/74	8/11/88	173.5	191.0	Herniated Vertebral Disc
LOW	1196 F	8/31/72	28	0.25	2.80	10.0	17.9	2/26/74	12/26/88	178.0	195.8	Carcinoma, Salivary Gland; Lung Tumor
LOW-SAC	1214 M	9/09/72	17	0.12	1.36	12.5	19.3	4/18/74	5/12/75	12.8	32.0	Sacrificed
LOW-SAC	1189 M	8/16/72	38	0.26	2.81	13.5	20.0	4/18/74	4/25/79	60.2	80.3	Sacrificed
LOW-SAC	930 M	4/27/71	38	0.27	2.92	13.0	19.2	11/30/72	12/28/72	0.9	20.1	Sacrificed
MED-LOW	1066 M	11/20/71	54	0.31	3.38	16.0	18.3	5/31/73	6/21/83	120.7	139.0	Malignant Lymphoma
MED-LOW	972 F	5/15/71	40	0.33	3.64	11.0	19.2	12/19/72	3/04/86	158.5	177.6	Allergic Bronchitis
MED-LOW	1089 F	12/22/71	41	0.34	3.73	11.0	17.3	5/31/73	8/21/88	182.7	200.0	Chronic Nephropathy
MED-LOW	1219 F	9/16/72	46	0.40	4.38	10.5	19.0	4/18/74	12/05/86	151.6	170.6	Chronic Nephropathy
MED-LOW	1158 M	5/15/72	73	0.43	4.71	15.5	17.7	11/06/73	6/16/88	175.3	193.1	Nasal Carcinoma
MED-LOW	1165 M	5/27/72	76	0.43	4.75	16.0	17.3	11/06/73	7/21/86	152.4	169.8	Pneumonia
MED-LOW	1309 M	8/18/73	60	0.44	4.80	12.5	18.5	3/04/75	4/ 87	145.6	164.1	Hemangiosarcoma, Liver

DOSE-EFFECT STUDIES WITH INHALED PU-238 OXIDE IN BEAGLES

			INITIAL ALVEOLAR DEPOSITION			INHALATION EXPOSURE			DEATH INFORMATION			
DOSE GROUP	DOG IDENT	BIRTH DATE	NCI	NCI/G LUNG	NCI/ KG	WEIGHT (KG)	AGE (MO)	EXPO DATE	DEATH DATE	MONTHS POST INH	AGE (MO)	COMMENTS ON DEAD DOGS
MED-LOW	1316 M	8/29/73	84	0.53	5.79	14.5	18.1	3/04/75	12/13/88	165.4	183.5	Ankylosis Spondylitis
MED-LOW	960 M	5/14/71	68	0.54	5.91	11.5	19.2	12/19/72	11/07/80	94.6	113.8	Malignant Lymphoma
MED-LOW	1072 M	11/26/71	98	0.54	5.94	16.5	18.1	5/31/73	9/22/83	123.7	141.9	Radiation Pneumonitis, Delayed
MED-LOW	1190 F	8/24/72	71	0.54	5.92	12.0	18.1	2/26/74	5/09/85	134.4	152.5	Lung Tumor
MED-LOW	982 M	5/20/71	76	0.58	6.33	12.0	19.0	12/19/72	1/29/86	157.3	176.4	Pneumonia; Carcinoma, Thyroid
MED-LOW	1040 M	8/19/71	84	0.61	6.72	12.5	18.2	2/22/73	3/04/81	96.3	114.5	Heart Failure
MED-LOW	1059 F	8/30/71	71	0.65	7.10	10.0	17.8	2/22/73	8/08/83	125.5	143.3	Malignant Lymphoma
MED-LOW	1108 F	1/19/72	84	0.69	7.64	11.0	16.4	5/31/73	1/14/87	163.5	179.8	Posterior Paralysis
MED-LOW	1000 F	5/31/71	70	0.71	7.78	9.0	18.7	12/19/72	12/02/87	179.4	198.1	Transitional Carcinoma, Urinary Bladder
MED-LOW	1056 M	8/27/71	97	0.71	7.76	12.5	17.9	2/22/73	6/17/86	159.8	177.7	Pneumonia; Carcinoma, Thyroid
MED-LOW	1004 M	5/31/71	116	0.73	8.00	14.5	19.6	1/18/73	4/30/87	171.3	191.0	Malignant Lymphoma; Lung Tumor; Carcinoma, Bile Duct
MED-LOW	1026 M	6/15/71	116	0.78	8.59	13.5	19.2	1/18/73	11/13/85	153.8	173.0	Hepatic Dysplasia
MED-LOW	1043 F	8/20/71	98	0.89	9.80	10.0	18.1	2/22/73	9/21/81	102.9	121.1	Empyema; Adenoma, Pituitary; Cushing's Disease
MED-LOW	1031 F	7/23/71	76	0.92	10.13	7.5	19.1	2/22/73	5/04/84	134.3	153.4	Pneumonia
MED-LOW	1212 F	9/09/72	111	1.12	12.33	9.0	17.6	2/26/74	6/24/88	171.9	189.5	Hepatocellular Carcinoma
MED-LOW-SAC	1310 M	8/18/73	54	0.34	3.72	14.5	18.5	3/04/75	4/01/77	24.9	43.4	Sacrificed
MED-LOW-SAC	1312 M	8/18/73	58	0.34	3.74	15.5	18.5	3/04/75	3/26/79	48.7	67.2	Sacrificed
MED-LOW-SAC	1311 M	8/18/73	54	0.36	4.00	13.5	18.5	3/04/75	4/03/78	37.0	55.5	Sacrificed
MED-LOW-SAC	1317 M	8/29/73	72	0.41	4.50	16.0	18.1	3/04/75	4/01/77	24.9	43.1	Sacrificed
MED-LOW-SAC	1318 M	8/29/73	67	0.45	4.96	13.5	18.1	3/04/75	3/08/76	12.2	30.3	Sacrificed

DOSE-EFFECT STUDIES WITH INHALED PU-238 OXIDE IN BEAGLES

			INITIAL ALVEOLAR DEPOSITION			INHALATION EXPOSURE			DEATH INFORMATION			
DOSE GROUP	DOG IDENT	BIRTH DATE	NCI	NCI/G LUNG	NCI/ KG	WEIGHT (KG)	AGE (MO)	EXPC DATE	DEATH DATE	MONTHS POST INH	AGE (MO)	COMMENTS ON DEAD DOGS
MED-LOW-SAC	929 F	4/27/71	41	0.50	5.47	7.5	19.2	11/30/72	1/25/73	1.8	21.0	Sacrificed
MED-LOW-SAC	926 M	4/15/71	75	0.55	6.00	12.5	19.5	11/30/72	2/28/73	3.0	22.5	Sacrificed
MED-LOW-SAC	1315 M	8/29/73	90	0.55	6.00	15.0	18.1	3/04/75	3/31/77	24.9	43.0	Sacrificed
MED-LOW-SAC	1319 M	8/29/73	99	0.67	7.33	13.5	18.1	3/04/75	3/09/76	12.2	30.3	Sacrificed
MEDIUM	1176 M	6/20/72	129	0.87	9.56	13.5	16.6	11/06/73	12/12/85	145.2	161.7	Hemangioma, Spleen
MEDIUM	1221 F	9/16/72	124	1.13	12.40	10.0	19.0	4/18/74	9/30/88	173.4	192.5	Malignant Lymphoma; Carcinoma, Bile Duct
MEDIUM	1195 M	8/24/72	228	1.38	15.20	15.0	18.1	2/26/74	7/29/87	161.0	179.1	Chronic Nephropathy; Adenoma, Bile Duct
MEDIUM	1053 F	8/27/71	148	1.42	15.58	9.5	17.9	2/22/73	2/02/85	143.3	161.2	Cushing's Disease
MEDIUM	997 M	5/31/71	203	1.60	17.65	11.5	19.6	1/18/73	5/08/86	159.6	179.3	Lung Tumor
MEDIUM	991 F	5/26/71	194	1.76	19.40	10.0	18.8	12/19/72	6/20/83	126.0	144.8	Transitional Carcinoma, Urinary Bladder
MEDIUM	1177 M	6/20/72	262	1.76	19.41	13.5	16.6	11/06/73	3/12/85	136.1	152.7	Bone Tumor
MEDIUM	1103 F	1/14/72	260	1.89	20.80	12.5	16.5	5/31/73	4/08/83	118.2	134.8	Bone Tumor; Lung Tumor
MEDIUM	973 F	5/15/71	271	2.24	24.64	11.0	19.2	12/19/72	10/08/84	141.6	160.8	Bone Tumor
MEDIUM	1091 F	12/22/71	243	2.60	28.59	8.5	17.3	5/31/73	11/10/86	161.3	178.6	Carcinoma, Thyroid
MEDIUM	1114 M	1/19/72	430	2.70	29.66	14.5	16.4	5/31/73	4/23/85	142.8	159.1	Bone Tumor; Carcinoma, Bile Duct
MEDIUM	1062 M	8/30/71	435	2.93	32.22	13.5	17.8	2/22/73	5/30/84	135.2	153.0	Bone Tumor; Lung Tumor
MEDIUM	1081 M	11/29/71	541	3.07	33.81	16.0	18.0	5/31/73	1/18/80	79.6	97.6	Hemangiosarcoma, Heart
MEDIUM	1030 F	7/23/71	340	3.25	35.79	9.5	19.1	2/22/73	4/14/83	121.7	140.7	Pneumonia; Radiation Pneumonitis
MEDIUM	1198 M	8/31/72	539	3.50	38.50	14.0	17.9	2/26/74	9/14/86	150.6	168.4	Penumonia; Lung Tumor
MEDIUM	952 F	5/14/71	365	3.69	40.56	9.0	19.2	12/19/72	6/03/83	125.4	144.7	Bone Tumor
MEDIUM	1166 M	5/27/72	673	4.08	44.87	15.0	17.3	11/06/73	6/23/84	127.5	144.9	Malignant Lymphoma

DOSE-EFFECT STUDIES WITH INHALED PU-238 OXIDE IN BEAGLES

			INITIAL ALVEOLAR DEPOSITION			INHALATION EXPOSURE			DEATH INFORMATION			
DOSE GROUP	DOG IDENT	BIRTH DATE	NCI	NCI/G LUNG	NCI/ KG	WEIGHT (KG)	AGE (MO)	EXPO DATE	DEATH DATE	MONTHS POST INH	AGE (MO)	COMMENTS ON DEAD DOGS
MEDIUM	1220 F	9/16/72	518	4.28	47.09	11.0	19.0	4/18/74	12/09/86	151.7	170.7	Malignant Lymphoma; Addison's Disease
MEDIUM	992 F	5/26/71	555	4.39	48.26	11.5	18.8	12/19/72	7/26/84	139.2	158.0	Bone Tumor
MEDIUM	983 M	5/20/71	617	4.67	51.42	12.0	19.0	12/19/72	12/29/83	132.3	151.3	Carcinoma, Adrenal; Carcinoma, Pituitary
MEDIUM-SAC	1032 M	7/23/71	162	1.40	15.43	10.5	16.3	11/30/72	12/08/72	0.3	16.6	Sacrificed
MEDIUM-SAC	932 F	4/28/71	216	1.79	19.64	11.0	19.1	11/30/72	1/25/73	1.8	21.0	Sacrificed
MEDIUM-SAC	931 F	4/28/71	289	2.39	26.27	11.0	19.1	11/30/72	12/28/72	0.9	20.0	Sacrificed
MEDIUM-SAC	934 M	4/28/71	454	3.06	33.63	13.5	19.1	11/30/72	3/01/73	3.0	22.1	Sacrificed
MED-HIGH	1191 F	8/24/72	591	4.48	49.25	12.0	19.8	4/18/74	3/21/77	35.1	54.9	Interstitial Pneumonitis
MED-HIGH	1157 M	5/15/72	700	4.71	51.85	13.5	17.7	11/06/73	3/02/84	123.8	141.6	Bone Tumor
MED-HIGH	1035 F	8/19/71	571	5.46	60.11	9.5	18.2	2/22/73	3/04/84	132.3	150.5	Bone Tumor; Cushing's Disease
MED-HIGH	1192 F	8/24/72	754	6.53	71.81	10.5	18.1	2/26/74	3/29/83	109.0	127.1	Bone Tumor
MED-HIGH	1140 M	5/01/72	1014	6.58	72.43	14.0	18.2	11/06/73	12/14/81	97.2	115.4	Bone Tumor
MED-HIGH	1071 M	11/26/71	1269	6.79	74.65	17.0	18.2	5/31/73	1/09/81	91.3	109.5	Bone Tumor; Lung Tumor
MED-HIGH	1173 M	5/27/72	1023	7.75	85.25	12.0	17.3	11/06/73	2/09/82	99.1	116.5	Bone Tumor
MED-HIGH	1178 M	6/20/72	1125	8.52	93.75	12.0	16.6	11/06/73	1/06/83	110.0	126.6	Bone Tumor; Lung Tumor
MED-HIGH	1047 M	8/20/71	900	8.61	94.74	9.5	18.1	2/22/73	10/05/82	115.4	133.5	Herniated Vertebral Disc
MED-HIGH	1109 F	1/19/72	1119	8.85	97.30	11.5	16.4	5/31/73	8/06/80	86.2	102.6	Bone Tumor; Lung Tumor; Addison's Disease
MED-HIGH	1160 F	5/27/72	1344	10.18	112.00	12.0	17.3	11/06/73	9/22/81	94.5	111.9	Bone Tumor; Lung Tumor
MED-HIGH	1211 M	9/09/72	1764	11.06	121.66	14.5	17.6	2/26/74	5/17/82	98.6	116.2	Bone Tumor
MED-HIGH	1096 F	1/11/72	1476	12.20	134.18	11.0	16.6	5/31/73	5/08/78	59.2	75.9	Addison's Disease

DOSE-EFFECT STUDIES WITH INHALED PU-238 OXIDE IN BEAGLES

			INITIAL ALVEOLAR DEPOSITION			INHALATION EXPOSURE			DEATH INFORMATION			
DOSE GROUP	DOG IDENT	BIRTH DATE	NCI	NCI/G LUNG	NCI/ KG	WEIGHT (KG)	AGE (MO)	EXPO DATE	DEATH DATE	MONTHS POST INH	AGE (MO)	COMMENTS ON DEAD DOGS
MED-HIGH	1218 F	9/16/72	1710	12.95	142.50	12.0	17.3	2/26/74	4/24/81	85.9	103.2	Bone Tumor
MED-HIGH	1092 M	12/22/71	1848	13.44	147.84	12.5	17.3	5/31/73	10/23/78	64.8	82.0	Bone Tumor
MED-HIGH	1027 M	6/15/71	2148	13.95	153.43	14.0	19.2	1/18/73	12/01/78	70.4	89.6	Bone Tumor; Lung Tumor
MED-HIGH	1115 F	1/27/72	1885	14.90	163.91	11.5	16.1	5/31/73	7/11/78	61.3	77.4	Bone Tumor
MED-HIGH	974 F	5/15/71	1718	15.62	171.80	10.0	20.2	1/18/73	5/24/78	64.1	84.3	Bone Tumor
MED-HIGH	1079 M	11/29/71	2620	15.88	174.67	15.0	18.0	5/31/73	2/12/78	56.4	74.5	Addison's Disease
MED-HIGH	1058 F	8/30/71	1907	16.51	181.62	10.5	17.8	2/22/73	11/01/79	80.3	98.1	Bone Tumor
HIGH	1002 M	5/31/71	2907	18.88	207.64	14.0	19.6	1/18/73	1/21/80	84.1	103.7	Bone Tumor; Lung Tumor
HIGH	1057 M	8/27/71	3116	20.98	230.81	13.5	17.9	2/22/73	3/07/79	72.4	90.3	Bone Tumor
HIGH	1009 M	6/02/71	3630	26.40	290.40	12.5	19.6	1/18/73	4/01/78	62.4	82.0	Lung Tumor; Osteoarthropathy
HIGH	1042 F	8/20/71	2959	28.32	311.47	9.5	18.1	2/22/73	11/10/78	68.6	86.7	Bone Tumor; Lung Tumor
HIGH	994 F	5/31/71	3453	31.39	345.30	10.0	19.6	1/18/73	7/04/76	41.5	61.1	Addison's Disease
HIGH	1006 F	6/02/71	3810	31.49	346.36	11.0	19.6	1/18/73	1/18/79	72.0	91.6	Bone Tumor; Lung Tumor
HIGH	975 F	5/15/71	3968	36.07	396.80	10.0	20.2	1/18/73	7/25/78	66.2	86.3	Bone Tumor; Lung Tumor
HIGH	1037 M	8/19/71	4854	44.13	485.40	10.0	18.2	2/22/73	11/21/78	68.9	87.1	Bone Tumor
HIGH	1143 M	5/01/72	7691	53.78	591.62	13.0	18.2	11/06/73	12/05/77	49.0	67.2	Bone Tumor; Lung Tumor
HIGH	1025 M	6/15/71	8479	57.10	628.07	13.5	19.2	1/18/73	3/17/77	49.9	69.1	Lung Tumor
HIGH	1064 M	8/30/71	9453	63.66	700.22	13.5	16.7	1/18/73	4/14/77	50.8	67.5	Bone Tumor; Lung Tumor
HIGH	1162 F	5/27/72	6959	70.29	773.22	9.0	17.3	11/06/73	12/19/78	61.4	78.8	Bone Tumor; Addison's Disease
HIGH	1175 F	6/20/72	6201	75.16	826.80	7.5	16.6	11/06/73	2/24/78	51.6	68.2	Lung Tumor

INHALED PLUTONIUM NITRATE IN DOGS

DOSE GROUP	DOG IDENT	BIRTH DATE	INITIAL ALVEOLAR DEPOSITION NCI	NCI/G LUNG	NCI/ KG	INHALATION EXPOSURE WEIGHT (KG)	AGE (MO)	EXPO DATE	DEATH INFORMATION DEATH DATE	MONTHS POST INH	AGE (MO)	COMMENTS ON DEAD DOGS
CONTROL	1356 M	5/11/74	0	0.00	0.00	13.0	20.3	1/20/76	4/07/87	134.5	154.9	Carcinoma, Adrenal
CONTROL	1365 M	5/14/74	0	0.00	0.00	10.0	20.2	1/20/76	7/16/88	149.8	170.1	Pneumonia
CONTROL	1376 F	6/17/74	0	0.00	0.00	9.5	19.1	1/20/76	5/11/80	51.7	70.8	Pneumonia
CONTROL	1393 M	6/22/74	0	0.00	0.00	9.5	21.9	4/20/76	6/19/87	133.9	155.9	Pneumonia
CONTROL	1409 M	7/07/74	0	0.00	0.00	12.5	21.5	4/20/76	7/17/89	158.9	180.3	Herniated Vertebral Disc
CONTROL	1418 M	7/16/74	0	0.00	0.00	10.5	23.3	6/23/76	8/26/89	158.1	181.4	Adenoma, Pituitary
CONTROL	1425 M	7/17/74	0	0.00	0.00	15.5	23.2	6/23/76	8/02/82	73.3	96.5	Epileptic Seizures
CONTROL	1455 F	8/05/74	0	0.00	0.00	6.0	20.5	4/20/76	8/20/87	136.0	156.5	Pyometra
CONTROL	1483 F	9/03/74	0	0.00	0.00	10.0	21.7	6/23/76		183.2	204.9	**Alive, ages as of 9/30/91**
CONTROL	1516 F	10/05/74	0	0.00	0.00	9.5	20.6	6/23/76		183.2	203.8	**Alive, ages as of 9/30/91**
CONTROL	1525 M	10/12/74	0	0.00	0.00	12.5	21.3	7/22/76	11/14/87	135.8	157.1	Transitional Carcinoma, Urethra
CONTROL	1526 M	10/12/74	0	0.00	0.00	11.0	21.3	7/22/76	8/28/90	169.2	190.5	Processing
CONTROL	1528 F	10/29/74	0	0.00	0.00	10.5	20.8	7/22/76	4/06/87	128.5	149.2	Cerebral Hemorrhage
CONTROL	1543 M	11/03/74	0	0.00	0.00	16.0	20.6	7/22/76	8/12/86	120.7	141.3	Herniated Vertebral Disc
CONTROL	1563 F	9/06/75	0	0.00	0.00	12.0	18.3	3/15/77		174.5	192.8	**Alive, ages as of 9/30/91**
CONTROL	1572 F	9/09/75	0	0.00	0.00	10.0	19.3	4/19/77	2/01/90	153.5	172.8	Endocarditis
CONTROL	1577 M	9/08/75	0	0.00	0.00	12.0	18.2	3/15/77	4/04/90	156.6	174.9	Hemangioma, Spleen (Ruptured)
CONTROL	1584 F	9/12/75	0	0.00	0.00	12.5	19.2	4/19/77	11/29/88	139.4	158.6	Carcinoma, Thyroid
CONTROL	1594 F	9/13/75	0	0.00	0.00	14.0	19.2	4/19/77	11/02/90	162.5	181.7	Pneumonia; Hepatocellur Carcinoma
CONTROL	1633 F	4/12/76	0	0.00	0.00	12.0	18.9	11/07/77	11/10/86	108.1	126.9	Carcinoma, Thyroid
CONTROL-SAC	1388 M	6/22/74	0	0.00	0.00	12.0	21.9	4/20/76	9/11/81	64.7	86.7	Sacrificed

INHALED PLUTONIUM NITRATE IN DOGS

DOSE GROUP	DOG IDENT	BIRTH DATE	INITIAL ALVEOLAR DEPOSITION NCI	NCI/G LUNG	NCI/ KG	INHALATION EXPOSURE WEIGHT (KG)	AGE (MO)	EXPO DATE	DEATH INFORMATION DEATH DATE	MONTHS POST INH	AGE (MO)	COMMENTS ON DEAD DOGS
CONTROL-SAC	1405 M	7/05/74	0	0.00	0.00	10.5	21.5	4/20/76	8/13/84	99.8	121.3	Heart Base Tumor
CONTROL-SAC	1450 F	7/23/74	0	0.00	0.00	13.5	20.9	4/20/76	11/04/81	66.5	87.4	Sacrificed
CONTROL-SAC	1509 M	9/26/74	0	0.00	0.00	11.5	20.9	6/22/76	10/30/86	124.3	145.1	Sacrificed
CONTROL-SAC	1608 M	9/20/75	0	0.00	0.00	12.0	17.8	3/15/77	2/14/91	167.0	184.8	Rhabdomyosarcoma
CONTROL-SAC	1638 F	4/22/76	0	0.00	0.00	9.0	18.5	11/07/77	9/08/87	118.0	136.5	Sacrificed
VEHICLE	1361 M	5/14/74	0	0.00	0.00	8.5	21.0	2/12/76	4/04/89	157.7	178.7	Heart Failure
VEHICLE	1381 F	6/21/74	0	0.00	0.00	8.5	19.7	2/12/76	12/05/89	165.7	185.5	Mammary Tumor
VEHICLE	1392 M	6/22/74	0	0.00	0.00	13.0	22.0	4/22/76	1/16/90	164.8	186.8	Sebaceous Carcinoma, Skin (Lung Metastasis)
VEHICLE	1406 M	7/05/74	0	0.00	0.00	13.5	21.6	4/22/76	1/21/88	141.0	162.6	Malignant Melanoma, Oral Cavity
VEHICLE	1412 F	7/15/74	0	0.00	0.00	9.0	19.0	2/12/76	7/06/89	160.8	179.7	Mammary Tumor
VEHICLE	1421 M	7/16/74	0	0.00	0.00	13.0	23.5	6/29/76	2/26/88	139.9	163.4	Mastocytoma
VEHICLE	1457 F	8/05/74	0	0.00	0.00	12.0	20.6	4/22/76	11/07/89	162.5	183.1	Hypothyroidism
VEHICLE	1491 F	9/05/74	0	0.00	0.00	8.0	21.8	6/29/76	5/10/89	154.3	176.1	Mammary Tumor
VEHICLE	1504 F	9/26/74	0	0.00	0.00	10.0	21.1	6/29/76	2/22/89	151.8	172.9	Malignant Lymphoma
VEHICLE	1514 M	9/26/74	0	0.00	0.00	14.0	21.1	6/29/76	8/06/82	73.2	94.3	Malignant Lymphoma
VEHICLE	1524 M	10/12/74	0	0.00	0.00	12.0	21.5	7/27/76	3/27/88	140.0	161.5	Herniated Vertebral Disc
VEHICLE	1531 F	10/29/74	0	0.00	0.00	9.0	20.9	7/27/76	8/15/91	180.6	201.5	Processing
VEHICLE	1542 M	11/03/74	0	0.00	0.00	12.0	20.8	7/27/76	5/01/89	153.1	173.9	Malignant Lymphoma
VEHICLE	1566 M	9/06/75	0	0.00	0.00	14.0	19.9	5/05/77	1/18/90	152.5	172.4	Malignant Lymphoma
VEHICLE	1578 M	9/08/75	0	0.00	0.00	10.5	19.9	5/05/77	2/13/90	153.3	173.2	Nephropathy
VEHICLE	1593 F	9/13/75	0	0.00	0.00	11.0	19.7	5/05/77	12/31/90	163.9	183.6	Nephropathy

INHALED PLUTONIUM NITRATE IN DOGS

			INITIAL ALVEOLAR DEPOSITION			INHALATION EXPOSURE			DEATH INFORMATION			
DOSE GROUP	DOG IDENT	BIRTH DATE	NCI	NCI/G LUNG	NCI/ KG	WEIGHT (KG)	AGE (MO)	EXPO DATE	DEATH DATE	MONTHS POST INH	AGE (MO)	COMMENTS ON DEAD DOGS
VEHICLE	1601 F	9/15/75	0	0.00	0.00	8.5	19.6	5/05/77	4/08/90	155.1	174.8	Nephropathy
VEHICLE	1620 M	2/29/76	0	0.00	0.00	11.0	21.1	12/01/77	1/06/87	109.2	130.2	Herniated Vertebral Disc
VEHICLE	1634 F	4/12/76	0	0.00	0.00	10.5	19.6	12/01/77		165.9	185.6	**Alive, ages as of 9/30/91**
VEHICLE	1651 F	4/26/76	0	0.00	0.00	11.0	19.2	12/01/77		165.9	185.1	**Alive, ages as of 9/30/91**
LOWEST	1416 M	7/16/74	0	0.00	0.00	12.0	22.1	5/20/76	2/15/90	164.9	187.0	Heart Failure
LOWEST	1458 F	8/05/74	0	0.00	0.00	10.5	21.5	5/20/76	9/21/89	160.1	181.6	Malignant Pheochromocytoma, Adrenal
LOWEST	1489 F	9/05/74	0	0.00	0.00	8.0	20.5	5/20/76	8/04/84	98.5	119.0	Carcinoma, Esophagus
LOWEST	1501 M	9/08/74	0	0.00	0.00	14.0	20.4	5/20/76	1/03/84	91.5	111.8	Carcinoma, Thyroid
LOWEST	1515 M	9/26/74	0	0.00	0.00	13.5	19.8	5/20/76	12/06/90	174.6	194.3	Processing
LOWEST	1573 M	9/08/75	0	0.00	0.00	11.5	19.4	4/19/77	9/06/90	160.6	179.9	Gastric Dilatation
LOWEST	1581 M	9/10/75	0	0.00	0.00	16.5	19.3	4/19/77	7/31/86	111.4	130.7	Hemangiosarcoma, Spleen
LOWEST	1596 M	9/13/75	0	0.00	0.00	14.0	19.2	4/19/77	7/02/91	170.4	189.6	Processing
LOWEST	1600 F	9/14/75	1	0.01	0.11	11.0	19.2	4/19/77	6/27/90	158.3	177.4	Nephropathy
LOWEST	1603 M	9/14/75	2	0.01	0.12	14.0	19.2	4/19/77	12/26/90	164.2	183.4	Nephropathy
LOWEST	1519 M	10/05/74	2	0.02	0.18	12.5	19.5	5/20/76	7/13/90	169.8	189.2	Processing
LOWEST	1570 F	9/08/75	2	0.02	0.18	10.0	19.4	4/19/77	6/19/87	122.0	141.3	Fibrosarcoma, Stomach
LOWEST	1465 F	8/19/74	4	0.03	0.35	12.0	21.0	5/20/76	5/16/89	155.9	176.9	Nephropathy
LOWEST	1470 F	8/21/74	3	0.03	0.29	10.5	21.0	5/20/76	4/09/84	94.7	115.6	Meningioma
LOWEST	1507 M	9/26/74	4	0.03	0.32	14.0	19.8	5/20/76	6/07/88	144.6	164.4	Malignant Melanoma, Oral Cavity
LOWEST	1592 F	9/13/75	4	0.03	0.29	13.5	19.2	4/19/77	10/17/89	149.9	169.1	Pneumonia
LOWEST	1607 M	9/20/75	5	0.03	0.35	13.0	19.0	4/19/77	7/26/88	135.2	154.2	Hepatocellular Carcinoma

INHALED PLUTONIUM NITRATE IN DOGS

DOSE GROUP	DOG IDENT	BIRTH DATE	INITIAL ALVEOLAR DEPOSITION NCI	NCI/G LUNG	NCI/ KG	INHALATION EXPOSURE WEIGHT (KG)	AGE (MO)	EXPO DATE	DEATH INFORMATION DEATH DATE	MONTHS POST INH	AGE (MO)	COMMENTS ON DEAD DOGS
LOWEST	1487 F	9/03/74	6	0.04	0.46	13.0	20.5	5/20/76	7/05/90	169.5	190.0	Processing
LOWEST	1583 F	9/12/75	4	0.04	0.40	9.5	19.2	4/19/77	10/13/89	149.8	169.0	Carcinoma, Thyroid
LOWEST	1565 F	9/06/75	8	0.06	0.67	11.5	19.4	4/19/77	9/28/85	101.3	120.7	Hemangiosarcoma, Spleen
LOWEST-SAC	1339 F	5/01/74	2	0.02	0.22	9.0	17.5	10/16/75	11/13/75	0.9	18.4	Sacrificed
LOWEST-SAC	1335 M	4/16/74	5	0.04	0.42	11.5	18.0	10/16/75	11/13/75	0.9	18.9	Sacrificed
LOWEST-SAC	1351 M	5/10/74	7	0.06	0.61	11.0	17.2	10/16/75	11/13/75	0.9	18.1	Sacrificed
LOW	1513 M	9/26/74	0	0.00	0.00	11.5	19.8	5/20/76	10/08/90	172.6	192.4	Processing
LOW	1520 M	10/05/74	1	0.01	0.12	10.5	19.5	5/20/76	5/21/90	168.0	187.5	Carcinoma, Bile Duct
LOW	1415 M	7/15/74	2	0.02	0.20	11.5	22.2	5/20/76	12/27/89	163.3	185.4	Transitional Carcinoma, Urinary Bladder
LOW	1575 M	9/08/75	3	0.02	0.19	14.0	19.4	4/19/77	12/28/87	128.3	147.6	Transitional Carcinoma, Urethra
LOW	1466 F	8/19/74	5	0.03	0.37	14.0	21.0	5/20/76	1/04/90	163.5	184.5	Nephropathy
LOW	1606 F	9/20/75	5	0.04	0.42	12.5	19.0	4/19/77	6/22/90	158.1	177.1	Hemangiosarcoma, Spleen
LOW	1579 M	9/09/75	8	0.05	0.59	14.0	19.3	4/19/77	6/05/90	157.5	176.9	Hepatocellular Carcinoma
LOW	1590 F	9/13/75	6	0.05	0.51	12.0	19.2	4/19/77	3/18/87	118.9	138.1	Mammary Tumor
LOW	1585 F	9/12/75	8	0.06	0.68	12.0	19.2	4/19/77	8/31/89	148.4	167.6	Carcinoma, Thyroid
LOW	1580 F	9/10/75	9	0.07	0.82	11.0	19.3	4/19/77		173.4	192.7	**Alive, ages as of 9/30/91**
LOW	1591 M	9/13/75	11	0.07	0.76	15.0	19.2	4/19/77	8/15/89	147.9	167.1	Malignant Lymphoma
LOW	1417 M	7/16/74	11	0.08	0.89	12.0	22.1	5/20/76	10/05/89	160.5	182.7	Malignant Lymphoma
LOW	1423 M	7/17/74	10	0.08	0.87	11.0	22.1	5/20/76	6/27/89	157.2	179.4	Panophthalmitis
LOW	1567 M	9/06/75	10	0.08	0.83	12.0	19.4	4/19/77	6/15/90	157.9	177.3	Nephritis
LOW	1472 F	8/21/74	10	0.09	1.01	10.0	21.0	5/20/76	11/22/89	162.1	183.1	Nephropathy; Carcinoma, Bile Duct

INHALED PLUTONIUM NITRATE IN DOGS

			INITIAL ALVEOLAR DEPOSITION			INHALATION EXPOSURE			DEATH INFORMATION			
DOSE GROUP	DOG IDENT	BIRTH DATE	NCI	NCI/G LUNG	NCI/ KG	WEIGHT (KG)	AGE (MO)	EXPO DATE	DEATH DATE	MONTHS POST INH	AGE (MO)	COMMENTS ON DEAD DOGS
LOW	1503 F	9/26/74	9	0.09	1.03	8.5	19.8	5/20/76	12/13/84	102.8	122.6	Carcinoma, Thyroid
LOW	1602 M	9/14/75	15	0.09	1.03	14.5	19.2	4/19/77	8/10/86	111.7	130.9	Epileptic Seizures
LOW	1484 F	9/03/74	11	0.10	1.08	10.0	20.5	5/20/76	10/26/90	173.2	193.7	Processing
LOW	1599 F	9/14/75	10	0.10	1.14	9.0	19.2	4/19/77	3/12/86	106.7	125.9	Carcinoma, Adrenal
LOW	1490 F	9/05/74	16	0.15	1.65	9.5	20.5	5/20/76	10/19/88	149.0	169.5	Mammary Tumor
MED-LOW	1386 M	6/21/74	34	0.21	2.36	14.5	22.0	4/20/76	1/04/86	116.5	138.5	Hemangiosarcoma, Spleen
MED-LOW	1413 F	7/15/74	29	0.24	2.68	11.0	18.2	1/20/76	3/01/85	109.3	127.5	Malignant Lymphoma
MED-LOW	1568 M	9/06/75	46	0.29	3.17	14.5	18.3	3/15/77	12/02/86	116.6	134.9	Pneumonia
MED-LOW	1595 M	9/13/75	50	0.29	3.23	15.5	18.0	3/15/77	1/09/90	153.9	171.9	Nephropathy
MED-LOW	1391 M	6/22/74	54	0.30	3.26	16.5	21.9	4/20/76	7/22/85	111.0	133.0	Carcinoma, Thyroid; Lung Tumor
MED-LOW	1587 M	9/12/75	53	0.31	3.40	15.5	18.1	3/15/77	1/14/86	106.0	124.1	Hemangiosarcoma, Subcutis; Lung Tumor
MED-LOW	1540 M	10/30/74	54	0.32	3.51	15.5	20.7	7/22/76	11/25/86	124.1	144.9	Lung Tumor
MED-LOW	1574 M	9/08/75	46	0.38	4.21	11.0	18.2	3/15/77	7/14/90	160.0	178.2	Lung Tumor
MED-LOW	1444 F	7/22/74	49	0.41	4.50	11.0	21.0	4/20/76	5/17/90	168.9	189.8	Transitional Carcinoma, Urinary Bladder
MED-LOW	1439 F	7/20/74	53	0.42	4.61	11.5	21.0	4/20/76	3/30/88	143.3	164.3	Malignant Lymphoma
MED-LOW	1523 F	10/12/74	55	0.42	4.60	12.0	21.3	7/22/76	12/21/90	173.0	194.3	Processing
MED-LOW	1380 M	6/17/74	63	0.46	5.06	12.5	19.1	1/20/76	5/24/87	136.1	155.2	Pneumonia
MED-LOW	1569 F	9/08/75	58	0.53	5.82	10.0	18.2	3/15/77	9/27/87	126.4	144.C	Lung Tumor
MED-LOW	1582 F	9/12/75	57	0.54	5.96	9.5	18.1	3/15/77	8/12/88	136.9	155.0	Mammary Tumor; Carcinoma, Bile Duct
MED-LOW	1427 F	7/17/74	68	0.62	6.81	10.0	21.1	4/20/76	8/23/89	160.1	181.2	Malignant Melanoma, Oral Cavity
MED-LOW	1363 M	5/14/74	85	0.74	8.09	10.5	20.2	1/20/76	5/12/87	135.7	155.9	Pneumonia; Carcinoma, Adrenal; Adenoma, Bile Duct

INHALED PLUTONIUM NITRATE IN DOGS

			INITIAL ALVEOLAR DEPOSITION			INHALATION EXPOSURE			DEATH INFORMATION			
DOSE GROUP	DOG IDENT	BIRTH DATE	NCI	NCI/G LUNG	NCI/ KG	WEIGHT (KG)	AGE (MO)	EXPO DATE	DEATH DATE	MONTHS POST INH	AGE (MO)	COMMENTS ON DEAD DOGS
MED-LOW	1604 M	9/14/75	85	0.74	8.10	10.5	18.0	3/15/77	4/03/90	156.6	174.6	Encephalopathy
MED-LOW	1530 F	10/29/74	72	0.76	8.41	8.5	20.8	7/22/76	9/17/86	121.9	142.6	Bone Tumor; Lung Tumor
MED-LOW	1456 F	8/05/74	61	0.79	8.68	7.0	20.5	4/20/76	4/21/87	132.0	152.5	Pneumonia
MED-LOW	1422 F	7/17/74	99	1.12	12.35	8.0	18.1	1/20/76	7/11/90	173.7	191.8	Processing
MED-LOW-SAC	1336 M	4/16/74	21	0.14	1.52	13.5	18.0	10/16/75	11/13/75	0.9	18.9	Sacrificed
MED-LOW-SAC	1341 F	5/10/74	19	0.16	1.78	10.5	17.2	10/16/75	11/13/75	0.9	18.1	Sacrificed
MED-LOW-SAC	1605 F	9/20/75	25	0.20	2.19	11.5	17.8	3/15/77	3/24/82	60.3	78.1	Sacrificed
MED-LOW-SAC	1389 M	6/22/74	27	0.23	2.54	10.5	21.9	4/20/76	5/04/76	0.5	22.4	Sacrificed
MED-LOW-SAC	1445 F	7/22/74	34	0.24	2.60	13.0	21.0	4/20/76	5/05/76	0.5	21.5	Sacrificed
MED-LOW-SAC	1390 M	6/22/74	43	0.30	3.29	13.0	21.9	4/20/76	5/04/76	0.5	22.4	Sacrificed
MED-LOW-SAC	1359 M	5/14/74	50	0.32	3.57	14.0	20.2	1/20/76	1/23/76	0.1	20.3	Sacrificed
MED-LOW-SAC	1344 F	5/10/74	41	0.33	3.60	11.5	17.2	10/16/75	11/14/75	1.0	18.2	Sacrificed
MED-LOW-SAC	1589 F	9/13/75	41	0.34	3.75	11.0	18.0	3/15/77	6/08/82	62.8	80.8	Sacrificed; Lung Tumor
MED-LOW-SAC	1588 M	9/12/75	50	0.36	3.98	12.5	18.1	3/15/77	3/22/78	12.2	30.3	Sacrificed
MED-LOW-SAC	1529 F	10/29/74	43	0.37	4.08	10.5	20.8	7/22/76	10/19/76	2.9	23.7	Sacrificed
MED-LOW-SAC	1375 F	6/17/74	50	0.40	4.35	11.5	19.1	1/20/76	1/23/76	0.1	19.2	Sacrificed
MED-LOW-SAC	1564 F	9/06/75	40	0.40	4.44	9.0	18.3	3/15/77	3/20/78	12.2	30.4	Sacrificed
MED-LOW-SAC	1539 M	10/30/74	65	0.45	4.99	13.0	20.7	7/22/76	10/20/76	3.0	23.7	Sacrificed
MED-LOW-SAC	1407 F	7/07/74	50	0.51	5.56	9.0	18.5	1/20/76	1/23/76	0.1	18.6	Sacrificed
MED-LOW-SAC	1576 M	9/08/75	70	0.53	5.86	12.0	18.2	3/15/77	3/17/82	60.1	78.3	Sacrificed
MED-LOW-SAC	1571 F	9/08/75	68	0.57	6.22	11.0	18.2	3/15/77	3/21/78	12.2	30.4	Sacrificed

INHALED PLUTONIUM NITRATE IN DOGS

			INITIAL ALVEOLAR DEPOSITION			INHALATION EXPOSURE			DEATH INFORMATION			
DOSE GROUP	DOG IDENT	BIRTH DATE	NCI	NCI/G LUNG	NCI/ KG	WEIGHT (KG)	AGE (MO)	EXPO DATE	DEATH DATE	MONTHS POST INH	AGE (MO)	COMMENTS ON DEAD DOGS
MED-LOW-SAC	1522 F	10/12/74	78	0.71	7.78	10.0	21.3	7/22/76	10/18/76	2.9	24.2	Sacrificed
MED-LOW-SAC	1598 F	9/14/75	93	1.06	11.65	8.0	18.0	3/15/77	3/10/82	59.8	77.8	Sacrificed
MEDIUM	1637 M	4/12/76	192	1.45	15.99	12.0	18.9	11/07/77	11/28/88	132.7	151.6	Lung Tumor
MEDIUM	1404 M	7/05/74	260	1.48	16.25	16.0	21.5	4/20/76	2/03/84	93.5	115.0	Pleuritis
MEDIUM	1521 F	10/12/74	205	1.49	16.37	12.5	21.3	7/22/76	6/07/85	106.5	127.8	Bone Tumor; Lung Tumor
MEDIUM	1656 M	4/26/76	211	1.54	16.90	12.5	18.4	11/07/77	1/02/91	157.8	176.2	Pneumonia; Lung Tumor
MEDIUM	1379 M	6/17/74	278	1.74	19.16	14.5	19.1	1/20/76	1/20/88	144.0	163.1	Carcinoma, Bile Duct; Lung Tumor; Bone Tumor
MEDIUM	1362 M	5/14/74	267	1.87	20.54	13.0	20.2	1/20/76	12/20/88	155.0	175.2	Bone Tumor; Hepatocellular Carcinoma; Carciroma, Bile Duct; Lung Tumors
MEDIUM	1639 F	4/22/76	248	2.05	22.57	11.0	18.5	11/07/77	12/24/89	145.5	164.1	Radiation Pneumonitis; Lung Tumor
MEDIUM	1647 M	4/23/76	294	2.05	22.58	13.0	18.5	11/07/77	1/13/90	146.2	164.7	Lung Tumor; Carcinoma, Bile Duct
MEDIUM	1640 M	4/22/76	307	2.06	22.71	13.5	18.5	11/07/77	3/20/84	76.4	94.9	Lung Tumor
MEDIUM	1645 F	4/23/76	257	2.13	23.39	11.0	18.5	11/07/77	8/07/86	105.0	123.5	Lung Tumor
MEDIUM	1534 M	10/28/74	295	2.14	23.57	12.5	20.8	7/22/76	5/26/85	106.1	126.9	Heart Failure
MEDIUM	1414 F	7/15/74	233	2.35	25.86	9.0	18.2	1/20/76	8/14/86	126.8	145.0	Bone Tumor; Lung Tumor; Carcinoma, Bile Duct
MEDIUM	1618 F	2/29/76	277	2.40	26.36	10.5	20.3	11/07/77	7/12/89	140.1	160.4	Bone Tumor
MEDIUM	1385 M	6/21/74	373	2.42	26.63	14.0	19.0	1/20/76	7/12/84	101.7	120.7	Bone Tumor; Lung Tumor
MEDIUM	1408 F	7/07/74	331	2.62	28.77	11.5	18.5	1/20/76	10/12/83	92.7	111.2	Bone Tumor
MEDIUM	1428 F	7/17/74	378	3.12	34.36	11.0	21.1	4/20/76	10/28/85	114.3	135.4	Bone Tumor; Lung Tumor
MEDIUM	1535 F	10/30/74	345	3.13	34.48	10.0	20.7	7/22/76	10/06/86	122.5	143.2	Bone Tumor; Lung Tumor
MEDIUM	1446 F	7/22/74	354	3.22	35.40	10.0	21.0	4/20/76	8/10/86	123.7	144.6	Pyometra; Adenoma, Bile Duct

INHALED PLUTONIUM NITRATE IN DOGS

DOSE GROUP	DOG IDENT	BIRTH DATE	INITIAL ALVEOLAR DEPOSITION NCI	NCI/G LUNG	NCI/ KG	INHALATION EXPOSURE WEIGHT (KG)	AGE (MO)	EXPO DATE	DEATH INFORMATION DEATH DATE	MONTHS POST INH	AGE (MO)	COMMENTS ON DEAD DOGS
MEDIUM	1364 M	5/14/74	463	3.24	35.65	13.0	20.2	1/20/76	8/02/84	102.4	122.6	Lung Tumor
MEDIUM	1387 F	6/22/74	345	4.48	49.30	7.0	19.0	1/20/76	8/13/80	54.8	73.7	Bone Tumor
MED-HIGH	1648 M	4/23/76	811	5.90	64.90	12.5	18.5	11/07/77	7/11/85	92.1	110.6	Bone Tumor; Lung Tumor
MED-HIGH	1659 F	4/29/76	990	7.20	79.22	12.5	18.3	11/07/77	8/19/83	69.4	87.7	Bone Tumor
MED-HIGH	1636 M	4/12/76	1212	8.48	93.25	13.0	18.9	11/07/77	5/03/83	65.8	84.7	Bone Tumor
MED-HIGH	1621 M	2/29/76	1334	8.66	95.26	14.0	20.3	11/07/77	11/19/84	84.4	104.7	Bone Tumor; Lung Tumor
MED-HIGH	1646 F	4/23/76	1061	8.77	96.45	11.0	18.5	11/07/77	11/11/82	60.1	78.6	Bone Tumor
MED-HIGH	1429 M	7/17/74	1376	9.62	105.85	13.0	23.2	6/23/76	5/29/81	59.2	82.4	Bone Tumor; Lung Tumor
MED-HIGH	1641 M	4/22/76	1275	9.66	106.24	12.0	18.5	11/07/77	6/28/85	91.7	110.2	Lung Tumor
MED-HIGH	1660 M	4/29/76	1518	10.22	112.41	13.5	18.3	11/07/77	9/05/84	81.9	100.2	Bone Tumor; Lung Tumor
MED-HIGH	1508 M	9/26/74	1716	10.76	118.37	14.5	20.9	6/23/76	1/24/80	43.0	63.9	Bone Tumor
MED-HIGH	1655 M	4/26/76	1094	11.05	121.56	9.0	18.4	11/07/77	3/18/85	88.3	106.7	Lung Tumor; Bone Tumor
MED-HIGH	1652 F	4/26/76	1320	12.00	131.95	10.0	18.4	11/07/77	7/20/83	68.4	86.8	Bone Tumor; Lung Tumor
MED-HIGH	1619 F	2/29/76	1490	12.32	135.50	11.0	20.3	11/07/77	1/21/83	62.5	82.7	Bone Tumor
MED-HIGH	1512 M	9/26/74	2411	14.61	160.71	15.0	20.9	6/23/76	12/23/79	42.0	62.9	Bone Tumor
MED-HIGH	1419 M	7/16/74	1559	14.92	164.11	9.5	23.3	6/23/76	10/22/82	76.0	99.2	Bone Tumor; Lung Tumor
MED-HIGH	1498 F	9/08/74	2018	16.68	183.45	11.0	21.5	6/23/76	4/09/82	69.5	91.0	Bone Tumor; Lung Tumor
MED-HIGH	1502 F	9/26/74	3008	20.25	222.80	13.5	20.9	6/23/76	1/21/81	55.0	75.9	Bone Tumor; Lung Tumor
MED-HIGH	1485 F	9/03/74	2330	21.18	233.00	10.0	21.7	6/23/76	12/30/80	54.2	75.9	Bone Tumor
MED-HIGH	1471 F	8/21/74	2508	21.71	238.62	10.5	22.1	6/23/76	5/01/79	34.2	56.3	Radiation Pneumonitis
MED-HIGH	1492 F	9/05/74	2473	24.98	274.82	9.0	21.6	6/23/76	10/16/80	51.8	73.4	Bone Tumor

INHALED PLUTONIUM NITRATE IN DOGS

DOSE GROUP	DOG IDENT	BIRTH DATE	INITIAL ALVEOLAR DEPOSITION NCI	NCI/G LUNG	NCI/ KG	INHALATION EXPOSURE WEIGHT (KG)	AGE (MO)	EXPO DATE	DEATH INFORMATION DEATH DATE	MONTHS POST INH	AGE (MO)	COMMENTS ON DEAD DOGS
MED-HIGH	1459 F	8/05/74	2645	26.72	293.89	9.0	22.6	6/23/76	9/25/80	51.1	73.7	Radiation Pneumonitis; Lung Tumor
MED-HIGH-SAC	1329 F	4/16/74	363	3.30	36.27	10.0	18.0	10/16/75	11/14/75	1.0	19.0	Sacrificed
MED-HIGH-SAC	1346 M	5/10/74	656	4.42	48.59	13.5	17.2	10/16/75	11/14/75	1.0	18.2	Sacrificed
MED-HIGH-SAC	1347 F	5/10/74	688	6.95	76.47	9.0	17.2	10/16/75	11/14/75	1.0	18.2	Sacrificed
HIGH	1518 M	10/05/74	3565	29.46	324.09	11.0	20.6	6/23/76	12/18/79	41.8	62.4	Radiation Pneumonitis; Lung Tumor
HIGH	1420 M	7/16/74	3840	30.36	333.91	11.5	23.3	6/23/76	7/12/78	24.6	47.9	Radiation Pneumonitis
HIGH	1517 F	10/05/74	5185	49.62	545.79	9.5	20.6	6/23/76	11/02/77	16.3	36.9	Radiation Pneumonitis
HIGH	1510 F	9/26/74	6969	55.09	606.02	11.5	20.9	6/23/76	11/09/77	16.6	37.5	Radiation Pneumonitis
HIGH	1424 M	7/17/74	7681	69.83	768.12	10.0	23.2	6/23/76	8/31/77	14.3	37.5	Radiation Pneumonitis

Publications and Presentations

Publications

1990

Arnold, G. E., A. K. Dunker, S. J. Johns, and R. J. Douthart. 1990. The sequence attributes method for determining correlations between amino acid sequence and protein secondary structure. In: *Current Research in Protein Chemistry: Techniques, Structure, and Function*, J. J. Villefranche, ed., pp. 405-415. Academic Press, New York.

Briant, J. K. 1990. Calculation of equivalent aerosol particle mobility in different mixtures of gases used to study convective transport in airways. *J. Aerosol Med.* 3(4):221-232.

Briant, J. K., and A. C. James. 1990. *Dissolution and Particle Size Characterization of Radioactive Contaminants in Hanford Facilities: Criteria for Methods of Measurement.* PNL-7438, Pacific Northwest Laboratory, Richland, Washington.

Brooks, A. L., G. J. Newton, L. J. Shyr, F. A. Seiler, and B. R. Scott. 1990. The combined effects of alpha particles and x rays on cell killing and micronuclei induction in lung epithelial cells. *Int. J. Radiat. Biol.* 58:799-811.

Cross, F. T. 1990. Health effects and risks of radon exposure. In: *Environmental Radon: Occurrence, Control and Health Hazards*, S. K. Majumdar, R. F. Schmalz, and E. W. Miller, eds., pp. 223-237. Pennsylvania Academy of Science, Easton, Pennsylvania.

Dagle, G. E., L. G. Smith, K. E. McDonald, J. F. McShane, and D. L. Stevens, Jr. 1990. Pulmonary carcinogenesis in rats given implants of shale oil in beeswax pellets. *J. Toxicol. Environ. Health* 29:399-407.

Gilbert, E. S., J. F. Park, F. T. Cross, and G. E. Dagle. 1990. Recent Pacific Northwest Laboratory beagle and rodent studies: Methods and results. *Radiat. Res.* 124(3):368-369 (abstract).

Hobbs, C. H., and F. T. Cross. 1990. Health effects of radon exposure in laboratory animals. *Fundam. Appl. Toxicol.* 13:630-6332.

Hui, T. E., J. W. Poston, and D. R. Fisher. 1990. The microdosimetry of radon decay products in the respiratory tract. *Radiat. Prot. Dosim.* 31(1/4):405-411.

Hulla, J. E., D. B. Mann, and D. L. Springer. 1990. Characterization of benzo[a]pyrene (BaP) adducts to the plasmid, pXP-14. *Toxicologist* 10:68 (abstract).

James, A. C. 1990. Reassessment of factors influencing lung dose from radon daughters. In: *Proceedings of the Technical Exchange Meeting on Assessing Radon Health Risks*, September 18-19, 1989, Grand Junction, Colorado, J. R. Duray, G. H. Langner, et al., eds. NTIS, Springfield, Virginia.

Jostes, R. F., J. A. Reese, J. E. Cleaver, M. Molero, and W. F. Morgan. 1990. Quiescent human lymphocytes do not contain DNA strand breaks detectable by alkaline elution. *Exp. Cell Res.* 182:513-520.

Jostes, R. F., T. L. Morgan, R. A. Gies, E. W. Fleck, K. P. Gaspar, and F. T. Cross. 1990. Molecular analysis of radon-induced mutants. *J. Cell. Biol.* 14A(Suppl.):55 (abstract).

Meznarich, H. K., and M. R. Sikov. 1990. Development of mouse embryonic forelimb in organ culture following irradiation. *Proc. Soc. Exp. Biol. Med.* 193:239A (abstract).

Meznarich, H. K., and M. R. Sikov. 1990. Effect of radiation on mouse embryonic limb development. In: *Abstracts*, Federation of American Societies for Experimental Biology, 74th Annual Meeting, April 1-15, 1990, Washington, D.C. *Fed. Am. Soc. Exp. Biol. J.* 4:A761 (abstract).

Moolgavkar, S. H., F. T. Cross, G. Luebeck, and G. E. Dagle. 1990. A two-mutation model for radon-induced lung tumors in rats. *Radiat. Res.* 121:28-37.

Park, J. F., G. E. Dagle, R. E. Weller, R. L. Buschbom, and G. J. Powers. 1990. Comparative distribution of inhaled $^{238}PuO_2$ in beagles. *Health Phys.* 58(Suppl. 1):S39 (abstract).

Rithidech, K., J. A. Hotchkiss, W. C. Griffith, R. F. Henderson, and A. L. Brooks. 1990. Chromosome damage in rat pulmonary alveolar macrophages following ozone inhalation. *Mutat. Res.* 24:67-73.

Sanders, C. L., and J. A. Mahaffey. 1990. Inhalation carcinogenesis of repeated exposures to high-fired $^{244}CmO_2$ in rats. *Health Phys.* 58(5):631-638.

Sikov, M. R., R. J. Traub, and H. K. Meznarich. 1990. *Contribution of Maternal Radionuclide Burdens to Prenatal Radiation Doses.* NUREG/CR-5631/PNL-7445. Prepared for the U.S. Nuclear Regulatory Commission by Pacific Northwest Laboratory, Richland, Washington.

Springer, D. L., J. E. Hulla, M. G. Horstman, B. L. Thomas, and S. C. Goheen. 1990. Preparation and partial characterization of hemoglobin adducts from trichloroethylene (TCE). *Toxicologist* 10:231 (abstract)

Zangar, R. C., D. W. Later, and D. L. Springer. 1990. Analysis of carbaryl metabolites using HPLC and supercritical fluid chromatograph (SFC). *Toxicologist* 10:334 (abstract).

1991

Bailey, M. R., A. Birchall, R. G. Cuddihy, A. C. James, and M. Roy. 1991. Respiratory tract clearance model for dosimetry and bioassay of inhaled radionuclides. *Radiat. Prot. Dosim.* 38(3/4)153-158.

Birchall, A., M. R. Bailey, and A. C. James. 1991. LUDEP: A lung dose evaluation program. *Radiat. Prot. Dosim.* 38(3/4):167-175.

Birchall, A., A. C. James, and C. R. Muirhead. 1991. Adequacy of personal air samplers for measuring plutonium intakes. *Radiat. Prot. Dosim.* 37(3):179-188.

Cross, F. T. 1991. A review of experimental animal radon health effect data. In: *Radiation Research, A Twentieth-Century Perspective,* Proceedings of the 9th International Congress of Radiation Research, Vol. 1, Congress Abstracts, W. C. Dewey and G. F. Whitmore, eds., p. 54 (abstract). Academic Press, San Diego, California.

Cross, F. T. 1991. Experimental studies on lung carcinogenesis and their relationship to future research on radiation-induced lung cancer in humans. In: *The Future of Human Radiation Research* (Section 2, Lung Cancer), G. B. Gerber, D. M. Taylor, E. Cardis, and J. W. Thiessen, eds., pp. 27-35. Report 22, British Institute of Radiology, London. Medical Physics Publishing, Madison, Wisconsin.

Cross, F. T. 1991. PNL research ranges from rocks to cancers. *Radon Research Notes* 6:1-3.

Cross, F. T. 1991. Pacific Northwest research focuses on toxicology of exposure. *Radon Research Notes* 6:3-4.

Cross, F. T., co-author. 1991. *State of Washington, Radon Health Effects Committee/ Radon Task Force Findings Report.* State of Washington, Olympia, Washington.

Dagle, G. E., J. F. Park, R. E. Weller, E. S. Gilbert, and R. L. Buschbom. 1991. Health effects of inhaled plutonium in dogs. In: *Radiation Research, A Twentieth-Century Perspective*, Proceedings of the 9th International Congress of Radiation Research, Vol. 1, Congress Abstracts, W. C. Dewey and G. F. Whitman, eds., p. 321 (abstract). Academic Press, San Diego, California.

Finch, G. L., W. T. Lowther, M. C. Hoover, and A. L. Brooks. 1991. Effects of berylliium metal particles on the viability and function of cultured rat alveolar macrophages. *J. Toxicol. Environ. Health* 34:103-114.

Fisher, D. R., T. E. Hui, and A. C. James. 1991. Model for assessing radiation dose to epithelial cells of the human respiratory tract from radon progeny. *Radiat. Prot. Dosim.* 38(1/3):73-80.

Fisher, D. R., R. L. Kathren, and M. J. Swint. 1991. Modified biokinetic model for uranium from analysis of acute exposure to UF_6. *Health Phys.* 60(3):335-342.

Fisher, D. R., C. C. Badger, H. Breitz, J. F. Eary, J. S. Durham, T. E. Hui, R. L. Hill, and W. B. Nelp. 1991. Internal radiation dosimetry for clinical testing of radiolabeled monoclonal antibodies. *Antibody Immunoconj. Radiopharmaceut.* 4(4):655-664.

Gies, R. A., F. T. Cross, G. E. Dagle, and R. L. Buschbom. 1991. The influence of exposure rate and level on the incidence and type of primary lung tumors in rats exposed to radon. *Health Phys.* 60(Suppl. 2): S32 (abstract).

James, A. C. 1991. Dosimetry of the respiratory tract and other organs: Implications for risk. In: *Radiation Research, A Twentieth-Century Perspective*, Proceedings of the 9th International Congress of Radiation Research, Vol. 1, Congress Abstracts, W. C. Dewey and G. F. Whitmore, eds., p. 53 (abstract). Academic Press, San Diego, California.

James, A. C., and A. Birchall. 1991. Implications of the ICRP Task Group's proposed lung model for internal dose assessments in the mineral sands industry. In: *Minesafe International, 1990,* Proceedings of an International Conference on Occupational Health and Safety in the Minerals Industry, September 10-14, 1990, Perth, Australia, pp. 210-222. Chamber of Mines and Energy of Western Australia, Perth.

James, A. C., J. R. Johnson, and D. R. Fisher. 1991. ICRP Task Group's dosimetry model for the respiratory tract: Implications for uranium. *Health Phys.* 60(2):S14 (abstract).

James, A. C., W. Stahlhofen, G. Rudolf, M. J. Eagan, W. Nixon, P. Gehr, and J. K. Briant. 1991. The respiratory tract deposition model proposed by the ICRP Task Group. *Radiat. Prot. Dosim.* 38(3/4):159-166.

James, A. C., P. Gehr, R. Masse, R. G. Cuddihy, F. T. Cross, A. Birchall, J. S. Durham, and J. K. Briant. 1991. Dosimetry model for bronchial and extrathoracic tissues of the respiratory tract. *Radiat. Prot. Dosim.* 37(4):221-230.

Jostes, R. F., T. E. Hui, A. C. James, F. T. Cross, J. L. Schwartz, J. Rotmensch, R. W. Atcher, H. H. Evans, J. Mencl, G. Bakele, and P. S. Rao. 1991. *In vitro* exposure of mammalian cells to radon: Dosimetric considerations. *Radiat. Res.* 127:211-219.

Leung, F. C. 1991. Growth factor and growth factor receptor in radiation carcinogenesis. *Radiat. Environ. Biophys.* 30:191-194.

Leung, F. C., L. R. Bohn, and G. E. Dagle. 1991. Elevated epidermal growth factor receptor binding in plutonium-induced lung tumors from dogs. *Proc. Soc. Exp. Biol. Med.* 196:385-389.

Leung, F. C., L. R. Bohn, and G. E. Dagle. 1991. Elevated epidermal growth factor receptor binding in dog lung tumors. In: *Proceedings, Eighth International Congress of Endocrinology*, July 17-23, 1988, Kyoto, Japan.

Mahaffey, J. A., J. R. Johnson, and C. L. Sanders. 1991. Robust estimation of nonlinear lung kinetics in animals exposed to alpha-emitting radionuclides. In: *The Analysis, Communication, and Perception of Risk: Advances in Risk Analysis, Vol. 9*, B. J. Garrick and W. C. Gekler, eds., pp. 401-410. Plenum, New York.

Mahaffey, J. A., F. T. Cross, J. R. Johnson, and M. C. Baechler. 1991. Prevention of lung cancer by remediation of residential exposure to radon daughters. *Radiat. Prot. Dosim.* 36:335-339.

Meznarich, H. K., L. A. Braby, and M. R. Sikov. 1991. Altered fibronectin levels in irradiated mouse blastocysts. *Fed. Am. Soc. Exp. Biol. J.* 5:1617A (abstract).

Meznarich, H. K., L. A. Braby, and M. R. Sikov. 1991. Expression of fibronectin in mouse blastocysts following irradiation. *Proc. Soc. Exp. Biol. Med.* 196(1):115A (Abstracts, Northwest Section).

Samet, J. M., R. E. Albert, J. D. Brain, R. A. Guilmette, P. K. Hopke, A. C. James, and D. G. Kaufman. 1991. *Comparative Dosimetry of Radon in Mines and Homes.* National Academy Press, Washington, D.C.

Sanders, C. L. 1991. Carcinogenesis in the lung following inhalation of $^{239}PuO_2$. In: *Proceedings*, Primer Congreso Regional Sobre Seguridad Radiologica y Nuclear, Buenas Aires, Argentina. *Seguridad Radiologica* 5:10.

Sanders, C. L., K. E. Lauhala, and G. E. Dagle. 1991. Brain tumors in the rat following inhalation of $^{239}PuO_2$. In: *Radiation Research: A Twentieth-Century Perspective,* Proceedings of the 9th International Congress of Radiation Research, Vol. 1, Congress Abstracts, W. C. Dewey and G. F. Whitmore, eds., p. 257 (abstract). Academic Press, San Diego, California.

Sikov, M. R., H. K. Meznarich, and R. J. Traub. 1991. Comparison of placental transfer and localization of cesium, strontium, and iodine in experimental animals and women. In: Meeting Report, CEIR/MRC Forum - Radionuclides and External Irradiation: Implications for the Embryo and Fetus. *Int. J. Radiat. Biol.* 60(3):553-555.

Sikov, M. R., F. T. Cross, T. J. Mast, H. E. Palmer, and A. C. James. 1991. Developmental toxicology and dosimetry studies of prenatal radon exposures in rats. *Proc. Soc. Exp. Biol. Med.* 196(1) (Abstracts, Northwest Section).

Wolff, S. F., R. Jostes, F. T. Cross, T. E. Hui, V. Afzal, and J. K. Wiencke. 1991. Adaptive response of human lymphocytes for the repair of radon-induced chromosomal damage. *Mutat. Res.* 250:299-306.

1992

Arnold, G. E., A. K. Dunker, S. J. Johns, and R. J. Douthart. 1992. Use of conditional probabilities for determining relationships between amino acid sequence and protein secondary structure. *Proteins Struct. Func. Genet.* 12:382-399.

Briant, J. K., and M. Lippman. 1992. Particle transport through a hollow canine airway cast by high-frequency oscillatory ventilation. *Exp. Lung Res.* 18:385-407.

Brooks, A. L., C. J. Mitchell, C. Lloyd, K. E. McDonald, and N. F. Johnson. 1992. Genotoxic effects of silicon carbide fibers. *In Vitro Toxicol.* 5(1):51-58.

Brooks, A. L., R. A. Guilmette, P. J. Haley, F. F. Hahn, B. A. Muggenberg, J. A. Mewhinney, and R. O. McClellan. 1992. Distribution and biological effects of inhaled $^{239}Pu(NO_3)_4$ in cynomolgus monkeys. *Radiat. Res.* 130:79-87.

Cross, F. T. 1992. A review of experimental animal radon health effects data. In: *Radiation Research: A Twentieth-Century Prospective*, Proceedings of the 9th International Congress of Radiation Research, Vol. 2, W. C. Dewey, M. Edington, R. J. M. Fry, E. J. Hall, and G. F. Whitmore, eds., pp. 476-481. Academic Press, New York.

Dagle, G. E., E. P. Moen, R. A. Adee, T. E. Hui, A. C. James, R. E. Filipy, and R. L. Kathren. 1992. Microdistribution and microdosimetry of thorium deposited in the liver. *Health Phys.* 63(1):41-45.

Hui, T. E., D. R. Fisher, O. W. Press, J. F. Eary, J. N. Weinstein, C. C. Gadger, and I. D. Bernstein. 1992. Localized beta dosimetry of ^{131}I-labeled antibodies in follicular lymphoma. *Med. Phys.* 19(1):97-104.

Hulla, J. E. 1992. The rat genome contains a p53 pseudogene: Detection of a processed pseudogene using PCR. *PCR Methods and Applications* 1:251-254.

Leung, F. C. 1992. Circadian rhythms of melatonin release from chicken pineal *in vitro*: Modified melatonin radioimmunoassay. *Soc. Exp. Biol. Med.* 198:826-832.

Minnick, M. F., L. C. Stilwell, J. M. Heineman, and G. L. Stiegler. 1992. A highly repetitive DNA sequence possibly unique to canids. *Gene* 110:235-238.

Sanders, C. L., and K. E. McDonald. 1992. Malignancy of proliferative pulmonary lesions in the Syrian hamster following inhalation of $^{239}PuO_2$. *J. Environ. Pathol. Toxicol. Oncol.* 11(3):151-156.

Schwartz, J. L., J. Rotmensch, R. W. Atcher, R. F. Jostes, F. T. Cross, T. E. Hui, D. Chen, S. Carpenter, H. H. Evans, J. Mencl, G. Bakale, and P. S. Rao. 1992. Interlaboratory comparison of different alpha particle and radon sources: Cell survival and relative biological effectiveness. *Health Phys.* 62(5):458-461.

Sikov, M. R. 1992. *Effects of Low-Level Fetal Irradiation on the Central Nervous System* (proceedings of a workshop). PNL-8009, Pacific Northwest Laboratory, Richland, Washington.

Sikov, M. R., R. J. Traub, T. E. Hui, H. K. Meznarich, and K. D. Thrall. 1992. *Contribution of Maternal Radionuclide Burdens to Prenatal Radiation Doses.* NUREG/CR-5631, PNL-7445, Rev. 1. Prepared for the U.S. Nuclear Regulatory Commission, Washington, D.C., by Pacific Northwest Laboratory, Richland, Washington.

In Press

Benson, J. M., A. L. Brooks, and R. F. Henderson. Comparative *in vitro* cytotoxicity of nickel compounds to pulmonary alveolar macrophages and to rat lung epithelial cells. *Adv. Environ. Sci. Technol.* (in press).

Briant, J. K., and A. C. James. Numerical simulation of aerosol particle transport by oscillating flow in respiratory airways. *Ann. Biomed. Eng.* (in press).

Brooks, A. L., K. Rithidech, N. F. Johnson, D. G. Thomassen, and G. J. Newton. Evaluating chromosome damage to estimate dose to tracheal epithelial cells. In: *Indoor Radon and Lung Cancer: Reality or Myth?*, F. T. Cross, ed., Proceedings of the 29th Hanford Symposium on Health and the Environment, October 15-19, 1990, Richland, Washington. Battelle Press, Columbus, Ohio (in press).

Brooks, A. L., K. E. McDonald, C. Mitchell, D. S. Culp, A. Lloyd, N. F. Johnson, and R. M. Kitchin. The combined genotoxic effects of radiation and occupational pollutants. In: *Current Topics in Occupational Health*, T. S. Tenforde, ed., Proceedings of the 30th Hanford Symposium on Health and the Environment, Richland, Washington. *Appl. Occup. Hyg. J.* (in press).

Cross, F. T. Experimental, statistical, and biological models of radon carcinogenesis. *Radiat. Prot. Dosim.* (in press).

Cross, F. T., G. E. Dagle, R. A. Gies, L. G. Smith, and R. L. Buschbom. Experimental animal studies of radon and cigarette smoke. In: *Indoor Radon and Lung Cancer: Reality or Myth?*, F. T. Cross, ed., Proceedings of the 29th Hanford Symposium on Health and the Environment, October 15-19, 1990, Richland, Washington. Battelle Press, Columbus, Ohio (in press).

Cross, F. T., J. Lubin, R. Masse, J. Samet, and G. A. Swedjemark. Inputs to the quantification of risk. In: *CEC/DOE Radon-Related Risk Recommendations Report*, Chapter 4 (in press).

Dagle, G. E., F. T. Cross, and R. A. Gies. Morphology of respiratory tract lesions in rats exposed to radon/radon progeny. In: *Indoor Radon and Lung Cancer: Reality or Myth?*, F. T. Cross, ed., Proceedings of the 29th Hanford Symposium on Health and the Environment, October 15-19, 1990, Richland, Washington. Battelle Press, Columbus, Ohio (in press).

Egert, G. H., R. L. Kathren, F. T. Cross, and M. A. Robkin. The effect of home weatherization on indoor radon concentrations. In: *Indoor Radon and Lung Cancer: Reality or Myth?*, F. T. Cross, ed., Proceedings of the 29th Hanford Symposium on Health and the Environment, October 15-19, 1990, Richland, Washington. Battelle Press, Columbus, Ohio (in press).

Fisher, D. R., T. E. Hui, V. P. Bond, and A. C. James. Microdosimetry of radon progeny: Application to risk assessment. In: *Indoor Radon and Lung Cancer: Reality or Myth?*, F. T. Cross, ed., Proceedings of the 29th Hanford Symposium on Health and the Environment, October 15-19, 1990, Richland, Washington. Battelle Press, Columbus, Ohio (in press).

Foreman, M. E., L. S. McCoy, and M. E. Frazier. Involvement of oncogenes in radon-induced lung tumors in the rat. In: *Indoor Radon and Lung Cancer: Reality or Myth?*, F. T. Cross, ed., Proceedings of the 29th Hanford Symposium on Health and the Environment, October 15-19, 1990, Richland, Washington. Battelle Press, Columbus, Ohio (in press).

Gilbert, E. S., F. T. Cross, C. L. Sanders, and G. E. Dagle. Models for comparing lung-cancer risks in radon- and plutonium-exposed experimental animals. In: *Indoor Radon and Lung Cancer: Reality or Myth?*, F. T. Cross, ed., Proceedings of the 29th Hanford Symposium on Health and the Environment, October 15-19, 1990, Richland, Washington. Battelle Press, Columbus, Ohio (in press).

Hoover, M. D., F. A. Seiler, G. L. Finch, P. J. Haley, A. F. Eidson, J. A. Mewhinney, D. E. Bice, A. L. Brooks, and R. K. Jones. Beryllium toxicity: An update. In: *Proceedings, Sixth Symposium on Space Nuclear Power Systems* (in press).

Hui, T. E., A. L. Brooks, and A. C. James. Microdosimetry of micronuclei induction and cell killing in mammalian cells irradiated in vitro by alpha particles. *Int. J. Radiat. Biol.* (in press).

Johnson, N. F., M. D. Hoover, D. G. Thomassen, Y. S. Cheng, A. Dalley, and A. L. Brooks. In vitro activity of silicon carbide whiskers in comparison to other industrial fibers using four cell culture systems. *Am. J. Ind. Med.* (in press).

Jostes, R. F., E. W. Fleck, R. A. Gies, T. E. Hui, T. L. Morgan, J. L. Schwartz, J. K. Wiencke, and F. T. Cross. Cytotoxic, clastogenic and mutagenic response of mammalian cells exposed *in vitro* to radon and its progeny. In: *Indoor Radon and Lung Cancer: Reality or Myth?*, F. T. Cross, ed., Proceedings of the 29th Hanford Symposium on Health and the Environment, October 15-19, 1990, Richland, Washington. Battelle Press, Columbus, Ohio (in press).

Leung, F. C., G. E. Dagle, and F. T. Cross. Involvement of growth factors and their receptors in radon-induced rat lung tumors. In: *Indoor Radon and Lung Cancer: Reality or Myth?*, F. T. Cross, ed., Proceedings of the 29th Hanford Symposium on Health and the Environment, October 15-19, 1990, Richland, Washington. Battelle Press, Columbus, Ohio (in press).

Mahaffey, J. A., M. A. Parkhurst, A. C. James, F. T. Cross, H. E. Palmer, M. C. R. Alavanja, S. Ezrine, P. Henderson, and R. Brownson. Feasibility study to evaluate affixing CR-39 to glass artifacts for estimating cumulative exposure to radon. *Health Phys.* (in press).

Perry, R. E., R. E. Weller, R. L. Buschbom, G. E. Dagle, and J. F. Park. Radiographically determined growth dynamics of primary lung tumors in dogs following inhalation of plutonium. *Am. J. Vet. Res.* (in press).

Sanders, C. L., and G. E. Dagle. A threshold model of pulmonary carcinogenesis: Carcinoma in the rat after deposition of plutonium or quartz. In: *Current Topics in Occupational Health*, T. S. Tenforde, ed., 30th Hanford Symposium on Health and the Environment, Richland, Washington. *Appl. Occup. Environ. Hyg. J.* (in press).

Sanders, C. L., G. E. Dagle, and J. A. Mahaffey. Incidence of brain tumors in rats exposed to an aerosol of $^{239}PuO_2$. *Int. J. Radiat. Biol.* (in press).

Sanders, C. L., R. A. Guilmette, and R. L. Kathren. Autoradiographic examination of soft tissues in a human case of acute ^{241}Am exposure. *Health Phys.* (in press).

Sikov, M. R., R. J. Traub, and H. K. Meznarich. Comparative placental transfer, localization, and effects of radionuclides in experimental animal and human pregnancies. In: *Proceedings of the AECL Research Fetal Dosimetry Workshop Conference*, June 25-26, 1991, Chalk River, Ontario Canada (in press).

Sikov, M. R., F. T. Cross, T. J. Mast, H. E. Palmer, and A. C. James. Developmental toxicity of radon exposures. In: *Indoor Radon and Lung Cancer: Reality or Myth?*, F. T. Cross, ed., Proceedings of the 29th Hanford Symposium on Health and the Environment, October 15-19, 1990, Richland, Washington. Battelle Press, Columbus, Ohio (in press).

Wasiolek, P. T., P. K. Hopke, and A. C. James. Assessment of exposure to radon decay products in realistic living conditions. *J. Exposure Anal. Environ. Epidemiol.* (in press).

Weller, R. E., G. E. Dagle, and J. F. Park. Primary pulmonary chondrosarcoma in a dog. *Vet. Pathol.* (in press).

Weller, R. E., R. E. Perry, R. L. Buschbom, G. E. Dagle, and J. F. Park. Radiographically determined growth dynamics of primary lung tumors in dogs following inhalation of plutonium. *Am. J. Vet. Res.* (in press).

Presentations

1990

Bailey, M. R., A. Birchall, R. G. Cuddihy, A. C. James, and M. Roy. 1990. Respiratory Tract Clearance Model for Dosimetry and Bioassay of Inhaled Radionuclides. Presented at the 3rd International Workshop on Respiratory Tract Dosimetry, July 1-3, 1990, Albuquerque, New Mexico.

Bair, W. J. 1990. Health Effects of Inhaled Radionuclides. Presented at the International Conference on Lung Diseases, May 20-24, 1990, Boston, Massachusetts.

Birchall, A., M. R. Bailey, and A. C. James. 1990. LUDEP: A Lung Dose Evaluation Program. Presented at the 3rd International Workshop on Respiratory Tract Dosimetry, July 1-3, 1990, Albuquerque, New Mexico.

Briant, J. K. 1990. Calculation of Mean Free Path in Different Gas Mixtures. Presented at the Annual Meeting of the American Association for Aerosol Research (AAAR), June 18-22, 1990, Philadelphia, Pennsylvania.

Brooks, A. L. 1990. The In Vitro Induction of Cell Killing and Chromosome Alterations by SiC Fibers. Presented at the Annual Meeting of the Environmental Mutagen Society, March 25-29, 1990, Albuquerque, New Mexico.

Brooks, A. L. 1990. Induction and Loss of Chromosome Aberrations in Rat Tracheal Epithelial Cells by Inhaled Radon and Its Progeny. Presented at the 38th Annual Meeting of the Radiation Research Society, April 7-12, 1990, New Orleans, Louisiana.

Brooks, A. L., K. Rithidech, N. F. Johnson, D. G. Thamassen, and G. J. Newton. 1990. Evaluating Chromosome Damage to Tracheal Epithelial Cells. Presented at the 29th Hanford Symposium on Health and the Environment, October 15-19, 1990, Richland, Washington.

Cross, F. T. 1990. Inhalation Hazards to Uranium Miners. Presented at the OPA Review of the DOE/OHER Radon Research Program, January 27, 1990, Burlington, California.

Cross, F. T. 1990. Overview of the 29th Hanford Symposium on Health and the Environment, "Indoor Radon and Lung Cancer: Reality or Myth?" Presented at the meeting of the Washington State Radon Health Effects Committee/Radon Task Force, December 18, 1990, Seattle, Washington.

Cross, F. T. 1990. The Radon Program. Presented at the LSC/DOE/OMB Meeting with Nancy Milton, Executive Office of the President, June 18-20, 1990, Richland, Washington.

Cross, F. T., and R. F. Jostes. 1990. Mechanisms of Radon Injury. Presented at the OPA Review of the DOE/OHER Radon Research Program, January 27, 1990, Burlington, California.

Cross, F. T., G. E. Dagle, R. A. Gies, L. G. Smith, and R. L. Buschbom. 1990. Experimental Animal Studies of Radon and Cigarette Smoke. Presented at the 29th Hanford Symposium on Health and the Environment, October 15-19, 1990, Richland, Washington.

Dagle, G. E., F. T. Cross, and R. A. Gies. 1990. Morphology of Respiratory Tract Lesions in Rats Exposed to Radon Progeny. Presented at the 29th Hanford Symposium on Health and the Environment, October 15-19, 1990, Richland, Washington.

Dagle, G. E., E. P. Moen, R. A. Adee, T. E. Hui, A. C. James, R. E. Filipy, and R. L. Kathren. 1990. Microdistribution of Thorium Deposited in the Liver. Presented at the Thorotrast Collaborator's Workshop, July 17, 1990, Rockville, Maryland.

Douthart, R. J. 1990. Computers and the Human Genome. Presented at "New Directions in Science and Technology," May 2, 1990, Western Oregon State College, Monmouth, Oregon (invited seminar).

Douthart, R. J. 1990. A Graphics Computer Interface to the Human Genome. Presented at the Association of Minority Health Professional Schools; and Research Centers in Minority Institutions: Program Planning Meeting for Participation in the Human Genome Initiative, July 21, 1990, Nashville, Tennessee (invited presentation).

Egert, G. H., R. L. Kathren, F. T. Cross, and M. A. Robkin. 1990. The Effect of Home Weatherization on Indoor Radon Concentrations. Presented at the 29th Hanford Symposium on Health and the Environment, October 15-19, 1990, Richland, Washington.

Fisher, D. R., T. E. Hui, and A. C. James. 1990. Model for Assessing Radiation Dose to Epithelial Cells of the Human Respiratory Tract from Radon Progeny. Presented at the 3rd International Workshop on Respiratory Tract Dosimetry, July 1-3, 1990, Albuquerque, New Mexico.

Fisher, D. R., T. E. Hui, V. P. Bond, and A. C. James. 1990. Microdosimetry of Radon Progeny: Application to Risk Assessment. Presented at the 29th Hanford Symposium on Health and the Environment, October 16-19, 1990, Richland, Washington.

Foreman, M. E., L. S. McCoy, and M. E. Frazier. 1990. Involvement of Oncogenes in Radon-Induced Lung Tumors in the Rat. Presented at the 29th Hanford Symposium on Health and the Environment, October 15-19, 1990, Richland, Washington.

Frazier, M. E. 1990. Oncogenes in Radiation Carcinogenesis. Presented at the DOE/OHER Radiation Biology Program Review, June 5-7, 1990, Chicago, Illinois.

Gilbert, E. S. 1990. Modeling Lung Cancer Risks in Laboratory Dogs Exposed to Inhaled Plutonium. Presented at the 1990 Joint Statistical Meetings, August 6-10, 1990, Anaheim, California.

Gilbert, E. S., F. T. Cross, C. L. Sanders, and G. E. Dagle. 1990. Models for Comparing Lung-Cancer Risks in Radon- and Plutonium-Exposed Experimental Animals. Presented at the 29th Hanford Symposium on Health and the Environment, October 15-19, 1990, Richland, Washington.

Gilbert, E. S., J. F. Park, F. T. Cross, and G. E. Dagle. 1990. Recent Pacific Northwest Laboratory Beagle and Rodent Studies: Methods and Results. Presented at the American Statistical Association Conference on Radiation and Health, July 8-12, 1990, Copper Mountain, Colorado.

Hui, T. E., D. R. Fisher, and A. C. James. 1990. Model for Assessing Radiation Dose to Epithelial Cells of the Human Respiratory Tract from Radon Daughters. Presented at the 3rd International Workshop on Respiratory Tract Dosimetry, July 1-3, 1990, Albuquerque, New Mexico.

Hulla, J. E., D. B. Mann, and D. L. Springer. 1990. Characterization of Benzo[a]pyrene Adducts to the Plasmid pXP-14. Presented at the 29th Annual Meeting of the Society of Toxicology, February 11-16, 1990, Miami Beach, Florida.

James, A. C. 1990. Dosimetry Modeling: Overview of Radon Dosimetry and the ICRP Task Group's Proposals for a New Lung Model. Presented at the American Statistical Association Conference on Radiation and Health, July 8-12, 1990, Copper Mountain, Colorado (invited lecture).

James, A. C. 1990. Lung Dosimetry Models and the Impact of Proposed Changes. Presented at the Workshop on Radiation Safety in the Mineral Sands Industry, September 12, 1990, Perth, Western Australia (invited lecture).

James, A. C. 1990. Recent Developments in Internal Dosimetry of Plutonium, Thorium, Uranium, and Radon Progeny. Presented at the Australian Radiation Laboratory, September 18, 1990, Melbourne, Victoria (invited lecture).

James, A. C. 1990. Respiratory Tract Dosimetry: What Does It Imply for Risk and Measurement of Indoor Exposure? Presented at the 29th Hanford Symposium on Health and the Environment, October 15-19, 1990, Richland, Washington.

James, A. C., and A. Birchall. 1990. Implications of the ICRP Task Group's Proposed Lung Model for Internal Dose Assessments in the Mineral Sands Industry. Presented at Minesafe International 1990, an International Conference on Occupational Health and Safety in the Minerals Industry, September 10-14, 1990, Perth, Western Australia (invited paper).

James, A. C., P. Gehr, R. Masse, R. G. Cuddihy, F. T. Cross, A. Birchall, J. S. Durham, and J. Briant. 1990. Dosimetry Model for Bronchial and Extrathoracic Tissues of the Respiratory Tract. Presented at the Third International Workshop on Respiratory Tract Dosimetry, July 1-3, 1990, Albuquerque, New Mexico.

James, A. C., W. Stahlhofen, G. Rudolf, M. J. Egan, W. Nixon, and J. K. Briant. 1990. The Respiratory Tract Deposition Model Proposed by the ICRP Task Group. Presented at the 3rd International Workshop on Respiratory Tract Dosimetry, July 1-3, 1990, Albuquerque, New Mexico.

Jostes, R. 1990. In Vitro Radon-Induced Chromosomal Damage in Human Peripheral Blood Lymphocytes. Presented at the 38th Annual Meeting of the Radiation Research Society, April 7-12, 1990, New Orleans, Louisiana.

Jostes, R. F., J. K. Wiencke, V. Afzal, S. Wolff, and F. T. Cross. 1990. In Vitro Radon-Induced Chromosomal Damage in Human Peripheral Blood Lymphocytes. Presented at the 38th Annual Meeting of the Radiation Research Society, April 7-12, 1990, New Orleans, Louisiana.

Jostes, R. F., T. L. Morgan, R. A. Gies, E. W. Fleck, K. P. Gaspar, and F. T. Cross. 1990. Molecular Analysis of Radon-Induced Mutants. Presented at the UCLA Colloquium on Ionizing Radiation Damage to DNA, January 16-20, 1990, Lake Tahoe, California.

Jostes, R. F., E. W. Fleck, R. A. Gies, T. E. Hui, T. L. Morgan, J. L. Schwartz, J. K. Wiencke, and F. T. Cross. 1990. Cytotoxic, Clastogenic and Mutagenic Response of Mammalian Cells Exposed *in Vitro* to Radon and Its Progeny. Presented at the 29th Hanford Symposium on Health and the Environment, October 15-19, 1990, Richland, Washington.

Kelman, B. J., and M. R. Sikov. 1990. Estimating Fetal Exposure to Toxic Materials. Presented at the Annual Meeting of the Society of Toxicology, February 12-16, 1990, Miami Beach, Florida.

Leung, F. C. 1990. Growth Factors/Receptors as Potential Molecular Markers for Radiation-Induced Lung Cancer. Presented at the 38th Annual Meeting of the Radiation Research Society, April 7-12, 1990, New Orleans, Louisiana.

Leung, F. C. 1990. Growth Factors/Growth Factor Receptor in Radiation Carcinogenesis. Presented at the Symposium on the "Relevance of Animal Models of Radiation Carcinogenesis in the Light of Developments in Molecular Biology, Institute of Applied Radiobiology and Immunology," October 22-23, 1990, TNO, Rijswijk, The Netherlands.

Leung, F. C., G. E. Dagle, and F. T. Cross. 1990. Involvement of Growth Factors and Their Receptors in Radon-Induced Rat Lung Tumors. Presented at the 29th Hanford Symposium on Health and the Environment, October 15-19, 1990, Richland, Washington.

Leung, F. C., G. E. Dagle, J. F. Park, and F. T. Cross. 1990. Growth Factors/Receptors as Potential Molecular Markers for Radiation-Induced Lung Cancer. Presented at the 38th Annual Meeting of the Radiation Research Society, April 7-12, 1990, New Orleans, Louisiana.

Leung, F. C., C. A. Poindexter, D. L. Miller, and L. E. Anderson. 1990. Biochemical and Hormonal Evaluation of Pineal Gland *In Vitro*. Presented at the 12th Annual Meeting of the Bioelectromagnetics Society, June 10-14, 1990, San Antonio, Texas.

Meznarich, H. K., and M. R. Sikov. 1990. Effect of Radiation on Mouse Embryonic Limb Development. Presented at the Annual Meeting of the Federation of American Societies for Experimental Biology, April 1-5, 1990, Washington, D.C.

Meznarich, H. K., L. A. Braby, and M. R. Sikov. 1990. Development of Mouse Limb Bud in Culture Following Irradiation. Presented to the Northwest Section of the Society for Experimental Biology and Medicine, October 6, 1990, Newport, Oregon.

Park, J. F., G. E. Dagle, R. E. Weller, R. L. Buschbom, and G. J. Powers. 1990. Comparative Distribution of Inhaled $^{238}PuO_2$ and $^{239}PuO_2$ in Beagles. Presented at the 35th Annual Meeting of the Health Physics Society, June 24-28, 1990, Anaheim, California.

Sanders, C. L. 1990. Low-Level $^{239}PuO_2$ Lifespan Studies. Presented at the DOE Review of Radiobiology Studies, June 6, 1990, Chicago, Illinois.

Sikov, M. R. 1990. Radiation and Chemical Dosimetry of the Embryo and Fetus. Presented at the Teratology Society Meeting, June 6-12, 1990, Victoria, British Columbia.

Sikov. M. R., H. K. Meznarich, and R. J. Traub. 1990. Comparison of Placental Transfer and Localization of Cesium, Strontium, and Iodine in Experimental Animals and Women. Presented at the CEIR/MRC Forum on Radionuclides and External Radiation: Implications for the Embryo and Fetus, November 9, 1990, London, England.

Sikov, M. R., F. T. Cross, T. J. Mast, H. E. Palmer, and A. C. James. 1990. Developmental Toxicology and Dosimetry Studies of Prenatal Exposure in Rats. Presented at the Annual Meeting of the Northwest Section of the Society for Experimental Biology and Medicine, October 5-6, 1990, Newport, Oregon.

Sikov, M. R., F. T. Cross, T. J. Mast, H. E. Palmer, and A. C. James. 1990. Developmental Toxicology of Radon Exposures. Presented at the 29th Hanford Symposium on Health and the Environment, October 15-19, 1990, Richland, Washington.

Springer, D. L., J. E. Hulla, M. G. Horstman, B. L. Thomas, and S. C. Goheen. 1990. Preparation and Partial Characterization of Hemoglobin Adducts from Trichloroethylene (TCE). Presented at the Annual Meeting of the Society of Toxicology, February 11-16, 1990, Miami Beach, Florida.

Zangar, R. C., D. W. Later, and D. L. Springer. 1990. Analysis of Carbaryl Metabolites Using HPLC and Supercritical Fluid Chromatograph (SFC). Presented at the 29th Annual Meeting of the Society of Toxicology, February 11-16, 1990, Miami Beach, Florida.

1991

Briant, J. K., A. C. James, and M. A. Parkhurst. 1991. Design and Calibration of an Ultrafine Radon Progeny Size-Spectrometer Utilizing Etched Tracks in CR-39 Plastic. Presented at the 1991 Meeting of the American Association for Aerosol Research, October 7-11, 1991, Traverse City, Michigan.

Brooks, A. L. 1991. Use of *In Vitro/In Vivo* Models of Carcinogenesis. Presented at the National Cancer Institute and Cancer Biology - Immunology Contracts Committee Review, October 6-9, 1991, Bethesda, Maryland.

Brooks, A. L., R. F. Kitchin, K. E. McDonald, and A. Vinson. 1991. Genotoxic Damage from Combined Exposures to Organic Solvents and Radiation. Presented at the Environmental Mutation Society Meeting, April 6-10, 1991, Orlando, Florida.

Brooks, A. L., K. E. McDonald, B. B. Kimsey, and R. M. Kitchin. 1991. The Induction of Chromosome Damage in Bone Marrow of Chinese Hamsters Following Combined Acute Gamma Ray Exposure and Internally Deposited ^{239}Pu. Presented at the 9th International Congress of Radiation Research, July 7-12, 1991, Toronto, Canada.

Brooks, A. L., D. S. Culp, A. L. Lloyd, K. E. McDonald, and R. M. Kitchin. 1991. Lack of Interaction Between Damage Produced by ^{60}Co Gamma Rays and Organic Solvents Methyl Isobutyl Ketone or Tributyl Phosphate on Cell Killing and Micronuclei. Presented at the Annual Meeting of the Pacific Northwest Association of Toxicologists, September 6, 1991, Seattle, WA.

Brooks, A. L., K. E. McDonald, C. Mitchell, A. Lloyd, N. F. Johnson, and R. M. Kitchin. 1991. The Combined Genotoxic Effects of Radiation and Occupational Pollutants. Presented at the 30th Hanford Symposium on Health and the Environment, "Current Topics in Occupational Health," October 29-November 1, 1991, Richland, Washington.

Brooks, A. L., M. R. Raju, M. K. Murphy, W. F. Harvey, G. J. Newton, and R. Guilmette. 1991. Comparison of the Effectiveness of Collimated and Non-Collimated Random ^{238}Pu Sources on the Induction of Micronuclei and Cell Killing in Lung Epithelial Cells. Presented at the 40th Annual Meeting of the Radiation Research Society, March 15-18, 1992, Salt Lake City, Utah.

Brooks, A. L., J. Adelstein, B. Boecker, K. Kase, A. Kronenburg, B. McNeil, R. Shore, and W. Templeton. 1991. Identification of Research Needs in Radiation Protection. Presented at the 40th Annual Meeting of the Radiation Research Society, March 15-18, 1992, Salt Lake City, Utah.

Cross, F. T. 1991. NIH Core Project Overview and Development and Application of the Animal Model. Presented at the NIH Radon Proposal Review Site Visit, February 21, 1991, Richland, Washington.

Cross, F. T. 1991. Experimental Studies on Lung Carcinogenesis and Their Relationship to Future Research in Radiation-Induced Lung Cancer in Humans. Presented at the Workshop on The Future of Human Radiation Research, March 4-8, 1991, Schloss, Elmau, Germany.

Cross, F. T. 1991. Overview of the DOE/RERF/IARC/CEC Scholl Elmau Workshop. Presented at the Meeting of the Washington State Radon Health Effects Committee/Radon Task Force, March 12, Seattle, Washington.

Cross, F. T. 1991. Can Animal Data Apply to Man? Presented at the DOE Science Writers' Workshop, "Radon Today: The Science and the Politics," April 25-26, 1991, Bethesda, Maryland.

Cross, F. T. 1991. A Review of Experimental Animal Radon Health Effects Data. Presented at the 9th International Congress of Radiation Research, July 7-12, 1991, Toronto, Canada.

Cross, F. T. 1991. Evidence of Risk from Animal Studies. Presented at the 1991 DOE/OHER Radon Contractors' Meeting, August 25-27, 1991, Albuquerque, New Mexico.

Cross, F. T. 1991. Progress on Risk in "Inhalation Hazards to Uranium Miners" and "Mechanisms of Radon Injury" Projects. Presented at the 1991 DOE/OHER Radon Contractors' Meeting, August 25-27, 1991, Albuquerque, New Mexico.

Cross, F. T. 1991. Experimental, Statistical, and Biological Models of Radon Carcinogenesis. Presented at the 5th International Symposium on the Natural Radiation Environment, September 22-28, 1991, Salzburg, Austria.

Cross, F. T. 1991. Radon Health Effects Data in Animals and Their Relationship to Human Data. Presented at the 5th Annual Conference of the American Association of Radon Scientists and Technologists, October 9-12, 1991, Rockville, Maryland.

Cross, F. T. 1991. Experimental Radon Health-Effect Studies. Presented to the Radiological Sciences Course 501, Biological Effects of Ionization Radiation, November 7, 1991, Washington State University Tri-Cities Campus, Richland, Washington.

Cross, F. T. 1991. The DOE and PNL Radon Program with Emphasis on Experimental Animal Studies. Presented at the Cellular and Mammalian Biology Section Meeting, November 7, 1991, Richland, Washington.

Cross, F. T. 1991. A Review of Experimental Animal Radon Health Effects Data. Presented at the 2nd IAEA/UNESCO/UNIDO/ICTP Workshop on Radon Monitoring in Radioprotection, Environmental and/or Earth Sciences, November 25-December 6, 1991, Trieste, Italy.

Cross, F. T., and G. E. Dagle. 1991. Lung Cancer in Rats Exposed to Radon/Radon Progeny. Presented at the 1991 International Symposium on Radon and Radon Reduction Technology, April 2-5, 1991, Philadelphia, Pennsylvania.

Dagle, G. E. 1991. Physicochemical Interactions and Tumor Induction in Bones by Inhaled $^{239}Pu(NO3)_4$. Presented at the Joint Bone Radiology Workshop, July 12-13, 1991, Toronto, Canada.

Dagle, G. E., J. F. Park, R. E. Weller, E. S. Gilbert, and R. L. Buschbom. 1991. Health Effects of Inhaled Plutonium in Dogs. Presented at the 9th International Congress of Radiation Research, July 7-12, 1991, Toronto, Canada.

Douthart, R. D. 1991. Computer Graphics As a Tool in Understanding Genomic Structures. Presented at the workshop "Computer-Based Analysis of Nucleic Acids and Protein Sequences," January 19, 1991, University of Washington Medical Center, Seattle, Washington (invited presentation).

Douthart, R. D. 1991. Graphics Sequence Representation and Analysis. Presented at the Sequence Analysis Workshop, in workshop "Computer-Based Analysis of Nucleic Acids and Protein Sequences," January 19, 1991, University of Washington Medical Center, Seattle, Washington (panel member and invited presentation).

Douthart, R. D. 1991. Computer Visualization of Large Genomic Structures. Presented at BBN, Inc., March 4, 1991, Cambridge, Massachusetts (invited presentation).

Douthart, R. D. 1991. "Metacodes in DNA and Protein Sequence," the Telluride Workshop on Open Problems of Computational Molecular Biology, June 2-8, 1991, Telluride, Colorado (invited participant).

Douthart, R. D., and D. A. Thurman. 1991. GnomeView: A Computer Graphics Window into the Human Genome. Presented at the Human Genome Workshop III, October 22, 1991, San Diego, California.

Douthart, R. D., D. A. Thurman, and J. E. Pelkey. 1991. GnomeView: A Genome Graphics Interface. Presented at the Human Genome Workshop, February 19, 1991, Santa Fe, New Mexico.

Elston, R. A. 1991. Future of the Coastal Shellfish Resource. Presented at the Washington Department of Fisheries Information Fair, January 17, 1991, Long Beach, Washington.

Hulla, J. E. 1991. Evidence of the Occurrence of a Processed p53 Pseudogene Within the Rat Genome. Presented at the Radiation Research Society Special Workshop, "Oncogenic Mechanisms in Radiation-Induced Cance ," January 16-19, 1991, Fort Collins, Colorado.

James, A. C. 1991. ICRP Lung Dosimetry - Status of the ICRP Task Group Proposals. Seminar presented to the Atomic Energy Control Board, April 22, 1991, Ottawa, Canada (invited presentation)

James, A. C. 1991. Developments in Lung and Body Organ Dosimetry for Radon, Thoron, and Their Short-Lived Progeny - What Are They Telling Us? Seminar presented to the National Radiological Protection Board, October 3, 1991, Chilton, England (invited presentation).

James, A. C., and J. K. Briant. 1991. Proposed New Concepts in ICRP Respiratory Tract Dosimetry with Application to Gases and Vapors. Presented at the 30th Hanford Symposium on Health and the Environment, "Current Topics in Occupational Health," October 29-November 1, 1991, Richland, Washington.

James, A. C., and K. D. Thrall. 1991. General Biokinetic Model for Radon, Thoron, and Their Short-Lived Progeny - What Are They Telling Us? Presented at the Annual Meeting of DOE/OHER Research Contractors, August 25-27, 1991, Albuquerque, New Mexico.

James, A. C., and K. D. Thrall. 1991. General Biokinetic Model for Radon, Thoron, and Their Short-Lived Progeny. Presented at the Annual Meeting of DOE/OHER Research Contractors, August 25-27, 1991, Albuquerque, New Mexico.

James, A. C., J. R. Johnson, and D. R. Fisher. 1991. ICRP Task Group Dosimetry Model for the Respiratory Tract: Implications for Uranium. Presented at the 36th Annual Meeting of the Health Physics Society, July 21-26, 1991, Washington, D.C.

Jostes, R. F., T. L. Morgan, E. W. Fleck, and F. T. Cross. 1991. Radiation-Induced Mutation Studies. Presented at the 1991 DOE/OHER Radon Contractors' Meeting, August 25-27, 1991, Albuquerque, New Mexico.

Kitchin, R. M., K. E. McDonald, B. B. Kimsey, and A. L. Brooks. 1991. Influence of Internally Deposited ^{144}Ce - ^{144}Pr on Chromosome Aberration Frequency Induced by Acute Exposure to ^{60}Co in Bone Marrow and Liver of Chinese Hamsters. Presented at the 9th International Congress of Radiation Research, July 7-12, 1991, Toronto, Canada.

Meznarich, H. K. 1991. Altered Fibronectin Levels in Irradiated Mouse Blastocysts. Presented at the Annual Meeting of the Federation of American Societies for Experimental Biology, April 1991, Atlanta, Georgia.

Meznarich, H. K. 1991. Fibronectin in Prenatally Irradiated Mouse Brains. Presented at the Regional Meeting for the Pacific Northwest Association of Toxicologists, September 1991, Seattle, Washington.

Morgan, T. L., L. A. Braby, E. W. Fleck, R. F. Jostes, and F. T. Cross. 1991. Model of Radiation Mutagenesis. Presented at the 24th Radiological and Chemical Physics Contractors Meeting, April 1991, New York, New York.

Sanders, C. L., and G. E. Dagle. 1991. A Threshold Model of Pulmonary Carcinogenesis: Carcinoma in the Rat After Deposition of Plutonium or Quartz. Presented at the 30th Hanford Symposium on Health and the Environment, "Current Topics in Occupational Health," October 29-November 1, 1991, Richland, Washington.

Sanders, C. L., G. E. Dagle, J. A. Mahaffey, and K. E. Lauhala. 1991. Increased Incidence of Brain Tumors in Rats Exposed to Plutonium Aerosol. Presented at the 9th International Congress of Radiation Research, July 7-12, 1991, Toronto, Canada.

Springer, D. L., C. G. Edmonds, D. M. Sylvester, and R. J. Bull. 1991. Hemoglobin Adducts as Biomarkers of Chemical Exposure. Presented at the 1991 Annual Meeting of the Society for Risk Analysis, December 8-11, 1991, Baltimore, Maryland.

Springer, D. L., S. C. Goheen, C. G. Edmonds, M. McCulloch, D. M. Sylvester, C. L. Sanders, and R. J. Bull. 1991. Presented at the 30th Annual Meeting of the Society of Toxicology, February 25-March 1, 1991, Dallas, Texas.

Stiegler, G. E. 1991. Evidence for *ras*-Oncogene Activation in Radiation-Induced Carcinogenesis. Presented at the Radiation Research Society Special Workshop, "Oncogenic Mechanisms in Radiation-Induced Cancer," January 16-19, 1991, Fort Collins, Colorado.

Stiegler, G. L., L. C. Stillwell, E. C. Sisk, and M. F. Minnick. 1991. Evidence for *ras*-Oncogene Activation in Radiation-Induced Oncogenesis. Presented at the 8th Annual Meeting of the Pacific Northwest Association of Toxicologists, September 6-7, 1991, Seattle, Washington.

Tenforde, T. S. 1991. Biological Interactions and Health Effects of Static and Extremely-Low-Frequency Electric and Magnetic Fields. Invited lectures presented at the Annual Meeting of the Asian Institution of Electrical Engineers, to the Department of Electrical and Electronic Engineering and to the Medical School Faculty, Tokushima University, at the Shikoku Electric Power Company in Takamatsu, and at a magnetobiology meeting sponsored by Kansai Electric Power Company, Osaka, November 7-17, 1991, Japan.

Thrall, B., and D. L. Springer. 1991. Altered Transcription by SP6 Polymerase. Presented at the 82nd Annual Meeting of the American Association for Cancer Research, May 15-18, 1991, Houston, Texas.

Thrall, B., M. J. Smerdon, and D. L. Springer. 1991. Sequence-Specific Modification of DNA by Benzo[a]pyrene Diolepoxide Determined by Inhibition of Polymerase Activities. Presented at the meeting of the American Association for Cancer Research, December 1-6, 1991, Banff, Alberta, Canada.

Watson, C. R. 1991. Workshop on "Future Directions for Radium Dial Painter Studies." Presented at Argonne National Laboratory, June 3-5, 1991, Argonne, Illinois (invited participant).

Watson, C. R. 1991. National Radiobiology Archives. Presented at the 36th Annual Meeting of the Health Physics Society, July 21-26, 1991, Washington, D.C.

Watson, C. R., Chairman. 1991. "The Control Beagle Workshop," convened by the National Radiobiology Project, December 16-17, 1991, Salt Lake City, Utah.

Weller, R. E. 1991. Canine Lymphoma: What's Old? What's New? Presented to the Southeast Washington Veterinary Medical Association, October 15, 1991, Pasco, Washington.

Zangar, R. C., D. R. Buhler, and D. L. Springer. 1991. Developmental Regulation of Cytochrome P450 IIC11 Enzyme Activity Correlates with mRNA Levels in DES-Imprinted Rats. Presented at the 30th Annual Meeting of the Society of Toxicology, February 25-March 1, 1991, Dallas, Texas.

1992

Brooks, A. L. 1992. Radioadaptive Response *In Vivo* in Chinese Hamsters Injected with Alpha- (^{239}Pu) or Beta-Gamma- (^{14}Ce) Emitting Radionuclides. Presented at the International Conference on Low Dose Irradiation and Biological Defense Mechanisms, July 11-19, 1992, Kyoto, Japan.

Cross, F. T. 1992. Evidence of Cancer Risk from Experimental Animal Radon Studies. Presented at the Pedagogical Symposium of the 203rd National Meeting of the American Chemical Society: "Radiation and Society," April 5-10, 1992, San Francisco, California (invited presentation).

Gies, R. A., F. T. Cross, G. E. Dagle, R. L. Buschbom, and J. C. Aryan. 1992. The Histomorphologic Effects of Inhaled Radon, Uranium Ore Dust, and Cigarette Smoke in the Tracheal Epithelium of the Rat. Presented at the 37th Annual Meeting of the Health Physics Society, June 21-25, 1992, Columbus, Ohio.

Jostes, R. F., Jr., T. E. Hui, R. A. Gies, and F. T. Cross. 1992. Use of the Single-Cell Gel Technique to Confirm Hit Probability Calculations in Mammalian Cells Exposed to Radon and Radon Progeny. Presented at the 40th Annual Meeting of the Radiation Research Society, March 14-18, 1992, Salt Lake City, Utah.

Sanders, C., D. M. Sylvester, and D. L. Springer. 1992. Recognition of Acrylamide Adducts in Peptides from Hemoglobin. Presented at the 31st Annual Meeting of the Society of Toxicology, February 23-27, 1992, Seattle, Washington.

Springer, D. L., C. G. Edmonds, D. M. Sylvester, C. Sanders, and R. J. Bull. 1992. Partial Characterization of Proteolytically Derived Peptides from Acrylamide-Adducted Hemoglobin. Presented at the 31st Annual Meeting of the Society of Toxicology, February 23-27, 1992, Seattle, Washington.

Thrall, B., and D. L. Springer. 1992. Sequence-Specific Blocks in DNA/RNA Polymerases Induced by Benzo[a]pyrene Diol Epoxide. Presented at the 31st Annual Meeting of the Society of Toxicology, February 23-27, 1992, Seattle, Washington.

Author Index

Author Index

Distribution

Distribution

OFFSITE

S. Addison
Radiological Safety Division
University of Washington
GS-05
Seattle, WA 98105

R. E. Albert, Professor
& Chairman
Department of Environmental
Health
University of Cincinnati
Medical Center
3223 Eden Avenue
Cincinnati, OH 45267-0056

E. L. Alpen
Donner Laboratory
University of California
Berkeley, CA 94720

A. Andersen
Center for Devices &
Radiological Health
Food & Drug Administration
5600 Fishers Lane, HFZ-100
Rockville, MD 20857

D. Anderson
ENVIROTEST
1108 NE 200th Street
Seattle, WA 98155-1136

G. Anderson
Department of Oceanography
University of Washington
Seattle, WA 98115

V. E. Archer
Rocky Mountain Center for
Occupational & Environmental
Health
Building 512
University of Utah
50 North Medical Drive
Salt Lake City, UT 84112

Assistant Secretary
Environment, Safety & Health
EH-1, FORS
U.S. Department of Energy
Washington, DC 20585

O. Auerbach
VA Hospital
East Orange, NJ 97919

J. A. Auxier
Auxier & Associates, Inc.
111 Mabry Hood Road
Suite 500
Knoxville, TN 37922

F. I. Badgley
13749 NE 41st Street
Seattle, WA 98125

R. E. Baker
8904 Roundleaf Way
Gaithersburg, MD 20879-1630

R. W. Barber
EH-33, GTN
U.S. Department of Energy
Washington, DC 20585

W. W. Barker, Chairman
Department of Biology
Central Washington University
Ellensburg, WA 98926

B. J. Barnhart
Office of Energy Research
U.S. Department of Energy
ER-72, GTN
Washington, DC 20585

N. F. Barr
ER-72, GTN
U.S. Department of Energy
Washington, DC 20585

M. M. Bashor, Ph.D.
ATSDR, Mail Stop E-28
1600 Clifton Road NE
Atlanta, GA 30333

J. W. Baum
Brookhaven National
Laboratory
Building 703-M
Upton, NY 11973

J. R. Beall
ER-72, GTN
U.S. Department of Energy
Washington, DC 20585

S. Benjamin
Director, CRHL
Foothills Campus
Colorado State University
Fort Collins, CO 80523

G. L. Bennett
Code RP
National Aeronautics & Space
Administration
Washington, DC 20585

R. P. Berube
EH-20, FORS
U.S. Department of Energy
Washington, DC 20585

PNL-8000, Pt. 1
UC-408

M. H. Bhattacharyya
BIM Div., Bldg. 202
Argonne National Laboratory
9700 South Cass Avenue
Argonne, IL 60439

R. W. Bistline
Rockwell International
Rocky Flats Plant
P. O. Box 464
Golden, CO 80401

B. B. Boecker
Inhalation Toxicology Research Institute
The Lovelace Foundation for Medical Education & Research
P. O. Box 5890
Albuquerque, NM 87185

V. P. Bond
Life Sciences, Chemistry and Safety
Brookhaven National Laboratory
Building 460
Upton, NY 11973

R. Borders
Health Protection Division
U.S. Department of Energy
P.O. Box 5400
Albuquerque, NM 87185

C. M. Borgstrom
Acting Director, NEPA
EH-25, Room 3E080
U.S. Department of Energy
1000 Independence Avenue SW
Washington, DC 20585

H. Box, Director
Biophysics
Roswell Park Cancer Institute
Elm & Carlton Streets
Buffalo, NY 14263-0001

J. D. Brain
Professor of Physiology
Director, Harvard Pulmonary Specialized Center of Research
Harvard University School of Public Health
665 Huntington Avenue
Boston, MA 02115

L. C. Brazley, Jr.
NE-22, GTN
U.S. Department of Energy
Washington, DC 20585

B. D. Breitenstein
Brookhaven National Laboratory
P.O. Box 83
Upton, NY 11973

F. W. Bruenger
Division of Radiobiology
Building 586
University of Utah
Salt Lake City, UT 84112

D. R. Buhler, Chairman
Toxicology Program
Oregon State University
Corvallis, OR 97331

R. J. Bull
Associate Professor of Pharmacology/Toxicology
College of Pharmacy
Pullman, WA 99164-6510

G. Burley
Office of Radiation Programs, ANR-458
Environmental Protection Agency
Washington, DC 20460

L. K. Bustad
College of Veterinary Medicine
Washington State University
Pullman, WA 99163

C. E. Carter
National Institute of Environmental Health Sciences
P.O. Box 12233
Research Triangle Park, NC 27709

H. W. Casey, Chairman
Department of Veterinary Pathology
School of Veterinary Medicine
Louisiana State University
Baton Rouge, LA 70803

R. J. Catlin
U.T. Health Science Center-Houston
13307 Queensbury Lane
Houston, TX 77079

N. Cohen
New York University Medical Center
P.O. Box 817
Tuxedo, NY 10987

W. Cool
Nuclear Regulatory Commission
Washington, DC 20585

D. K. Craig
Savannah River Laboratories
P.O. Box 616
Aiken, SC 29802

E. P. Cronkite
Medical Department
Brookhaven National Laboratory
Upton, NY 11973

J. Crowell
The Maxima Corporation
107 Union Valley Road
Oak Ridge, TN 37830

G. Davis
Vice President & Chairman
Medical Sciences Division
Oak Ridge Associated Universities
P.O. Box 117
Oak Ridge, TN 37830-0117

The Honorable Gail de Planque
U.S. Nuclear Regulatory Commission
Washington, DC 20555

G. P. Dix
3028 St. Tropex Street
Las Vegas, NV 89128

T. J. Dobry, Jr.
DP-221, GTN
U.S. Department of Energy
Washington, DC 20585

DOE/Office of Scientific & Technical Information (12)

DOE - Savannah River Operations Office
Environmental Division
P.O. Box A
Aiken, SC 29801

D. Doyle
Argonne National Laboratory
9700 South Cass Avenue
Argonne, IL 60439

H. Drucker
Argonne National Laboratory
9700 South Cass Avenue
Argonne, IL 60439

J. A. Louis Dubeau
Urological Cancer Research Laboratory
USC Comprehensive Cancer Center
University of Southern California
Los Angeles, CA 90033-0800

G. D. Duda
ER-72, GTN
U.S. Department of Energy
Washington, DC 20585

A. P. Duhamel
ER-74, GTN
U.S. Department of Energy
Washington, DC 20585

D. Dungworth
Associate Dean of Research and Professor & Chairman
Department of Veterinary Pathology
School of Veterinary Medicine
University of California
Davis, CA 95616

Dr. Patricia W. Durbin
Division of Biology and Medicine
Lawrence Berkeley Laboratory
University of California
Berkeley, CA 94704

K. F. Eckerman
Health Studies Section
Health and Safety Research Division
Oak Ridge National Laboratory
P.O. Box 2008
Oak Ridge, TN 37831-6383

C. W. Edington, Director
National Academy of Sciences
JH 554
2101 Constitution Avenue, NW
Washington, DC 20418

G. R. Eisele
Medical Division
Oak Ridge Associated Universities
P.O. Box 117
Oak Ridge, TN 37830

M. Eisenbud
711 Bayberry Drive
Chapel Hill, NC 27514

N. B. Everett
Department of Biological Structure
University of Washington
School of Medicine
Seattle, WA 98105

H. Falk, M.D.
CDC
CEHIC/EHHE
1600 Clifton Road NE
Atlanta, GA 30333

K. P. Ferlic
Office of Scientific & Engineering Recruitment, Training & Development
TR-1
U.S. Department of Energy
Washington, DC 20585

B. H. Fimiani
Battelle, Pacific Northwest Laboratories
Washington Operations
370 L'Enfant Promenade, Suite 900
901 D Street, SW
Washington, DC 20024

M. E. Frazier
Office of Health and Environment
Office of Energy Research
U.S. Department of Energy
ER-72, GTN
Germantown, MD 20875

H. L. Friedell
Biochemical Oncology
Case-Western Reserve University
2058 Abington Road
Wearn B21
Cleveland, OH 44106

T. Fritz
Argonne National Laboratory
9700 South Cass Avenue
Argonne, IL 60439

D. J. Galas
Office of Energy Research
ER-63
U.S. Department of Energy
Washington, DC 20585

D. E. Gardner
Northrop Services, Inc.
P.O. Box 12313
Research Triangle Park,
NC 27709

T. F. Gesell
Idaho State University
Campus Box 8106
Pocatello, ID 83209

R. D. Gilmore, President
Environmental Health
Sciences, Inc.
Nine Lake Bellevue Building
Suite 220
Bellevue, WA 98005

M. Goldman
Department of Radiological
Sciences (VM)
University of California
Davis, CA 95616

R. Goldsmith, Director
Office of Epidemiology & Health
Surveillance, EH-42
U.S. Department of Energy
Washington, DC 20585

G. Goldstein
Office of Epidemiology & Health
Surveillance
EH-42
U.S. Department of Energy
Washington, DC 20585

J. A. Graham
ECAO, Mail Drop 52
Environmental Protection
Agency
Research Triangle Park,
NC 27711

R. A. Griesemer, Director
National Toxicology Program
National Institutes of Health
P.O. Box 12233
Research Triangle Park,
NC 27709

G. H. Groenewold
Energy and Mineral Research
Center
University of North Dakota
Box 8123, University Station
Grand Forks, ND 58202

F. F. Hahn
Lovelace Inhalation Toxicology
Research Institute
P.O. Box 5890
Albuquerque, NM 87115

E. J. Hall
Radiological Research
Laboratory
Columbia University
630 West 168th Street
New York, NY 10032

R. Hamlin
Department of Veterinary
Physiology
The Ohio State University
1900 Coffey Road
Columbus, OH 43201

W. Happer
ER-1, FORS
U.S. Department of Energy
Washington, DC 20585

J. W. Healy
51 Grand Canyon Drive
White Rock, NM 87544

C. H. Hobbs
Inhalation Toxicology Research
Institute
The Lovelace Foundation for
Medical Education & Research
P.O. Box 5890
Albuquerque, NM 87185

L. M. Holland
Los Alamos National
Laboratory
P.O. Box 1663
Los Alamos, NM 87545

R. Hornung
DSHEFS, NIOSH
Robert A. Taft Laboratories
4676 Columbia Parkway
Cincinnati, OH 45220

J. E. Hulla
Hulla Scientific
125 University Avenue
Missoula, MT 59801

R. O. Hunter, Jr.
ER-1, FORS
U.S. Department of Energy
1000 Independence Avenue SW
Washington, DC 20585

F. Hutchinson
Department of Therapeutic
Radiology, HRT 315
Yale University
School of Medicine
333 Cedar Street
New Haven, CT 06510-8040

H. Ishikawa, General Manager
Nuclear Safety Research
Association
P.O. Box 1307
Falls Church, VA 22041

E. D. Jacobson
Center for Devices &
Radiological Health
Food & Drug Administration
5600 Fishers Lane, HFZ-100
Rockville, MD 20857

A. W. Johnson
San Diego State University
6310 Alvardo Court, Suite 110
San Diego, CA 92120

Dr. B. M. Jones
V-243 Carolina Meadows
Chapel Hill, NC 27514

R. K. Jones
The Lovelace Foundation for
Medical Education & Research
Building 9200, Area Y
Sandia Base
Albuquerque, NM 87108

G. Y. Jordy, Director
ER-30, GTN
U.S. Department of Energy
Washington, DC 20585

C. M. Kelly
Air Products and Chemicals,
Inc.
Corporate Research and
Development
P.O. Box 538
Allentown, PA 18105

A. R. Kennedy
Department of Radiation
Oncology
University of Pennsylvania
School of Medicine
3508 Market Street
Philadelphia, PA 19204-3357

R. T. Kratzke
NP-40
U.S. Department of Energy
Germantown, MD 20875

W. M. Leach
Food & Drug Administration
5600 Fishers Lane, HFZ-100
Rockville, MD 20857

Librarian
Documents Department--
The Libraries
Colorado State University
Ft. Collins, CO 80523

Librarian
Electric Power Research
Institute
3412 Hillview Avenue
P.O. Box 10412
Palo Alto, CA 94303

Librarian
Health Sciences Library, SB-55
University of Washington
Seattle, WA 98195

Librarian
Los Alamos National Laboratory
Report Library, MS P364
P.O. Box 1663
Los Alamos, NM 87545

Librarian
Oregon Regional Primate
Research Center
505 NW 185th Avenue
Beaverton, OR 97006

Library
Serials Department
(#80-170187)
University of Chicago
1100 East 57th Street
Chicago, IL 60637

Librarian
Washington State University
Pullman, WA 99164-6510

J. B. Little
Department of Physiology
Harvard School of Public
Health
665 Huntington Avenue
Boston, MA 02115

A. B. Lovins
Rocky Mountain Institute
1739 Snowmass Creek Road
Snowmass, CO 81654-9199

W. Lowder
Environmental Measurements
Laboratory
U.S. Department of Energy
376 Hudson Street
New York, NY 10014-3621

D. L. Lundgren
Inhalation Toxicology Research
Institute
P.O. Box 5890
Albuquerque, NM 87185

O. R. Lunt
Laboratory of Biomedical &
Environmental Sciences
University of California
900 Veteran Avenue
Los Angeles, CA 90024-1786

J. R. Maher
ER-65, GTN
U.S. Department of Energy
Washington, DC 20585

D. D. Mahlum
Board of Radiation Research
Room 342
2101 Constitution NW
Washington, D.C. 20318

T. D. Mahony
750 Swift Boulevard
Richland, WA 99352

S. Marks
8024 47th Place West
Mukilteo, WA 98275

D. R. Mason
Nuclear Safety Branch
U.S. Department of Energy
P.O. Box A
Aiken, SC 29801

W. H. Matchett
Graduate School
New Mexico State University
Box 3G
Las Cruces, NM 88003-0001

H. M. McCammon
ER-74, GTN
U.S. Department of Energy
Washington, DC 20585

R. O. McClellan, President
Chemical Industry Institute of Toxicology
P.O. Box 12137
Research Triangle Park, NC 27709

J. F. McInroy
Los Alamos National Laboratory
Mail Stop K484
P.O. Box 1663
Los Alamos, NM 87545

Medical Officer
Monsanto Research Corp.
Mound Laboratory
P.O. Box 32
Miamisburg, OH 45342

T. Meinhardt
DSHEFS, NIOSH
Robert A. Taft Laboratories
4676 Columbia Parkway
Cincinnati, OH 45220

C. B. Meinhold, President
National Council on Radiation Protection and Measuremnets
7910 Woodmont Avenue
Suite 800
Bethesda, MD 20814

H. Menkes
Assistant Professor of Medicine & Environmental Medicine
The John Hopkins University
Baltimore, MD 21205

D. B. Menzel
Southern Occupational Health Center
University of California, Irvine
Irvine, CA 92717

S. Michaelson
University of Rochester Medical Center
Rochester, NY 14642

C. Miller
P.O. Box 180
Watermill, NY 11976

S. Miller
Department of Radiobiology
University of Utah
Salt Lake City, UT 84112

W. A. Mills
Committee on Interagency Radiation Research & Policy Coordination (CIRRPC)
1346 Connecticut Avenue NW
Suite 530
Washington, DC 20036

K. Z. Morgan
1984 Castleway Drive
Atlanta, GA 30345

P. E. Morrow
Department of Biophysics
Medical Center
University of Rochester
Rochester, NY 14642

O. R. Moss
Chemical Industry Institute of Toxicology
P.O. Box 12137
Research Triangle Park, NC 27709

W. F. Mueller
New Mexico State University
Box 4500
Las Cruces, NM 88003-4500

D. S. Nachtwey
NASA-Johnson Space Center
Mail Code SD-5
Houston, TX 77058

R. Nathan
Battelle Project Management Division
505 King Avenue
Columbus, Ohio 43201

National Library of Medicine
TSD-Serials
8600 Rockville Pike
Bethesda, MD 20014

N. S. Nelson
Office of Radiation Programs (ANR-461)
Environmental Protection Agency
401 M Street SW
Washington, DC 20460

P. Nettesheim
National Institutes of Environmental Health Sciences
Research Triangle Park, NC 27711

W. R. Ney
Executive Director
National Council on Radiation Protection and Measurements
7910 Woodmont Avenue
Suite 800
Bethesda, MD 20814

S. W. Nielsen
Department of Pathology
New York State Veterinary College
Cornell University
Ithaca, NY 14850

R. A. Nilan
Division of Sciences
Washington State University
Pullman, WA 99164

M. Nolan
10958 Rum Cay Court
Columbia, MD 21044

Nuclear Regulatory Commission
Advisory Committee on Reactor Safeguards
Washington, DC 20555

A. F. Perge
RW-43, FORS
U.S. Department of Energy
Washington, DC 20585

D. F. Petersen
Los Alamos National Laboratory
P.O. Box 1663
Los Alamos, NM 87545

G. R. Petersen, Director
Epidemiologic Studies Division
Office of Epidemiology and Health Surveillance, EH-42
U.S. Department of Energy
Washington, DC 20585

L. E. Peterson
Epidemiology Research Unit/UTSPH
P.O. Box 20186
Houston, TX 77225

H. J. Pettengill
Deputy Assistant Secretary of Health
EH-40, GTN
U.S. Department of Energy
Washington, DC 20585

H. Pfuderer
Oak Ridge National Laboratory
P.O. Box X
Oak Ridge, TN 37830

O. G. Raabe
Laboratory for Energy-Related Health Research
University of California
Davis, CA 95616

R. Rabson
Division of Biological Energy Research
ER-17, GTN
U.S. Department of Energy
Washington, DC 20585

D. P. Rall, Director
National Institutes of Environmental Health Sciences
P.O. Box 12233
Research Triangle Park, NC 27709

R. D. Reed, Chief
Rocky Flats Area Office
Albuquerque Operations Office
U.S. Department of Energy
P.O. Box 928
Golden, CO 80402-0928

C. R. Richmond
Oak Ridge National Laboratory
4500N, MS-62523
P.O. Box 2008
Oak Ridge, TN 37831-6253

B. Robinson
Monsanto Research Corp.
Mound Laboratory
P.O. Box 32
Miamisburg, OH 45342

S. L. Rose
ER-72, GTN
U.S. Department of Energy
Washington, DC 20585

G. Runkle, Chief
U.S. Department of Energy, AL
HPB/EHD
P.O. Box 5400
Albuquerque, NM 87115

G. Saccomanno
Pathologist and Director of Laboratories
St. Marys and V. A. Hospitals
Grand Junction, CO 81501

U. Saffiotti
Laboratory of Experimental Pathology
National Cancer Institute
Building 41, Room C-105
Bethesda, MD 20892

L. Sagan
Electric Power Research Institute
3412 Hillview Avenue
P.O. Box 10412
Palo Alto, CA 94304

M. Sage
CDC (F-28)
CEHIC
1600 Clifton Road NE
Atlanta, GA 30333

J. M. Samet
New Mexico Tumor Registry
University of New Mexico
Cancer Research and Treatment Center
Albuquerque, NM 87131

R. A. Scarano
Mill Licensing Section
Nuclear Regulatory Commission
Washington, DC 20585

R. A. Schlenker
Environmental Health & Safety Department
Building 201
Argonne National Laboratory
9700 South Cass Avenue
Argonne, IL 60439

C. R. Schuller
Battelle - Seattle
4000 NE 41st Street
Seattle, WA 98105

M. Schulman
ER-70, GTN
U.S. Department of Energy
Washington, DC 20585

T. M. Seed
BIM 202
Argonne National Laboratory
9700 South Cass Avenue
Argonne, IL 60439

R. B. Setlow
Brookhaven National Laboratory
Upton, NY 11973

R. Shikiar
Battelle - Seattle
4000 NE 41st Street
Seattle, WA 98105

H. P. Silverman
Beckman Instruments
2500 Harbor Blvd.
Fullerton, CA 92634

W. K. Sinclair
National Council on Radiation Protection
7910 Woodmont Avenue
Suite 800
Bethesda, MD 20814

D. H. Slade
ER-74, GTN
U.S. Department of Energy
Washington, DC 20585

D. A. Smith
ER-72, GTN
U.S. Department of Energy
Washington, DC 20585

G. S. Smith
New Mexico State University
Box 3-I
Las Cruces, NM 88003-0001

J. M. Smith
CDC
CEHIC
1600 Clifton Road NE
Atlanta, GA 30333

M. Smith
Department of Ecology
NUC Waste Library
PV-11 Building 99 South Sound
Olympia, WA 98504

Dr. H. Spitz
Department of Mechanical, Industrial, & Nuclear Engineering
University of Cincinnati
MS 072
Cincinnati, OH 45267

J. N. Stannard
17441 Plaza Animado #132
San Diego, CA 92128

R. W. Starostecki
U.S. Department of Energy
1000 Independence Ave. SW
Washington, DC 20585

R. J. Stern
EH-10, FORS
U.S. Department of Energy
Washington, DC 20585

K. G. Steyer
Nuclear Regulatory Commission
Washington, DC 20555

E. T. Still
Kerr-McGee Corporation
P.O. Box 25861
Oklahoma City, OK 73125

B. Stuart
Brookhaven National Laboratory
Upton, NY 11973

D. Swanger
Biology Department
Eastern Oregon State College
La Grande, OR 97850

J. Swinebroad
EH-43, GTN
U.S. Department of Energy
Washington, DC 20585

M. Tanaka
Physics Library
510A
Brookhaven National Laboratory
Upton, NY 11973

G. N. Taylor
Division of Radiobiology
Building 351
University of Utah
Salt Lake City, UT 84112

Technical Information Service
Savannah River Laboratory
Room 773A
E. I. duPont de Nemours
& Company
Aiken, SC 29801

R. G. Thomas
Argonne National Laboratory
Environment Research
Building 203
9700 South Cass Avenue
Argonne, IL 60439

T. Thomas
Health Physics and Industrial
Hygiene
EH-41
U.S. Department of Energy
Washington, DC 20585

P. W. Todd
Center for Chemical
Engineering
National Bureau of Standards
(773.10)
325 Broadway
Boulder, CO 80303

G. E. Tripard
Acting Director, NRC
Washington State University
Pullman, WA 99164-1300

P. T'so
Division of Biophysics
Room 3120
School of Hygiene & Public
Health
The Johns Hopkins University
615 North Wolfe Street
Baltimore, MD 21205

A. C. Upton
New York University Medical
Center
Institute of Environmental
Medicine
P.O. Box 817
Tuxedo, NY 10987

B. Valett
NORCUS
390 Hanford Street
Richland, WA 99352

E. J. Vallario
15228 Red Clover Drive
Rockville, MD 20853

R. L. Van Citters, Dean
Research and Graduate
Programs
University of Washington
Seattle, WA 98105

Dr. C. R. Vest
Marymount University
2807 North Glebe Road
Arlington, VA 22207

G. J. Vodapivc
DOE - Schenectady Naval
Reactors Office
P.O. Box 1069
Schenectady, NY 12301

G. L. Voelz
Los Alamos National
Laboratory
MS-K404
P.O. Box 1663
Los Alamos, NM 87545

B. W. Wachholz
Radiation Effects Branch
National Cancer Institute
EPN,
6130 Executive Blvd.
Rockville, MD 20842

N. Wald
School of Public Health
University of Pittsburgh
Pittsburgh, PA 15213

A. Waldo
U.S. Department of Energy
(EH-231)
1000 Independence Avenue SW
Washington, DC 20585

R. A. Walters
Assistant to the Associate
Director
Los Alamos National Laboratory
MS-A114
P.O. Box 1663
Los Alamos, NM 87545

P. Watson
Associate Professor
Department of Chemistry
Oregon State University
Corvallis, OR 97331

M. E. Weaver
Professor of Anatomy
University of Oregon Health
Science Center
School of Dentistry
Portland, OR 97201

M. H. Weeks
U.S. AEHA, Bldg. 2100
Edgewood Arsenal
Aberdeen Proving Ground,
MD 21014

I. Wender
Department of Chemical
Engineering
1249 Benedum Hall
University of Pittsburgh
Pittsburgh, PA 15261

W. W. Weyzen
Electric Power Research Institute
3412 Hillview Avenue
P.O. Box 10412
Palo Alto, CA 94303

K. Wilzbach
Argonne National Laboratory
9700 South Cass Avenue
Argonne, IL 60439

F. J. Wobber
U.S. Department of Energy
ER-75, GTN
Germantown, MD 20875

R. W. Wood
PTRD, OHER
ER-71, GTN
U.S. Department of Energy
Washington, DC 20585

Dr. Chui-hsu Yang
NASA Johnson Space Center
NASA Road 1
Mail Code: SD4
Houston, TX 77058

Dr. Shalomo Yaniv
Office of Nuclear Regulatory Research
Nuclear Regulatory Commission
Washington, DC 20555

P. L. Ziemer, Ph. D.
Assistant Secretary
Environment, Safety and Health
EH-1, FORS
U.S. Department of Energy
Washington, DC 20585

FOREIGN

Dr. Asker Aarkrog
Riso National Laboratory
ECO/MIL
DK-4000 Roskilde
DENMARK

G. E. Adams, Director
Medical Research Council
Radiobiology Unit
Harwell, Didcot
Oxon OX11 ORD
ENGLAND

A. L. Alejandrino, Head
Biomedical Research, ARD
Republic of the Philippines
Philippine Nuclear Research Institute
P.O. Box 932
Manila
THE PHILIPPINES

M. Anderson
Library
Department of National Health & Welfare
Ottawa, Ontario
CANADA

Atomic Energy of Canada, Ltd.
Scientific Document Distribution Office
Station 14
Chalk River Nuclear Laboratories
Chalk River, Ontario KOJ 1JO
CANADA

D. C. Aumann
Institut für Physikalische Chemie
Universität Bonn
Abt. Nuklearchemie
Wegelerstraße 12
5300 Bonn 1
GERMANY

M. R. Balakrishnan, Head
Library & Information Services
Bhabha Atomic Research Centre
Bombay-400 085
INDIA

G. W. Barendsen
Laboratory for Radiobiology
AMC, FO 212
Meibergdreef 9
1105 AZ Amsterdam
THE NETHERLANDS

A. M. Beau, Librarian
Département de Protection Sanitaire
Commissariat à l'Énergie Atomique
BP 6
F-92265 Fontenay-aux-Roses
FRANCE

G. Bengtsson
Director-General
Statens Stralskyddsinstitut
Box 60204
S-104 01 Stockholm
SWEDEN

D. J. Beninson
Director, Licenciamento de Instalaciones Nulceares
Comisión Nacional de Energía Atómica
Avenida del Libertador 8250
2° Piso Of. 2330
1429 Buenos Aires
ARGENTINA

A. Bianco
Viale Seneca, 65
10131 Torino
ITALY

J. Booz
KFA Jülich Institut für Medezin
Kernsforschungsanlage Jülich
Postfach 1913
D-5170 Jülich
GERMANY

M. J. Bulman, Librarian
Medical Research Council
Radiobiology Unit
Harwell, Didcot
Oxon OX11 ORD
ENGLAND

M. Calamosia
ENEA-LAB Fisica E
Tossicologia Aerosol
Via Mazzini 2
I-40138 Bologna
ITALY

Cao Shu-Yuan, Deputy Head
Laboratory of Radiation
Medicine
North China Institute of
Radiation Protection
P.O. Box 120
Tai-yuan, Shan-Xi
PEOPLE'S REPUBLIC OF
CHINA

M. Carpentier
Commission of the European
Communities
200 Rue de la Loi
J-70 6/16
B-1049 Brussels
BELGIUM

M. W. Charles
Nuclear Electric PLC
Radiological Protection Branch
Berkeley Nuclear Laboratories,
Berkeley
Gloucestershire GL 13 9PB
ENGLAND

Chen Xing-An
Laboratory of Industrial Hygiene
Ministry of Public Health
2 Xinkang Street
Deshengmenwai, Beijing
PEOPLE'S REPUBLIC OF
CHINA

R. Clarke
National Radiological
Protection Board
Harwell, Didcot
Oxon OX11 ORQ
ENGLAND

G. F. Clemente, Director
Radiation Toxicology
Laboratory
National Committee of Nuclear
Energy (CNEN)
Casaccia Centre for Nuclear
Studies (CSN)
Casella Postale 2400
I-00100 Roma
ITALY

H. Coffigny
Institut de Protection et de
Sûreté Nucléaire
Département de Protection
Sanitaire
Service de Pathologie
Expérimentale
BP 6
F-92265 Fontenay-aux-Roses
FRANCE

Commission of the European
Communities
DG XII - Library SDM8 R1
200 Rue de la Loi
B-1049 Brussels
BELGIUM

M. S. Davies
Medical Research Council
20 Park Crescent
London W1N 4AL
ENGLAND

Deng Zhicheng
North China Institute of
Radiation Protection
Tai-yuan, Shan-Xi
PEOPLE'S REPUBLIC OF
CHINA

M. Di Paola
ENEA, PAS/VALEPID
C.R.E. Casaccia
Casella Postale 2400
I-00100 Roma
ITALY

Director
Commissariat à l'Énergie
Atomique
Centre d'Etudes Nucléaires
Fontenay-aux-Roses (Seine)
FRANCE

Director
Laboratorio di Radiobiologia
Animale
Centro di Studi Nucleari Della
Casaccia
Comitate Nazionale per
l'Energia Nucleare
Casella Postale 2400
I-00100 Roma
ITALY

D. Djuric
Institute of Occupational and
Radiological Health
11000 Beograd
Deligradoka 29
YUGOSLAVIA

M. Dousset
Health Ministry
Frue de la Gruerie
F-91190 Gifsur Yvette
FRANCE

J. Eapen
Biochemistry Division
Bhabha Atomic Research
Centre
Bombay-400 085
INDIA

Estação Agronómica Nacional
Biblioteca
2780 Oeiras
PORTUGAL

PNL-8000, Pt. 1
UC-408

L. Feinendegen, Director
Institut für Medezin
Kernsforschungsanlage Jülich
Postfach 1913
D-5170 Jülich
GERMANY

T. M. Fliedner
Institut für Arbeits- u. Sozialmedizin
Universität Ulm
Oberer Eselsberg M 24, 309
D-7900 Ulm
GERMANY

L. Friberg
The Karolinska Institute
Stockholm
SWEDEN

R. M. Fry, Head
Office of the Supervising Scientist for the Alligator Rivers Region
P.O. Box 387
Bondi Junction NSW 2022
AUSTRALIA

A. Geertsema
Sasol Technology (Pty), Ltd.
P.O. Box 1
Sasolburg 9570
REPUBLIC OF SOUTH AFRICA

T. Giuseppe
ENEA-PAS-FIBI-AEROSOL
Via Mazzini 2
I-40138 Bologna
ITALY

H. L. Gjørup, Head
Health Physics Department
Atomic Energy Commission
Research Establishment
Risø, Roskilde
DENMARK

A. R. Gopal-Ayengar
73-Mysore Colony
Mahul Road, Chembur
Bombay-400 074
INDIA

C. L. Greenstock
Radiation Biology
AECL Research
Chalk River, Ontario
KOJ 1JO
CANADA

R. V. Griffith
International Atomic Energy Agency
Wagramerstraße 5
P.O. Box 200
A-1400 Vienna
AUSTRIA

Y. Hamnerius
Applied Electron Physics
Chalmers University of Technology
S-412 96 Göteborg
SWEDEN

G. P. Hanson, Chief
Radiation Medicine Unit
World Health Organization
CH-1211 Geneva 27
SWITZERLAND

J. L. Head
Department of Nuclear Science & Technology
Royal Naval College, Greenwich
London SE10 9NN
ENGLAND

W. Hofmann
Division of Biophysics
University of Salzburg
Hellbrunner Str 34
A-5020 Salzburg
AUSTRIA

J. Inaba, Director
Division of Comparative Radiotoxicology
National Institute of Radiological Sciences
9-1, Anagawa-4-chome
Chiba-shi 260
JAPAN

International Atomic Energy Agency
Documents Library
Attn: Mrs. Javor
Kaerntnerring 11
A-1010 Vienna 1
AUSTRIA

E. Iranzo
Jefe, División Protección Radiológica
Junta de Energia Nuclear
Cuidad Universitari
Madrid 3
SPAIN

W. Jacobi
Institut für Strahlenschutz
Post Schleissheim
Ingolstadter Landstrasse 1
D-8042 Neuherberg
GERMANY

K. E. Lennart Johansson
Radiofysiska Inst.
Regionsjukhuset
S-901-82 Umeå
SWEDEN

A. M. Kellerer
Institut für Strahlenbiologie
GSF
Ingelstädter Landstr. 1
D-8042 Neuherberg b. München
GERMANY

T. Kivikas
Studsvik Nuclear
S-611 82 Nyköping
SWEDEN

H.-J. Klimisch
BASF Aktiengesellschaft
Abteilung Toxikologie, Z470
D-6700 Ludwigshafen
GERMANY

H. E. Knoell
Battelle-Institut e.V.
Am Römerhof 35
Postfach 900160
D-6000 Frankfurt am Main 90
GERMANY

T. Kumatori
National Institute of
Radiological Sciences
9-1, Anagawa-4-chome
Chiba-shi 260
JAPAN

J. Lafuma, Head
Département de Protection
Sanitaire
Commissariat à l'Énergie
Atomique/IPSN
BP 6
F-92260 Fontenay-aux-Roses
FRANCE

J. R. A. Lakey
Department of Nuclear Science
& Technology
Royal Naval College
Greenwich Naval college
SW10 9NN
ENGLAND

Li De-Ping
Professor and Director of North
China
Institute of Radiation
Protection, NMI
P.O. Box 120
Tai-yuan, Shan-Xi
PEOPLE'S REPUBLIC OF
CHINA

Librarian
Alberta Environmental Centre
Bag 4000
Vegreville, Alberta T9C 1T4
CANADA

Librarian
Centre d'Etudes Nucléaires de
Saclay
P.O. Box 2, Saclay
Fig-sur-Yvette (S&O)
FRANCE

Librarian
CSIRO
314 Albert Street
P.O. Box 89
East Melbourne, Victoria
AUSTRALIA

Librarian
CSIRO
Division of Wildlife and Ecology
P.O. Box 84
Lyneham, ACT 2602
AUSTRALIA

Librarian
HCS/EHE
World Health Organization
CH-1211 Geneva 27
SWITZERLAND

Librarian
Kernforschungzentrum
Karlsruhe
Institut für Strahlenbiologie
Postfach 3640
D-75 Karlsruhe 1
GERMANY

Librarian
Max-Planck Institut für
Biophysics
Forstkasstraße
D-6000 Frankfurt/Main
GERMANY

Librarian
Medical Research Council
Radiobiology Unit
Chilton
Oxon OX11 ORD
ENGLAND

Librarian
Ministry of Agriculture,
Fisheries & Food
Fisheries Laboratory
Lowestoft, Suffolk NR33 OHT
ENGLAND

Librarian
National Institute of
Radiological Sciences
9-1, Anagawa-4-chome
Chiba-shi 260
JAPAN

Librarian
Supervising Scientist for the
Alligator Rivers Region
Level 23, Bondi Junction Plaza
P.O. Box 387
Bondi Junction NSW 2022
AUSTRALIA

Library
Atomic Energy Commission of
Canada, Ltd.
Whiteshell Nuclear Research
Establishment
Pinawa, Manitoba ROE 1L0
CANADA

Library
Department of Meteorology
University of Stockholm
Arrhenius Laboratory
S-106 91 Stockholm
SWEDEN

B. Lindell
National Institute of Radiation Protection
Fack S-104 01
Stockholm 60
SWEDEN

J. R. Maisin
Radiobiology Department
C.E.N. - S.C.K.
Mol
BELGIUM

A. M. Marko
9 Huron Street
Deep River, Ontario KOJ 1PO
CANADA

R. Masse
Institut de Protection et de Sûreté Nucléaire
Département de Protection Sanitaire
Service d'Etudes Appliquées de Protection Sanitaire
BP 6
F-92260 Fontenay-aux-Roses
FRANCE

H. Matsudaira
Director General
National Institute of Radiological Sciences
9-1, Anagawa-4-chome
Chiba-shi 260
JAPAN

O. Matsuoka
Research Consultant
Abiko Research Laboratory
Central Research Institute of Electric Power Industry
1646, Abiko, Abiko City
Chiba-ken 270-11
JAPAN

N. Matsusaka
Department of Veterinary Medicine
Faculty of Agriculture
Iwate University
Ueda, Morioka
Iwate 020
JAPAN

S. Mattsson
Department of Radiation Physics
Malmö General Hopsital
S-214 01 Malmö
SWEDEN

R. G. C. McElroy
Atomic Energy Commission of Canada, Ltd.
Dosimetric Research Branch
Chalk River, Ontario KOJ 1JO
CANADA

F.-I. S. Medina
Cytogenetics Laboratory
Biomedical Research Division
A.R.C.
Philippine Atomic Energy Commission
P.O. Box 932
Manila
THE PHILIPPINES

M. L. Mendelsohn
Radiation Effects Research Foundation
1-8-6 Nakagawa
Nagasaki 850
JAPAN

Meng Zi-Qiang
Department of Environmental Science
Shanxi University
Tai-yuan, Shan-Xi
PEOPLE'S REPUBLIC OF CHINA

P. Metalli
ENEA-PAS
CRE Casaccia
Casella Postale 2400
I-00100 Roma
ITALY

H. J. Metivier
Institut de Protection et de Sûreté Nucléaire
Centre d'Études de Service de Fontenay-aux-Roses
BP 6
F-92265 Fontenay-aux-Roses
FRANCE

A. R. Morgan
Biotechnology
Building 353
AEA Technology
Harwell, Didcot
Oxfordshire OX11 ORA
ENGLAND

Y. I. Moskalev
Institute of Biophysics
Ministry of Public Health
Givopisnaya 46
Moscow
RUSSIA

J. Muller
7 Millgate Crescent
Willowdale, Ontario M2K 1L5
CANADA

D. K. Myers, Head
Radiation Biology Branch
Atomic Energy Commission of Canada, Ltd.
Chalk River, Ontario
CANADA

J. C. Nériot, Deputy Director
Département de Protection
Centre d' Etudes Nucléaires
BP 6
F-92260 Fontenay-aux-Roses
FRANCE

R. Osborne
Atomic Energy Commission of Canada, Ltd.
Biology and Health Physics Division
Chalk River Nuclear Laboratories
P.O. Box 62
Chalk River, Ontario KOJ 1JO
CANADA

J. Pacha
Silesian Medical School
Fac. of Pharmacy
Ul. Jagiellonska 4
41-200 Sosnowiec
POLAND

H. G. Paretzke
GSF Institut für Strahlenschutz
Ingolstadter Landstraße 1
D-8042 Neuherberg
GERMANY

N. Parmentier
Département de Protection Sanitaire
Centre d'Etudes Nucléaires
BP 6
F-92260 Fontenay-aux-Roses
FRANCE

G. Patrick
Medical Research Council
Radiobiology Unit
Harwell, Didcot
Oxon OX11 ORD
ENGLAND

O. Pavlovski
Institute of Biophysics
Ministry of Public Health
Givopisnaya 46
Moscow D-182
RUSSIA

R. Perraud
Commissariat à l'Énergie Atomique
BP 1
87640 Razes
FRANCE

G. Premazzi
Commission of the European Communities
Joint Research Centre
Ispra Establishment
I-21020 Ispra
ITALY

V. Prodi
Department of Physics
University of Bologna
Via Irnerio 46
I-40126 Bologna
ITALY

O. Ravera
Commission of the European Communities, C.C.R.
I-21020 Ispra (Varese)
ITALY

REP Institutes TNO
TNO Division of Health Research Library
P.O. Box 5815
151 Lange Kleiweg
2280 HV Rijswijk
THE NETHERLANDS

Reports Librarian
Harwell Laboratory,
Building 465
UKAEA
Harwell, Didcot
Oxon OX11 ORB
ENGLAND

P. J. A. Rombout
Inhalation Toxicology Department
National Institute of Public Health and Environmental Protection
P.O. Box 1
NL-3720 BA Bilthoven
THE NETHERLANDS

M. Roy
Institut de Protection et de Sûreté Nucléaire
Département de Protection Sanitaire
Service d'Etudes Appliquées de Protection Sanitaire
BP 6
F-92260 Fontenay-aux-Roses
FRANCE

F. A. Sacherer
Battelle-Institut e.V.
Am Römerhof 35
Postfach 900160
D-6000 Frankfurt am Main 90
GERMANY

W. Seelentag, Chief Medical Officer
Radiation Health Unit
World Health Organization
CH-1211 Geneva 27
SWITZERLAND

J. Sinnaeve
Biology, Radiation Protection Medical Research
Commission of the European Communities
200 Rue de la Loi
B-1049 Brussels
BELGIUM

H. Smith
International Commission on Radiological Protection
P.O. Box 35
Didcot
Oxon OX11 ORJ
ENGLAND

J. W. Stather
National Radiological Protection Board
Building 383
Chilton, Didcot
Oxon OX11 ORQ
ENGLAND

M. J. Suess
Regional Officer for Environmental Hazards
World Health Organization
8, Scherfigsvej
DK-2100 Copenhagen
DENMARK

Sun Shi-quan, Head
Radiation-Medicine Department
North China Institute of Radiation Protection, MNI
P.O. Box 120
Tai-yuan, Shan-Xi
PEOPLE'S REPUBLIC OF CHINA

G. Tarroni
EHEA-AMB-BIO-FITS
Viale G. B. Ercolani 8
I-40138 Bologna
ITALY

D. M. Taylor
5 Branwen Close
The Sanctuary
Culverhouse Cross
Cardiff CF5 4NE
ENGLAND

K. H. Tempel
Institut für Pharmakologie, Toxikologie und Pharmazie
Fachbereich Tiermedizin der Universität München
Veterinärstraße 13
D-8000 München 22
GERMANY

J. W. Thiessen
Radiation Effects Research Foundation
1-8-6 Nakagawa
NAGASAKI, 850
JAPAN

United Nations Scientific Committee on the Effects of Atomic Radiation
Vienna International Center
P.O. Box 500
A-1400 Vienna
AUSTRIA

D. Van As
Atomic Energy Corporation
P.O. Box 582
Pretoria 0001
REPUBLIC OF SOUTH AFRICA

Dame Janet Vaughan
1 Fairlawn End
First Turn
Wolvercote
Oxon OX2 8AP
ENGLAND

J. Vennart
Bardon, Ickleton Road, Wantage
Oxon OX12 9OA
ENGLAND

Vienna International Centre Library
Gifts and Exchange
P.O. Box 100
A-1400 Vienna
AUSTRIA

V. Volf
Kernforschungzentrum Karlsruhe
Institut für Genetik und Toxikologie von Spaltstoffen
Postfach 3640
D-7500 Karlsruhe 1
GERMANY

G. Walinder
Unit of Radiological Oncology
University of Agricultural Sciences
P.O. Box 7031
S-750 07 Uppsala
SWEDEN

Wang Hengde
North China Institute of Radiation Protection
P.O. Box 120
Tai-yuan, Shan-Xi
PEOPLE'S REPUBLIC OF CHINA

Wang Renzhi
Institute of Radiation Medicine
27# Tai Ping Road
Beijing 100850
PEOPLE'S REPUBLIC OF CHINA

Wang Ruifa, Associate Director
Laboratory of Industrial Hygiene
Ministry of Public Health
2 Xinkang Street
P.O. Box 8018
Deshengmenwai, Beijing 100088
PEOPLE'S REPUBLIC OF CHINA

Wang Yibing
North China Institute of Radiation Protection
P.O. Box 120
Tai-yuan, Shan-Xi
PEOPLE'S REPUBLIC OF CHINA

Wei Lü-Xin
Laboratory of Industrial Hygiene
Ministry of Public Health
2 Xinkang Street
Deshengmenwai, Beijing 100088
PEOPLE'S REPUBLIC OF CHINA

J. Wells
Radiobiology Laboratory
Radiation Biophysics
Nuclear Electric
Berkeley Nuclear Laboratories
Berkeley
Gloucestershire GL 13 9PB
ENGLAND

B. C. Winkler, Director of Licensing
Raad Op Atomic
Atoomkrag Energy Board
Privaatsk X 256
Pretoria 0001
REPUBLIC OF SOUTH AFRICA

Wu De-Chang
Institute of Radiation Medicine
27# Tai Ping Road
Beijing
PEOPLE'S REPUBLIC OF CHINA

Yao Jiaxiang
Laboratory of Industrial Hygiene
2 Xinkang Street
Deshengmenwai, Beijing 100088
PEOPLE'S REPUBLIC OF CHINA

Kenjiro Yokoro, Director
Research Institute for Nuclear Medicine & Biology
Hiroshima University
Kasumi 1-2-3, Minami-ku
Hiroshima 734
JAPAN

V. Zeleny
Institute of Experimental Biology and Genetics
Czechoslovak Academy of Sciences
Bidekpvocla 1-83
Pragie 4
CZECHOSLOVAKIA

Zhu Zhixian
China Research Institute of Radiation Protection
Ministry of Nuclear Industry
P.O. Box 120
Tai-yuan, Shan-Xi
PEOPLES REPUBLIC OF CHINA

ONSITE

DOE Richland Operations Office (3)

P. W. Kruger A5-90
E. C. Norman A5-51
Public Reading Room A1-65

WSU Tri-Cities University Center

H. R. Gover, Librarian H2-52

Hanford Environmental Health Foundation (4)

S. E. Dietert H1-03
R. L. Kathren H1-01
W. C. Milroy H1-02
T. Henn H1-02

U. S. Testing

V. H. Pettey H2-51

Westinghouse Hanford Co.

D. E. Simpson B3-51

Pacific Northwest Laboratory (249)

R. R. Adee P8-13
R. C. Adams K6-52
L. E. Anderson K4-28
R. W. Baalman K1-50 (10)
J. F. Bagley K1-45
W. J. Bair K1-50 (15)
C. A. Baldwin P7-58 (15)
L. A. Braby P8-47
J. K. Briant P7-53
A. L. Brooks P7-53
J. A. Buchanan P7-82
R. L. Buschbom P7-82
D. P. Chandler K4-13
T. D. Chikalla P7-75
B. J. Chou K4-10
M. L. Clark K4-16
T. T. Claudson K1-66
J. A. Creim K4-28
F. T. Cross K4-13
G. E. Dagle K4-10
J. R. Decker K4-16
H. S. DeFord K4-16
J. A. Dill K4-16
R. J. Douthart K4-13
R. D. DuBois P8-47
F. N. Eichner P7-03
C. E. Elderkin K6-08
J. J. Evanoff K4-10
J. W. Falco K6-78
D. R. Fisher K3-53
L. G. Florek K4-16
M. E. Foreman P7-56
W. C. Forsythe K4-16
K. M. Gideon K4-10
R. A. Gies K4-13
A. W. Gieschen K4-16
E. S. Gilbert P7-82
M. F. Gillis K1-50
W. A. Glass K4-13
B. J. Greenspan K4-16
D. K. Hammerberg K4-16
B. K. Hayden K4-16
L. A. Holmes K1-29
M. G. Horstman K4-10
V. G. Horstman P7-58
J. R. Houston A3-60

PNL-8000, Pt. 1
UC-408

A. C. James K3-51
A. E. Jarrell K4-10
J. R. Johnson K3-53
R. F. Jostes K4-13
D. R. Kalkwarf P7-50
M. T. Karagianes P7-57
R. M. Kitchin P7-56
M. Knotek K1-48
S. A. Kreml P7-58 (2)
E. G. Kuffel K4-16
W. W. Laity K2-15
K. E. Lauhala P7-58
C. L. Leach K4-10
F. C. Leung K4-13
M. K. Lien P8-47
J. A. Mahaffey P7-82
E. M. Maloney K4-13
D. B. Mann P7-53
T. J. Mast K4-10
K. E. McDonald P7-56
P. W. Mellick K4-10
M. E. Mericka K4-10
H. K. Meznarich P7-53
D. L. Miller P7-53
J. H. Miller P8-47
M. C. Miller P7-44
R. A. Miller K4-10
T. L. Morgan P8-47
J. E. Morris P7-56
D. A. Mueller P7-50
D. A. Nelson K2-44
J. M. Nelson P8-47
J. F. Park P7-58 (50)
R. W. Perkins P7-35
J. T. Pierce K4-10
C. A. Poindexter K4-16
G. J. Powers P7-53
H. A. Ragan K4-13
R. A. Renne K4-10
D. N. Rommereim K4-28
R. L. Rommereim K4-10
C. O. Romsos K4-10
E. J. Rossignol K4-16
S. E. Rowe K4-10
P. S. Ruemmler K4-10
J. L. Ryan P7-25
C. L. Sanders H2-52
L. B. Sasser P7-53
G. F. Schiefelbein K2-03
J. E. Schmaltz K1-86
L. C. Schmid K1-34
R. P. Schneider P7-56
L. E. Sever P7-82
B. D. Shipp K1-73
M. R. Sikov P7-53
J. C. Simpson K1-86
E. C. Sisk P7-56
L. G. Smith P7-58
D. L. Springer P7-53
J. G. Stephan K3-56
R. G. Stevens P7-82
D. L. Stewart K6-91
G. L. Stiegler P7-56
L. C. Stillwell P7-56
G. M. Stokes K1-74
K. L. Swinth K3-55
W. L. Templeton K1-30
T. S. Tenforde K1-50 (10)
R. M. Thomas P7-53
R. C. Thompson P7-58
B. D. Thrall P7-50
L. H. Toburen P8-47
R. J. Traub K3-57
V. D. Tyler K4-13
H. R. Udseth P8-19
B. E. Vaughan K1-66
M. B. Walter K6-96
C. R. Watson P7-82
R. J. Weigel K4-16
R. E. Weller P7-52
R. B. Westerberg K4-16
T. J. Whitaker K2-21
E. L. Wierman P7-52 (2)
R. E. Wildung P7-54
W. R. Wiley K1-46
L. D. Williams K1-41
W. E. Wilson P8-47
J. D. Zimbrick P7-58 (10)
Health Physics Department Library
Life Sciences Library (2)
Publishing Coordination
Technical Report Files (5)

END

DATE
FILMED
2/23/93